

1
2
3
4
5
6
7
8

DRAFT
**Assessment of the Responses of the
Caloosahatchee River Estuary to
Low Freshwater Inflow in the
Dry Season**



9
10
11
12
13
14
15
16
17
18
19
20
21

August 2016

Prepared by:
Christopher Buzzelli, Peter Doering, Yongshan Wan, Teresa Coley, Detong Sun,
Zhiquiang Chen, Cassandra Thomas, Don Medellin and Toni Edwards

Coastal Ecosystems Section
South Florida Water Management District
3301 Gun Club Rd.
West Palm Beach, FL 33406

22

ACKNOWLEDGEMENTS

23 This document resulted from significant efforts by personnel in the Coastal Ecosystem
24 Section at the South Florida Water Management District. R. Chamberlain at the St. Johns
25 River Water Management District deserves special recognition for his contributions to
26 studies of freshwater inflows and the ecological attributes of the Caloosahatchee River
27 Estuary. We acknowledge the considerable efforts of S.G. Tolley et al. at Florida Gulf
28 Coast University for their study of zooplankton and ichthyoplankton, and P. Montagna and
29 T. Palmer at Texas A&M University-Corpus Christi for their analyses of historical
30 macrobenthic data. The document greatly benefitted from constructive reviews provided
31 by S. Gray, J. Brown, and S. Memberg at the South Florida Water Management District.

DRAFT

EXECUTIVE SUMMARY

The Caloosahatchee River minimum flow and level (MFL) was established in 2001, reviewed in 2003, and is being reevaluated for 2017. MFL criteria define the point at which additional withdrawals of water will result in significant harm to the water resources (Sections 373.042 and 373.0421, Florida Statutes). The purpose of this study was to provide a comprehensive assessment of the effects of dry season freshwater inflow on the Caloosahatchee River Estuary (CRE). This effort was composed of 11 component studies focused on hydrodynamics, water column and benthic habitats, and faunal indicators. The different indicators respond to inflow on different scales (days-years) and are located along the salinity gradient between the upstream water control structure (S-79) and the estuary mouth (~42 kilometers). The component studies emphasized the relationships between the indicators and inflows through the S-79 structure in the dry season (November–April). The indicator inflow (Q_I) was defined as the inflow rates below which there would be negative impacts, not significant harm.

The CRE has been structurally altered including the installation of the S-79 structure and the Sanibel Causeway, removal of oyster reefs around Shell Point, and channelization. These irreversible modifications have enhanced upstream salt transport throughout the estuary. Inflow-salinity relationships are influenced by the Tidal Basin downstream of S-79, which provides an estimated 18% of the total freshwater input over the period of record from 1966 through 2014. There were wide inter-annual variations in S-79 inflows (445 ± 218 cubic feet per second [cfs]) associated with a salinity of 10 at Fort Myers. Total dry season inflows less than 500 cfs appeared to promote bottom water hypoxia in the upper CRE as the chlorophyll *a* maximum migrated upstream over the deeper channel. Inflows less than 412 ± 165 cfs could lead to impingement of zooplankton assemblages on S-79, compressing their habitat. Flows less than 238 ± 256 could result in loss of preferred salinity habitat (<10) for juvenile fish in the upper estuary. Inflows of 501 ± 525 cfs and 296 ± 410 cfs supported stationary habitats in the upper (benthic macrofauna) and lower (oyster bed) CRE. Average inflows greater than 545 ± 774 cfs in the dry season from 1993 to 1999 promoted low salinity conditions for the survival of *Vallisneria americana* (tape grass). Conversely, the vegetated habitat declined as the average salinity at Fort Myers exceeded 10 from 2007 to 2013. Lee County blue crab harvest (1984–2013) was reduced when the average dry season inflows were less than 400 ± 57 cfs. The area of sawfish habitat area between S-79 and Shell Point was maximized when inflow from S-79 was 270 cfs in the 2007 dry season. There were three important results:

1. The magnitude of minimum indicator inflows (Q_I) from S-79 ranged from 237 cfs to 545 cfs among the 11 estimates.
2. Seasonally averaged S-79 inflows less than the Q_I for each indicator could result in phytoplankton blooms in the upper CRE (less than 10 kilometers from S-79), compress the water column habitat for zooplankton and ichthyoplankton against the structure, alter the composition of the macrobenthic community in the upper estuary, prevent the survival of *Vallisneria*, shrink the available habitat for the endangered sawfish, and lead to reduced harvest of blue crabs the following year.

- 73
74
75
76
3. Flow through S-79 accounts for 82% of the total inflow. The Tidal Basin inflows account for the remaining 18%. Assuming a median Q_I at S-79 of 400 cfs, the Tidal Basin flows are estimated at 88 cfs for a total inflow of 488 cfs.

DRAFT

77	TABLE OF CONTENTS	
78	Acknowledgements	ii
79	Executive Summary	iii
80	List of Figures.....	ix
81	List of Tables	xvi
82	Acronyms and Abbreviations	xxi
83	Science Summary	1
84	Purpose of Study	1
85	Background Information	1
86	Alterations of the South Florida Landscape and Caloosahatchee River MFL	
87	Watershed.....	1
88	Freshwater Inflow and Estuaries	4
89	Freshwater Inflow and the Caloosahatchee River Estuary	5
90	Methods.....	8
91	Description of Component Studies.....	8
92	Importance of Uncertainty.....	9
93	Quantification of Indicator Freshwater Inflows in the Dry Season.....	9
94	Results.....	10
95	Summaries of Component Studies	10
96	Component 1: Three Dimensional Model Evaluation of Physical and Structural Alterations of	
97	the Caloosahatchee River and Estuary: Impact on Salt Transport	10
98	Component 2: Analysis of the Relationship between Freshwater Inflow at S-79 and Salinity in	
99	the Caloosahatchee River Estuary 1993–2013.....	11
100	Component 3: Relationships between Freshwater Inflows and Water Quality Attributes during	
101	the Dry Season in the Caloosahatchee River Estuary	11
102	Component 4: Zooplankton Response to Freshwater Inflow in the Caloosahatchee River	
103	Estuary	11
104	Component 5: Ichthyoplankton Response to Freshwater Inflow in the Caloosahatchee River	
105	Estuary	12
106	Component 6: Summary and Interpretation of Macrobenthic Community Properties Relative	
107	to Salinity and Inflow in the Caloosahatchee River Estuary	12
108	Component 7: Relationships between Salinity and the Survival of <i>Vallisneria americana</i> in the	
109	Caloosahatchee River Estuary.....	12
110	Component 8: Development and Application of a Simulation Model for <i>Vallisneria americana</i>	
111	in the Caloosahatchee River Estuary.....	12
112	Component 9: Assessment of Dry Season Salinity and Freshwater Inflow Relevant for Oyster	
113	Habitat in the Caloosahatchee River Estuary	13
114	Component 10: Ecohydrological Controls on Blue Crab Landings and Minimum Freshwater	
115	Inflow to the Caloosahatchee River Estuary	13
116	Component 11: Relationships between Freshwater Inflow, Salinity and Potential Habitat for	
117	Sawfish (<i>Pristis pectinata</i>) in the Caloosahatchee River Estuary	14
118	Quantification of Indicator Freshwater Inflows in the Dry Season.....	14
119	Discussion.....	17

120	Component Studies	20
121	Component Study 1: Three-Dimensional Model Evaluation of Physical and Structural	
122	Alterations of the Caloosahatchee River and Estuary: Impact on Salt Transport.....	20
123	Abstract	20
124	Introduction	20
125	Methods.....	21
126	Study Site.....	21
127	Alterations within the Caloosahatchee River Estuary MFL Watershed.....	22
128	Hydrodynamic Model of the CRE.....	24
129	Hydrodynamic Model Scenarios.....	25
130	Results 29	
131	Validation of the Existing Condition	29
132	Hydrodynamic Model Scenarios.....	32
133	Theoretical Considerations for Salt Intrusion	34
134	Discussion	35
135	Component Study 2: Analysis of the Relationship between Freshwater Inflow at S-79	
136	and Salinity in the Caloosahatchee River Estuary 1993–2013	36
137	Abstract	36
138	Introduction	36
139	Methods.....	37
140	Results	39
141	Discussion	39
142	Component Study 3: Relationships between Freshwater Inflows and Water Quality	
143	Attributes during the Dry Season in Caloosahatchee River Estuary	44
144	Abstract	44
145	Introduction	44
146	Methods.....	45
147	Adaptive Protocol Release Study.....	45
148	Long-Term Monitoring of Chlorophyll a.....	47
149	Segmented Simulation Model of the Caloosahatchee River Estuary	48
150	Results	50
151	Adaptive Protocol Release Study.....	50
152	Long-Term Monitoring of Chlorophyll a.....	54
153	Segmented Simulation Model of the CRE.....	56
154	Discussion	58
155	Component Study 4: Zooplankton Response to Freshwater Inflow in the	
156	Caloosahatchee River Estuary	60
157	Abstract	60
158	Introduction	60
159	Methods.....	61
160	Florida Gulf Coast University Plankton Surveys 2008–2010	61
161	Data Analysis.....	62
162	Results and Discussion.....	65
163	Component Study 5: Ichthyoplankton Response to Freshwater Inflow in the	
164	Caloosahatchee River Estuary	76

165	Abstract	76
166	Introduction	76
167	Methods.....	76
168	Results and Discussion.....	78
169	Component Study 6: Summary and Interpretation of Macrobenthic Community	
170	Properties Relative to Salinity and Inflow in the Caloosahatchee River Estuary.....	83
171	Abstract	83
172	Introduction	83
173	Methods.....	84
174	Results and Discussion.....	86
175	Component Study 7: Relationships between Salinity and the Survival of <i>Vallisneria</i>	
176	<i>americana</i> in the Caloosahatchee River Estuary	92
177	Abstract	92
178	Introduction	92
179	Methods.....	96
180	<i>Vallisneria</i> Monitoring in the Caloosahatchee River Estuary	96
181	Salinity Monitoring in the CRE	96
182	Data Analyses	97
183	Results	98
184	Discussion	102
185	Component Study 8: Development and Application of a Simulation Model for	
186	<i>Vallisneria americana</i> in the Caloosahatchee River Estuary	104
187	Abstract	104
188	Introduction	104
189	Methods.....	105
190	Study Site.....	105
191	Empirical Data	106
192	Model Boundaries.....	107
193	Model Mathematical Structure.....	107
194	Model Calibration, Sensitivity, and Application.....	114
195	Results	115
196	Discussion	121
197	Component Study 9: Assessment of Dry Season Salinity and Freshwater Inflow	
198	Relevant for Oyster Habitat in the Caloosahatchee River Estuary.....	123
199	Abstract	123
200	Introduction	123
201	Methods.....	125
202	Results	126
203	Discussion	128
204	Component Study 10: Ecohydrological Controls on Blue Crab Landings and	
205	Minimum Freshwater Inflow to the Caloosahatchee River Estuary.....	130
206	Abstract	130
207	Introduction	130
208	Methods.....	131
209	Study Area	131
210	Inflow Characteristics	132
211	Data Sources	132

212	Relationships between Hydrologic Variables and Blue Crab Catch	133
213	Statistical Analyses	133
214	Loss of Water Resource Function and Recovery in Relation to Rainfall.....	134
215	Determination of Flow Associated with Rainfall.....	136
216	Results	136
217	Relationships between Hydrologic Variables and Blue Crab Catch	136
218	Loss of Water Resource Function and Recovery in Relation to Rainfall.....	140
219	Return Frequency.....	143
220	Discussion	144
221	Component Study 11: Relationships between Freshwater Inflow, Salinity, and	
222	Potential Habitat for Sawfish (<i>Pristis pectinata</i>) in the Caloosahatchee River Estuary	
223	146
224	Abstract	146
225	Introduction	146
226	Methods.....	148
227	Bathymetric Analyses	148
228	Hydrodynamic Modeling	148
229	Data Analyses	151
230	Results	151
231	Discussion	152
232	References	156
233		

234

LIST OF FIGURES

235	Figure 1. A) The Caloosahatchee River Estuary MFL Watershed with its sub-	
236	watersheds and major water control structures and B) locations for the	
237	monitoring of salinity, water quality and oyster habitat for the CRE. The	
238	map includes SAV monitoring sites in the upper CRE.....	3
239	Figure 2. A) Total rainfall to the Caloosahatchee River Estuary MFL Watershed by	
240	water year and season and B) stacked bar chart for the total freshwater	
241	inflow (millions of ac-ft per year). Included are the long-term averages	
242	from WY1997–WY2014, WY2012, WY2013 and WY2014.....	6
243	Figure 3. Graphical results showing the range (bar) and average + standard deviation	
244	(point + error bar and text) of the estimated indicator inflows (QI) for	
245	each of the component studies.	16
246	Figure 4. The Caloosahatchee River Estuary MFL Watershed with its sub-	
247	watersheds and major water control structures. The future location of the	
248	C-43 Storage Reservoir is also shown.	22
249	Figure 5. Comparison of bathymetry of the model domain for the CRE: (top left)	
250	the 1887 bathymetry for the entire domain, (bottom left) the 1887	
251	bathymetry focused on the CRE, (top right) the 2003 bathymetry for the	
252	entire domain, and (bottom right) the 2003 bathymetry focused on the	
253	CRE.....	26
254	Figure 6. Salinity and inflow monitoring stations in the CRE used for model	
255	validation. Both freshwater inflow and salinity are monitored at the S-79	
256	structure.....	28
257	Figure 7. Freshwater inflow (cfs) from S-79 (blue) and the tidal basin downstream	
258	of S-79 (red).....	28
259	Figure 8. Modeled (red line) and measured (black dash) tidal elevations at (A) S-79,	
260	(B) I-75, (C) Shell Point, and (D) Sanibel Island from March to April	
261	2011.....	29
262	Figure 9. Modeled (red line) and measured (blue line) tidal discharge at (A) Shell	
263	Point, and (B) Marker 52 from October 15, 2008, to April 15, 2009.....	30
264	Figure 10. Modeled (red line) and measured (black dash) hourly surface and bottom	
265	salinity at I-75 (A and B) , Fort Myers (C and D) , and Shell Point (E and	
266	F) from March to April 2010.....	31
267	Figure 11. Modeled (red line) and measured (black dash) daily surface and bottom	
268	salinity at S-79 (A and B) and Ft. Myers (C and D) from 2001 to 2010.....	32
269	Figure 12. Comparison between average daily surface salinity at Fort Myers (red	
270	line) and five different physical alteration scenarios (black dash) from	
271	2001 to 2010: (A) removal of S-79; (B) removal of Sanibel Causeway;	
272	(C) restoration of oyster bar at the mouth; (D) refill of the navigational	
273	channel; and (E) reestablishment of predevelopment bathymetry.	33

274	Figure 13. (A) Time series of average monthly inflow from the S-79 structure to the	
275	CRE and average monthly salinity at the Fort Myers monitoring station.	
276	(B) Negative relationship between inflow (Q_{S79}) and salinity (S_{FIM})	
277	represented by an exponential decay equation. All months from the POR,	
278	WY1993–WY2013, are included.....	38
279	Figure 14A–L. Series of scatter plots and fitted exponential decay equations between	
280	average monthly inflow at S-79 (cfs) and average monthly salinity at the	
281	Fort Myers monitoring station since WY1993.	40
282	Figure 14M–U. Series of scatter plots and fitted exponential decay equations	
283	between average monthly inflow at S-79 (cfs) and average monthly	
284	salinity at Fort Myers since WY1993.	41
285	Figure 15. Time series of the calculated amount of freshwater inflow from S-79	
286	associated with a salinity of 10 at Fort Myers (Q_{calc}). The average Q_{calc} is	
287	shown (445 cfs).....	43
288	Figure 16. (A) Map of the CRE in Southwest Florida from the Adaptive Protocol	
289	Release Study showing the major structures (S-79 and bridges), the	
290	distance downstream of S-79 (white circles), and the locations for the nine	
291	vertical profiling stations (yellow call-outs). (B) Site map for monitoring	
292	in the CRE.....	47
293	Figure 17. Schematic and definition of process terms that influence phytoplankton	
294	biomass (e.g. CHL) in the simulation model for the CRE.....	49
295	Figure 18. Results of the APRS from March 8, 2012, March 21, 2012, and April 12,	
296	2012: (A) surface water salinity versus distance downstream of S-79; and	
297	(B) surface water CHL versus distance downstream of S-79.....	51
298	Figure 19. Interpolated depth versus distance contour plots derived from vertical	
299	profiling from the APRS for three different cruise dates. The APRS	
300	station designations shown in Figure 16A are provided along the top of	
301	each plot. The horizontal axis is oriented from right to left to represent	
302	distance downstream of S-79. The vertical axis is depth. The top three	
303	plots show salinity ranging from 0 to 3 to >35.0. The middle three plots	
304	show CHL ranging from 0 to 2 to >15.0. The bottom three plots show DO	
305	concentrations ranging from 0 to 2 to >9.0.....	52
306	Figure 20. Hyperbolic relationship between average (avg) freshwater inflow 14 days	
307	(d) before cruise date for the APRS and the location of the CHL_{max} in	
308	surface water of the CRE. Results from all cruises from dry seasons in	
309	2012 and 2013 ($n = 15$).....	53
310	Figure 21. Time series of water column CHL observed at station CES03 in the upper	
311	CRE. Average daily inflow at S-79 (right axis) is shown in grey.	54
312	Figure 22. Scatterplots of water column CHL observed at station CES03 in the upper	
313	CRE versus the average daily inflow at S-79: (A) inflow on CES03	

314	sampling date; (B) inflow averaged over 14 days (d) prior to the sampling	
315	date; (C) inflow averaged over 21 days prior to sampling date; (D) inflow	
316	averaged over 21 d prior to sampling date; (E) inflow averaged over 35	
317	days prior to sampling date.	55
318	Figure 23. Time series of water column CHL concentration predicted for the upper	
319	CRE (0–16 km downstream of S-79) using the simulation model. Data	
320	points represent the average CHL concentration averaged among four	
321	stations in the upper CRE (S-79, CES01, CES02, and CES03). Also	
322	shown are daily average flows from S-79.	56
323	Figure 24. Results from simulation model of the CRE. Average monthly inflow at	
324	S-79 (cfs) versus average monthly CHL concentration ($\mu\text{g L}^{-1}$) in	
325	upstream Segment 1. The zoomed scatterplot highlights inflows <500 cfs.	
326	57
327	Figure 25. Zooplankton sampling stations. Distances in kilometers from Shell Point.	
328	The Franklin Lock and Dam are located at about 43.5 km upstream of	
329	Shell Point. Data collected from 2008 to 2010 was used in this study.	61
330	Figure 26. Change point analysis using conditional regression. The Y-axis is the	
331	position of the 90 th abundance decile in the CRE. The x-axis is discharge	
332	averaged over a number of days before sampling, which ranged between	
333	0 and 60.	65
334	Figure 27. Volume of the CRE in 1-km increments. Shell Point (0 km) to the S-79	
335	(43 km).	66
336	Figure 28. COA for various taxa during the study period. Upstream of the reference	
337	line at 30 km, habitat volume is reduced.	67
338	Figure 29. Potential habitat volume as a function of the position of rkm_U (left) for	
339	different taxa. IDR as a function of the position of rkm_U (right).	71
340	Figure 30. Map of ichthyoplankton sampling stations from 1986–1989 in the	
341	Caloosahatchee River Estuary.	77
342	Figure 31. Ichthyoplankton abundance (number per cubic meter [$\#/m^3$]) across	
343	stations. Bars with the same letters are not significantly different ($p >$	
344	0.05). Data were retransformed from $\log(x+1)$ transformed analysis.	78
345	Figure 32. Ichthyoplankton abundance (number per cubic meter [$\#/m^3$]) under	
346	different inflow regimes (1 = 0–150 cfs; 2 and 3 = 151–600 cfs; 4 = 601–	
347	1,200 cfs; 5 = 1,201–2,500 cfs; 6 = >2,500 cfs) (1986–1989 study). Bars	
348	with the same letters are not significantly different ($p >$ 0.05). Data were	
349	retransformed from $\log(x+1)$ transformed analysis.	79
350	Figure 33. Ichthyoplankton abundance of different life stages at each station over	
351	different months compared to abundance of zooplankton (1986–1989	
352	study).	80

353	Figure 34. Juvenile fish abundance (number per cubic meter [$\#/m^3$]) relative to 30-	
354	day average salinity and the running median of abundance (right axis; red	
355	line) to establish a salinity envelope of preference.	81
356	Figure 35. COA for juvenile fish compared to density-weighted salinity at different	
357	inflow regimes (1 = 0–150 cfs; 2 and 3 = 151–600 cfs; 4 = 601–1,200 cfs;	
358	5 = 1,201–2,500 cfs; 6 = >2,500 cfs) (1986–1989 study).	81
359	Figure 36. Frequency distribution of density-weighted salinity for juvenile fish.	82
360	Figure 37. (A) Location map for macrobenthic sampling in the CRE. Included are	
361	sampling macrobenthic stations (B1 through B7; yellow), the long-term	
362	salinity stations (red), and the upstream location of freshwater inflow (S-	
363	79; green). (B) Map of the CRE with the macrobenthic sampling stations	
364	(B1 through B7; red) and four estuarine zones determined in this study.	85
365	Figure 38. (A) Long-term average salinity in the dry season at Bridge 31 in the upper	
366	CRE (open bars; left axis) superimposed on daily freshwater inflow at S-	
367	79 (grey fill; right axis). (B) The percentage of dry season days where	
368	salinity ranged from 0 to 4 (S_{0-4}) at Bridge 31 in the upper CRE (open	
369	bars; left axis) superimposed on daily freshwater inflow at S-79 (grey fill;	
370	right axis).	91
371	Figure 39. 1993 map of SAV habitat density in the CRE from Hoffaker (1994).	95
372	Figure 40. Location map for the CRE including the S-79 water control structure,	
373	water quality monitoring sites, SAV monitoring sites (upper CRE), and	
374	the location of continuous salinity recorders.	97
375	Figure 41. (A) Time series of daily average surface water salinity at Fort Myers from	
376	January 1992 to April 2014. (B) Time series of average <i>Vallisneria</i> shoot	
377	densities ($\# m^{-2}$) at Sites 1 (filled circle) and 2 (open square) in the CRE	
378	from 1998 to 2007. Average daily surface salinity at Fort Myers is shown	
379	as the grey filled time series (right axis).	99
380	Figure 42. Combination plot showing <i>Vallisneria</i> shoot densities (unit per m^2 [unit	
381	m^{-2}]; left axis) from monitoring Sites 1 and 2 as a function of the 30-day	
382	moving average salinity at Ft. Myers. The red line depicts the	
383	probabilities of break points in the relationship between shoot density and	
384	salinity.	100
385	Figure 43. (A) Time series of average seasonal salinity at Fort Myers from 1993 to	
386	2014. The shaded areas mark two separate seven-year periods (1993–	
387	1999; 2007–2014). (B) Time series of average seasonal shoot density	
388	from 1998 to 2007. Data before this period were qualitative. Monitoring	
389	methods changed to detect presence versus absence since 2008.	101
390	Figure 44. Proportional mortality plot showing the number of days where salinity at	
391	Fort Myers was >10 versus the percent of initial shoots remaining. See	
392	text and Table 22 for details of analysis.	102

393	Figure 45. Location map for the CRE including the S-79 water control structure,	
394	water quality monitoring sites, SAV monitoring sites, and the location of	
395	continuous salinity recorders.	106
396	Figure 46. Conceptual model for response of <i>Vallisneria</i> shoots to variable	
397	temperature (T_w), irradiance at the bottom (I_z), and salinity (S). See	
398	Tables 1 and 2 for model equations and coefficients, respectively. Surface	
399	irradiance (I_0), turbidity (NTU), chlorophyll <i>a</i> (CHL), and color were	
400	used to calculate I_z . S was used as a term to estimate color. Depth (h) was	
401	calculated using water level (η) and sediment elevation (z). A suite of	
402	coefficients— optimum temperature (T_{opt}), <i>Vallisneria</i> constants for	
403	photosynthesis (KT1) and (KT2), maximum rate of photosynthesis (P_m),	
404	and the half-saturation irradiance value (I_k)—are combined with T_w and	
405	shoot biomass to calculate gross production (G). Respiration (R) is	
406	influenced by a temperature effect (T_{fx}) and S . S also influences the rate	
407	of shoot mortality (M). Loss due to grazing (G_z) is a function of the shoot	
408	biomass and the basal grazing rate (kG_z).	108
409	Figure 47. (A) Time series of daily water temperature in ° C (C) at Fort Myers from	
410	1998 to 2012. (B) Relationship between water temperature in ° C (C) and	
411	the shoot gross production rate (fT_{shoot}).	109
412	Figure 48. (A) Time series of daily salinity predicted for SAV monitoring Site 1	
413	from 1998 to 2014 (black line; left axis) and freshwater inflow at S-79	
414	(cubic meters per second [$m^3 s^{-1}$]; grey fill; right axis). (B) Scalar	
415	multiplier for the negative effects of salinity on gross photosynthesis	
416	(fS_{gross} ; solid) and positive effects on shoot mortality (fS_{loss} ; dashed).	112
417	Figure 49. Monthly time series at CES04 monitoring site in the Caloosahatchee	
418	Estuary for (A) turbidity (NTU) and (B) CHL.	113
419	Figure 50. Time series of altered daily salinity in the dry season as input to the 1998–	
420	1999 loop model.	114
421	Figure 51. (A) Time series of the submarine light extinction coefficient (k_t ; m^{-1} ; left	
422	axis) and daily freshwater inflow at S-79 (cfs; right axis). (B) Time series	
423	of the percent of light at the bottom ($\%I_0$; left axis) and daily freshwater	
424	inflow at S-79 (cfs; right axis).	118
425	Figure 52. (A) Time series of <i>Vallisneria</i> shoot density (average + standard	
426	deviation) from Site 1 near Beautiful Island in the CRE. (B) Linear	
427	regression between total number of <i>Vallisneria</i> shoots and total dry	
428	weight biomass of shoots (grams dry weight [gdw]) from controlled	
429	mesocosm experiments. (C) Time series of Site 1 <i>Vallisneria</i> shoot	
430	biomass (average + standard deviation) derived by converted shoot	
431	density using the regression equation.	119

432	Figure 53. Time series (1998–2014) of average seasonal <i>Vallisneria</i> shoot biomass	
433	from the model superimposed on average seasonal values at Site 1 (1998–	
434	2008). Daily inflow at S-79 shown as shaded area with right axis.....	120
435	Figure 54. Plot of % increase in dry season salinity versus average shoot biomass. A	
436	55% increase in dry season salinity values resulted in net mortality of	
437	<i>Vallisneria</i>	120
438	Figure 55. Location map for Cape Coral and Shell Point sampling sites, oyster	
439	habitat derived from side-scan mapping (red), and average densities	
440	(colored circles) in the lower CRE.....	125
441	Figure 56. Conceptual model of the effects of salinity (S) on oyster survival and	
442	growth. Generalized freshwater inflows that could account for the target	
443	salinity range are shown at the bottom.	126
444	Figure 57. Time series of average daily freshwater inflow at S-79 (cfs; right axis;	
445	shaded fill) and salinities at Cape Coral (red) and Shell Point (black) from	
446	May 1, 2005, to April 30, 2014.....	127
447	Figure 58. Location of Lee County and the Caloosahatchee River and CRE. Over	
448	60% of land area in Lee County drains into the CRE and San Carlos Bay.	
449	132
450	Figure 59. Monthly landings of hard shell blue crabs in Lee County Florida. Data	
451	from the Florida Fish and Wildlife Conservation Commission’s Florida	
452	Wildlife Research Institute.	133
453	Figure 60. Normality test of natural log-transformed dry season rainfall during	
454	WY1966–WY2013. (Note: cm – centimeters.)	135
455	Figure 61. (A) Dry season (November–April) rainfall in Lee County. (B) Annual	
456	landings of hard shell blue crabs.....	137
457	Figure 62. Functional regression of hard shell blue crab landings on the previous	
458	year’s dry season rainfall (unadjusted data).....	139
459	Figure 63. Functional regression of the increase in CPUE from one year to the next	
460	on the dry season rainfall occurring during the first of the two years. Data	
461	from Figure 61	141
462	Figure 64. Exponential relationships between dry season rainfall in Lee County and	
463	discharge to the CRE at S-79 (top panel) or total discharge (bottom	
464	panel).....	142
465	Figure 65. Results of spectral analysis. Periodicity of de-trended blue crab landings	
466	(top panel) and dry season rainfall (bottom panel) in Lee County for	
467	WY1986–WY2013. Results indicate that both time series show major	
468	fluctuation with a period of about six years.....	143
469	Figure 66. (A) Hypothetical relationship between inflow at S-79 (Q_{S79} ; cfs) and the	
470	downstream locations of the S_{12} and S_{27} . (B) Hypothetical relationship	
471	between inflow at S-79 and the area for sawfish in the CRE.	149

472	Figure 67. Schematic of method used to combine sawfish habitat requirements, the	
473	bathymetry of the CRE, and the hydrodynamic model (CH3D) to estimate	
474	A_{saw} . (Note: A and V – A_{saw} and habitat volume [V_{saw}]; DEM – digital	
475	elevation model; and SP – Shell Point.).....	150
476	Figure 68. (A) Bathymetric contour map for the CRE. (B) Frequency histogram	
477	depicting the bottom area for each of several CRE depth classes.	153
478	Figure 69. Results of bathymetric analyses depicting the area (km^2) and volume (10^6	
479	m^3) of the 0- to 1-m depth contour relative to distance downstream of S-	
480	79.....	154
481	Figure 70. The gradient in average salinities in nearshore environments predicted	
482	over a range of inflows (0, 150, 300, 450, 650, 800, and 1,000 cfs) from	
483	May 2007.	154
484	Figure 71. (A) The position of the S_{12} and S_{27} salinity isohalines as a function of dry	
485	season inflow. (B) The A_{saw} and V_{saw} as a function of dry season inflow.	
486	(C) Scatterplot and polynomial curve fit between inflow at S-79 and the	
487	A_{saw}	155
488		

489

LIST OF TABLES

490	Table 1. List of component studies and the basic description of research methods.	8
491	Table 2. Summary of component studies, the method used to estimate the indicator	
492	inflow (QI), and the range and average + standard deviation (Avg + SD)	
493	values for QI (cfs). The median value for QI over all estimates is provided	
494	(362 cfs).	15
495	Table 3. Model performance statistics for hourly tidal elevation calculated over the	
496	period from 2007 to 2011.	29
497	Table 4. Model performance statistics for hourly and daily salinity calculated over	
498	the period from 2007 to 2011 and from 2001 to 2011, respectively. [Note	
499	$\text{m}^3 \text{s}^{-1}$ – cubic meters per second.]	30
500	Table 5. Model performance statistics for hourly and daily salinity calculated over	
501	the period from 2007 to 2011 and from 2001 to 2011, respectively.....	32
502	Table 6. Difference of monthly average surface (S) and bottom (B) salinity between	
503	each scenario and the existing condition at I-75 and Fort Myers in May	
504	of 2001, 2007, 2008, and 2011.	33
505	Table 7. Summary from analysis of average monthly inflow at S-79 (cfs) and average	
506	monthly salinity at Fort Myers. An exponential decay curve was used to	
507	describe the relationship between the average monthly values for each	
508	water year. Table values for each water year include the average inflow	
509	(Q_{S79}) and salinity at Fort Myers (S_{FIM}), curve fit parameters (r^2 , a , and	
510	b), and the calculated inflow to achieve a salinity of 10 at Fort Myers (Q_I).	
511	42
512	Table 8. Results from the APRS on the CRE in the 2012 dry season. Included are	
513	the 14-day average inflow at S-79 (Q_{S79}), the location of the salinity of 10	
514	isohaline in km from S-79 (S_{10}), and the location and value for the	
515	maximum concentration of chlorophyll a (CHL_{max})......	50
516	Table 9. Descriptive statistics for (CHL ($\mu\text{g L}^{-1}$) at station CES03 in the CRE from	
517	April 1999 to April 2014. The data set was split into dry (November-	
518	April) and wet (May–October) seasons. Included are the number of	
519	samples, range, median, average and standard deviation (Avg \pm SD), and	
520	the coefficient of variation expressed as a percentage (CV =	
521	(SD/Avg)*100).	54
522	Table 10. Model calibration results to simulation CHL concentration ($\mu\text{g L}^{-1}$) in the	
523	upper CRE (0–16 km from S-79) from 2002 to 2009. Included are the	
524	average + standard deviation for pooled monitoring data (CES01, CES02,	
525	CES03, and S-79) and the model. The correlation coefficient (r) between	
526	the data and the model was calculated using monthly average	
527	concentrations ($n = 96$ months).	56

528	Table 11. Summary of daily average inflows at S-79 (cfs) when the CHL	
529	concentrations were $>11 \mu\text{g L}^{-1}$. Results from both field monitoring (top	
530	row) and the upper segment of the Caloosahatchee River Estuary	
531	simulation model (bottom row; Buzzelli et al. 2014b). Water column	
532	CHL concentrations were determined at station CES03 from April 1999	
533	to April 2014 (n = 259). Using the model, water column CHL	
534	concentrations were predicted for the upper CRE (0 to 16 km from S-79)	
535	every day from 2002 to 2009 (n = 2,120 days). Values include the	
536	averages and standard deviations (Avg \pm SD) for CHL and the freshwater	
537	inflows from S-79 (Q_{S79} ; cfs). Results are for dry season days only	
538	(November – April) for both the field (n = 123) and model (n = 1,450).....	58
539	Table 12. Sampling stations for biological and water quality data (May 2008 to April	
540	2010). Depth represents the mean maximum water depth recorded at each	
541	station during biological sampling. (Note: D = downstream and U =	
542	upstream stations within each zone, with zones as described in text.).....	62
543	Table 13. List of organisms evaluated for potential habitat compression and	
544	impingement on S-79.....	63
545	Table 14. Regression relationships between freshwater inflow at S-79 (x) and the	
546	location of the center of abundance (rkmU; y) in the sampling space. n is	
547	the number of observations, a is the intercept, b is the slope, p is the level	
548	of statistical significance, r^2 is the coefficient of determination. Days are	
549	the number of days prior to each sampling date that inflow (Q) was	
550	averaged. In general regression equations were of the form $\text{rkmU} = a - b$	
551	$(\ln(Q+1))$ except where noted. Also given is the inflow required to locate	
552	the center of abundance at 30 km upstream of Shell Point where volume	
553	of the estuary begins to increase.	66
554	Table 15. Linear regression relationships between the distance-weighted COA (x)	
555	and the location (river km) of the 10 th (KM_10) and 90 th (KM_90)	
556	abundance deciles (y). n is the number of observations, a is the intercept,	
557	b is the slope, and r^2 is the coefficient of determination. All regression	
558	were statistically significant at $p < 0.05$ except where noted (ns = not	
559	significant and * denotes $p < 0.10$).	69
560	Table 16. Results of change point analysis to evaluate impingement on the Franklin	
561	Lock and Dam (S-79). Constant is the river km where the location of the	
562	90 th abundance quantile stops changing as inflows decrease, indicating	
563	impingement. CP is the inflow at which the 90 th decile begins to move	
564	downstream as inflow increases. U and L indicate upper and lower limits	
565	of the 95% confidence interval. Decile data for <i>A. mitchelli</i> adults were	
566	natural log transformed for the analysis. Results for Anchoa and Gobiidae	
567	not included in calculation of means and standard deviations.....	75

568	Table 17. Summary of dominant macrobenthic taxa and relationship with salinity in	
569	the CRE (Montagna and Palmer 2014).....	87
570	Table 18. Seasonal ranges for salinity zones in the CRE based on classifications	
571	provided by Bulger et al. 1993.....	89
572	Table 19. The number and percentages of dry season days for average daily salinity	
573	values at BR31 over a series of salinity class criteria (0 to 1, 1 to 2, 2 to	
574	3, 3 to 4, >4, and all dry season days) from WY1993 to WY2012.....	90
575	Table 20. Summary of <i>Vallisneria</i> salinity tolerances from a variety of studies in	
576	different locations.	93
577	Table 21. Descriptive statistics for salinity values at Fort Myers. Two equal subsets	
578	of data were extracted from the long-term (1992–2014) time series.	
579	Period 1 was from May 1, 1993 to October 31, 1999. Period 2 was from	
580	May 1, 2007 to October 31, 2013.	101
581	Table 22. Time periods and data used to calculate percent change in <i>Vallisneria</i>	
582	shoot densities relative to salinity criteria at Fort Myers. See text and	
583	Figure 44 for details and results.....	102
584	Table 23. List of equations to simulate dynamics of <i>Vallisneria americana</i> shoot	
585	biomass. See Buzzelli et al. (2012, 2014b) for mathematical details.	110
586	Table 24. List of <i>Vallisneria</i> model coefficients. See Buzzelli et al. (2012, 2014b)	
587	for mathematical details.....	111
588	Table 25. Results of sensitivity tests for the effects of physiological coefficients on	
589	predicted <i>Vallisneria</i> shoot biomass. The maximum rate of	
590	photosynthesis (P _m ; per day), the basal rate of respiration (k _R ; per day),	
591	the initial shoot biomass (C _{init} ; gdw m ⁻²), the shoot loss rate due to	
592	salinity (k _{Sloss} ; per day), and the basal grazing rate (k _{Gz} ; square meter	
593	per grams dry weight [m ² gdw ⁻¹]) were varied by +10% and +50% in	
594	independent model simulations. Simulations spanned 18 years (1997–	
595	2014 = 6,574 days). Provided are the coefficient values, the predicted	
596	biomass ranges (C _{shoot} ; gdw m ⁻²), the average and standard deviations	
597	(Avg ± SD) of predicted biomass (gdw m ⁻²), and the percent difference	
598	between the base model values (base) and each sensitivity test averaged	
599	over all simulation days (%Difference = ((observed –	
600	expected)/expected)*100).....	116
601	Table 26. Dry season (November–April) average and standard deviations (Avg ±	
602	SD) for model variables from WY1998–WY2014. Variables include	
603	freshwater inflow at S-79 (Q _{S79}) and the tidal basin (Q _{TB} ; cfs), salinity at	
604	<i>Vallisneria</i> monitoring site 1 (S _{val1}), temperature at Ft. Myers (T; °C),	
605	total light extinction coefficient (k _t ; m ⁻¹), the percentage of surface light	
606	at the bottom (%I ₀ ; unitless), and model <i>Vallisneria</i> shoot biomass (C _{shoot} ;	
607	gdw m ⁻²). The range of model <i>Vallisneria</i> shoot biomass for each dry	

608	season is also provided. See text for description of model input and	
609	response variables.	117
610	Table 27. Results from simulation model of <i>Vallisneria</i> . Shown are dry seasons with	
611	average daily salinities >10 at Monitoring Site 1 in the CRE from	
612	WY1999 to WY2012. All values based on daily salinity >10 including	
613	the total number of days in the dry season, the average and standard	
614	deviation (Avg \pm SD) of salinity for those days, the initial and final dates	
615	bracketing consecutive days where salinity >10, the initial shoot density,	
616	and the percentage of initial shoots lost during the consecutive days. The	
617	model biomass reaches a minimum of 0.1 gdw m ⁻² , which converts to	
618	~8 shoots m ⁻²	121
619	Table 28. Summary of salinity tolerances for different oyster life stages.....	124
620	Table 29. Seasonal ranges, averages (Avg), and standard deviations (SD) for salinity	
621	values recorded at Cape Coral and Shell Point from 2005 to 2014.	127
622	Table 30. The number (n) and percentages (%) of dry season days with measured	
623	average (Avg) daily salinity values (\pm standard deviation [SD]) at Cape	
624	Coral that were <10, 10 to 15, 15 to 20, 20 to 25, and > 25 from 2005 to	
625	2014. Included are descriptive statistics (range; Avg \pm SD) for salinity	
626	and freshwater inflow at S-79 (cfs) for each salinity class.	128
627	Table 31. The number (n) and percentages (%) of dry season days with measured	
628	average (Avg) daily salinity values (\pm standard deviation [SD]) at Shell	
629	Point that were <10, 10 to 15, 15 to 20, 20 to 25, and > 25 from 2005 to	
630	2014. Included are descriptive statistics (range; Avg \pm SD) for salinity	
631	and freshwater inflow at S-79 (cfs) for each salinity class. (Note: NA –	
632	not applicable.).....	128
633	Table 32. Annual and seasonal (wet versus dry) rainfall (inches) in Lee County and	
634	discharge (cfs) at the Franklin Lock and Dam and total discharge to the	
635	estuary (sum of S-79 and Tidal Basin). Values are average (standard	
636	deviation). POR was WY1981–WY2013.	136
637	Table 33. Mean annual landings in pounds per year (lbs/yr) of hard and soft shell	
638	blue crabs for WY1986–WY2013. Values are average (standard	
639	deviation).	137
640	Table 34. Correlation of unadjusted hydrologic variables with unadjusted estimates	
641	of CPUE. n=28 in all cases. Statistical significance: * p<0.10, ** p<0.05,	
642	and ***p<0.01.	138
643	Table 35. Correlations between hydrologic variables and CPUE after adjustment for	
644	long-term trend (de-trended) and autocorrelation (corrected) as	
645	appropriate. Included are correlations lagged by one year for dry	
646	(November–May) season Lee County rainfall, freshwater discharge	

647 through S-79, and total discharge calculated as the sum of S-79 and the
648 Tidal Basin. 140

649 **Table 36.** Estimates of the preceding water year’s dry season rainfall (Lee County)
650 that produce annual catches of hard shelled crabs that will return to the
651 long-term mean CPUE (1.26 lbs/trap) after one to three years of average
652 dry season rainfall (12.45 inches). Estimates were made using a
653 regression technique and a probabilistic Monte Carlo approach. Also
654 given are the dry season discharge at S-79 and total discharge (S-79 +
655 Tidal Basin) associated with the dry season rainfall in Lee County. 141

656 **Table 37.** Average dry season rainfall for potential significant harm and associated
657 return interval and probability of occurrences from Monte Carlo
658 simulations. 144

659

DRAFT

ACRONYMS AND ABBREVIATIONS

660		
661	° C	degrees Celsius
662	# m ⁻²	number per square meter
663	# m ⁻³	number per cubic meter
664	% I ₀	percentage of surface irradiance at the bottom (model parameter)
665	η	variable water level
666	μg L ⁻¹	micrograms per liter
667	μmoles m ⁻² s ⁻¹	micromoles per square meter per second
668	ac-ft	acre-feet
669	a _{CHL}	attenuation factor for chlorophyll <i>a</i> (model parameter)
670	a _{color}	constant for salinity-color relationship (model parameter)
671	AM2	amplitude at the water level tide (M ₂) determined for Fort Myers
672		(model parameter)
673	ANCOVA	analysis of covariance
674	ANOVA	analysis of variance
675	a _{NTU}	attenuation factor for turbidity (model parameter)
676	APRS	Adaptive Protocol Release Study
677	A _{saw}	area of sawfish habitat
678	b _{color}	constant for salinity-color relationship (model parameter)
679	C&SF Project	Central and Southern Florida Flood Control Project
680	CERP	Comprehensive Everglades Restoration Plan
681	cfs	cubic feet per second
682	CH3D	Curvilinear Hydrodynamic Three Dimensional Model
683	CHL	chlorophyll <i>a</i> concentrations
684	CHL _{max}	chlorophyll <i>a</i> maximum concentration
685	C _{init}	initial <i>Vallisneria</i> biomass values (model parameter)
686	C _{max}	maximum <i>Vallisneria</i> biomass (model parameter)
687	COA	center of abundance
688	CPUE	catch per unit effort
689	CRE	Caloosahatchee River Estuary
690	C _{shoot}	changes in aboveground biomass of <i>Vallisneria</i> (model parameter)
691	DBHYDRO	South Florida Water Management District's corporate
692		environmental database

693	DO	dissolved oxygen
694	FDEP	Florida Department of Environmental Protection
695	fS _{gross}	gross production (model parameter)
696	fS _{loss}	mortality (model parameter)
697	fT _{shoot}	photosynthesis-irradiance relationship (model parameter)
698	G	gross production of <i>Vallisneria</i> (model parameter)
699	gdw m ⁻²	grams dry weight per square meter
700	GPS	global positioning system
701	G _{shoot}	gross production of <i>Vallisneria</i> (model parameter)
702	Gz	grazing on <i>Vallisneria</i> (model parameter)
703	Gz _{shoot}	herbivorous grazing on <i>Vallisneria</i> (model parameter)
704	h	depth (model parameter)
705	I ₀	irradiance at the water surface (model parameter)
706	IDR	inter-decile range
707	I _k	half-saturation irradiance value (model parameter)
708	I _z	irradiance at the sediment (model parameter)
709	k _{color}	attenuation coefficient for color (model parameter)
710	kg	kilogram
711	kGz	basal grazing rate for <i>Vallisneria</i> (model parameter)
712	km	kilometer
713	kM	basal rate of mortality for <i>Vallisneria</i> (model parameter)
714	km ²	square kilometers
715	kR	basal rate of respiration for <i>Vallisneria</i> (model parameter)
716	kS _{loss}	salinity-specific loss rate model parameter)
717	k _t	total attenuation coefficient for submarine light (model parameter)
718	kT1	<i>Vallisneria</i> temperature constant for photosynthesis (model
719		parameter)
720	kT2	<i>Vallisneria</i> temperature constant for photosynthesis (model
721		parameter)
722	k _w	total attenuation coefficient for pure water (model parameter)
723	lbs/trap	pounds per trap
724	lbs/trap/inch	pounds per trap per inch
725	LORS2008	Lake Okeechobee Regulation Schedule 2008

726	LOSA	Lake Okeechobee Service Area
727	m	meter
728	M	shoot mortality of <i>Vallisneria</i> (model parameter)
729	m ⁻¹	per meter
730	m ²	square meter
731	m ⁻²	per square meter
732	M ₂	tidal water level
733	m ³	cubic meter
734	MDS	multi-dimensional scaling
735	MFL	minimum flows and levels
736	mg L ⁻¹	milligrams per liter
737	M _{shoot}	salinity-based mortality of <i>Vallisneria</i> (model parameter)
738	n	sample size
739	NEEPP	Northern Everglades and Estuaries Protection Program
740	NOAA	National Oceanic and Atmospheric Administration
741	NTU	turbidity (model parameter)
742	PhM ₂	phase angle of the water level tide (M ₂) determined for Fort Myers
743		(model parameter)
744	P _m	maximum rate of photosynthesis (model parameter)
745	POR	period of record
746	P _{photo}	photoperiod (model parameter)
747	Q _{S79}	Flow at S-79
748	r	root mean square correlation coefficient
749	R	respiration of <i>Vallisneria</i> (model parameter)
750	rkm	distance of a station from Shell Point
751	rkm _U	density-weighted center of abundance for each sampling event
752	RMS	root mean square
753	R _{shoot}	respiration for <i>Vallisneria</i> (model parameter)
754	S	salinity
755	S ₁₂	position of salinity of 12
756	S ₂₇	position of salinity of 27
757	SAV	submersed aquatic vegetation
758	SFWMD	South Florida Water Management District

759	S_{val1}	daily salinity at SAV monitoring Site 1 (model parameter)
760	T_{fx}	temperature effect (model parameter)
761	TM2	period of the water level tide (M2) determined for Fort Myers
762		(model parameter)
763	T_{opt}	optimum temperature (model parameter)
764	T_w	water temperature (model parameter)
765	USACE	United States Army Corps of Engineers
766	WY	Water Year
767	z	base level of the habitat (model parameter)

DRAFT

768

SCIENCE SUMMARY

769 Purpose of Study

770 The purpose of this study was to provide a comprehensive and quantitative assessment
771 of the effects of freshwater inflow on the hydrology and ecology of the Caloosahatchee
772 River Estuary (CRE) in the dry season (November to April). The dry season was chosen
773 for this study because these are the times when freshwater inflows are diminished and
774 negative responses from various ecological indicators are most likely to occur. It also
775 coincides with the times when the MFL criteria are most likely to be exceeded. The
776 objectives were (1) to compile and document information about freshwater inflows into
777 and salinity distributions within the CRE, and (2) to examine the responses of a suite of
778 ecological indicators to dry season freshwater inflows. This effort was conducted in support
779 of the 2017 update to the minimum flows and levels (MFL) (Sections 373.042 and
780 373.0421, Florida Statutes) for the Caloosahatchee River [Rule 40E-8.221(2), Florida
781 Administrative Code]. Specifically, this study explored new data collected since adoption
782 of the MFL, analyzed older data using updated statistical approaches, and applied recently
783 developed ecological models.

784 Freshwater discharge, tides and wind drive the estuarine salinity gradients, which
785 influence all ecological processes in the water column and sediments. Organisms ranging
786 in size and complexity from plankton to fish respond to fluctuations in inflow and salinity
787 over a range of time scales. This study relied on multiple research components to examine
788 inflow-salinity response patterns for phytoplankton, zooplankton, benthic communities,
789 submersed aquatic vegetation (SAV), oyster beds, blue crabs (*Callinectes sapidus*), and
790 sawfish (*Pristis pectinata*).

791 The Franklin Lock and Dam (S-79) located near Olga, Florida serves as the upstream
792 boundary for the CRE (**Figures 1A and 1B**). Freshwater inflow has been measured at this
793 location since its completion in 1966. Although a majority of the total freshwater inflow is
794 through the S-79 structure, there is ungauged input of fresh water from tributaries and
795 groundwater in the Tidal Basin downstream of the structure. Recent estimates of the Tidal
796 Basin's contribution have improved with data availability and advancements in modeling.
797 However, all analyses of indicator responses were conducted relative to measured inflow
798 at the S-79 water control structure. The contribution of the Tidal Basin was incorporated
799 into the final assessment of the magnitude of total inflows to the estuary (total inflows = S-
800 79 + Tidal Basin).

801 Background Information

802 Alterations of the South Florida Landscape and Caloosahatchee River 803 Estuary MFL Watershed

804 The CRE and the C-43 canal were connected to Lake Okeechobee through the
805 evolution of the Central and South Florida Flood Control Project (C&SF Project). The
806 C&SF Project is a complete system of canals, storage areas, and water control structures
807 spanning the area from Lake Okeechobee to both the east and west coasts, and from
808 Orlando south to the Everglades. It was designed and constructed during the 1950s and
809 1960s by the United States Army Corps of Engineers (USACE) to provide flood control

810 and improve navigation and recreation. Most of the water bodies within the C&SF Project
811 have specific regulation schedules that are federally mandated by USACE.

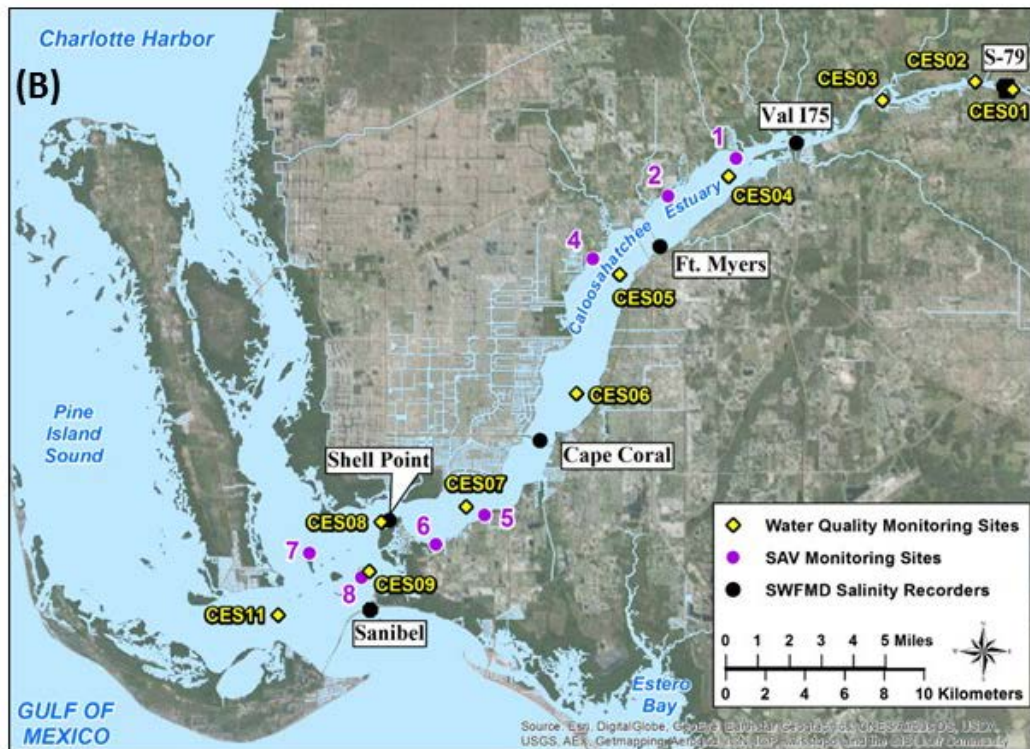
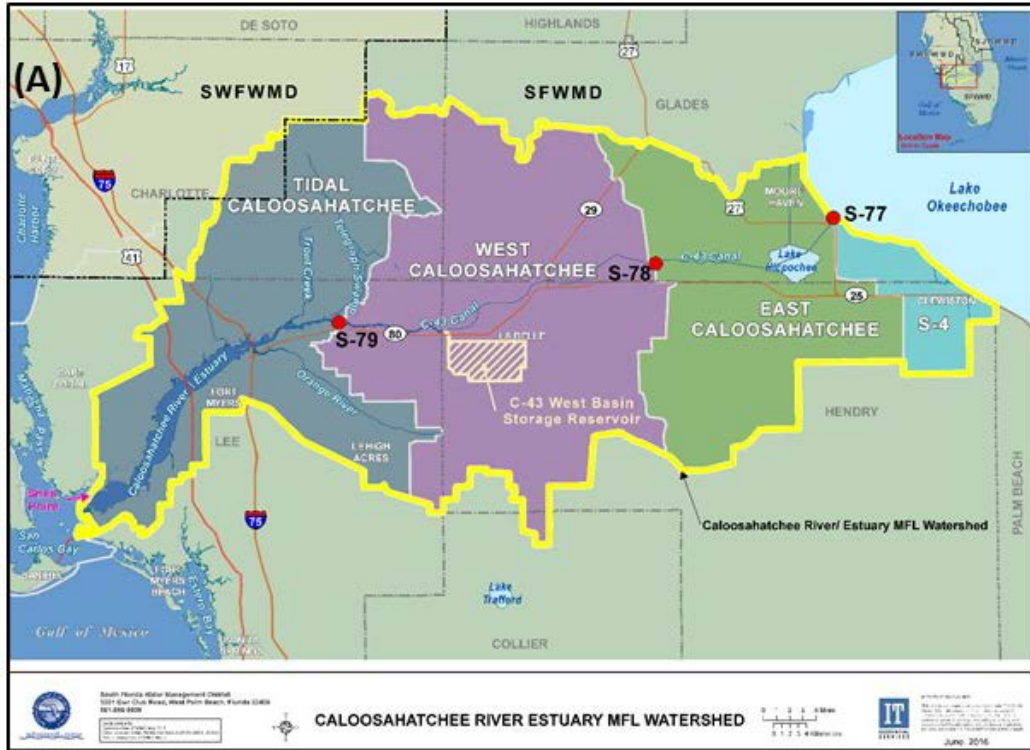
812 The South Florida Water Management District (SFWMD) is the local sponsor of the
813 C&SF Project. In its capacity as local sponsor, SFWMD operates and maintains the C&SF
814 Project. The operations require water to be moved out of certain water bodies when stages
815 are above the regulation schedule to provide flood protection.

816 As a result of the C&SF Project, the modern South Florida aquatic landscape is highly
817 engineered featuring ~3,380 kilometers (km) of canals, ~1,225 water control structures,
818 more than 70 pumping stations, heavily managed wetlands, densely populated coastal
819 watersheds, and highly impacted estuaries (Ogden et al. 2005, Obeysekera et al. 2011).
820 This includes the region between Lake Okeechobee and the Gulf of Mexico encompassing
821 the CRE Minimum Flows and Levels (MFL) Watershed and CRE (**Figure 1A**; SFWMD
822 2015). The portion of the watershed located upstream of the S-79 Structure is referred to
823 as the C-43 Watershed or C-43 Basin. The portion of the watershed located downstream of
824 the S-79 Structure is referred to as the Tidal Caloosahatchee sub-watershed or Tidal Basin.
825 Flows from the S-79 structure to the CRE are part of the C&SF Project. Water management
826 must balance resource needs by protecting the natural system while simultaneously
827 providing water supply, flood control and recreation opportunities. As a result of these
828 structural alterations, the availability of water that can be delivered to the CRE from the
829 regional system to meet these needs is constrained.

830 In addition to the alterations described above, a multitude of other structural and
831 physical alterations have occurred to the CRE MFL Watershed, historic Caloosahatchee
832 River (now the C-43 canal), and CRE. These alterations changed the historical hydrologic
833 conditions of the CRE MFL Watershed and downstream water bodies. A network of
834 secondary and tertiary canals in the CRE MFL Watershed is connected to the C-43 canal
835 and CRE. These canals provide navigational access or convey water for both drainage and
836 irrigation to accommodate agricultural, urban and other land uses in the watershed. Based
837 on the 2012 land use land cover data, the primary land use type within the CRE MFL
838 Watershed today is agricultural, which comprises 41.5%. Urban and built up land use
839 comprises 18% and wetlands comprise approximately 15.1%.

840 Historically, the Caloosahatchee River was sinuous as it originated near Lake Flirt ~2
841 miles (3.2 km) east of La Belle at Fort Thompson. Beginning in the 1880s, the river channel
842 was straightened, deepened, and connected to Lake Okeechobee. This resulted in a loss of
843 76 river bends and 8.2 miles (13.2 km) of river length (Antonini et al. 2002). Dredging
844 alterations continued and, by 1918, three combination lock and spillway structures had
845 been constructed at Moore Haven, Citrus Center, and Fort Thompson (USACE 1957,
846 Section 6.B.6). Flows within the historic Caloosahatchee River (now the C-43 canal) are
847 controlled through the operation of multiple water control structures (S-77, S-78, and S-
848 79) as these structures regulate downstream freshwater transport. The final lock and dam
849 structure (S-79) was completed in 1966 at Olga to assure freshwater supply and prevent
850 upstream saltwater intrusion. Discharges from Lake Okeechobee and the C-43 Canal
851 (between the S-77 and S-79 structures) are regulated by USACE.

852



853
854
855
856

Figure 1. A) The Caloosahatchee River Estuary MFL Watershed with its sub-watersheds and major water control structures and **B)** locations for the monitoring of salinity, water quality and oyster habitat for the CRE. The map includes SAV monitoring sites in the upper CRE.

857 Early descriptions of the CRE characterize it as barely navigable due to extensive
858 shoals and oyster bars (Sackett 1888). Some of the alterations that have occurred include
859 dredging a large navigational channel (Intracoastal Waterway) and secondary navigational
860 channels, removing oyster bars upstream of Shell Point for roadway construction,
861 removing the gulf bar at the mouth of the CRE, and the creation of two islands for
862 construction of the Sanibel Causeway across the mouth of San Carlos Bay. Seven
863 automobile bridges and one railroad bridge now connect the north and south shores of
864 the estuary.

865 There are other more recent significant changes that affect water availability including
866 the Lake Okeechobee Regulation Schedule that went into effect in 2008 (LORS2008),
867 adaptive protocols for Lake Okeechobee, and establishment of a restricted allocation area
868 for the Lake Okeechobee Service Area (LOSA). The restricted allocation area rule for
869 LOSA that was adopted in 2008 limits allocations from Lake Okeechobee and integrated
870 conveyance canal systems that are hydraulically connected to and receive surface water
871 from Lake Okeechobee (SFWMD 2012b). This includes the C-43 and C-44 canals. The
872 current regulation schedule (LORS2008) regulates the stage in Lake Okeechobee
873 approximately one foot lower than the previous Water Supply and Environment Regulation
874 Schedule. The adaptive protocols for Lake Okeechobee are intended to provide operational
875 flexibility to facilitate environmental benefits without impacting other lake uses. The
876 adaptive protocols were modified for use with the LORS2008 in the *Final Adaptive*
877 *Protocols for Lake Okeechobee Operations* (SFWMD 2010), which was finalized on
878 September 16, 2010.

879 The potential for removing the existing structural and physical alterations affecting the
880 C-43 canal and the CRE may not be economically or technically feasible. Much of the
881 existing development within the downstream water bodies is dependent upon the modern
882 functions of these alterations (e.g. flood protection, navigation, water supply and
883 transportation). For this reason, SFWMD has been strategically focused on making
884 improvements within the watershed rather than the downstream estuary. Programs and
885 projects to improve water regimes and ecosystem health, or both, include the Dispersed
886 Water Management Program; Caloosahatchee Storage/Treatment Project; Comprehensive
887 Everglades Restoration Plan (CERP), including the CERP Caloosahatchee River (C-43)
888 West Basin Storage Reservoir; Northern Everglades and Estuaries Protection Program
889 (NEEPP); and other smaller projects (SFWMD 2012a).

890 **Freshwater Inflow and Estuaries**

891 Small estuaries and embayments with sub-tropical climates and managed inflow are
892 particularly susceptible to reduced freshwater input on scales of days (event-scale) to years
893 (Schlacher et al. 2008, Buzzelli 2011, Azevedo et al. 2014). Inflows are managed because
894 many estuarine rivers have dams at the upstream boundary (Montagna et al. 2002a) similar
895 to the CRE. Low inflow increases hydrodynamic residence time as the upstream
896 encroachment of saltier water can establish a cascade of low inflow-related ecological
897 responses (Sheldon and Alber 2006, Wan et al. 2013).

898 Submarine light often increases throughout the estuary with the reduced input of
899 colored dissolved organic matter that freshwater inflow provides (Bowers and Brett 2008,
900 Chen et al. 2015). Reduced flushing coupled with enhanced light in the surface layer can
901 stimulate the rapid proliferation of phytoplankton in the upper estuary on scales of days to

902 weeks (Murrell et al. 2007, Lancelot and Muylaert 2011, Cloern et al. 2014). Zooplankton
903 and ichthyoplankton assemblages often shift upstream with their food resources
904 (phytoplankton) while remaining within favorable salinity zones (Flannery et al. 2002).
905 However, there is the possibility of habitat impingement and/or compression if upstream
906 movement of planktonic assemblages is bounded by a water control structure (Crowder
907 1986, Tolley et al. 2010). The overall biological productivity in estuaries is proportional to
908 freshwater inflow (Livingston et al. 1997, Gillson 2011).

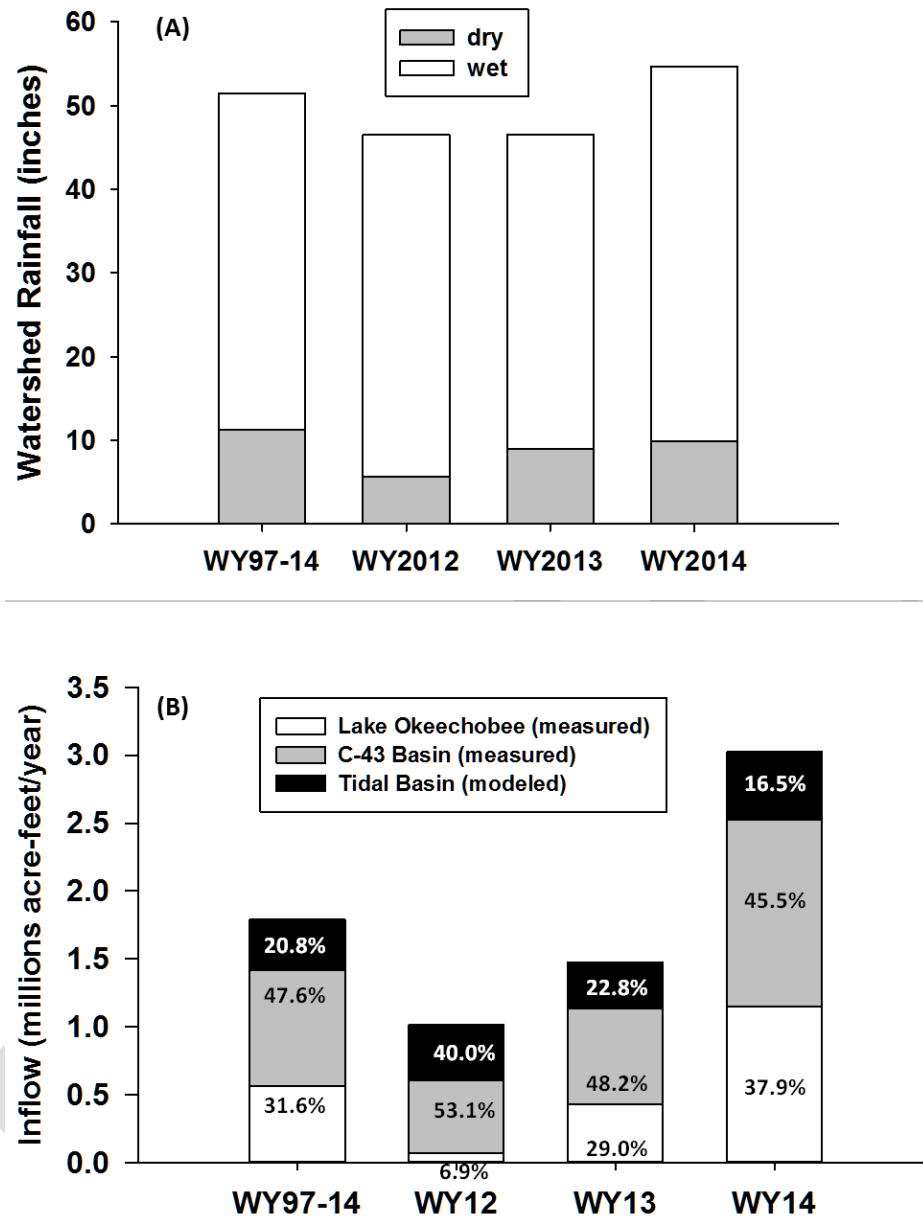
909 Saltwater encroachment can alter the composition and density of the macrobenthic
910 community upon which many estuarine fish and crustaceans are dependent (Palmer et al.
911 2011, Montagna et al. 2013). The freshwater macrophyte *Vallisneria americana* (tape
912 grass) provides essential habitat in the oligohaline portion of many estuaries. However, it
913 is very sensitive to increases in the frequency and duration of elevated salinity (Doering et
914 al. 2002, French and Moore 2003, Rozas and Minello 2006). Increased salinity also can
915 impact the survival of the eastern oyster (*Crassostrea virginica*) through the introduction
916 of marine parasites and predators (Livingston et al. 2000, Petes et al. 2012). The life
917 histories of many coastal fish populations rely on favorable salinity gradients as they utilize
918 estuaries as nursery and feeding areas (Whitfield et al. 2012, Stevens et al. 2013, Sheaves
919 et al. 2015). Finally, long-term reductions in freshwater inflow can be associated with
920 declining harvests of important fishery species (Wilber 1994, Gillson 2011).

921 Fluctuations in freshwater inflows over time scales ranging from weeks to years have
922 altered salinity regimes and impacted the ecology of the CRE (Chamberlain and Doering
923 1998, Barnes 2005). Changes in freshwater inflows and salinity have been shown to affect
924 the distribution and dynamics of many taxa and communities including phytoplankton and
925 zooplankton (Tolley et al. 2010, Radabaugh and Peebles 2012), SAV (Doering et al. 2001,
926 2002, Lauer et al. 2011), oysters and pathogens (La Peyre et al. 2003, Barnes et al. 2007,
927 Volety et al. 2009), fauna inhabiting oyster reefs (Tolley et al. 2005, Tolley et al. 2006),
928 and fishes (Collins et al. 2008, Heupel and Simpfendorfer 2008, Simpfendorfer et al. 2011,
929 Poulakis et al. 2013; Stevens et al. 2013).

930 **Freshwater Inflow and the Caloosahatchee River Estuary**

931 South Florida has a subtropical climate featuring dry (November–April) and wet (May–
932 October) seasons (Childers et al. 2006, Moses et al. 2013, SFWMD 2015). Event-scale
933 weather, extreme intra-annual seasonal variations in precipitation, and longer-term climatic
934 fluctuations (3–6 years) are incorporated into water management (Obeysekera et al. 2007).
935 In order to include both a wet and a dry season, a water year (WY) is defined as the time
936 from May 1 to April 30 of the subsequent year.

937 The long-term annual average (WY1997–WY2014) rainfall within the CRE MFL
938 Watershed was 51.5 inches with 21.9% in the dry season and 78.1% in the wet season
939 (**Figure 2A**). Freshwater discharge at the S-79 structure represents the combined
940 contribution of rainfall-driven runoff from the CRE MFL Watershed as well as releases
941 from Lake Okeechobee. The average annual total inflow (WY1997–WY2014) was 1.8 x
942 10⁶ acre-feet (ac-ft) (2,220 x 10⁶ cubic meters [m³]). Over this time period, the relative
943 contributions from Lake Okeechobee, the C-43 Watershed upstream of S-79, and the Tidal
944 Basin downstream of S-79 averaged 31.6%, 47.6% and 20.8%, respectively (**Figure 2B**).



945

946

947

948

Figure 2. A) Total rainfall to the Caloosahatchee River Estuary MFL Watershed by water year and season and **B)** stacked bar chart for the total freshwater inflow (millions of ac-ft per year). Included are the long-term averages from WY1997–WY2014, WY2012, WY2013 and WY2014.

949

950

951

952

953

954

955

The CRE is bounded upstream by the S-79 structure and downstream by San Carlos Bay at the mouth (**Figure 1A**). The surface area of the CRE is 67.6 square kilometers (km²) (6,764 hectares = 16,715 acres) with an average depth of 2.7 meters (Buzzelli et al. 2013b). Average flushing time ranges from 5 to 60 days (Wan et al. 2013, Buzzelli et al. 2013c). A variety of physical, chemical and biological variables are regularly monitored by SFWMD and other organizations (**Figure 1B**). Freshwater inflow has been measured at S-79 since 1966 and is reported as daily average cubic feet per second (cfs). Surface and bottom

956 salinity have been monitored at multiple locations (S-79, Val I75, Fort Myers, Cape Coral,
957 Shell Point, and Sanibel) since the 1990s and is reported as average daily values. Salinity
958 is derived from a dimensionless ratio and therefore has no units in reporting (Millero 2010).
959 The distribution and density of SAV have been determined at the upper stations (1, 2, and
960 4) since 1998 and the in the lower estuary (5, 6, 7, and 8) bi-monthly since 2004. Oyster
961 population attributes have been monitored seasonally at multiple locations in the lower
962 estuary near Shell Point since 2000.

963 The term “ecohydrology” was coined to describe the integrative management of coastal
964 basins based on the linkages among inflows, circulation, environmental conditions, habitat
965 attributes, and biological integrity (Peterson 2003, Wolanski et al. 2004). Essential to this
966 conceptualization are resource-based approaches to quantify minimum freshwater inflows
967 (Chamberlain and Doering 1998, Alber 2002). This approach seeks to identify the
968 historical inflow regime, the biological resources to be protected, and the environmental
969 conditions required to sustain them and determine inflow regimes needed to maintain the
970 desired conditions (Palmer et al. 2011). Choosing an indicator resource that responds to
971 freshwater inflow in a timeframe appropriate for management can be problematic (Dale
972 and Beyeler 2001, Alber 2002). In many cases, there are limited data for, or changes in,
973 the indicator resource that preclude extraction of useful information from the existing data.

974 The Caloosahatchee River MFL criteria were based on the salinity tolerance of
975 *Vallisneria americana* (Doering et al. 1999, Doering et al. 2001, Doering et al. 2002,
976 SFWMD 2003). *Vallisneria* was selected as an indicator because of its location in the
977 estuary, its sensitivity to enhanced salinity, and its important habitat functions (sediment
978 stabilization, nursery area, and food web support for invertebrate and vertebrate fauna). An
979 independent peer review in 2000 of the SFWMD MFL document (SFWMD 2000)
980 emphasized four problematic research areas: 1) lack of a hydrodynamic/salinity model;
981 2) lack of a numerical population model for *Vallisneria americana*; 3) no quantification of
982 the habitat value of *Vallisneria* beds; and 4) lack of documentation of the effects of MFL
983 flows on downstream estuarine biota (SFWMD 2003). A research program was initiated in
984 2001 to address some of these concerns and a review of the MFL criteria was conducted
985 (SFWMD 2003).

986 There has been much effort towards addressing the problematic areas identified in the
987 peer review. Salinity data collected at 15-minute intervals at multiple locations between S-
988 79 and Shell Point have been central to the development and calibration of a three-
989 dimensional hydrodynamic model (Qiu 2002, 2006, Qiu and Wan 2013, Wan et al. 2013).
990 Additionally, the long-term time series of salinity at Fort Myers (1992–present) and other
991 locations are essential to a wide range of water quality and ecological studies supporting
992 water management (SFWMD 2012a, SFWMD 2015). The Florida Department of
993 Environmental Protection (FDEP), SFWMD, and United States Geological Survey jointly
994 conducted a flow monitoring program from October 2008 to March 2013 to measure stage
995 and flow at several locations in the Tidal Basin of the CRE (Telegraph Creek, Orange
996 River, Popash Creek, Billy’s Creek, Hancock Creek, Marker 52, and Shell Point). Lee
997 County has monitored Whiskey Creek since April 1994. These data were collected to
998 support further development and calibration of the Tidal Basin Model (Wan and Konyha
999 in press).

1000 The distribution and abundance of *Vallisneria* have been documented since 1997
1001 (SFWMD 2015). Additionally, studies of the responses of *Vallisneria* to variable salinity

1002 and temperature (Doering et al. 2001, Doering et al. 2002, Bartleson et al. 2014) provided
 1003 an information base for both empirical assessments and the development of a simulation
 1004 model (this document). Site-specific assessment of *Vallisneria* habitat value has been
 1005 impeded by the greatly reduced distribution and density of *Vallisneria* since droughts in
 1006 2001 and 2007–2008. Oyster beds were identified as stationary indicators of salinity and
 1007 freshwater inflow in the lower estuary (Volety et al. 2009, Buzzelli et al. 2013a). Oyster
 1008 population attributes have been monitored in the lower CRE as part of CERP since 2005
 1009 (RECOVER 2014).

1010 The Conservancy of Southwest Florida filed a petition on September 3, 2010,
 1011 requesting immediate initiation of rulemaking to revise the Caloosahatchee River MFL
 1012 Rule. The SFWMD Governing Board denied this petition. However, SFWMD committed
 1013 to review and update the Caloosahatchee River MFL Rule after conducting the appropriate
 1014 scientific analyses based on the best available information.

1015 Methods

1016 Description of Component Studies

1017 This effort was composed of 11 component studies to evaluate the effects of reduced
 1018 freshwater inflow on the CRE in the dry season (**Table 1**). While the estimation of estuarine
 1019 inflow requirements using multiple indicators offers a system of checks and balances, the
 1020 quantitative assessment of the responses of a particular resource to variable levels of inflow
 1021 can be very difficult (Adams et al. 2002).

1022 This multi- and inter-disciplinary assessment of the relationships between inflow,
 1023 circulation, salinity, habitats and biological responses represents the best available
 1024 scientific knowledge of the CRE. While the respective component studies targeted specific
 1025 concerns regarding the physical and ecological characteristics, together they offer a holistic
 1026 understanding of the impacts of diminished freshwater inflow on estuarine ecology.

1027 **Table 1.** List of component studies and the basic description of research methods.
 1028 Studies 2 through 11 resulted in estimates of indicator inflow magnitudes.

	Study	Method
1	Hydrodynamics	Influence of alterations on hydrodynamics
2	Inflow versus Salinity	Monthly freshwater-salinity relationships at Fort Myers
3	Water Quality	Fine-scale relationships between water quality and inflow
4	Zooplankton	Inflow, zooplankton impingement, and habitat compression
5	Ichthyoplankton	Relationships between ichthyoplankton and inflow
6	Benthic Fauna	Macrofauna-salinity patterns relative to inflow
7	<i>Vallisneria</i> Data	Empirical relationships between <i>Vallisneria</i> , salinity, and inflow
8	<i>Vallisneria</i> Model	Model exploration of <i>Vallisneria</i> , salinity, light, and inflow
9	Oyster Habitat	Assess conditions for oyster survival in the lower CRE
10	Blue Crabs	Relationships between blue crab landings, rainfall, and inflow
11	Sawfish	Area and volume of sawfish habitat with variable dry season inflow

1029 **Importance of Uncertainty**

1030 Uncertainty is a fundamental property that can propagate through computational
1031 schemes and contribute to interpretative errors (Regan et al. 2002, Lehrter and Cebrian
1032 2010). It is important that the uncertainty associated with proposed environmental actions
1033 be evaluated, quantified and properly explained so that all stakeholders can better connect
1034 changes in ecological systems to effective scientific inquiry and improved management
1035 (Lamon et al. 1996, Halpern et al. 2006). Limits in data quantity, data quality and an
1036 understanding of dynamic processes increase uncertainty in predictive models (Reckhow
1037 1994). Although assessments of environmental risk using models can be inherently
1038 uncertain, the information contained in uncertainty can be applied to benefit environmental
1039 decision making (Reckhow 1994). For example, data gaps and missing information can be
1040 identified by evaluating uncertainty and variability (Ahn and James 2001).

1041 Unlike environmental management of rivers or lakes, salinity serves as the connection
1042 between biotic resources in the receiving basin and the rate of freshwater inflow in estuaries
1043 (Alber 2002). Spatial and temporal salinity variations are complicated by wind and
1044 atmospheric frontal passages, tidal exchange, and vertical mixing. Thus, it is very difficult
1045 to directly relate freshwater inflows, hydrodynamic processes, and biological responses in
1046 coastal basins. Difficulties arise from a combination of scalar mismatches, complexity and
1047 uncertainty, temporal and spatial lags, and an overall lack of data.

1048 This study included estimations of freshwater inflow associated with observed or
1049 simulated responses of selected estuarine indicators. These estimations were based on data,
1050 information, assumptions, discussions, and calculations, which carry varying amounts of
1051 inherent and systematic uncertainty. Despite inevitable uncertainty, this document provides
1052 the best available information through which to better understand the potential responses
1053 of selected indicators to salinity regimes within the CRE in the dry season.

1054 **Quantification of Indicator Freshwater Inflows in the Dry Season**

1055 This study applied elements of a resource-based approach to the quantification of
1056 freshwater inflows that might be limiting to the ecological functioning of the CRE in the
1057 dry season. The component studies emphasized the relationships between the indicators
1058 and inflows through the S-79 structure. The term “indicator inflow” or Q_I was defined as
1059 the S-79 inflow threshold below which there might be detrimental effects. There were 11
1060 different approaches to estimate Q_I (Study Components 2 through 11).

- 1061 1. Component Study 1 utilized hydrodynamic modeling as a tool to explore changes
1062 in circulation and salinity caused by structural alterations at the estuary scale but
1063 did not provide estimates of inflows relative to estuarine response variables.
- 1064 2. Component Study 2 used the relationship between average monthly inflow at S-79
1065 and average monthly salinity at Fort Myers to estimate the quantity of fresh water
1066 associated with a salinity value of 10 from WY1993 to WY2013
- 1067 3. Component Study 3 emphasized the relationship between low inflow and elevated
1068 chlorophyll *a* concentrations (CHL) to estimate Q_I when CHL in the upper CRE
1069 was greater than the impaired estuarine waters target of 11 micrograms per liter
1070 ($\mu\text{g L}^{-1}$) (FDEP 2009). This approach was applied independently to both empirical
1071 and model-derived CHL values.

- 1072 4. Component Study 4 estimated Q_I as the inflow threshold below which the upstream
1073 movement of the zooplankton community would be impinged against the S-
1074 79 structure.
- 1075 5. Component Study 5 utilized salinity tolerances of ichthyoplankton to estimate the
1076 habitat area with reduced inflow.
- 1077 6. Component Study 6 estimated Q_I from inflows on the days when the salinity in the
1078 upper CRE was greater than the tolerance range associated with the characteristic
1079 benthic macrofauna community.
- 1080 7. Component Study 7 extracted dry season days where the salinity at Fort Myers
1081 ranged from 9 to 10 from WY1993 to WY1999 when *Vallisneria* was abundant to
1082 calculate Q_I .
- 1083 8. Component Study 8 applied a *Vallisneria* simulation model to identify the salinity
1084 and inflows where *Vallisneria* experienced net mortality.
- 1085 9. Component Study 9 extracted days where the salinity at Cape Coral was 20–25
1086 from WY2005 to WY2014 concurrent with oyster monitoring to calculate Q_I .
- 1087 10. Component Study 10 examined the relationships between rainfall and Lee County
1088 blue crab catch data.
- 1089 11. Component Study 11 assessed the inflows that maximize the area of favorable
1090 habitat for the endangered sawfish in the dry season.

1091 Results

1092 Summaries of Component Studies

1093 ***Component 1: Three Dimensional Model Evaluation of Physical and Structural*** 1094 ***Alterations of the Caloosahatchee River and Estuary: Impact on Salt Transport***

1095 Hydrodynamic modeling of estuaries provides a platform to assess the effects of
1096 physical alterations on hydrodynamics, transport, and mixing. This study component
1097 utilized a three dimensional hydrodynamic model (Curvilinear Hydrodynamic Three
1098 Dimensional Model or CH3D) of the CRE to compare simulated salinities between the
1099 existing condition and the reversal of five historical physical alterations to the estuary.
1100 Alterations included (1) removal of the S-79 water control structure; (2) removal of the
1101 downstream causeway (Sanibel); (3) backfill of the oyster bar near the estuary mouth; (4)
1102 backfill of the navigation channel; and (5) the reestablishment of predevelopment
1103 bathymetry. Model results indicated that refilling the navigation channel had profound
1104 effects with a five-fold reduction in dry season salinity distributions. The reduced salt
1105 transport was more pronounced with the predevelopment bathymetry because the estuary
1106 was much shallower. Increased estuary depth and cross-sectional area significantly
1107 increase salt transport to the upper estuary. Increased salt transport can push biologically
1108 relevant isohalines further upstream depending upon freshwater inflow conditions.

1109 **Component 2: Analysis of the Relationship between Freshwater Inflow at S-79 and**
1110 **Salinity in the Caloosahatchee River Estuary 1993–2013**

1111 The upstream migration of salt with reduced freshwater inflow alters the composition
1112 and productivity of oligohaline habitats in estuaries. This process can be problematic in
1113 subtropical estuaries with regulated freshwater inflow such as the CRE in southwestern
1114 Florida. This study component examined relationships between average monthly inflow
1115 (Q) and mid-estuary salinity (S) from 1993 to 2013. An exponential decay equation was fit
1116 to the inflow-salinity (Q-S) relationship for each water year (May 1 to Apr 30). Annual
1117 equations were used to estimate the inflow rate associated with salinity = 10 at the Fort
1118 Myers monitoring station (Q_{calc}). Inflows varied both intra- and inter-annually. Q_{calc} ranged
1119 from 70 cfs to 773 cfs with an average of 445 ± 218 cfs. At the estuary and annual scales,
1120 the quantity of fresh water to support a particular salinity target varied greatly. This
1121 variance was related to the variations in freshwater inputs from both the C-43 Watershed
1122 located upstream of S-79 and the downstream tidal basin.

1123 **Component 3: Relationships between Freshwater Inflows and Water Quality**
1124 **Attributes during the Dry Season in the Caloosahatchee River Estuary**

1125 Decreased flushing with reduced inflow can lead to the deposition of phytoplankton
1126 biomass and bottom water hypoxia in estuaries. The highest CHL and lowest DO
1127 concentrations occur in the upper CRE under low inflows. This study component utilized
1128 event-scale water quality data, long-term monitoring of CHL, and simulation modeling of
1129 phytoplankton dynamics to evaluate low freshwater inflows that could contribute to water
1130 quality problems in the upper CRE. Although more research is needed, it is hypothesized
1131 that dry season inflows of less than approximately 500-600 cfs may promote bottom water
1132 hypoxia in the deeper channel of the upper CRE. Field and model results indicated that
1133 CHL concentrations greater than the water quality standard of $11 \mu\text{g L}^{-1}$ were associated
1134 with inflows of 469 ± 689 cfs and 269 ± 493 cfs, respectively. Low level inflows (<500
1135 cfs) need to be further studied to better quantify the discharge required to mitigate the
1136 potential for hypoxia in the upper CRE.

1137 **Component 4: Zooplankton Response to Freshwater Inflow in the Caloosahatchee**
1138 **River Estuary**

1139 Freshwater inflow to some estuaries, including the CRE, is regulated through control
1140 structures. Zooplankton assemblages provide an essential food web link whose position in
1141 the estuary fluctuates with inflow. Unfortunately, zooplankton habitat can be both
1142 impinged and compressed due to the presence of a water control structure as inflow is
1143 reduced in the dry season. This study assessed impingement and habitat compression for
1144 zooplankton under reduced inflow. Data were from a study of the CRE conducted by
1145 Florida Gulf Coast University from 2008 to 2010. Zooplankton samples were collected
1146 monthly at each sampling site at night during a flood tide. The centers of abundance (COA)
1147 for the 13 taxa investigated migrated downstream and upstream as freshwater inflow
1148 increased and decreased, respectively. Both habitat compression and impingement were
1149 potentially harmful for zooplankton assemblages in the estuary. Impingement was possible
1150 if inflow from the S-79 structure ranged and averaged 98–566 cfs and 412 ± 165 ,
1151 respectively. Almost all taxa investigated (except *Menidia*) experienced habitat
1152 compression if the COA was < 12 km downstream of S-79.

1153 **Component 5: Ichthyoplankton Response to Freshwater Inflow in the**
1154 **Caloosahatchee River Estuary**

1155 Ichthyoplankton communities are key components of food webs in the upper,
1156 oligohaline reaches of most estuaries. This study analyzed historical (1986-1989) data to
1157 evaluate effects of salinity and freshwater inflow on ichthyoplankton communities in the
1158 Caloosahatchee River and Estuary. Abundance of ichthyoplankton was greatest when 30-
1159 day inflows at S-79 averaged between 151 and 600 cfs. Juvenile fish appeared to prefer
1160 salinities <10 and their abundance was centered just downstream of Station 2 near Beautiful
1161 Island. Flows at S-79 associated with a salinity of 10 in this region averaged 237.5 ± 255.5
1162 cfs. Flows less than this could result in loss of favorable habitat.

1163 **Component 6: Summary and Interpretation of Macrobenthic Community**
1164 **Properties Relative to Salinity and Inflow in the Caloosahatchee River Estuary**

1165 The composition, distribution, and density of benthic invertebrate communities
1166 (macrofauna) can be used as indicators of salinity and inflow for estuaries. The goal of this
1167 study component was to explore the relationships between inflow, salinity, and benthic
1168 macrofauna in the CRE. Benthic samples were collected every 2 to 4 months at seven
1169 stations during two periods (February 1986–April 1989 and October 1994–December
1170 1995). The abundance, diversity, and composition of the macrofaunal community were
1171 determined relative to observed fluctuations in salinity. Four distinct zones emerged based
1172 on salinity ranges and the composition of the macrobenthic community. Conditions
1173 conducive to maintain the characteristic community observed during the sampling periods
1174 in the most upstream zone (salinity = 0 to 4, 0 to 7 km from S-79) occurred on 54% of dry
1175 season days from 1993 to 2012. The indicator inflows (Q_I) ranged from 0 to 3,720 cfs and
1176 averaged 501 ± 525 cfs for the days where salinity was 3 to 4 ($N = 181$).

1177 **Component 7: Relationships between Salinity and the Survival of *Vallisneria***
1178 ***americana* in the Caloosahatchee River Estuary**

1179 *Vallisneria americana* is sensitive to increased salinity in many estuaries, including the
1180 CRE. Much of the historical *Vallisneria* observed from 1993 to 1999 in the CRE has been
1181 lost since droughts in 2001 and 2007–2008. This study examined relationships between
1182 *Vallisneria* and salinity through change-point analysis, assessment of long-term patterns of
1183 abundance, and exploration of the effects of salinity exposure time. Change-point analysis
1184 revealed salinity thresholds of 4, 9, and 15. Dry season average daily salinity was ~5 and
1185 rarely exceeded 10 when *Vallisneria* was abundant from 1993 to 1999. Indicator inflows
1186 (Q_I) ranging and averaging 0 to 3,160 and 545 ± 774 , respectively, were associated with
1187 dry season salinity values of 9 to 10 (sample size [n] = 63) at Fort Myers from 1993 to
1188 1999. In contrast, *Vallisneria* was virtually absent from 2007 to 2013 as dry season average
1189 daily salinity exceeded 10. Negative changes in shoot density can be rapid as ~50 to 60%
1190 of the aboveground material was lost if salinity was >10 for 2 to 3 weeks. These results
1191 highlight the effects of both the magnitude and duration of environmental conditions that
1192 can inhibit *Vallisneria* survival in the CRE.

1193 **Component 8: Development and Application of a Simulation Model for *Vallisneria***
1194 ***americana* in the Caloosahatchee River Estuary**

1195 Monitoring of *Vallisneria* densities in the upper CRE from 1998 to 2007 was
1196 accompanied by mesocosm experiments to determine relationships between salinity and

1197 growth. This study built upon these efforts by developing a simulation model to examine
1198 the effects of temperature, salinity, and light on *Vallisneria* survival and biomass in the
1199 upper CRE from 1998 to 2014. The effects of salinity on *Vallisneria* mortality were
1200 explored through using an 8-year experimental model based on favorable conditions from
1201 1998 to 1999. Using the experimental model, the dry season salinity was systematically
1202 increased in 5% increments until the net annual biomass accumulation of *Vallisneria* was
1203 negative. A five-fold increase in grazing was required to stabilize model biomass under
1204 optimal conditions. A 55% salinity increase to 12 promoted shoot mortality in the
1205 experimental model. Annual inflow-salinity relationships for Fort Myers were used to
1206 estimate that dry season inflows ranging from 15.2 to 629.0 cfs and averaging 342 ± 180
1207 cfs were associated with a salinity of 12 at Fort Myers. Model results suggested that an
1208 estimated 85.4% and 86.7% of the shoots were lost in the dry seasons of 2001 and 2007,
1209 respectively.

1210 ***Component 9: Assessment of Dry Season Salinity and Freshwater Inflow Relevant***
1211 ***for Oyster Habitat in the Caloosahatchee River Estuary***

1212 Short- and long-term alteration of salinity distributions in estuaries with variable
1213 freshwater inflow affects the survival, abundance, and extent of oyster habitat. The
1214 objective of this study was to evaluate salinity conditions at two locations (Cape Coral and
1215 Shell Point) in the CRE. Salinity data from the 2006–2014 dry seasons (November–April)
1216 were categorized relative to oyster habitat criteria and related to freshwater inflow. Daily
1217 salinity was within the appropriate range for oysters (10–25) on 70.1% of the observations.
1218 Daily inflow ranged from 0 to 2,000 cfs and averaged 296 ± 410 cfs when salinity ranged
1219 from 20 to 25 at Cape Coral in the dry season. The influence of the marine parasite
1220 *Perkinsus marinus* (dermo) is limited due to the subtropical climate where temperature is
1221 low when salinity is high (dry season) and temperature is high when salinity is low (wet
1222 season). Overall salinity patterns were favorable for oyster survival at the upstream extent
1223 of oyster habitat in the CRE.

1224 ***Component 10: Ecohydrological Controls on Blue Crab Landings and Minimum***
1225 ***Freshwater Inflow to the Caloosahatchee River Estuary***

1226 A long-term record (28 years) was used for blue crab landings in the CRE to establish
1227 relationships between (1) changes in hydrology and changes in water resource function and
1228 (2) the magnitude of the functional loss and time to recover. Annual catch per unit effort
1229 (CPUE), computed from monthly landings of crabs and measures of fishing effort,
1230 represented the resource function. Annual landings expressed as both unadjusted and de-
1231 trended CPUE were found to be significantly correlated with hydrologic variables, rainfall
1232 and freshwater inflow, during the previous year's dry season. Increases in CPUE from one
1233 year to the next were also positively related to dry season rainfall in the first of the two
1234 years. Geometric mean functional regressions and Monte Carlo simulations were used to
1235 identify the dry season rainfall associated with losses of water resource function (CPUE)
1236 that required 1, 2, or 3 years of average dry season rainfall to recover. A spectral analysis
1237 indicated that time series of both dry season rainfall and blue crab catch had periodicities
1238 of 5.6 years. A Monte Carlo analysis revealed that the rainfall associated with two- and
1239 three-year recoveries had return intervals of 5.8 and 8.2 years, respectively.

1240 **Component 11: Relationships between Freshwater Inflow, Salinity and Potential**
1241 **Habitat for Sawfish (*Pristis pectinata*) in the Caloosahatchee River Estuary**

1242 The smalltooth sawfish is an endangered species that historically ranged from Texas to
1243 North Carolina. The distribution and abundance of sawfish have declined due to over-
1244 fishing and habitat loss. Presently, the CRE is an important sawfish nursery. Juvenile
1245 sawfish habitat can be characterized as nearshore environments <1 meter in depth, where
1246 salinities range from 12 to 27. This study quantified sawfish habitat with variable inflow
1247 to the CRE in the dry season using a combination of bathymetric analyses and
1248 hydrodynamic modeling. Inflows of 150–300 cfs positioned the 12 and 27 salinities in the
1249 shallowest part of the estuary (10 to 30 km downstream). Specifically, the area of sawfish
1250 habitat was greatest (5.7 km²) when inflow through the S-79 structure was 270 cfs in the
1251 dry season. Under reduced inflow, the habitat migrated into the channel above Beautiful
1252 Island where it was compressed against S-79. Higher inflows pushed S₂₇ out of the estuary.

1253 **Quantification of Indicator Freshwater Inflows in the Dry Season**

1254 While there were 10 separate component studies that generated values for Q_I , the water
1255 quality component provided both empirically-based and modeled estimates using the same
1256 selection criteria (**Table 2** and **Figure 3**). Among 11 different calculations, the estimated
1257 magnitude of Q_I was least from the phytoplankton model (269 ± 493 cfs), the sawfish
1258 habitat assessment (270 cfs), analysis of ichthyoplankton data (237 ± 255 cfs), and
1259 evaluation of conditions relative to oyster tolerances (296 ± 410 cfs). While an inflow rate
1260 of 545 ± 774 cfs was estimated to inhibit *Vallisneria* survival, the modeling exercise
1261 predicted that inflow rates less than 342 ± 180 cfs could lead to *Vallisneria* mortality. There
1262 was a wide range of sample sizes (n) used to estimate Q_I among the calculations (2 to 422).
1263 For example, 16 annual values were used in Component 2 (S-79 inflow versus salinity at
1264 Fort Myers) compared to 181 daily values derived in Component 6 (benthic fauna). Four
1265 of the approaches used the salinity requirements of an indicator resource as a guide to select
1266 corresponding dry season inflows (benthic fauna, *Vallisneria* data, oysters, and sawfish).
1267 Each of these four estimates generally resulted in a wide range of possible inflows and
1268 therefore, large standard deviations that were greater than the average values. On the other
1269 hand, estimates among the customized approaches from the other five component studies
1270 (S-79 inflow versus salinity, zooplankton, ichthyoplankton, *Vallisneria* model and blue
1271 crabs) had narrower ranges and less variance (**Table 2**). For example, Q_I estimated for
1272 zooplankton and ichthyoplankton assemblages averaged 412 ± 165 cfs and 237 ± 255 cfs,
1273 respectively. As a result of the method, a single value for Q_I was estimated from assessment
1274 of sawfish habitat (270 cfs).

1275

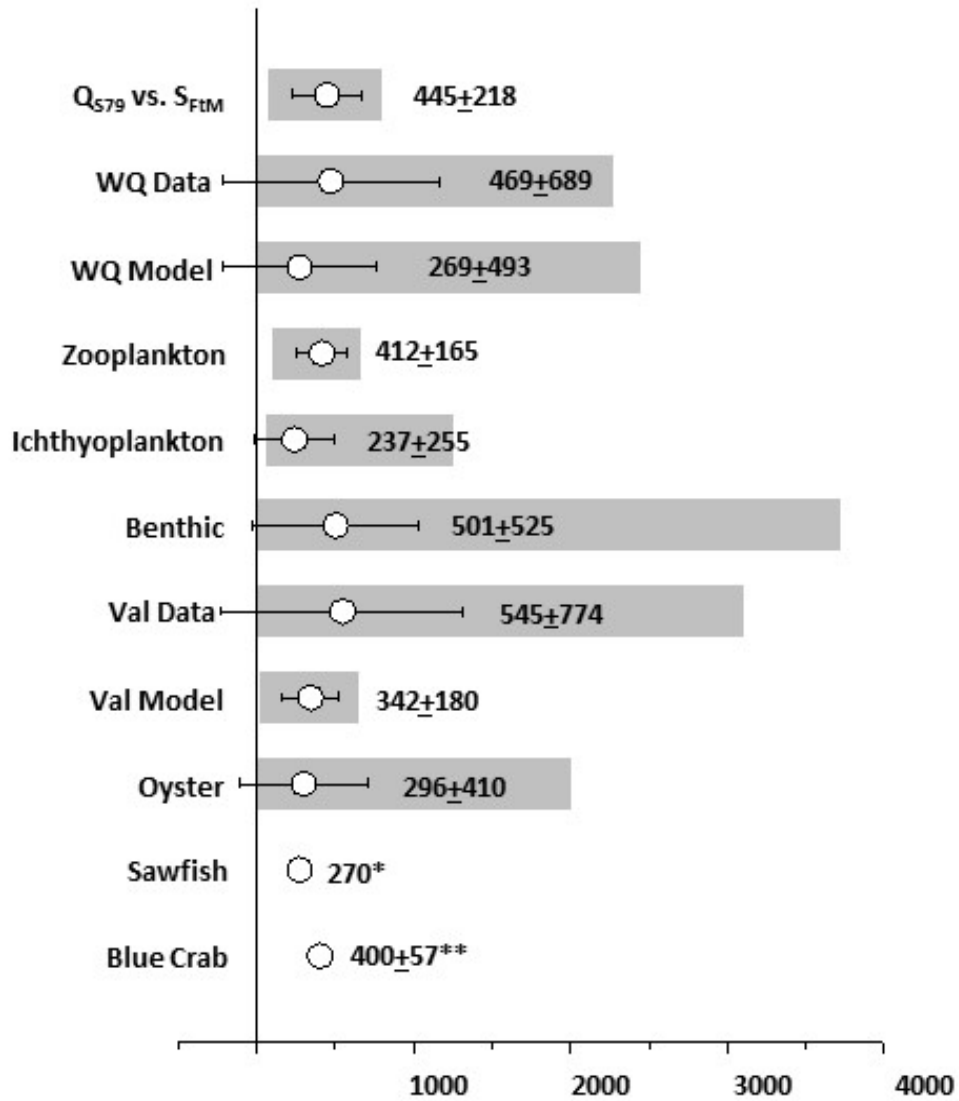
1276
1277
1278**Table 2.** Summary of component studies, the method used to estimate the indicator inflow (Q_I), and the range and average + standard deviation (Avg + SD) values for Q_I (cfs). The median value for Q_I over all estimates is provided (362 cfs).

Component	Method	Q _I (cfs)	
		Range	Avg + SD
1 Hydrodynamics	Hydrodynamic model used to evaluate long-term structural modifications to the CRE	Not applicable (NA)	NA
2 Inflow versus Salinity	Based on calculated inflow at S-79 associated with S-10 at Fort Myers from monthly average long-term data (WY1993–WY2013; n = 16)	70–720	445 ± 218
3 Water Quality - Data	Estimated using monthly average dry season CHL > 11 µg L ⁻¹ observed at CES03 linked to daily freshwater inflow (n = 8).	0–2,270	469 ± 689
Water Quality – Model	Estimated using daily average dry season CHL > 11 µg L ⁻¹ predicted in the upper CRE linked to daily freshwater inflow (n = 58).	0–2,450	269 ± 493
4 Zooplankton	Estimated using monthly zooplankton center of abundance (2008–2010) and lagged inflows with conditional regression (n = 7).	98–566	412 ± 165
5 Ichthyoplankton	Estimated using monthly ichthyoplankton center of abundance (2008–2010) and 30-day average salinity at Fort Myers (n = 11).	62–1191	237 ± 255
6 Benthic Fauna	Benthic fauna data used to establish optimal salinity in the upper reaches of the CRE (optimum salinity = 3–4). Long-term (WY1993–WY2012) inflow at S-79 and salinity at BR31 were used to calculate inflow on dry seasons days meeting optimal salinity criteria (n = 181).	0–3,720	501 ± 525
7 <i>Vallisneria</i> Data	Estimated using maximum salinity tolerance (salinity = 9–10) and dry season Fort Myers salinity data from period when <i>Vallisneria</i> was abundant (WY1993–WY1999; n = 63).	0–3,160	545 ± 774
8 <i>Vallisneria</i> Model	Simulation series where dry season daily salinity was proportionally increased until <i>Vallisneria</i> biomass stabilized in optimized 8 year-model version. Estimated inflows from dry season days in 1998–1999 where salinity at Val Site 1 ranged from 6.3 to 6.5 (n = 32).	0–526	342 ± 180
9 Oyster Habitat	Estimated from maximum salinity tolerance (salinity = 20–25) and dry season daily salinity at Cape Coral from WY2005 to WY2014 (n = 422).	0–2,000	296 ± 410
10 Blue Crabs	Estimated using rainfall/discharge associated with significant harm to Lee County blue crab fishery from WY1981 to WY2013 (n = 2).		400 ± 57 ^a
11 Sawfish	Estimated using hydrodynamic model to quantify relationship between the area that was <1 meter and 12–27 salinity and inflow.		270 ^b

1279
1280
1281

a. Average from two estimates.

b. Only one value estimated for sawfish.



1282

1283

1284

1285

1286

1287

1288

Figure 3. Graphical results showing the range (bar) and average + standard deviation (point + error bar and text) of the estimated indicator inflows (QI) for each of the component studies.

See **Table 2** and text for calculation details related to each estimate.

*Only one value was estimated for sawfish.

**Average from two estimates.

1289 Discussion

1290 The purpose of this study was to provide a comprehensive and quantitative assessment
1291 of the effects of freshwater inflow during the dry season on the hydrology and ecology of
1292 the CRE in the dry season (November–April). It is unique in its scope to incorporate
1293 multiple indicators along the length of the estuary that respond to fluctuations in discharge
1294 or salinity on time scales ranging from days (water quality) to decades (blue crab
1295 catch data).

1296 There were three important findings from this study:

- 1297 1. The magnitude of minimum indicator inflows (Q_I) from the S-79
1298 structure ranged from 237 cfs to 545 cfs among the 11 estimates.
- 1299 2. Seasonally averaged S-79 inflows less than the Q_I for each indicator
1300 could result in phytoplankton blooms in the upper CRE (<10 km from S-
1301 79), compress the water column habitat for zooplankton and
1302 ichthyoplankton against the structure, alter the composition of the
1303 macrobenthic community in the upper estuary, prevent the survival of
1304 *Vallisneria*, shrink the available habitat for the endangered sawfish, and
1305 lead to reduced harvest of blue crabs the following year.
- 1306 3. Flow through S-79 accounts for 82% of the total inflow. The Tidal Basin
1307 inflows account for the remaining 18%. Assuming a median Q_I at S-79
1308 of 400 cfs, the Tidal Basin flows are estimated at 88 cfs for a total inflow
1309 of 488 cfs.

1310 Increased salinity through combinations of seawater encroachment and reduced
1311 freshwater input influences species composition, physiological processes and trophic
1312 dynamics (Gonzalez-Ortegon and Drake 2012). For example, long-term reductions in
1313 discharge to Apalachicola Bay in the northern Gulf of Mexico altered the food web leading
1314 to decreased biological productivity over time (Livingston et al. 1997). Therefore, it is
1315 important to describe the freshwater dry season inflows necessary to establish estuarine
1316 salinity gradients in both dynamic (water column) and static (benthic) habitats (Wolanski
1317 et al. 2004, Palmer et al. 2011).

1318 Salinity varies over many time scales through complex hydrodynamic processes that
1319 integrate rainfall, surface inflows, submarine groundwater discharge, wind events and tidal
1320 exchanges (Zheng and Weisberg 2004). Thus, simple correlations between inflow and
1321 salinity may be influenced by ungauged freshwater inputs. The diffuse inputs through
1322 submarine groundwater discharge is particularly difficult to quantify and model (Langevin
1323 2003, Burnett et al. 2006). Recent efforts to measure and model the contribution of the
1324 Tidal Basin to total freshwater inflow to the CRE provided an estimate of ~18% over all
1325 dry seasons from 1966 to 2014 (Wan and Konyha in press; this study). The relative
1326 contribution of the Tidal Basin ranged from 5 to 90% with values <10% in very wet dry
1327 seasons (1995, 2005, and 2006) and values >70% in the driest times (1982, 1990, 2001,
1328 and 2008). This potentially important source of fresh water must be incorporated into
1329 hydrodynamic models to account for changes in salinity that affects estuarine processes.

1330 The balance between downstream transport of fresh water and the upstream
1331 encroachment of salinity creates gradients that influence all biogeochemical processes and
1332 patterns. The gradient can be represented by lines of equal salinity (e.g. isohalines) whose
1333 positions fluctuate up and down the estuary with freshwater inflow(s), tidal cycles and
1334 meteorological phenomena (e.g. fronts, winds, and storms). Particular isohalines provide
1335 useful indications of desirable (or undesirable) salinity conditions for sentinel organisms
1336 or communities (Jassby et al. 1995). For example, low salinity conditions indicative of a
1337 functional oligohaline benthic community served as the most upstream biological
1338 indicator. Salinity at this upstream location is extremely sensitive to fine scale changes in
1339 freshwater inflow. This sensitivity combined with the complexity and dynamism of
1340 macrobenthic assemblages accounted for the variability of the estimated Q_1 (501 ± 525
1341 cfs)—a range associated with salinity zones for characteristic macrobenthic communities
1342 in the dry season (Palmer et al. 2015).

1343 Estimated mean daily dry season inflows of 300 to 550 cfs were associated with
1344 suitable dynamic and stationary habitats (water column and *Vallisneria*, respectively)
1345 located in the upper estuary around Beautiful Island (~10–15 km from S-79). Dry season
1346 inflows within this range should serve to maintain the area of maximum phytoplankton
1347 production and biomass from 9 to 16 km downstream. Maintaining the area of maximum
1348 CHL ≥ 12 km downstream should diminish the potential for the accumulation of phyto-
1349 detritus and hypoxia in the upstream bottom water. Overall, the relationships between dry
1350 season inflow (<500 cfs), the magnitude and position of the CHL maximum concentrations,
1351 and bottom water hypoxia in the upper CRE are complex and poorly understood.

1352 *Vallisneria* was historically observed from 1993 to 1999 from Beautiful Island to Fort
1353 Myers (Hoffaker 1994, Bortone and Turpin 2000). The acute sensitivity of this organism
1354 to increased salinity makes it an excellent candidate for the resource-based approach of
1355 prescribing freshwater inflows (Chamberlain and Doering 1998, Doering et al. 2002). Dry
1356 season freshwater inflows of 545 ± 774 cfs from 1993 to 1999 promoted the maximum
1357 tolerable salinity (9 to 10) for the survival of *Vallisneria*. Conversely, the *Vallisneria*
1358 habitat disappeared as the average salinity at Fort Myers exceeded 10 from 2007 to 2013.
1359 *Vallisneria* habitat in the CRE has not recovered from drought-induced stress in 2001 and
1360 2007–2008 when salinity was >10 for 4 to 5 months. Loss of mature shoots greatly inhibits
1361 the potential for habitat reestablishment. There were signs of recovery on a scale of 3 to 6
1362 years as salinity declined from 2003 to 2006. However, increased salinity in the upper CRE
1363 from 2007 to 2009 and again in 2012 severely limited the potential for *Vallisneria* survival.

1364 There were three different indicator inflow estimates from analyses centered near Fort
1365 Myers (~20 km downstream of S-79). Fort Myers represents a location in the middle of the
1366 CRE just downstream of the *Vallisneria* beds where variations in basinwide total
1367 freshwater inflow are the main drivers for salinity (Wan et al. 2013, SFWMD 2015). This
1368 study estimated that S-79 inflows averaging 445 ± 218 cfs were related to a salinity of 10
1369 at this location. While a coarse-scale assessment, there are wide variations in the inflow
1370 from S-79 that accounts for a target salinity at Fort Myers (e.g. 10). For example, more
1371 inflow is required from S-79 to maintain the magnitude and position of indicator isohalines
1372 when Tidal Basin inputs are diminished due to extended periods of drought.

1373 Inflows from S-79 ranging from ~225 to 425 cfs maintain zooplankton and
1374 ichthyoplankton assemblages in downstream locations (~10–20 km and 10–30 km,
1375 respectively). Peak zooplankton abundance is often located downstream of the maximum
1376 CHL but can migrate far upstream under severely reduced inflow. It is under these
1377 circumstances the water column biota could experience habitat impingement and
1378 compression against S-79. As with water quality, there should be further study of the
1379 effects of low inflow on planktonic dynamics in the upper estuary.

1380 Oyster habitat located from Cape Coral to the mouth of the CRE served as the most
1381 seaward indicator of freshwater inflows. While oysters are excellent indicators to detect
1382 changes in and responses to environmental conditions, salinity in the lower estuary is
1383 highly influenced by oceanic processes. Assessment of the time series of inflows based on
1384 oyster salinity criteria (salinity of 20–25) resulted in reasonable but variable estimates of
1385 Q_1 (296 ± 409 cfs). The relatively high variability was because a wide salinity range was
1386 applied (20–25) at a downstream location (Cape Coral ~30 km from S-79).

1387 Estimates of the indicator inflows for the two mobile fauna species (blue crabs and
1388 sawfish) resulted from widely different approaches. Salinity gradients must be adequate
1389 for these two populations to most effectively utilize the estuary as a nursery (Wilbur 1994,
1390 Poulakis et al., 2013). The blue crab CPUE being proportional to freshwater inputs in the
1391 previous dry season demonstrates both the connectivity and lags between rainfall, inflows,
1392 salinity, and biotic responses. At the seasonal time scale, dry season mean monthly inflows
1393 of ~270 cfs would position the 12 to 27 salinity range ~10 to 30 km downstream of S-79,
1394 thus maximizing the potential sawfish habitat area. Dry season mean monthly inflows <270
1395 cfs could confine the sawfish habitat to the deeper, upper CRE where there is much less
1396 shoal area and lead to habitat compression against the structure. Upstream migration into
1397 a bathymetrically compressed habitat potentially places juvenile sawfish in closer
1398 proximity to larger predators such as bull sharks (*Carcharhinus leucas*) (Poulakis et al.
1399 2011).

1400

COMPONENT STUDIES

1401 **Component Study 1: Three-Dimensional Model Evaluation of** 1402 **Physical and Structural Alterations of the Caloosahatchee River** 1403 **and Estuary: Impact on Salt Transport**

1404 *Detong Sun and Yongshan Wan*

1405 **Abstract**

1406 Hydrodynamic modeling of estuaries provides a platform to assess the effects of
1407 physical alterations on hydrodynamics, transport, and mixing. This study component
1408 utilized a three dimensional hydrodynamic model (CH3D) of the CRE to compare
1409 simulated salinities between the existing condition and the reversal of five historical
1410 physical alterations to the estuary. Alterations included: (1) removal of the S-79 water
1411 control structure; (2) removal of the downstream causeway (Sanibel); (3) backfill of the
1412 oyster bar near the estuary mouth; (4) backfill of the navigation channel; and (5) the
1413 reestablishment of predevelopment bathymetry. Model results indicated that refilling the
1414 navigation channel had profound effects with a five-fold reduction in dry season salinity
1415 distributions. The reduced salt transport was more pronounced with the predevelopment
1416 bathymetry because the estuary was much shallower. Increased estuary depth and cross-
1417 sectional area significantly enhance salt transport to the upper estuary. Increased salt
1418 transport can push biologically relevant isohalines further upstream depending upon
1419 freshwater inflow conditions.

1420 **Introduction**

1421 Hydrodynamic processes integrate freshwater inputs, wind events, and tidal exchanges
1422 to establish salinity conditions and modulate biodiversity and biological productivity.
1423 Estuaries are very sensitive to anthropogenic changes including urbanization, physical
1424 alterations of the estuarine systems, nutrient enrichment, and climate change (Alber 2002).
1425 Physical alterations such as dredging and dams change natural inflows, impact
1426 hydrodynamics and mixing with the coastal ocean, and dramatically affect salinity and
1427 water quality gradients in the estuary (Day et.al. 1989). Anthropogenic changes to tributary
1428 rivers can have pronounced influence on both the quality and quantity of freshwater inputs
1429 to estuaries. Additionally, deep navigational channels can alter circulation, increase the
1430 upstream encroachment of saltwater, and promote hypoxia and anoxia.

1431 The impacts of physical alterations on estuarine systems are noted worldwide. The
1432 Wadden Sea in the Netherlands and the Mississippi Delta in the United States serve as two
1433 examples of how physical alterations have changed coastal systems. In the Wadden Sea,
1434 coastal land reclamation was designed to protect natural resources while allowing for urban
1435 and agricultural development (Saundry and Cleveland 2011). In the Mississippi Delta,
1436 changes following the construction of dikes that cut the sources of riverine sediment, and
1437 dredging of canals led to significant hydrologic changes (Deegan et al. 1984, Barras et al.
1438 2004, Day et al. 2005). In both cases, large areas of coastal ecosystem have been altered or
1439 destroyed.

1440 Such changes are also evident in South Florida where river channels were dredged and
1441 widened for navigational purposes and water control structures were constructed near the
1442 heads of the estuaries (Kimes et al. 1999, Antonini et al. 2002, Ogden et al. 2005). The
1443 modern landscape is highly engineered featuring ~3,380 km of canals, ~1,225 water control
1444 structures, more than 70 pumping stations, heavily managed wetlands, densely populated
1445 coastal watersheds, and highly impacted estuaries (Ogden et al. 2005; Obeysekera et al.
1446 2011). These structural alterations have dramatically changed the watershed hydrological
1447 conditions as well as the geomorphology of the rivers and estuaries. In addition,
1448 agricultural and municipal demands for fresh water have increased. All these modifications
1449 have altered freshwater discharges to the estuaries (SFWMD 2012).

1450 Physical alterations at the landscape scale may have possibly irreversible impacts on
1451 estuarine ecosystems (Dyer and Orth 1994). Quantitative evaluation of these alterations
1452 remains a difficult task. Previous estuarine studies used hydrodynamic models to
1453 investigate saltwater intrusion in dredged navigational channels. Liu et al. (2001) utilized
1454 a vertical (laterally integrated) two-dimensional numerical model to study the
1455 hydrodynamic characteristics and extended saltwater intrusion in the Tanshui River
1456 estuarine system (Taiwan). The UnTRIM San Francisco Bay-Delta model, an unstructured
1457 grid hydrodynamic model, was used to study saltwater intrusion associated with deepening
1458 the Sacramento Deep Water Ship Channel (MacWilliams et al. 2009). In Louisiana, a semi-
1459 implicit version of Estuary and Coastal Model was used to study saltwater intrusion in
1460 navigation channels in Lake Pontchartrain (Georgiou 1999). In Florida, the Environmental
1461 Fluid Dynamics Code hydrodynamic model of the St. John's River was used to study the
1462 impact from dredging Jacksonville Harbor (USACE 2008). A more recent study applied
1463 the Finite Volume Coastal Ocean Model to explore the effects of changes to the
1464 navigational channel on circulation in Tampa Bay (Zhu et al. 2015).

1465 The CRE has a watershed characterized by extensive agriculture and urbanization, is
1466 influenced by both unregulated and regulated freshwater inflow, and contains valuable
1467 biological resources (Chamberlain and Doering 1998a, Doering et al. 2006, SFWMD
1468 2012). Through climatic variations, landscape modification, flood protection, and managed
1469 operations, the CRE can experience reduced freshwater inflow during the dry season. In
1470 many estuaries reduced freshwater inflow over time can result in the landward
1471 encroachment of salinity (Cloern and Jassby 2012). In the case of the CRE, upstream
1472 saltwater intrusion can reduce the extent of vegetated freshwater habitat (i.e., *Vallisneria*
1473 *americana*), impact community composition in the water column and benthos, and
1474 compress the oligohaline area of the estuary that is essential to a variety of faunal
1475 populations (Doering et al. 2002, Simpfendorfer et al. 2011, Stevens et al. 2013).

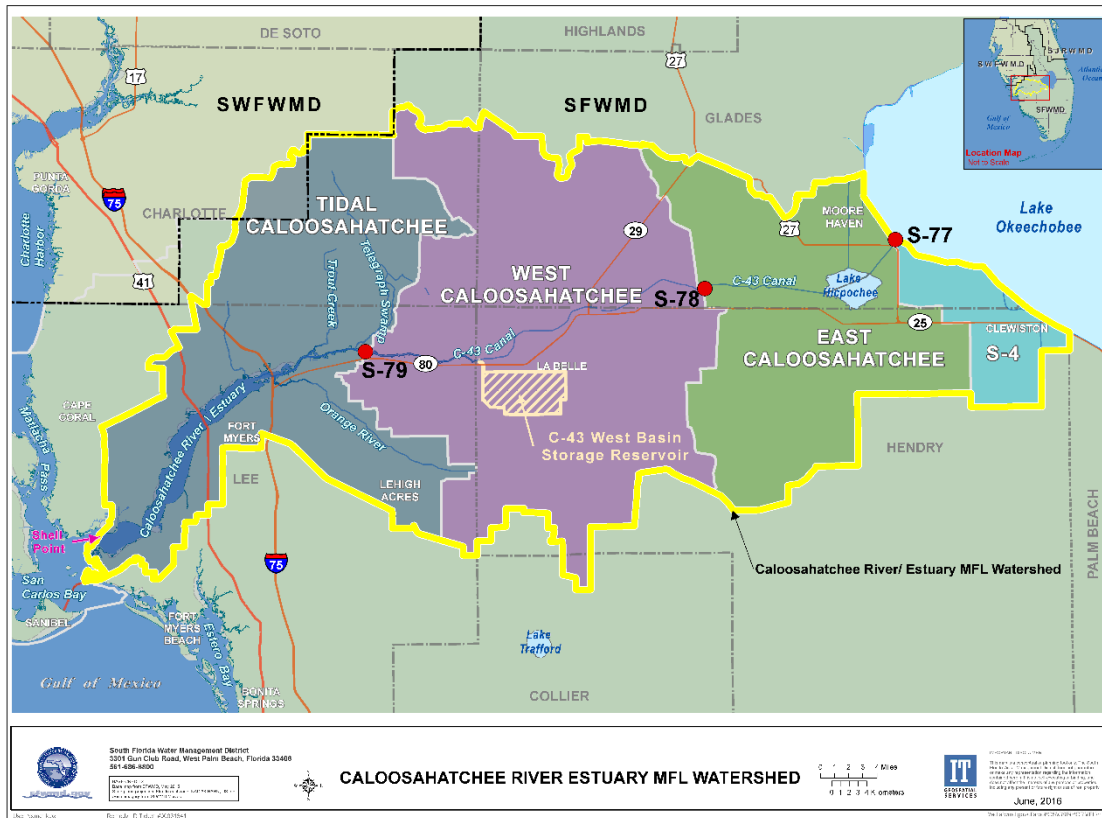
1476 The objective of this study was to use a hydrodynamic model to evaluate the effects of
1477 physical alterations on salinity distribution in the CRE. CH3D was applied to the CRE.
1478 This study intended to quantify and rank the effects of different physical and structural
1479 alterations over the past century on modern day estuarine salinity patterns.

1480 **Methods**

1481 **Study Site**

1482 The Caloosahatchee River and Estuary are located in Southwest Florida (**Figure 4**).
1483 The modern day C-43 Canal runs 67 km from Lake Okeechobee to the Franklin Lock and

1484 Dam (S-79 structure), which marks the upstream boundary of the estuary that extends 42
 1485 km downstream to Shell Point. The system has been modified to provide for navigation,
 1486 water supply, salinity control, and flood protection on both a local and regional scale
 1487 (Chamberlain and Doering 1998a, Doering et al. 2006). The CRE is a funnel-shaped
 1488 estuary whose width ranges from ~0.2 km in the upper portion to ~2.5 km near the mouth.
 1489 The total surface area of the estuary is about 65 km² (Buzzelli et al. 2013b). The narrow
 1490 section between the S-79 structure and Beautiful Island (~15 km downstream) was
 1491 physically altered by channelization with an average depth of ~6 meters (m) while the
 1492 downstream estuary has an average depth of 1.5 m.



1493
 1494 **Figure 4.** The Caloosahatchee River Estuary MFL Watershed with its sub-watersheds and major
 1495 water control structures. The future location of the C-43 Storage Reservoir is also shown.

1496 ***Alterations within the Caloosahatchee River Estuary MFL Watershed***

1497 The CRE and the C-43 canal were connected to Lake Okeechobee through the
 1498 evolution of the C&SF Project. The C&SF Project is a complete system of canals, storage
 1499 areas, and water control structures spanning the area from Lake Okeechobee to both the
 1500 east and west coasts, and from Orlando south to the Everglades. It was designed and
 1501 constructed during the 1950s by USACE to provide flood control and improve navigation
 1502 and recreation. In its role as a local sponsor, SFWMD is subject to balancing the water
 1503 resource needs by providing flood control, water supply, recreation and protection for the
 1504 natural system. As a result of structural alterations to the watershed, the existing C&SF

1505 Project has constraints on the availability of water that can be delivered to the CRE from
1506 the regional system.

1507 In addition to the alterations described above, a multitude of other structural and
1508 physical alterations have occurred to the CRE MFL Watershed, historic Caloosahatchee
1509 River, and the CRE. These alterations changed the historical hydrologic conditions of the
1510 CRE MFL Watershed and its receiving water bodies. The CRE MFL Watershed is a system
1511 that has been highly altered from its natural state by human intervention to meet multiple
1512 objectives. Various land uses in a watershed dictate water demands and runoff volumes to
1513 estuarine receiving waters located downstream of S-79. A network of secondary and
1514 tertiary canals exists in the CRE MFL Watershed that is hydrologically connected to the
1515 C-43 canal and the CRE. These canals are used for navigational access or convey water for
1516 both drainage and irrigation to accommodate existing agriculture, urban development and
1517 other land uses in the watershed.

1518 The primary land use type within the CRE MFL Watershed today is agricultural, which
1519 comprises 41.5% of the total area. Urban and built up land uses occupy the next largest
1520 group (18%), followed by wetlands (15.1%) and upland forest (14%).

1521 Historically, the Caloosahatchee River, present day C-43 canal, was a sinuous river,
1522 originating near Lake Flirt, ~2 miles (3.2 km) east of La Belle at Fort Thompson. Beginning
1523 in the 1880s, the river channel was straightened, deepened, and connected to Lake
1524 Okeechobee. This resulted in a loss of 76 river bends and 8.2 miles (13.2 km) of river
1525 length (Antonini et al. 2002). Dredging alterations continued and, by 1918, three
1526 combination lock and spillway structures had been constructed at Moore Haven, Citrus
1527 Center, and Fort Thompson (USACE 1957, Section 6.B.6). Flows within the historic
1528 Caloosahatchee River (now the C-43 canal) are controlled through operation of multiple
1529 water control structures (S-77, S-78, and S-79), and these structures regulate freshwater
1530 inflows to the downstream estuary. The final lock and dam structure (S-79) was completed
1531 in 1966 at Olga to assure freshwater supply and prevent upstream saltwater intrusion.
1532 Discharges from Lake Okeechobee and the C-43 Watershed or Basin (between the S-77
1533 and S-79 structures) are regulated by USACE for various purposes, including flood control,
1534 water supply, and navigation. The modern C-43 canal spans 70 km from the S-77 structure
1535 at Lake Okeechobee to the S-79 structure (**Figure 4**).

1536 The total effect of these alterations has been the loss of surface water storage in the
1537 CRE MFL Watershed, which has altered the magnitude, timing, and distribution of
1538 freshwater inflows to the estuary at the S-79 structure. As is typical of a watershed
1539 characterized by extensive drainage features (Hopkinson and Vallino 1995), runoff is more
1540 variable with higher wet season discharges and lower dry season discharges. Large
1541 volumes of fresh water during the wet season can flush all salt water from the tidally
1542 influenced sections of the water body. By contrast, inflow at S-79 can stop entirely during
1543 the dry season. Salt water intrudes to S-79, sometimes reaching a salinity of 20
1544 (Chamberlain and Doering 1998a, 1998b). Fluctuations of this magnitude at the head and
1545 mouth of the system cause mortality of organisms at both ends of the salinity gradient
1546 (Doering et al. 2002).

1547 The first recorded survey of the waterbodies (CRE and historic Caloosahatchee River)
1548 within the watershed was conducted by Captain W.M. Black of the United States Army
1549 Engineers in 1887 (Black 1887). This survey indicated that the estuary was much shallower

1550 than today. An extensive shoal (<1.6-m depth) spanned the mouth where the estuarine river
1551 discharged to San Carlos Bay. This shoal was part of an extensive tidal delta which
1552 bordered the eastern portion of the bay. Navigation was inhibited along the entire length
1553 by the shoal and oyster bars, which extended ~27 km upstream to Fort Myers. The
1554 historical river channel from Fort Myers to LaBelle was shallow (~1 m), long (~70 km),
1555 and crooked. Early descriptions of the estuary characterize it as barely navigable due to
1556 extensive shoals and oyster bars (Sackett 1888). Some of the alterations that have occurred
1557 include dredging a large navigational channel (Intracoastal Waterway) and secondary
1558 navigational channels, removing oyster bars upstream of Shell Point for roadway
1559 construction, removing the gulf bar at the mouth of the Caloosahatchee River Estuary, and
1560 the creation of two islands for construction of the Sanibel Causeway across the mouth of
1561 San Carlos Bay. Seven automobile bridges and one railroad bridge now connect the north
1562 and south shores of the estuary.

1563 The potential for removing the existing structural and physical alterations affecting the
1564 historic Caloosahatchee River (C-43 canal) and the CRE may not be feasible. Much of the
1565 existing development within these downstream water bodies is dependent upon the
1566 conditions these alterations currently provide (e.g., flood protection, navigation, water
1567 supply, transportation, etc.).

1568 **Hydrodynamic Model of the CRE**

1569 The CH3D model, originally developed by Sheng (1986), is a non-orthogonal
1570 curvilinear grid model capable of simulating complicated hydrodynamic processes
1571 including wind driven, density driven, and tidal circulation. The model has a robust
1572 turbulence closure scheme for accurate simulation of stratified flows in estuaries and
1573 coastal waters (Sheng 1986, Sheng 1987, Sheng and Villaret 1989). The non-orthogonal
1574 nature of the model enables it to represent the complex geometry of a tidal estuary such as
1575 the CRE. The model includes a circulation model to simulate three-dimensional
1576 hydrodynamics and a salinity model to simulate salt transport. The model is driven by
1577 external forcing prescribed at the boundaries including tidal forcing at the ocean boundary,
1578 freshwater inflow from the watershed, and meteorological forcing including wind and
1579 rainfall. The CH3D model has been successfully applied to many waterbodies including
1580 east coast Florida estuaries such as the Indian River Lagoon, St. Lucie Estuary (Sun 2009,
1581 Wan et al. 2012) and Loxahatchee River Estuary (Sun 2004).

1582 The Caloosahatchee Estuary CH3D model was developed from the Charlotte Harbor
1583 CH3D model (Sheng 2002). The original Charlotte Harbor model was calibrated using two
1584 months of hydrodynamic and salinity data collected during summer at six stations located
1585 in and around Pine Island Sound and the Peace River. SFWMD extended the model to the
1586 CRE using 16 months of continuous monitoring data (Qiu 2002, SFWMD 2003). The
1587 Caloosahatchee Estuary CH3D model was further calibrated with three years of salinity
1588 observations (October 2001–December 2004) at five stations in the estuary for the
1589 evaluation of various alternative plans of the Southwest Florida Feasibility Study and the
1590 Caloosahatchee River (C-43) West Basin Storage Reservoir Project (Sheng and Zhang
1591 2006, Qiu 2006, USACE and SFWMD 2010). An external peer review of the model was
1592 conducted in 2006 for this application (Qiu 2006). The latest calibration of the model was
1593 conducted with data collected up to 2010 at seven locations in the estuary to support the

1594 development of the Lake Okeechobee Adaptive Protocols (SFWMD 2010, Wan et al.
1595 2013).

1596 The Caloosahatchee Estuary CH3D model domain covers the entire estuarine system,
1597 including Caloosahatchee Estuary, Charlotte Harbor, Pine Island Sound, San Carlos Bay,
1598 Estero Bay, and the major tributaries, as well as about 30 km offshore in the Gulf of Mexico
1599 (**Figure 5**). The horizontal grid has 166 x 128 elements with 5,266 water cells allowing
1600 fine enough resolution to represent the numerous islands, including the two islands
1601 constructed as part of the Sanibel Causeway. The higher resolution within the CRE and
1602 San Carlos Bay (50–100 m) provides a more detailed representation of the complex
1603 shoreline and the navigation channel. Five vertical layers evenly spaced over the water
1604 column enable simulation of density stratification within the estuary.

1605 ***Hydrodynamic Model Scenarios***

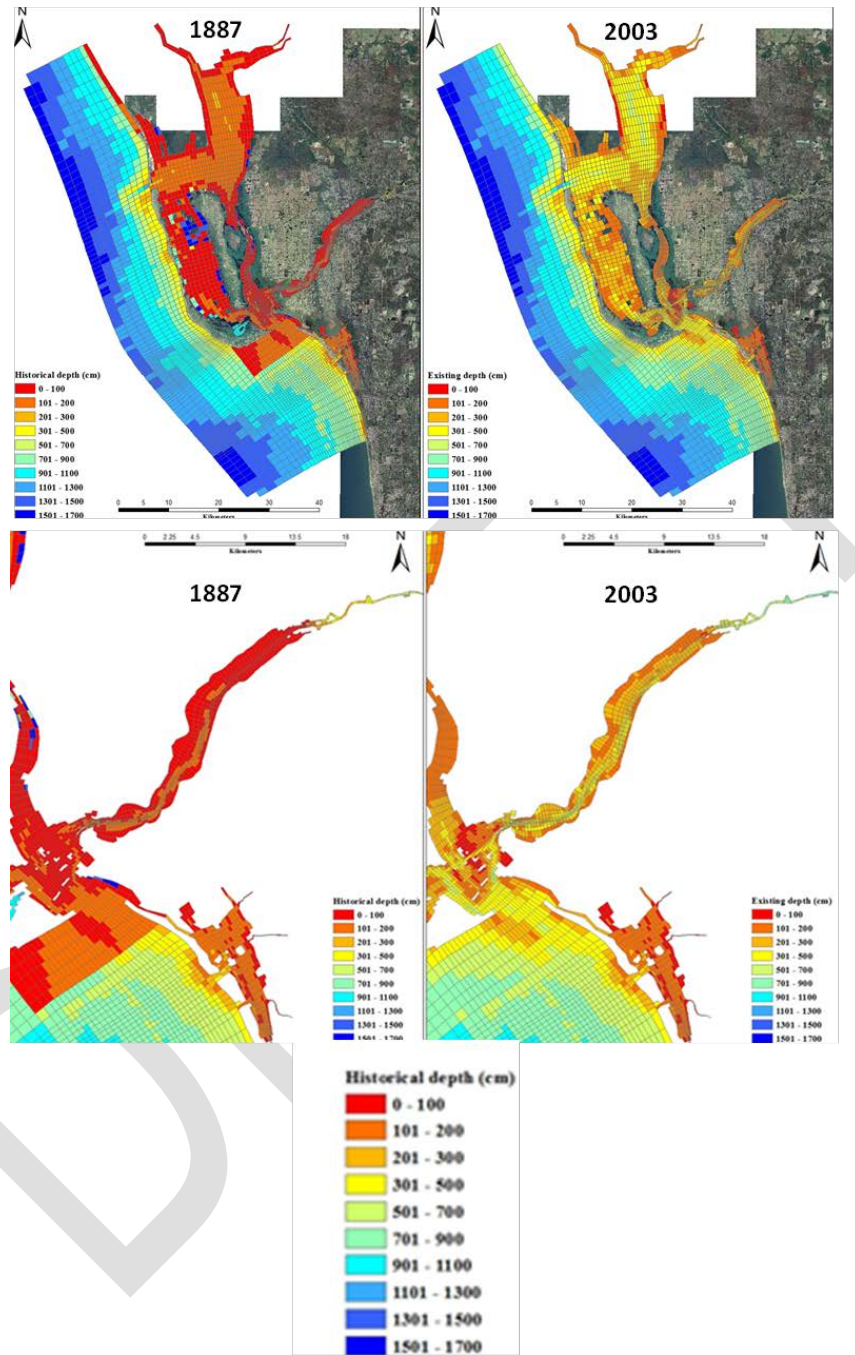
1606 The effects of physical alterations on saltwater intrusion were quantified by comparing
1607 the results of altered scenarios with the existing condition under the same boundary forcing.
1608 This modeling strategy allowed for isolation of the effects of each physical alteration on
1609 salinity patterns. The existing condition was based on bathymetric survey data collected in
1610 2003. Five model scenarios were designed to simulate reversals of the historical alterations:
1611 (1) removal of S-79 water control structure at the upstream boundary, (2) removal of the
1612 Sanibel Causeway at the downstream boundary, (3) backfilling of the oyster bar near Shell
1613 Point, (4) filling the navigational channel throughout the estuary, (5) reestablishing the
1614 predevelopment bathymetry from the Captain Black's survey.

1615 The first model scenario investigated the potential effects of removing the S-79 lock
1616 and dam on the distribution of salinity in the estuary. To simulate this effect, the model
1617 grid was extended from S-79 to S-78. Discharge at S-79 is a combination of discharge at
1618 S-78 and runoff from the intervening West Caloosahatchee sub-watershed (**Figure 4**).
1619 Runoff from the watershed was calculated as the difference between discharges at S-79
1620 versus S-78. This simulation applied measured flow at S-78 with the difference between
1621 the two discharges redistributed along the C-43 canal west of S-78.

1622 In the second scenario, the CH3D model grid was modified to eliminate the causeway
1623 with its two man-made islands. Estuarine circulation and salinity patterns are heavily
1624 influenced by the input of salt water at the downstream boundary. Thus, this scenario
1625 simulated the influence of the causeway on salinity within the estuary. Removal of the
1626 Sanibel Causeway was implemented by activating the “island” cells of the causeway and
1627 assigning them an elevation equal to the average of the submerged neighboring cells (i.e.
1628 removal of the two islands).

1629 The effects of the removal of the historical oyster bar were modeled by increasing the
1630 elevation of selected areas near Shell Point where historical oyster bars were dredged. This
1631 was accomplished by increasing the bottom elevation 0.6 m near the mouth of the CRE.
1632 Similarly, the effect of dredging the navigation channel was simulated by changing the
1633 elevation of the exiting navigation channel to that of the neighboring cells. The lower CRE
1634 and the majority of San Carlos Bay and Pine Island Sound were significantly shallower
1635 historically, mostly <1.5 m in depth, compared to ~2 to 5 m deep in the present existing
1636 condition (**Figure 5**). The increase in depth was apparently due to the dredging of

1637 navigational channels including the Intracoastal Waterway. This was done by changing the
 1638 channel depths in the CH3D model grid from the mouth to S-79 to a maximum of 1.5 m.



1639
 1640 **Figure 5.** Comparison of bathymetry of the model domain for the CRE: (top left) the 1887
 1641 bathymetry for the entire domain, (bottom left) the 1887 bathymetry focused on the CRE, (top
 1642 right) the 2003 bathymetry for the entire domain, and (bottom right) the 2003 bathymetry focused
 1643 on the CRE.

1644 The final hydrodynamic model scenario incorporated the bathymetric survey data
 1645 generated by Captain Black into the existing model grid to represent the predevelopment
 1646 condition. Historical bathymetry from Captain Black’s 1887 survey was interpolated to the

1647 modified model grid which was extended to the S-78 structure (**Figure 5**). Similar to the
1648 S-79 removal scenario, freshwater inflow was applied at the location of S-78 and
1649 distributed along the river between S-79 and S-78 with the same total freshwater inflow as
1650 the existing condition.

1651 The model was calibrated using data from October 1, 2001, to December 31, 2011 (11
1652 year or 3,744 days). For each run, predicted salinities at Fort Myers and I-75 were
1653 compared to those from the existing condition to examine the impact from the change.
1654 These two locations were selected for their proximity to the existing MFL compliance
1655 monitoring point and monitoring associated with the implementation of the most recent
1656 operational schedule.

1657 The existing boundary conditions including tidal water levels, freshwater inflow, and
1658 meteorological forcing remained the same for all model scenarios. Tidal data collected at
1659 a National Oceanic and Atmospheric Administration (NOAA) station located in Naples,
1660 Florida were used as the ocean boundary condition. The upstream boundary condition
1661 resulted from measured freshwater inflow at the S-79 structure available from the
1662 SFWMD's corporate environmental database, DBHYDRO (access the database using
1663 http://my.sfwmd.gov/dbhydroplsql/show_dbkey_info.main_menu) and predicted inflow
1664 from tributaries in the Tidal Basin downstream of S-79 (Konya and Wan 2011).

1665 Freshwater inflow through the S-79 structure and the Tidal Basin exhibited significant
1666 inter-annual, seasonal, and daily variations during the simulation period. The surface
1667 boundary condition was driven by wind and rainfall/evaporation data available from
1668 DBHYDRO. Incoming fresh water at the upstream boundary was assigned a salinity of 0.0
1669 while salinity at the downstream boundary was set at constant value of 35.0. Salinity time
1670 series observed at the monitoring stations located along the length of the estuary were
1671 interpolated over the model domain to serve as the initial condition. Three years of tidal
1672 discharge data (October 2007–September 2010) measured at the two transects at Shell
1673 Point and Marker 52 (**Figure 6**) provided a validation of the sum of tidal flow and
1674 freshwater discharge (**Figure 7**). Water levels were recorded at some of these stations.
1675 During the simulation, the Manning's bottom friction coefficient was held constant at 0.025
1676 (Qiu et al. 2006).

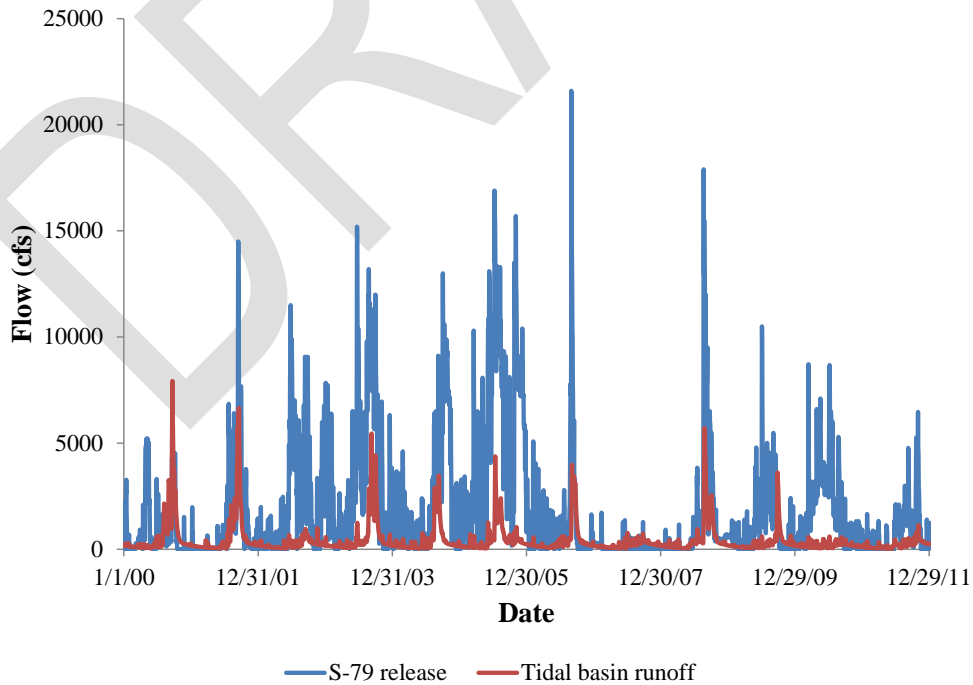
1677 Validation of the existing condition involved long-term data for water level and salinity
1678 along with more recent tidal discharge data determined along two transects in the estuary.
1679 Seven continuous salinity monitoring stations maintained by SFWMD, including S-79,
1680 BR-31, I-75, Fort Myers, Cape Coral, Shell Point, and Sanibel, provided hourly and daily
1681 data for salinity validation (**Figure 7**). Salinity is measured at two depths: surface (defined
1682 at 20% of the total depth below surface) and bottom (defined as 20% of the total depth
1683 above the bottom). Hourly salinity data and model results for the same five-year period
1684 were compared at five stations: S-79, BR-31, I-75, Fort Myers, and Shell Point.

1685



1686
1687
1688

Figure 6. Salinity and inflow monitoring stations in the CRE used for model validation. Both freshwater inflow and salinity are monitored at the S-79 structure.



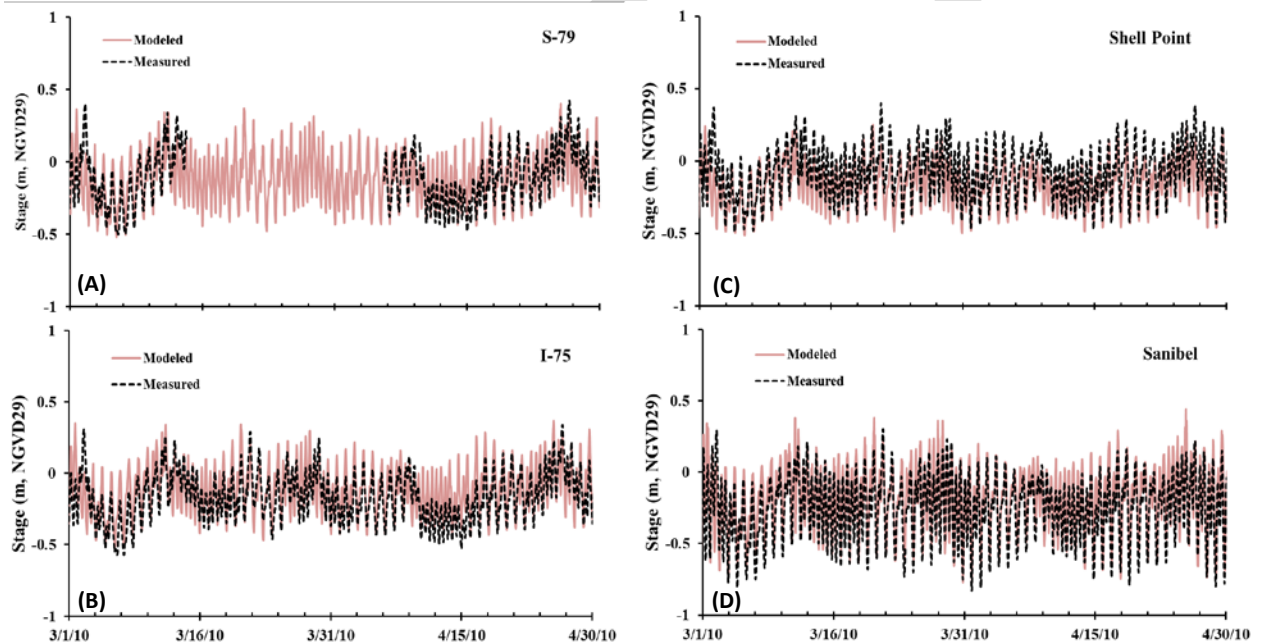
1689
1690

Figure 7. Freshwater inflow (cfs) from S-79 (blue) and the tidal basin downstream of S-79 (red).

1691 **Results**

1692 **Validation of the Existing Condition**

1693 The modeled tidal water surface elevation was compared to measured water elevations
 1694 at four locations: S-79, I-75, Shell Point, and Sanibel Causeway (**Figure 8**). Only two
 1695 months (March and April, 2010) were presented. Overall, predicted water levels agreed
 1696 with the measurement at all the four sites in terms of tidal range, tidal phase, and subtidal
 1697 movement. The root mean square (RMS) error and correlation coefficient (r) along with
 1698 the relative error defined by the RMS error divided by the average tidal range were
 1699 calculated from the model results and the field observations over a five-year period (2007
 1700 to 2011; **Table 3**). Despite the relatively larger RMS error at Shell Point due to a small
 1701 datum offset observed at that location, the RMS errors were within 15% of average tidal
 1702 range. One possible source of error is the long open tidal boundary in the Gulf of Mexico
 1703 where only tidal information at Naples was provided. Tidal range in the upper estuary (S-79
 1704 and BR-31) was slightly over-predicted possibly due to inadequate representation of the
 1705 shoreline, floodplain, and bathymetry in this part of the estuary.

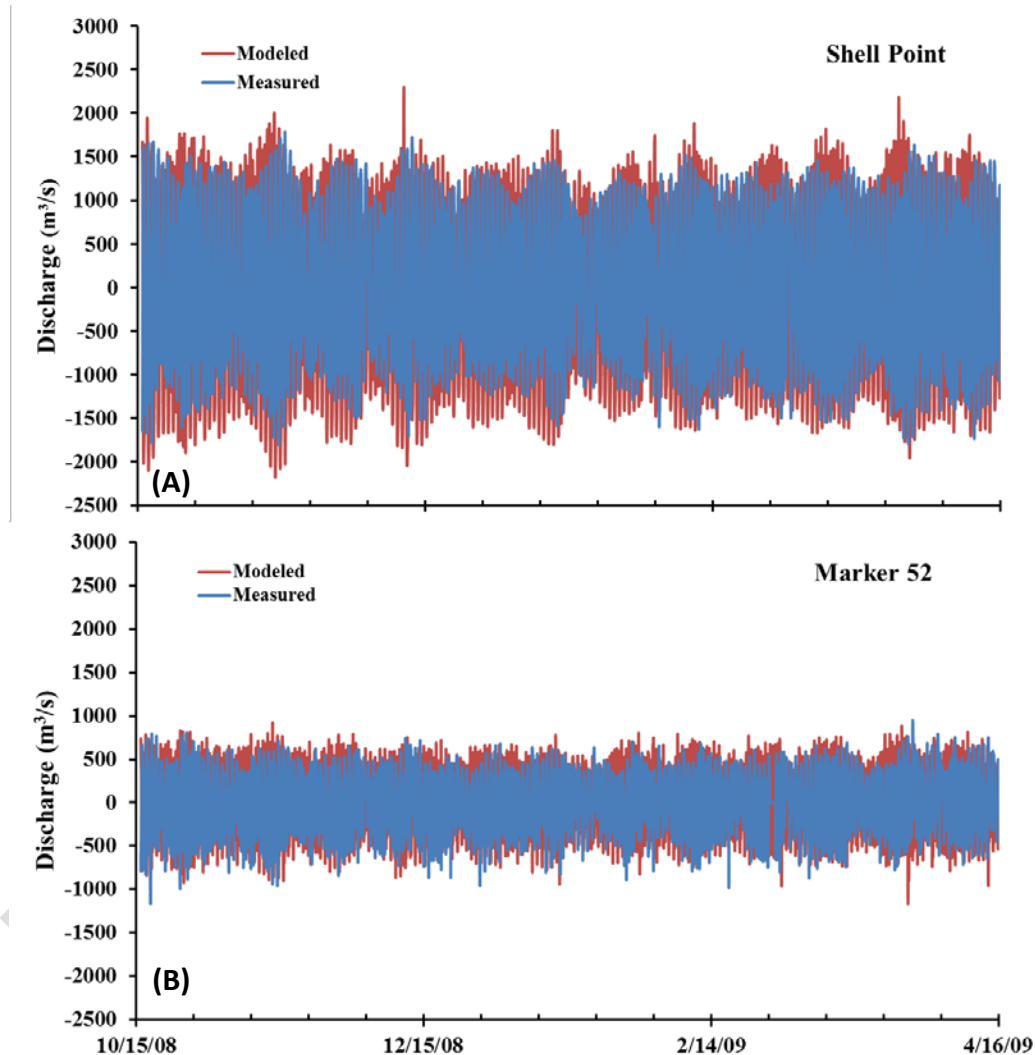


1706
 1707 **Figure 8.** Modeled (red line) and measured (black dash) tidal elevations at (A) S-79, (B) I-75, (C)
 1708 Shell Point, and (D) Sanibel Island from March to April 2011.

1709 **Table 3.** Model performance statistics for hourly tidal
 1710 elevation calculated over the period from 2007 to 2011.

Station	r	RMS Error (m)	Relative Error
S-79	0.86	0.11	12.3%
I-75	0.88	0.12	12.5%
Shell Point	0.91	0.15	15%
Sanibel	0.94	0.10	10%

1711 The discharge at Shell Point is due to the combined contribution determined along three
 1712 subtransects, which in sum account for the total discharge at the mouth of the estuary
 1713 (Figure 9). This total discharge was much larger than that at Marker 52 located about 20
 1714 km upstream near Fort Myers. The tidal component was dominant relative to the freshwater
 1715 inflow at the two downstream transects. Model representation of tidal transport agreed with
 1716 the empirical observations (Table 4).



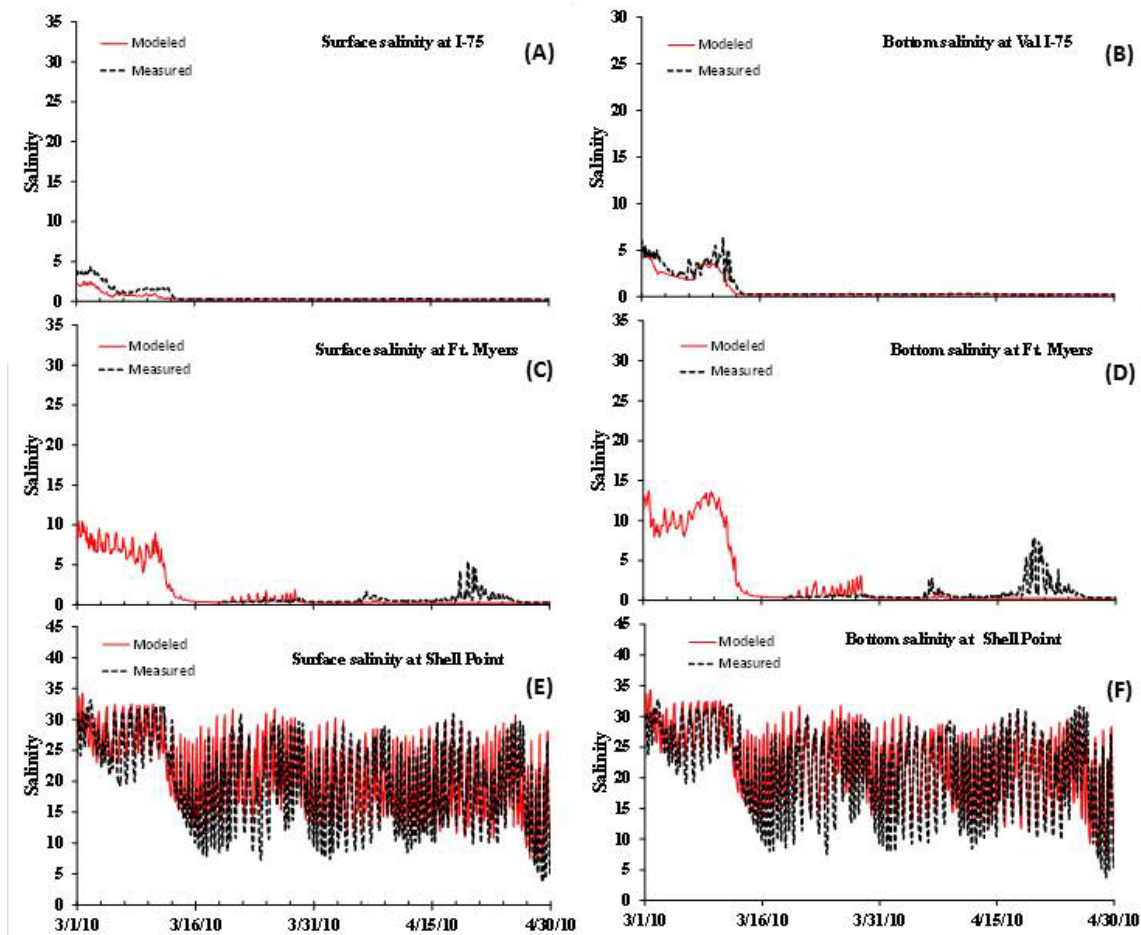
1717
 1718 **Figure 9.** Modeled (red line) and measured (blue line) tidal discharge at (A) Shell Point, and (B)
 1719 Marker 52 from October 15, 2008, to April 15, 2009.

1720 **Table 4.** Model performance statistics for hourly and daily
 1721 salinity calculated over the period from 2007 to 2011 and from
 1722 2001 to 2011, respectively. [Note $\text{m}^3 \text{s}^{-1}$ – cubic meters per
 1723 second.]

Station	r	RMS Error ($\text{m}^3 \text{s}^{-1}$)	Relative Error
Shell point	0.82	446	17.3%
Marker 52	0.85	221	18.1%

1724

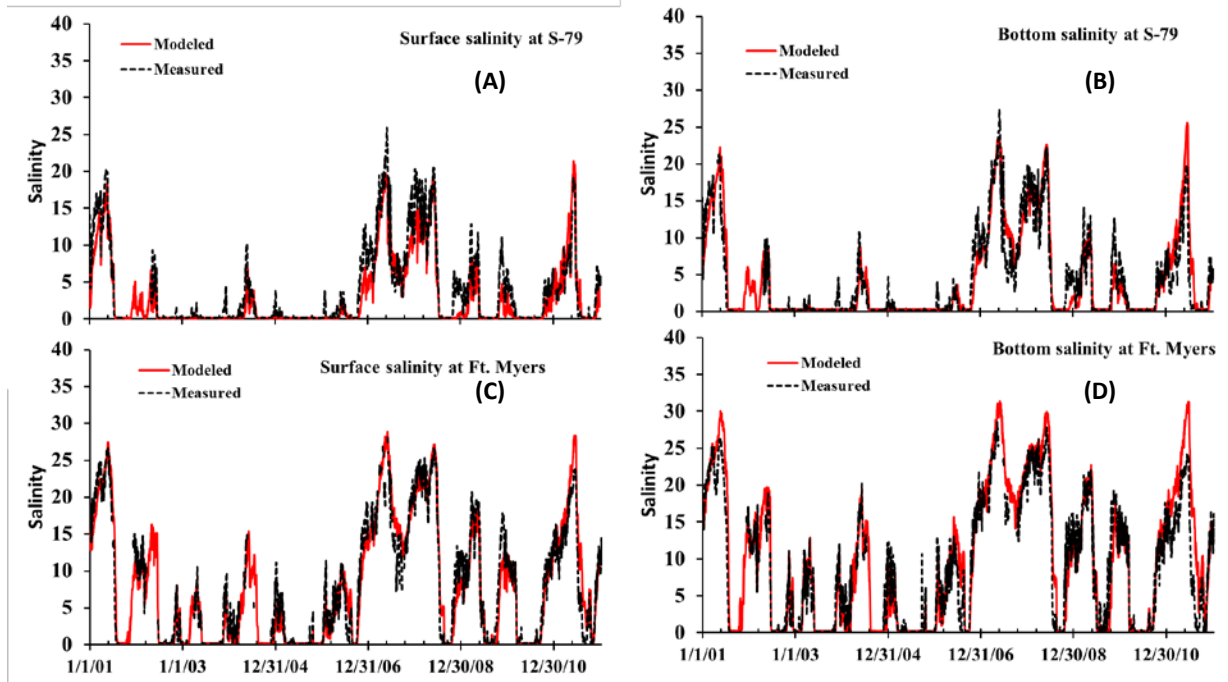
1725 Salinities predicted using the model agreed to the hourly data from 2010 (I-75, Fort
 1726 Myers, and Shell Point; **Figure 10**), and, the daily data for the entire period (S-79 and Fort
 1727 Myers; **Figure 11**). This included good representation of fine-scale variations (e.g.
 1728 stratification), daily variability, and seasonal patterns. Simulation of short-term (daily or in
 1729 the order of a few days) salinity fluctuations was more reliable at downstream sites (Shell
 1730 Point and Fort Myers) than at upstream sites (S-79 and BR-31). This was possibly due to
 1731 a damping effect inherent in the modeling transport scheme. There was little difference (r
 1732 = 0.9; RMS 2.5–3.5) between hourly salinities predicted by the model and those measured
 1733 from 2007 to 2011 (**Table 5**). The reliability of the salinity prediction was greater at the
 1734 daily time scale at all locations. These results suggest that the model is a reliable tool for
 1735 salinity prediction to support decision making regarding water management operations for
 1736 the CRE.



1737

1738 **Figure 10.** Modeled (red line) and measured (black dash) hourly surface and bottom salinity at I-
 1739 75 (**A and B**), Fort Myers (**C and D**), and Shell Point (**E and F**) from March to April 2010.

1740



1741
1742
1743

Figure 11. Modeled (red line) and measured (black dash) daily surface and bottom salinity at S-79 (A and B) and Ft. Myers (C and D) from 2001 to 2010.

1744
1745

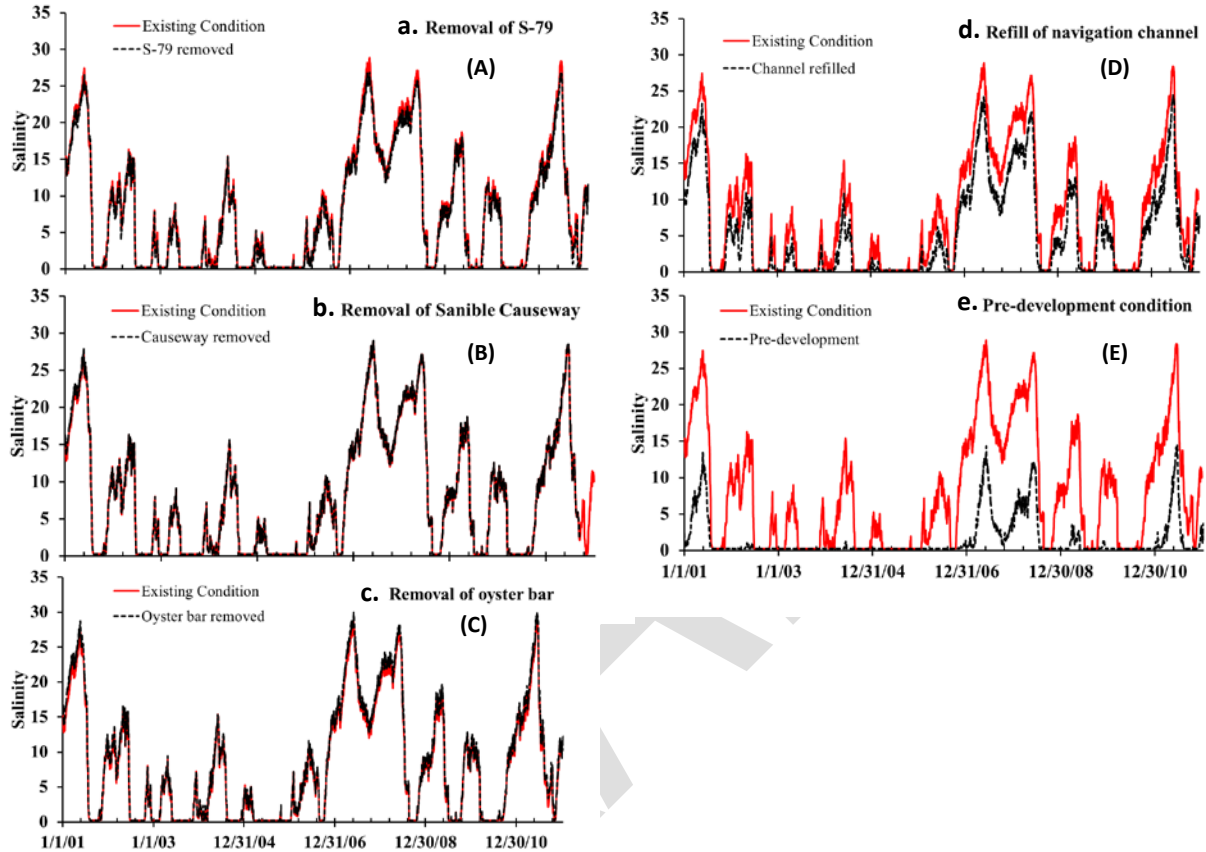
Table 5. Model performance statistics for hourly and daily salinity calculated over the period from 2007 to 2011 and from 2001 to 2011, respectively.

Station	Hourly (2007 to 2011)				Daily (2001 to 2011)			
	Surface		Bottom		Surface		Bottom	
	r	RMS	r	RMS	r	RMS	r	RMS
S-79	0.92	2.68	0.92	3.27	0.94	2.17	0.93	2.25
BR-31	0.94	2.44	0.90	3.41	0.95	1.91	0.91	2.65
I-75	0.94	2.32	0.93	2.91	0.94	2.27	0.93	2.87
Fort Myers	0.94	3.22	0.92	5.11	0.96	2.31	0.94	2.98
Cape Coral					0.97	2.46	0.97	2.95
Shell Point	0.89	3.58	0.88	3.79	0.94	2.78	0.92	2.90
Sanibel					0.84	2.03	0.86	2.80

1746 **Hydrodynamic Model Scenarios**

1747 The total freshwater inflow entering the CRE was the same between the existing
 1748 condition and the scenario where S-79 was removed. Salinity decreased slightly during the
 1749 dry season without the control structure at the estuary head (Figure 12A). The relative
 1750 difference in salinity was greater at I-75 (not shown) than at Fort Myers with a more
 1751 noticeable deviation in the bottom water. Salinity at Fort Myers did not change
 1752 significantly with the removal of the Sanibel Causeway (Figure 12B). However, there was
 1753 a slight increase in salinity at Sanibel during the dry season (data not shown). While dry
 1754 season salinity at Fort Myers increased slightly when the oyster bar was reestablished, this
 1755 effect diminished in the upstream direction (Figure 12C). In contrast, filling the
 1756 navigational channel led to reductions in salinity throughout the CRE during the dry season
 1757 (Figure 12D). Finally, reintroduction of the predevelopment bathymetry resulted in

1758 significantly lower salinity in upstream regions of the estuary relative to the existing
 1759 condition (**Figure 12E**). Except for the four drought years (2001, 2007, 2008, and 2011),
 1760 the estuary would be nearly fresh upstream of Fort Myers even during the dry season.
 1761 Changes in both average surface and bottom salinities at I-75 and Fort Myers were most
 1762 pronounced in the scenarios that decreased the depth of the navigational channel or across
 1763 the entire model grid (**Table 6**).



1764
 1765 **Figure 12.** Comparison between average daily surface salinity at Fort Myers (red line) and five
 1766 different physical alteration scenarios (black dash) from 2001 to 2010: (A) removal of S-79; (B)
 1767 removal of Sanibel Causeway; (C) restoration of oyster bar at the mouth; (D) refill of the
 1768 navigational channel; and (E) reestablishment of predevelopment bathymetry.

1769 **Table 6.** Difference of monthly average surface (S) and bottom (B) salinity between each
 1770 scenario and the existing condition at I-75 and Fort Myers in May of 2001, 2007, 2008, and 2011.

Scenario		2001		2007		2008		2011	
		I-75	Fort Myers						
S-79 Removal	S	-1.03	-0.84	-2.57	-1.49	-1.61	-1.04	-1.54	-0.95
	B	-2.56	-1.31	-3.27	-1.88	-2.59	-1.40	-2.62	1.59
Causeway Removal	S	0.14	0.15	0.16	0.16	0.12	0.14	0.15	0.17
	B	0.15	0.18	0.17	0.16	0.13	0.14	0.16	0.16
Restore Oyster Bar	S	0.75	0.49	1.33	0.95	1.38	1.02	1.46	1.02
	B	1.01	1.23	1.39	1.33	1.46	1.37	1.56	1.56
Refill Navigation Channel	S	-5.7	-4.5	-5.5	-4.5	-5.7	-5.0	-5.6	-4.7
	B	-4.8	-4.8	-5.1	-4.9	-5.7	-5.4	-5.0	-5.1
Predevelopment	S	-14.4	-14.8	-17.1	-15.3	-15.9	-14.1	-14.7	-14.7
	B	-15.4	-14.2	-19.1	-16.2	-17.9	-17.9	-17.4	-16.4

1771 **Theoretical Considerations for Salt Intrusion**

1772 In many estuaries reduced freshwater inflow over time can result in the landward
 1773 salinity encroachment (Cloern and Jassby 2012). There have been many attempts to address
 1774 the problem based on theoretical and experimental approaches. With a prismatic channel,
 1775 analytical solutions of salt transport equations have been given by various authors (Ippen
 1776 and Harleman 1961, Ippen 1966, Prandle 1985, 2004, 2009, Savenije 1992, 2005, Kuijper
 1777 and Van Rijn 2011). When averaged on tidal time scales, the one-dimensional salt
 1778 continuity equation can be simplified to a balance between the seaward advective salt
 1779 transport and the landward dispersive transport (Savenije 2005):

$$1780 \quad u_r S + D_x \frac{dS}{dx} = 0 \quad (1)$$

1781 Where x is the distance from the mouth, u_r is the river discharge velocity, S is salinity,
 1782 and D_x is the dispersive coefficient. Each parameter was averaged over multiple tidal cycles
 1783 and the channel cross-sectional area. The transport due to advection is caused by the
 1784 velocity associated with freshwater discharge, whereas the longitudinal dispersive
 1785 transport is caused by tidally- and density-driven processes. Longitudinal dispersion in
 1786 estuaries can be particularly difficult to measure and model (Jay et al. 1997, Austin 2004,
 1787 Geyer et al. 2008, Spencer et al. 2014). Nevertheless, the theory can still provide qualitative
 1788 guidance.

1789 The most important parameters influencing salt intrusion are the tidal characteristics
 1790 (tidal amplitude and peak tidal velocity), the river parameters (discharge and average cross-
 1791 sectional velocity) and the geometric parameters (depth, width, and convergence length
 1792 scale). Using a tidally averaged approach and assuming the following relation between the
 1793 dispersion coefficient D_x and river discharge velocity u_r (Van Der Burgh 1972) results in

1794 **Equation 2:**

$$1795 \quad \frac{dD_x}{dx} = -K u_r \quad (2)$$

1796 where K is a calibration coefficient (Van Der Burgh coefficient) between 0 and 1. The salt
 1797 balance equation can be solved and the maximum salt intrusion length L_{max} (defined as the
 1798 salt penetration length at high slack water) can be expressed as (Savenije 2005, Kuijper
 1799 and Van Rijn 2011) **Equation 3:**

$$1800 \quad L_{max} = L_a \ln\left(1 + \frac{D_0 A_0}{K L_a Q_r}\right) \quad (3)$$

1801 where L_a is the convergent length scale for the cross-section area $A = A_0 \exp(-x/L_a)$, A_0 is
 1802 the cross-section area at the mouth, D_0 is the dispersive coefficient at the mouth, and Q_r is
 1803 the river discharge. For prismatic estuaries, **Equation 3** is reduced to the following:

$$1804 \quad L_{max} = \frac{D_0 A_0}{K Q_r} \quad (4)$$

1805 Savenije (2005) also found an empirical relationship for the dispersive coefficient at
 1806 the mouth:

$$1807 \quad D_0 \sim 1400 \hat{u}_0 h_0 \quad (5)$$

1808 where \hat{u}_0 is the peak tidal velocity and h_0 is the depth at the mouth.

1809 Thus, it is evident from **Equations 3** through **5** that salt intrusion length would increase
1810 significantly with increasing depth h and cross-section area A . This theoretical
1811 consideration is consistent with the numerical simulation results of the last two of scenarios
1812 of physical alteration (e.g. refilling the estuarine channel and return to the predevelopment
1813 bathymetry).

1814 **Discussion**

1815 This study applied a three-dimensional, curvilinear hydrodynamic model (CH3D) to
1816 investigate the impact of physical alterations on salinity in the CRE. Simulated salinity
1817 distributions and time series from five different scenarios representing physical alterations
1818 to the estuary were compared to those from the existing condition. Intra- and inter-annual
1819 variations in the model's existing salinity conditions were validated using extensive data
1820 collected from 2000 to 2011. With all forcing being kept the same, the modeled salinity of
1821 the existing conditions was compared with five cases in which historical physical
1822 alterations of the estuary were reversed, including (1) removal of the S-79 structure, (2)
1823 removal of the Sanibel Causeway, (3) backfill of the oyster bar, (4) backfill of the
1824 navigation channel, and (5) the predevelopment bathymetry.

1825 Model results indicated that the construction of the Sanibel Causeway, the removal of
1826 the oyster bar near the estuarine mouth, and the S-79 water control structure had little effect
1827 on salinity of the CRE. Potential effects of these alterations were localized and spatially
1828 limited. In contrast, dredging the navigational channels greatly increased salinities
1829 throughout the estuary. Under the pre-development bathymetry, before dredging, salinity
1830 was dramatically lower in the estuary upstream of Fort Myers being nearly fresh in the dry
1831 season except for the drought years of 2001, 2007, 2008, and 2011. Dredging and
1832 deepening of the estuary was one of the primary activities that changed the pattern of salt
1833 transport in the estuary. This is consistent with the analytical theory about the significance
1834 of estuary depth and cross-sectional area in salt intrusion. There are two factors that could
1835 explain this difference. On the one hand, refilling the channel provided more resistance to
1836 salt intrusion; on the other hand, the volume of the estuary was significantly reduced, but
1837 the amount of freshwater input remained the same, resulting in reduced salinity in the
1838 estuary. Since these physical changes are unlikely to be reversed, the results may have
1839 important implications in the development of realistic inflow goals to protect the estuarine
1840 ecosystem. This modeling evaluation provides a framework for understanding the
1841 influence of different structural alterations on resulting salinity distributions. It should be
1842 recognized that these irreversible alterations act as constraints on the ability to restore
1843 historical hydrologic conditions to the CRE.

1844

1845

1846 **Component Study 2: Analysis of the Relationship between**
1847 **Freshwater Inflow at S-79 and Salinity in the Caloosahatchee**
1848 **River Estuary 1993–2013**

1849 *Christopher Buzzelli*

1850 **Abstract**

1851 The upstream migration of salt with reduced freshwater inflow alters the composition
1852 and productivity of oligohaline habitats in estuaries. This process can be problematic in
1853 subtropical estuaries with regulated freshwater inflow such as the CRE in southwest
1854 Florida. This study component examined relationships between average monthly inflow
1855 (Q) and mid-estuary salinity (S) from 1993 to 2013. An exponential decay equation was fit
1856 to the inflow-salinity (Q-S) relationship for each water year (May 1 to April 30). Annual
1857 equations were used to estimate the inflow rate associated with a salinity of 10 at the Fort
1858 Myers monitoring station (Q_{calc}). Inflows varied both intra- and inter-annually. Q_{calc} ranged
1859 from 70 cfs to 773 cfs with an average of 445 ± 218 cfs. At the estuary and annual scales,
1860 the quantity of fresh water to support a particular salinity target varied greatly. This
1861 variance was related to the variations in freshwater inputs from both the watershed located
1862 upstream of S-79 and the downstream tidal basin.

1863 **Introduction**

1864 Life histories of many estuarine organisms are directly dependent upon temporal and
1865 spatial variations in salinity (Livingston et al. 1997, Palmer et al. 2011, Whitfield et al.
1866 2012). The vertical and horizontal patterns of salinity can be quantified using lines of equal
1867 salinity (e.g. isohalines) whose positions fluctuate with freshwater inflow, tidal cycles, and
1868 meteorological phenomena (e.g. fronts, winds, and storms; Jassby et al. 1995). Upstream
1869 or downstream shifts in isohaline position can narrow the optimal habitat for estuarine
1870 organisms or move them further away from their optimal locations (Sklar and Browder
1871 1998). Data analyses and research to provide guidelines for freshwater management should
1872 rely upon appropriate physical and ecological indicators and seek clear breakpoints in
1873 relationships between inflow, salinity, and biological responses (Montagna et al. 2002a).
1874 Therefore, isohaline position can be used as an indicator of ecological conditions in
1875 estuaries (Jassby et al. 1995).

1876 The CRE has a watershed characterized by extensive agriculture and urbanization, is
1877 influenced by freshwater inflow from several sources, and contains valuable biological
1878 resources (Chamberlain and Doering 1998a, Doering et al. 2006, SFWMD 2012). Through
1879 combinations of climatic variations, landscape modification, and managed operations, the
1880 CRE can experience variable freshwater inflow during the dry season. In many estuaries
1881 reduced freshwater inflow over time can result in the landward encroachment of salinity
1882 (Cloern and Jassby 2012). In the case of the CRE, upstream salt migration can reduce the
1883 extent of vegetated freshwater habitat (i.e., *Vallisneria americana*), impact community
1884 composition in the water column and benthos, and compress the oligohaline area of the
1885 estuary essential to a variety of faunal populations (Doering et al. 2002, Simpfendorfer et
1886 al. 2011, Palmer et al. 2011, Stevens et al. 2013).

1887 Continuous salinity recorders have been in place near Fort Myers, Florida since 1992.
 1888 The objective of this study was to quantify inter-annual variations in the estimated
 1889 freshwater inflow from S-79 associated with a salinity of 10 (S_{10}) at Fort Myers.

1890 Methods

1891 This analysis focused on the average daily freshwater inflow at the Franklin Lock and
 1892 Dam (S-79; Q_{S79} ; cfs) and did not include consider freshwater inputs from tributaries or
 1893 groundwater downstream of S-79. Inflows from January 1, 1992, to May 1, 2013, were
 1894 downloaded from the publicly available database, DBHYDRO, at SFWMD, which can be
 1895 accessed at http://my.sfwmd.gov/dbhydropls/sql/show_dbkey_info.main_menu. Average
 1896 daily salinity determined at the Fort Myers station (S_{FIM}) over the same period of record
 1897 (POR) was downloaded and combined with the inflow data. The two data sets were used
 1898 to generate a time series of average monthly values (**Figure 13A**). The overall relationship
 1899 between average monthly inflow (Q_{S79} ; cfs) and average monthly salinity at Fort Myers
 1900 (S_{FIM}) follows a negative exponential form (**Figure 13**; Qiu and Wan 2013):

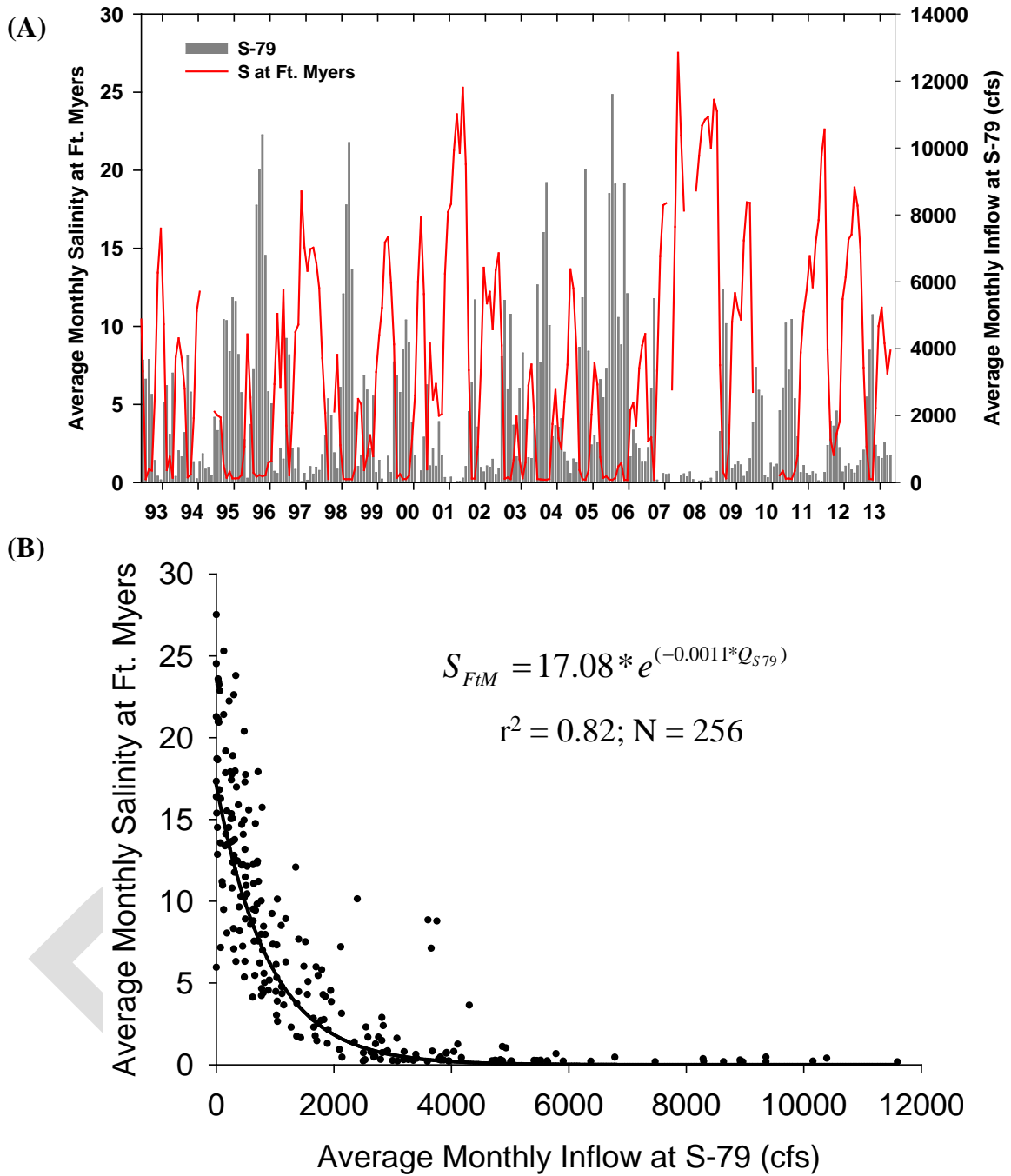
$$1901 \quad S_{FIM} = a * e^{(-b * Q_{S79})} \quad (6)$$

1903 The average monthly inflow and salinities were categorized by water year to derive 21
 1904 individual years of coupled inflow-salinity records ($n = 12$ per water year). Scatter plots
 1905 similar to **Figure 13B** were generated for each water year (**Figure 14A-U**). The negative
 1906 exponential curve fit to the scatter plots for each year resulted in estimates of r^2 and two
 1907 equation parameters (a , b) to calculate salinity at Fort Myers. There were five water years
 1908 for which the relationship was unusable. The high inflows throughout WY1995 resulted in
 1909 average monthly salinities <5 . Inflow and salinities in the dry (November–April) and wet
 1910 (May–October) seasons were anomalous in WY2006 as tropical storms in 2005 led to
 1911 extreme freshwater releases from Lake Okeechobee from late 2005 to the middle of 2006
 1912 (**Figure 13A**). Precipitous decreases to inflow in WY2007 due to drought rendered the
 1913 curve-fitting procedure meaningless. Similarly, the greatly reduced inflow and exacerbated
 1914 salinity in WY2008 resulted in an uncertain mathematical relationship. Finally, the salinity
 1915 sensor was unavailable for several months in WY2010. The negative exponential equation
 1916 for each of the remaining 16 water years was solved to predict Q_{S79} required for S_{10} (Q_{calc}):

$$1917 \quad Q_{calc} = \frac{\ln(S_{10}) - \ln(a)}{-b} \quad (7)$$

1919

1920



1921
1922
1923
1924
1925

Figure 13. (A) Time series of average monthly inflow from the S-79 structure to the CRE and average monthly salinity at the Fort Myers monitoring station. (B) Negative relationship between inflow (Q_{S79}) and salinity (S_{FM}) represented by an exponential decay equation. All months from the POR, WY1993–WY2013, are included.

1926
1927

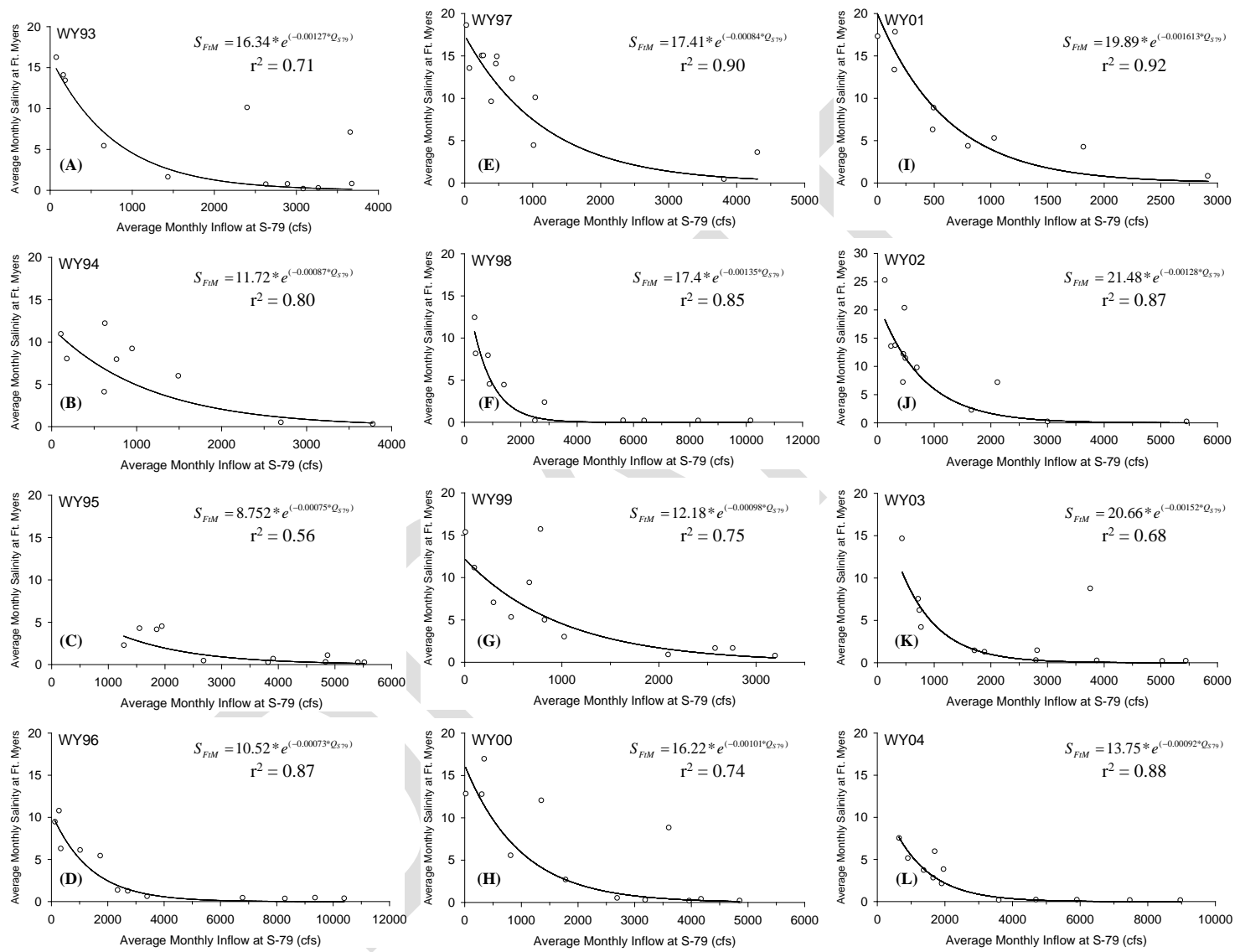
1928 **Results**

1929 Average monthly inflows varied both intra- and inter-annually from WY1993 to
1930 WY2013 (**Figure 14A-U**). As noted, inflows were extremely low (<300 cfs) in WY2008
1931 (**Figure 14P**). The maximum monthly inflows were comparatively low in WY1993 (1,997
1932 cfs), WY1994 (1,073 cfs), WY1997 (1,069 cfs), WY1999 (1,238 cfs), WY2000 (2,256
1933 cfs), WY2001 (664 cfs), WY2002 (1,291 cfs), WY2003 (2,500 cfs), WY2009 (1,397 cfs),
1934 WY2011 (1,576 cfs), and WY2013 (1,585 cfs; Table A2-1). Average monthly salinity at
1935 Fort Myers ranged from 5.5 to 11.0 among these years. By contrast, average monthly
1936 inflows were comparatively high in WY1996 (3,905 cfs), WY1998 (3,445 cfs), WY2004
1937 (3,394 cfs), WY2005 (2,817 cfs), and WY2006 (5,074 cfs; **Table 7**). Average monthly
1938 salinities were 3.9, 3.8, 2.7, 5.1, and 2.0, respectively, for these water years under
1939 comparatively higher freshwater inflow.

1940 The degree of fit (r^2) for the relationship between average monthly inflow and average
1941 monthly salinity at Fort Myers ranged from 0.71 to 0.96 among 17 water years (**Table 7**).
1942 r^2 was lowest in WY1993 (0.71) and WY2003 (0.68) and greatest in WY2001 (0.92),
1943 WY2009 (0.93), WY2011 (0.96), and WY2013 (0.93). Q_{calc} to achieve S_{10} at Fort Myers
1944 ranged from 70 cfs (WY1996) to 773 cfs (WY2013) with an average (\pm standard deviation)
1945 of 445 ± 218 cfs over all water years (**Figure 15**).

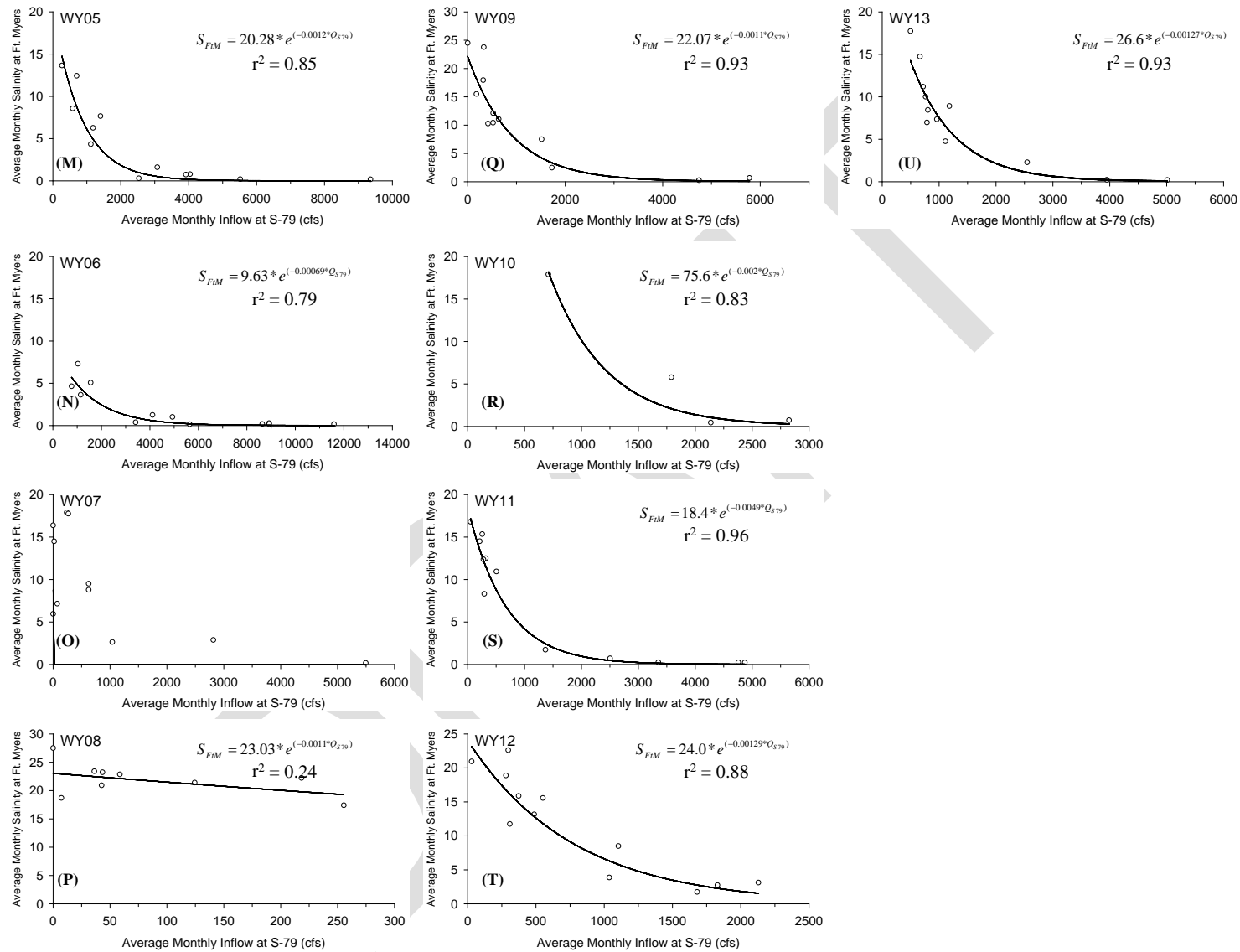
1946 **Discussion**

1947 This study demonstrated that the amount of freshwater inflow at the head of the CRE
1948 varies greatly both intra- and inter-annually. This has implications for attempts to establish
1949 inflow requirements to the estuary. The quantity of freshwater delivered from S-79
1950 associated with a salinity target of 10 at Fort Myers varied from 70-773 cfs depending upon
1951 the contribution from the downstream Tidal Basin. In fact, the amount of ungauged
1952 freshwater input from the Tidal Basin is likely to be a key component to the total freshwater
1953 budget for the estuary. Modeling of freshwater inputs from tributaries and groundwater in
1954 the downstream Tidal Basin is ongoing and these inputs have been incorporated into the
1955 CRE CH3D Model (Wan et al. 2013).



1956
1957
1958

Figure 14A–L. Series of scatter plots and fitted exponential decay equations between average monthly inflow at S-79 (cfs) and average monthly salinity at the Fort Myers monitoring station since WY1993.



1959
1960
1961

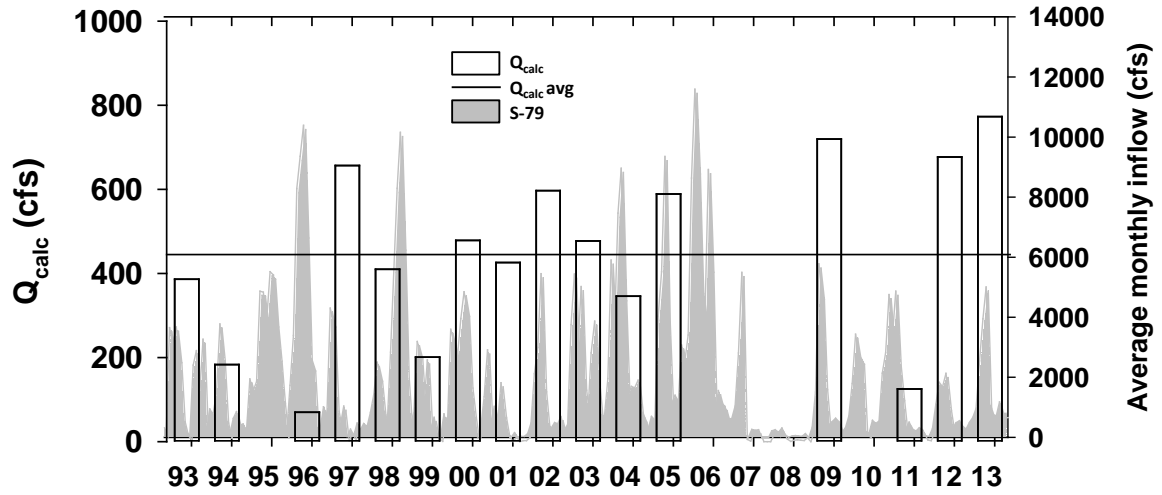
Figure 14M–U. Series of scatter plots and fitted exponential decay equations between average monthly inflow at S-79 (cfs) and average monthly salinity at Fort Myers since WY1993.

1962
1963
1964
1965
1966

Table 7. Summary from analysis of average monthly inflow at S-79 (cfs) and average monthly salinity at Fort Myers. An exponential decay curve was used to describe the relationship between the average monthly values for each water year. Table values for each water year include the average inflow (Q_{S79}) and salinity at Fort Myers (S_{FtM}), curve fit parameters (r^2 , a , and b), and the calculated inflow to achieve a salinity of 10 at Fort Myers (Q_i).

Water Year	Q_{S79} (cfs)	S_{FtM}	r^2	a	b	Q_i (cfs)
1993	1,997	5.5	0.71	16.34	0.00127	386
1994	1,073	7.0	0.80	11.72	0.00087	183
1995	3,152	1.4				
1996	3,905	3.9	0.87	10.52	0.00073	70
1997	1,069	11.0	0.90	17.41	0.00084	657
1998	3,445	3.8	0.85	17.40	0.00135	410
1999	1,238	6.4	0.75	12.18	0.00098	201
2000	2,256	6.1	0.74	16.22	0.00101	479
2001	664	12.0	0.92	19.89	0.00161	426
2002	1,291	10.3	0.87	21.48	0.00128	597
2003	2,500	3.9	0.68	20.66	0.00152	477
2004	3,394	2.7	0.88	13.75	0.00092	346
2005	2,817	5.1	0.85	20.28	0.00120	589
2006	5,074	2.0				
2007	953	8.8				
2008	113	21.6				
2009	1,397	11.4	0.93	22.07	0.00110	720
2010	1,516	7.5				
2011	1,576	7.8	0.96	18.40	0.00487	125
2012	844	11.6	0.88	24.00	0.00129	677
2013	1,585	7.7	0.93	26.63	0.00127	773
Average	1,993	7.6				445 ± 218

1967



1968
1969
1970

1971

Figure 15. Time series of the calculated amount of freshwater inflow from S-79 associated with a salinity of 10 at Fort Myers (Q_{calc}). The average Q_{calc} is shown (445 cfs).

DRAFT

1972 **Component Study 3: Relationships between Freshwater Inflows**
1973 **and Water Quality Attributes during the Dry Season in**
1974 **Caloosahatchee River Estuary**

1975 *Christopher Buzzelli, Peter Doering, Teresa Coley, and Zhiqiang Chen*

1976 **Abstract**

1977 Decreased flushing with reduced inflow can lead to the deposition of phytoplankton
1978 biomass and bottom water hypoxia in estuaries. The highest CHL and lowest DO
1979 concentrations occur in the upper CRE under low inflows. This study component utilized
1980 event-scale water quality data, long-term monitoring of CHL, and simulation modeling of
1981 phytoplankton dynamics to evaluate low freshwater inflows that could contribute to water
1982 quality problems in the upper CRE. Although more research is needed, it is hypothesized
1983 that dry season inflows of less than approximately 500-600 cfs may promote bottom water
1984 hypoxia in the deeper channel of the upper CRE. Field and model results indicated that
1985 CHL concentrations greater than the water quality standard of $11 \mu\text{g L}^{-1}$ were associated
1986 with inflows of 469 ± 689 cfs and 269 ± 493 cfs, respectively. Low level inflows (<500
1987 cfs) need to be further studied to better quantify the discharge required to mitigate the
1988 potential for hypoxia in the upper CRE.

1989 **Introduction**

1990 Bottom water hypoxia (DO concentrations ≤ 3 milligrams per liter [mg L^{-1}]) is
1991 increasingly common in many estuaries (Diaz and Rosenberg 2008, Committee on
1992 Environment and Natural Resources 2010). Recurring hypoxia negatively impacts benthic
1993 fauna, fish populations, fishery harvest, and ecosystem energy flow (Breitburg 2002,
1994 Powers et al. 2005, Diaz and Rosenberg 2008, Rabalais et al. 2010). The potential for
1995 bottom water hypoxia is directly related to phytoplankton blooms as phytoplankton detritus
1996 stimulates DO consumption below the pycnocline (Paerl et al. 2006, Livingston 2007,
1997 Kemp et al. 2009, Committee on Environment and Natural Resources 2010). Processes can
1998 be complex due to spatial and temporal lags among hydrodynamic drivers, phytoplankton
1999 production and deposition, and bottom water hypoxia.

2000 Relationships between freshwater inflow and phytoplankton production in estuaries are
2001 dependent upon the time scales of transport, growth, and grazing (Cloern et al. 2014).
2002 Reduced inflow can promote phytoplankton blooms through longer water residence time,
2003 decreased vertical mixing, and enhanced light in the surface layer (Lancelot and Muylaert
2004 2011, Wan et al. 2013, Cloern et al. 2014). Anthropogenic factors such as increased water
2005 temperature from climate change, reductions in filter feeders, and increased nutrient loads
2006 can stimulate phytoplankton production in excess of consumption (Kemp et al. 2009).
2007 Phyto-detritus not consumed or transported downstream reaches bottom sediments through
2008 vertical settling (Cloern et al. 2014).

2009 Estuarine phytoplankton production can be viewed on annual, seasonal, and event
2010 (<1 month) time scales (Cloern and Jassby 2009). Phytoplankton dynamics at the event-
2011 scale can be particularly acute in small estuaries with subtropical climate and managed
2012 freshwater inflows (Schlacher et al. 2008, Buzzelli 2011, Azevedo et al. 2014).
2013 Phytoplankton responses to pulsed river discharges are sometimes modulated by
2014 zooplankton grazing (Wolanski et al. 2004). However, low flow conditions favor

2015 phytoplankton growth in excess of loss, upstream migration of the chlorophyll maximum
2016 (CHL_{max}), and hypoxia in the upstream bottom water (Schlacher et al. 2008). Upstream
2017 encroachment of CHL_{max} is common for micro-tidal Gulf of Mexico estuaries with
2018 subtropical climates and vertical stratification under reduced flushing (Murrell et al. 2007).
2019 The CRE possesses many of these characteristics.

2020 Changes to freshwater inflow have altered salinity regimes and the overall ecology of
2021 the estuary (Chamberlain and Doering 1998a, Barnes 2005). The CHL_{max} (~30 µg L⁻¹)
2022 moves upstream towards the water control structure at the estuarine head (S-79) under low
2023 inflows (0–500 cfs; Doering et al. 2006, Tolley et al. 2010, Radabaugh and Peebles 2012,
2024 Buzzelli et al. 2014a). When this occurs, the highest CHL and lowest DO concentrations
2025 can be coincidentally located upstream (Doering and Chamberlain, 1998). Like many
2026 estuaries, hypoxia develops through increased residence time, reduced vertical mixing, and
2027 increased deposition of phyto-detritus (Tolley et al. 2010, Radabaugh and Peebles 2012).
2028 This process was particularly evident in 2000 as the CRE experienced a decline in bottom
2029 water DO one to two months following a phytoplankton bloom (Doering et al. 2006).
2030 Reduced freshwater inflow results in the proliferation of diatoms in the upper CRE (Tolley
2031 et al. 2010). While this can stimulate the food web, unconsumed phyto-detritus can
2032 contribute to bottom water hypoxia.

2033 There is limited information on the effects of low level freshwater inflows on patterns
2034 of salinity and water quality in the CRE. Additionally, it is very difficult to rely on the CHL
2035 concentration as an indicator of freshwater inflow. This is because CHL is itself an
2036 uncertain indicator of a variety of non-linearly related physical, biogeochemical, and
2037 biological processes (Buzzelli 2011, Cloern et al. 2014). The objective of this study
2038 component was to consider relationships between freshwater inflows and water quality
2039 attributes during the dry season. Of interest were freshwater discharges that position the
2040 CHL_{max} in the upper estuary, thus potentially enhancing deposition of phyto-detritus and
2041 hypoxic conditions in the bottom waters. This was accomplished through three synergistic
2042 approaches. First, fine-scale detection of water quality gradients with managed freshwater
2043 inflows (Adaptive Protocol Release Study [APRS]) was applied to better understand
2044 patterns at the event scale in the dry season. Second, analysis of long-term monitoring data
2045 provided a platform to examine patterns of CHL with intra- and inter-annual variations in
2046 inflow. Finally, a simulation model of phytoplankton dynamics was used to examine CHL
2047 patterns with variable transport and material cycling in the upper CRE over a range of
2048 scales.

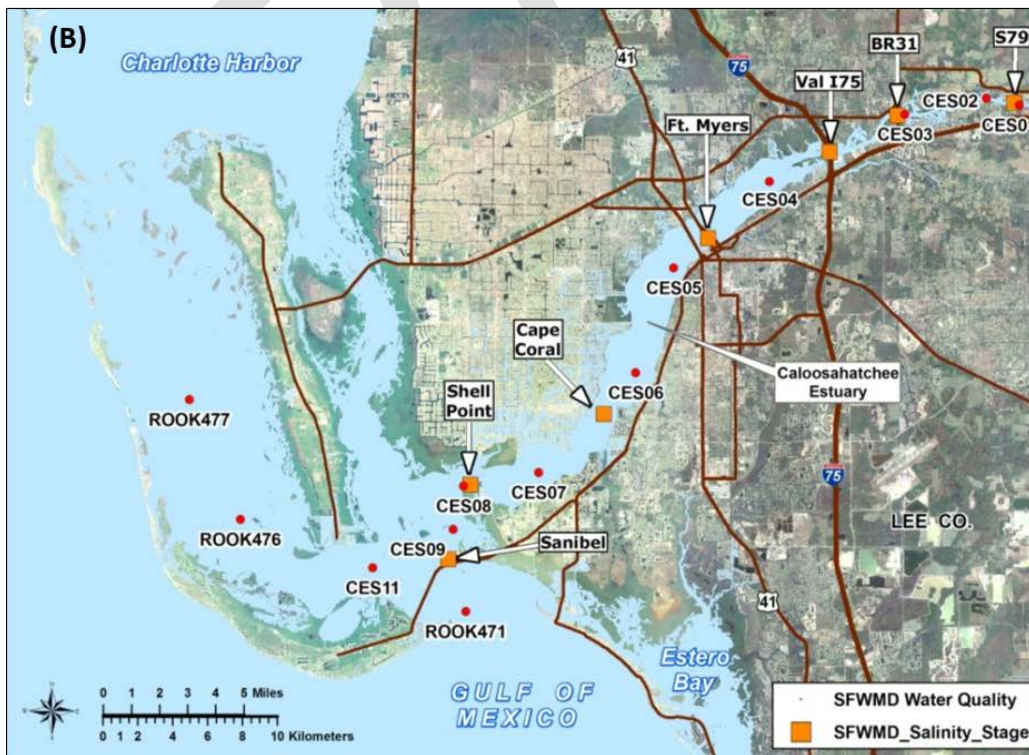
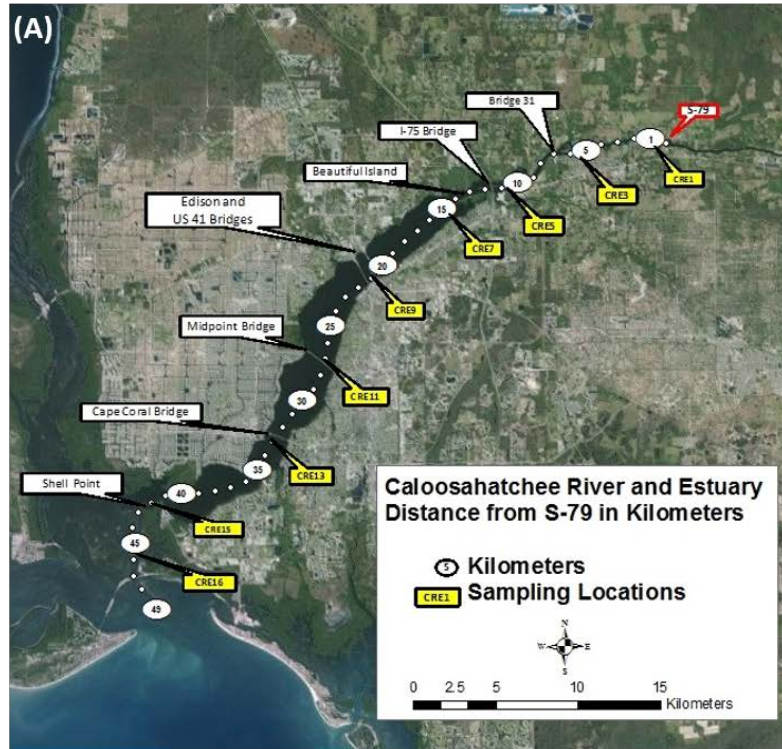
2049 **Methods**

2050 ***Adaptive Protocol Release Study***

2051 This study presented a unique opportunity to evaluate the potential effects of short-term
2052 inflows on water quality and plankton abundances during the dry season. It was unique
2053 because it combined the operational capacity to regulate inflow through S-79 with
2054 ecological responses along the CRE salinity gradient and rapid in situ data acquisition (e.g.,
2055 flow-through system; Madden and Day 1992, Lane et al. 2007, Buzzelli et al. 2014a).

2056 The APRS focused on the event scale to assess potential effects of short-term pulses of
2057 fresh water on water column ecological attributes along the length of the CRE. A total of
2058 23 APRS research cruises were conducted during in dry seasons (November – April)

2059 between January 2012 and April 2014. The cruises utilized a combination of continuous
2060 flow-through technology and a series of vertical sampling stations. Cruises covered a total
2061 distance of ~42 km from S-79 to San Carlos Bay (**Figure 16**).



2062

2063 **Figure 16. (A)** Map of the CRE in Southwest Florida from the Adaptive Protocol Release Study
2064 showing the major structures (S-79 and bridges), the distance downstream of S-79 (white circles),
2065 and the locations for the nine vertical profiling stations (yellow call-outs). **(B)** Site map for
2066 monitoring in the CRE.

2067 The flow-through system offers a novel method of acquiring in situ surface water data
2068 while the research vessel is under way. The system consists of an intake ram attached to
2069 the stern, a flow meter, a Trimble global position system (GPS), an YSI 6600 multi-probe
2070 instrument, a bathymetric profiler, and a laptop computer with Streamline GEO software.
2071 The YSI 6600 was set up to record temperature, salinity, pH, turbidity, DO, and in situ
2072 CHL every 5 seconds. The intake ram was at 0.5 m below the water surface with an in-line
2073 pump to ensure continuous water flow through the system. Streamline Geo software
2074 permitted integration of the GPS and surface water data into an ArcGIS shape file useful
2075 both to display surface water properties in real time and for the post-processing of spatial
2076 data. Approximately 7–8 hours were required to travel from S-79 to San Carlos Bay at an
2077 average speed of 15.2 km per hour resulting in an average distance of 15–26 m between
2078 surface water recordings (Buzzelli et al. 2014a).

2079 Patterns of surface water salinity and CHL with distance downstream from S-79 from
2080 three dates in 2012 (March 8, March 21, and April 12) were included in this study. Since
2081 the cruises occurred approximately every two weeks, the downstream location of the
2082 maximum CHL concentration (CHL_{max}) on each date was plotted versus freshwater inflow
2083 at S-79 averaged over the previous 14 days. All the cruise dates from 2012 and 2013 were
2084 included in a separate assessment of the longitudinal variation in isohalines and the
2085 CHL_{max} . Cruise data taken under higher discharges in 2014 (0–2,030 cfs; 761 ± 569 cfs)
2086 were omitted from this analysis.

2087 On each of the cruises, the research vessel stopped at several mid-channel stations
2088 along the mid-estuary axis to conduct vertical profiling of temperature, salinity, pH, DO,
2089 turbidity, and CHL with the YSI 6600 multi-probe instrument. Recordings using the multi-
2090 probe instrument occurred at 1-meter intervals between the surface and bottom allowing
2091 for instrument stabilization between successive recordings. The vertical profiles for
2092 salinity, CHL, and DO were interpolated in two-dimensions (distance and depth) using a
2093 kriging technique to compare patterns among the three selected cruise dates.

2094 ***Long-Term Monitoring of Chlorophyll a***

2095 Water quality concentrations are monitored at approximately monthly intervals at
2096 multiple locations in the CRE (stations beginning with CES; **Figure 16B**). These data are
2097 available from SFWMD's DBHYDRO database, which can be accessed via the following
2098 link: http://www.sfwmd.gov/dbhydroplsql/show_dbkey_info.main_menu. CHL
2099 concentrations at CES03 in the upper CRE from April 1999 to April 2014 were included
2100 in this assessment. Since the relationships between freshwater inflow and estuarine
2101 indicators are often lagged in time and space, CHL was related to inflow averaged over
2102 different time periods. The monitoring dates were combined with a freshwater inflow series
2103 at S-79, which included the inflow on the sampling date (0 day) and inflow averaged 7 to
2104 35 days prior. The relationship between CHL concentrations at CES03 was plotted over all
2105 time periods. The combined CHL-inflow data set was queried to determine freshwater
2106 inflows associated with the Impaired Waters Rule (Rule 62-303.353, Florida

2107 Administrative Code) annual average CHL value of $11 \mu\text{g L}^{-1}$. This exercise resulted in the
2108 determination of freshwater inflows linked to increased phytoplankton production in the
2109 upper CRE.

2110 ***Segmented Simulation Model of the Caloosahatchee River Estuary***

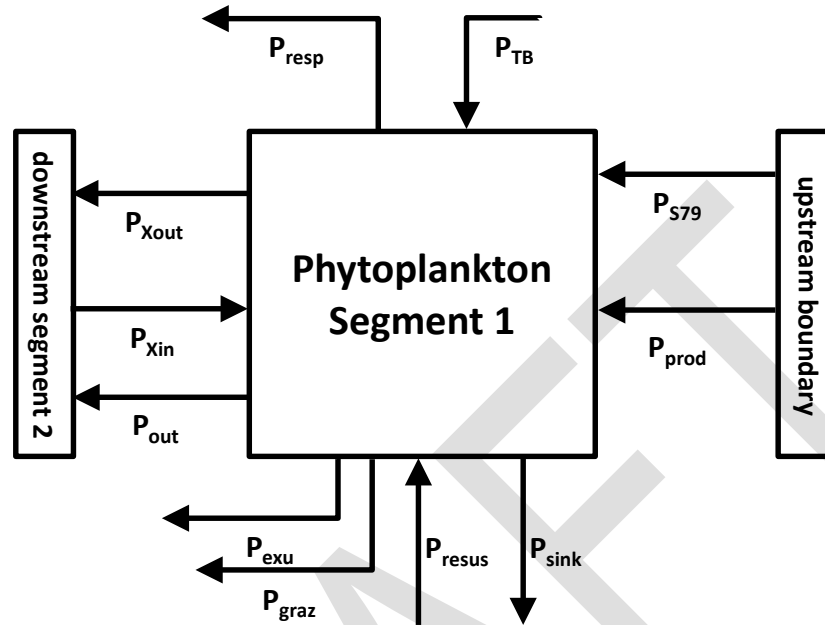
2111 The CRE was split into three segments for development of a simulation modeling
2112 framework (Buzzelli et al. 2014b, 2014c). This model application focused on Segment 1
2113 in the upper CRE (16.1 km from S-79; 1.5×10^7 square meters [m^2]; $2.1 \times 10^7 \text{ m}^3$, see
2114 **Figure 16** for River km). The model framework includes a box model for transport,
2115 external inputs, forcing functions that drive model processes, and biogeochemical process
2116 equations and coefficients (Buzzelli et al. 2014b). The biogeochemical models use an
2117 integration interval of 0.03125 days (45 minutes) over simulations spanning 2,922 days
2118 from 2002 to 2009. The box model was driven by daily time series for freshwater inflow
2119 at the estuarine head and salinity for each segment and the downstream boundary. Physical
2120 transport of a water column constituent was the sum of advection, lateral inputs from
2121 tributaries and ground water, and non-tidal dispersion. The time series for estuarine head
2122 from 2002 to 2009 (2,922 days) at S-79 was derived from DBHYDRO. The loadings of
2123 water column constituents at the upstream boundary were calculated as the product of the
2124 estuarine head and average monthly concentrations.

2125 A watershed model was used to estimate the daily lateral input from tributaries and
2126 ground water (Y. Wan, unpublished data). The loadings of water column constituents from
2127 the tributaries and ground water were the product of the lateral inflows to each segment
2128 and the corresponding average monthly input concentration derived from Lee County,
2129 Florida monitoring stations. Time series for the average daily salinity of each segment were
2130 generated using a predictive statistical model developed for the CRE (Qiu and Wan 2013).

2131 Each of the three segments included a water column submodel to simulate the
2132 concentration of phytoplankton carbon, organic nitrogen and phosphorus, ammonium,
2133 nitrate-nitrite, ortho-phosphate, and sediment microalgae. Biogeochemical processes were
2134 modulated by variations in temperature, depth, and submarine light. The total attenuation
2135 coefficient for submarine light contained contributions from pure water, color, turbidity,
2136 and CHL. Attenuation due to color was estimated using a negative exponential relationship
2137 with average salinity of the segment (McPherson and Miller 1994, Bowers and Brett 2008,
2138 Buzzelli et al. 2012). Time series for the average turbidity of each segment were derived
2139 from monitoring data available through DBHYDRO. Phytoplankton was a key variable
2140 since it receives external inputs of CHL from the watershed, is the primary sink for
2141 inorganic nitrogen and phosphorus, is the primary source of autochthonous organic
2142 nitrogen and phosphorus, is important in submarine light extinction, and serves as an
2143 ecological indicator (Doering et al. 2006, Buzzelli 2011, Buzzelli et al. 2014b). The amount
2144 of phytoplankton biomass (e.g. CHL) is calculated every time step depending upon five
2145 source terms (input from S-79, input from the Tidal Basin, production, resuspension from
2146 the bottom, and dispersion) and six sink terms (downstream outflow, dispersion,
2147 respiration, sinking, exudation, and grazing; **Figure 17**).

2148 Dry season (November–April) results from the base model simulations (2002–2009) in
2149 Segment 1 were used in this study. Daily model predictions of CHL in the upper CRE were
2150 calibrated using monthly CHL concentrations averaged among the S-79, CES01, CES02,
2151 and CES03 locations (Buzzelli et al. 2014b). Similar to the field data, the model output was

2152 queried to determine freshwater inflows associated with the Impaired Waters Rule annual
 2153 average CHL value of $11 \mu\text{g L}^{-1}$. This exercise resulted in the determination of the desirable
 2154 freshwater inflows below which there was the potential for phytoplankton blooms in the
 2155 upper CRE.



- P_{in} = Input from upstream boundary
- P_{prod} = Gross production
- P_{TB} = Input from the tidal basin
- P_{resp} = Respiration
- P_{sink} = Sinking from water column
- P_{resus} = Resuspension from bottom
- P_{graz} = Loss to grazing
- P_{exu} = Loss to exudation
- P_{Xin} = Upstream non-tidal exchange
- P_{Xout} = Downstream non-tidal exchange
- P_{out} = Downstream transport

$$dPhytdt^{-1} = [(P_{S79} + P_{TB} + P_{prod} + P_{resus} + P_{Xin}) - (P_{out} + P_{Xout} + P_{resp} + P_{sink} + P_{exu} + P_{graz})]$$

2156
 2157 **Figure 17.** Schematic and definition of process terms that influence phytoplankton biomass (e.g.
 2158 CHL) in the simulation model for the CRE.

2159

2160 **Results**2161 ***Adaptive Protocol Release Study***

2162 Freshwater inflow to the CRE through S-79 declined from January to March 2012
 2163 before reaching 0.0 cfs on March 27, 2012 (Buzzelli et al. 2014a). Two-week average
 2164 inflow decreased from 627.8 cfs to 556.3 cfs between March 8 and March 21 (**Table 8**).
 2165 There were a total of 1,559, 2,177, and 2,085 surface water recordings along the length of
 2166 the CRE on March 8, March 21, and April 12, respectively (Buzzelli et al. 2014a). These
 2167 highly resolved spatial data permitted visualization of the longitudinal patterns of salinity
 2168 and CHL with changes in freshwater inflow (Fig. A3-3). The locations of the salinity of 10
 2169 isohaline moved upstream with reduced inflow; it was located 14.6 km from S-79 on March
 2170 8 but only 0.7 km from S-79 on April 12 (**Table 8**). Salinity ranged 5 to 6 from 0 to 14 km
 2171 downstream before increasing from 6 to 35 over the remaining 26 km on March 8 (**Figure**
 2172 **18A**). There were obvious variations in salinity along the length of the CRE on this date.
 2173 On March 21, salinity ranged from 6 to 7 over the initial 10 km after which it increased
 2174 linearly with distance downstream. Finally, salinity at S-79 was ~10 on April 12 after the
 2175 cessation of inflow. It increased gradually down to ~14 km before exhibiting a smooth,
 2176 linear increase over the remaining length of the estuary.

2177 **Table 8.** Results from the APRS on the CRE in the 2012 dry season. Included are the 14-day
 2178 average inflow at S-79 (Q_{S79}), the location of the salinity of 10 isohaline in km from S-79 (S_{10}),
 2179 and the location and value for the maximum concentration of chlorophyll a (CHL_{max}).

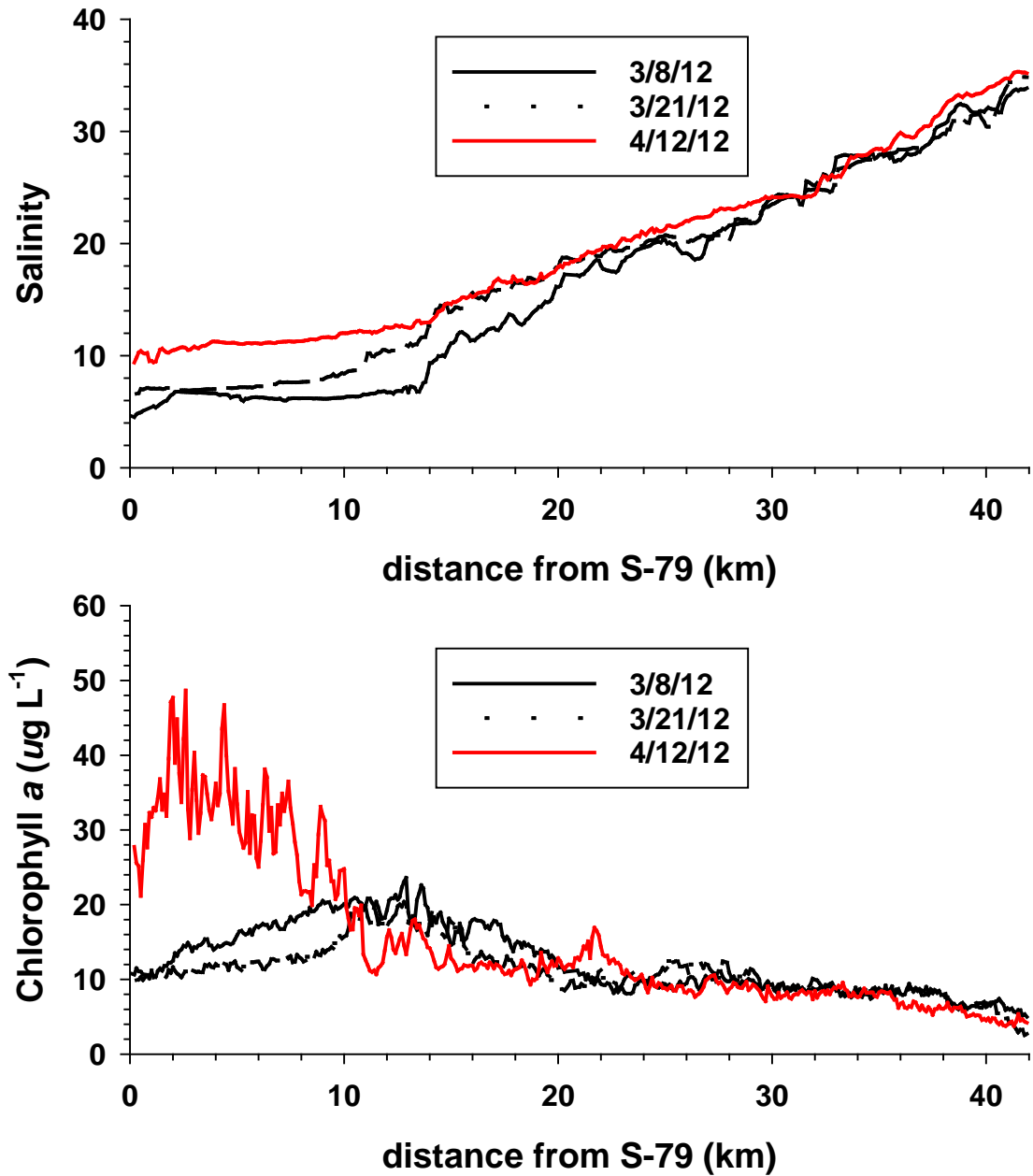
Date	Q_{S79} (cfs)	S_{10} (km)	CHL_{max} (km)	CHL_{max} ($\mu\text{g L}^{-1}$)
3/8/12	627.8	14.6	12.9	11.1
3/21/12	556.3	11.1	12.8	10.2
4/12/12	0.0	0.7	2.6	25.6

2180

2181 Similar to the salinity of 10 isohaline, the CHL_{max} migrated upstream with reduced
 2182 discharge. While it was located at 12.8 km downstream of S-79 on March 21, it moved
 2183 upstream to 2.6 km as inflow decreased leading up to the April 12 cruise (**Table 8**). There
 2184 was great variability in CHL (20–48 $\mu\text{g L}^{-1}$) from 0 to 10 km on April 12 compared to the
 2185 previous two cruise dates (**Figure 18B**). Thus, the location of the CHL_{max} in the upper
 2186 estuary increased dramatically from 10.2 $\mu\text{g L}^{-1}$ on March 21 to 25.6 $\mu\text{g L}^{-1}$ on April 12
 2187 (**Table 8**). CHL declined to 10–15 $\mu\text{g L}^{-1}$ from 20 to 42 km downstream on all three cruise
 2188 dates.

2189

2190



2191

2192

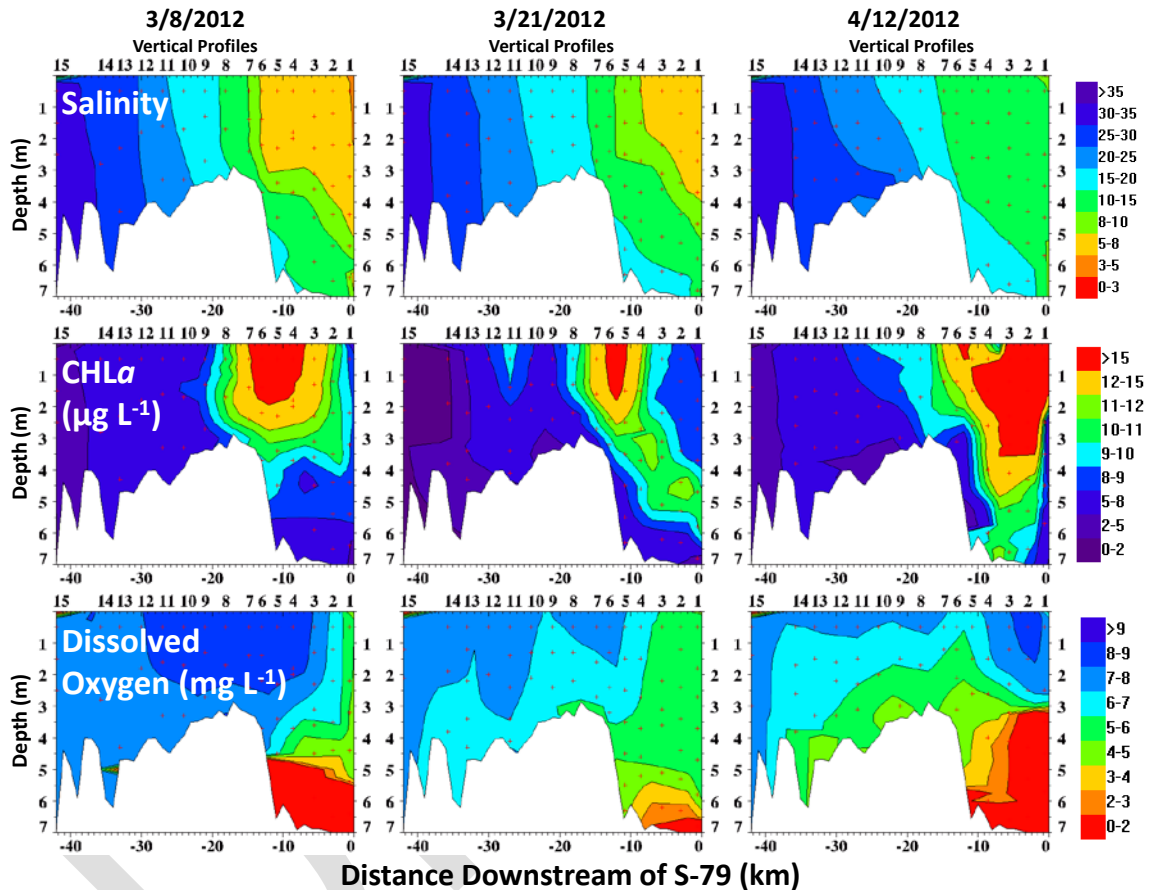
2193

2194

Figure 18. Results of the APRS from March 8, 2012, March 21, 2012, and April 12, 2012: (A) surface water salinity versus distance downstream of S-79; and (B) surface water CHL versus distance downstream of S-79.

2195

2196 Interpolated contour plots derived from the vertical profiles validated upstream salinity
 2197 and CHL encroachment as inflow decreased (**Figure 19**). These profiles and plots
 2198 illustrated depth-dependent patterns including a surface lens of freshwater that contributed
 2199 to vertical salinity stratification on March 8 (**Figure 19**, top left; Buzzelli et al. 2014a). It
 2200 appeared that the vertical stratification evident in March gave way to horizontal gradients
 2201 as saltier water moved upstream by April (**Figure 19**, top center and top right). There
 2202 appeared to be a topographic influence on hydrodynamic and biogeochemical processes
 2203 due to the decrease in depth from 6 km (~7 m) to 15 km (~2.5 m) downstream of S-79.



2204

2205 **Figure 19.** Interpolated depth versus distance contour plots derived from vertical profiling from
 2206 the APRS for three different cruise dates. The APRS station designations shown in **Figure 16A**
 2207 are provided along the top of each plot. The horizontal axis is oriented from right to left to
 2208 represent distance downstream of S-79. The vertical axis is depth. The top three plots show
 2209 salinity ranging from 0 to 3 to >35.0. The middle three plots show CHL ranging from 0 to 2 to
 2210 >15.0. The bottom three plots show DO concentrations ranging from 0 to 2 to >9.0.

2211

2212 The CHL_{max} was located ~13 to 20 km downstream under inflows of 500 to 1,000 cfs
2213 over all cruises in 2012 and 2013 (**Figure 20**). Thus, the CHL_{max} extended vertically down
2214 a couple of meters as it was located in a shallower area of the estuary. This was evident on
2215 March 8 followed by a slight deepening of the surface layer CHL_{max} on March 21 (**Figure**
2216 **19** middle left and middle center). The estuarine water parcel containing a greater amount
2217 of phytoplankton biomass located farther upstream on April 12 extended much deeper in
2218 the water column (~4.5 m; **Figure 19**, right center). These attributes of depth, inflow, and
2219 primary production affect the potential for bottom water hypoxia in the upper CRE (**Figure**
2220 **19**, bottom row). Although there were bottom water DO concentrations ≤ 3 mg L⁻¹ on
2221 March 8 and March 21, the vertical and horizontal extent of bottom water hypoxia was
2222 much greater on April 12.



2223
2224 **Figure 20.** Hyperbolic relationship between average (avg) freshwater inflow 14 days (d) before
2225 cruise date for the APRS and the location of the CHL_{max} in surface water of the CRE. Results
2226 from all cruises from dry seasons in 2012 and 2013 (n = 15).

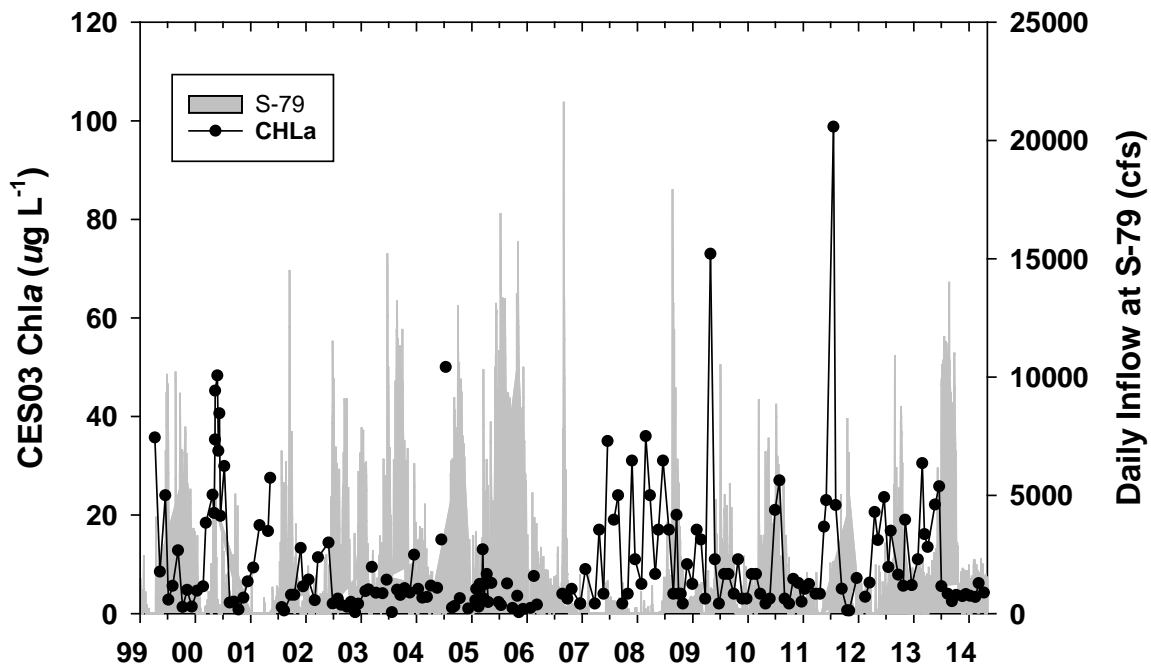
2227

2228 **Long-Term Monitoring of Chlorophyll a**

2229 CHL at CES03 (7 km downstream of S-79) ranged from a minimum of $0.3 \mu\text{g L}^{-1}$ to
 2230 maximum values of 73.0 and $98.8 \mu\text{g L}^{-1}$ in the dry and wet seasons, respectively (**Table**
 2231 **9** and **Figure 21**). CHL was low ($<10 \mu\text{g L}^{-1}$) from 2002 to 2006 but appeared to be more
 2232 variable from 2007 to 2011. The highest values were observed on April 28, 2009 ($73.0 \mu\text{g}$
 2233 L^{-1}) and July 20, 2011 ($98.8 \mu\text{g L}^{-1}$). The seasonally averaged concentrations were highly
 2234 variable in dry and wet seasons (8.6 ± 10.2 and 12.2 ± 15.0 , respectively). The coefficient
 2235 of variation was $>100\%$ in both seasons. Averaging inflow over an increasing number of
 2236 days preceding the field sampling at CES03 did not improve the correlation between the
 2237 observed CHL concentrations and freshwater discharge (**Figure 22**).

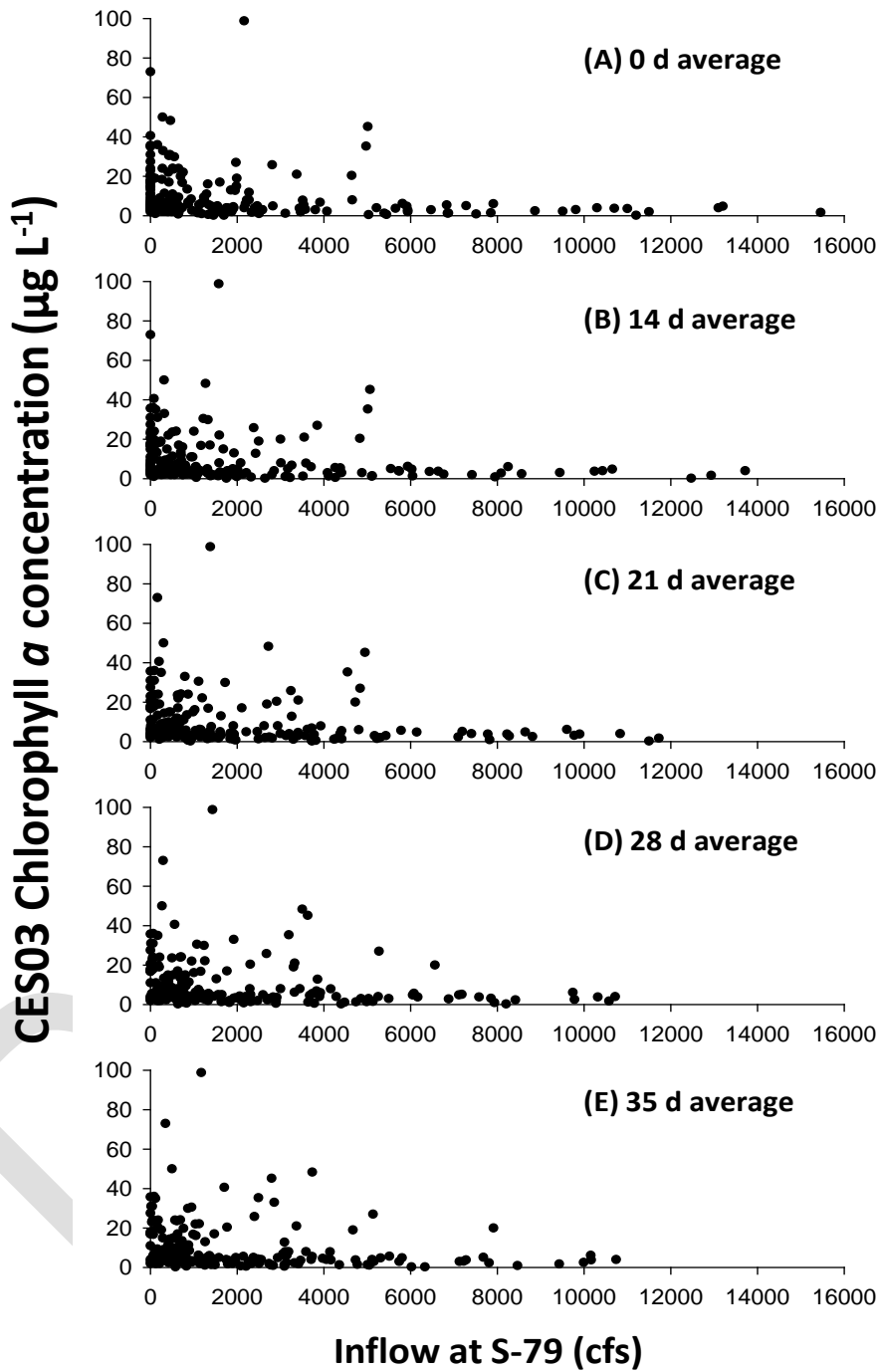
2238 **Table 9.** Descriptive statistics for (CHL ($\mu\text{g L}^{-1}$) at station CES03 in the CRE from April 1999 to
 2239 April 2014. The data set was split into dry (November–April) and wet (May–October) seasons.
 2240 Included are the number of samples, range, median, average and standard deviation (Avg \pm SD),
 2241 and the coefficient of variation expressed as a percentage (CV = (SD/Avg)*100).

Season	Number	Range	Median	Avg \pm SD	CV (%)
Dry	93	0.3–73.0	5.5	8.6 ± 10.2	118
Wet	93	0.3–98.8	5.2	12.2 ± 15.0	123



2242 **Figure 21.** Time series of water column CHL observed at station CES03 in the upper CRE.
 2243 Average daily inflow at S-79 (right axis) is shown in grey.

2244



2245

2246

2247

2248

2249

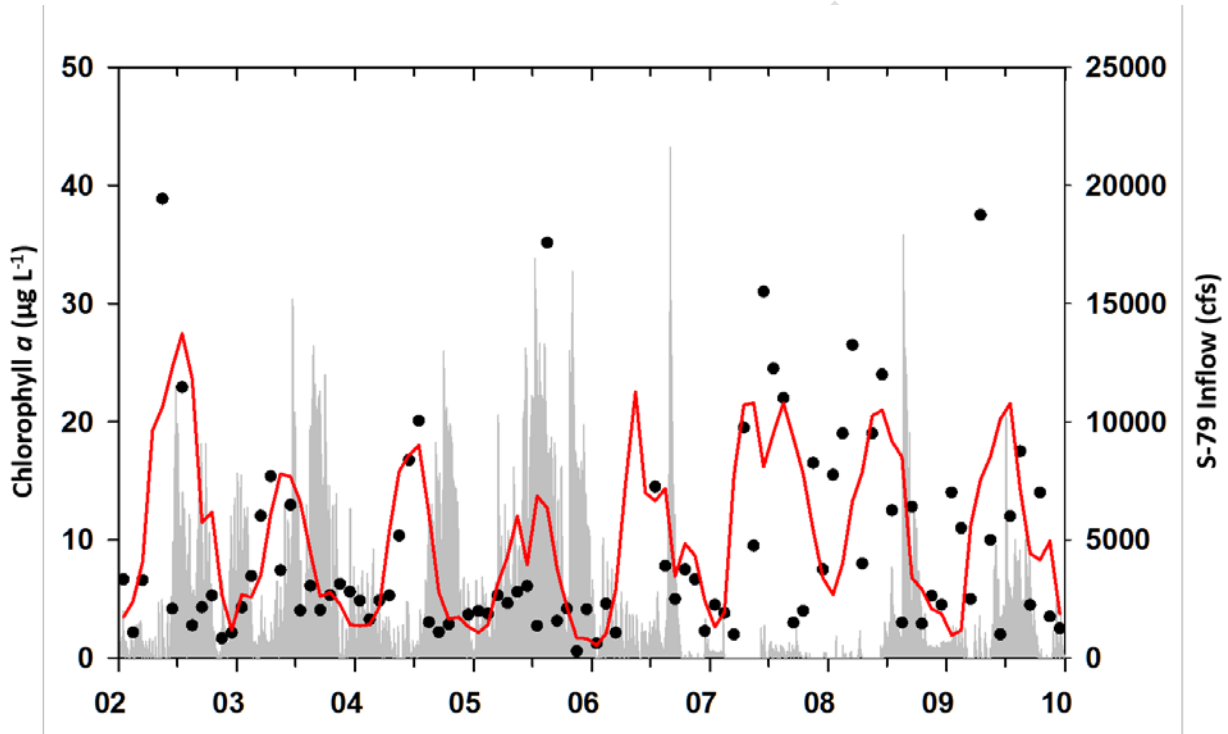
2250

2251

Figure 22. Scatterplots of water column CHL observed at station CES03 in the upper CRE versus the average daily inflow at S-79: (A) inflow on CES03 sampling date; (B) inflow averaged over 14 days (d) prior to the sampling date; (C) inflow averaged over 21 days prior to sampling date; (D) inflow averaged over 21 d prior to sampling date; (E) inflow averaged over 35 days prior to sampling date.

2252 **Segmented Simulation Model of the CRE**

2253 Average daily CHL concentrations predicted for the upper CRE ranged from 0.6 to
 2254 31.3 $\mu\text{g L}^{-1}$ from 2002 to 2009 (**Figure 23**). The model was a reliable predictor as CHL
 2255 approximated the average concentrations determined among multiple stations in the upper
 2256 CRE ($r = 0.61\text{--}0.76$; **Table 10**). Values were generally higher in the wet season (14.2 ± 4.0
 2257 $\mu\text{g L}^{-1}$) compared to the dry season ($6.8 \pm 2.3 \mu\text{g L}^{-1}$; **Table 10**). The simulation model
 2258 predicted that average monthly CHL during the dry season in the upper CRE decreases
 2259 exponentially with increased freshwater inflow (**Figure 24**). However, there was a wide
 2260 range of CHL concentrations that were possible when inflows were <500 cfs.

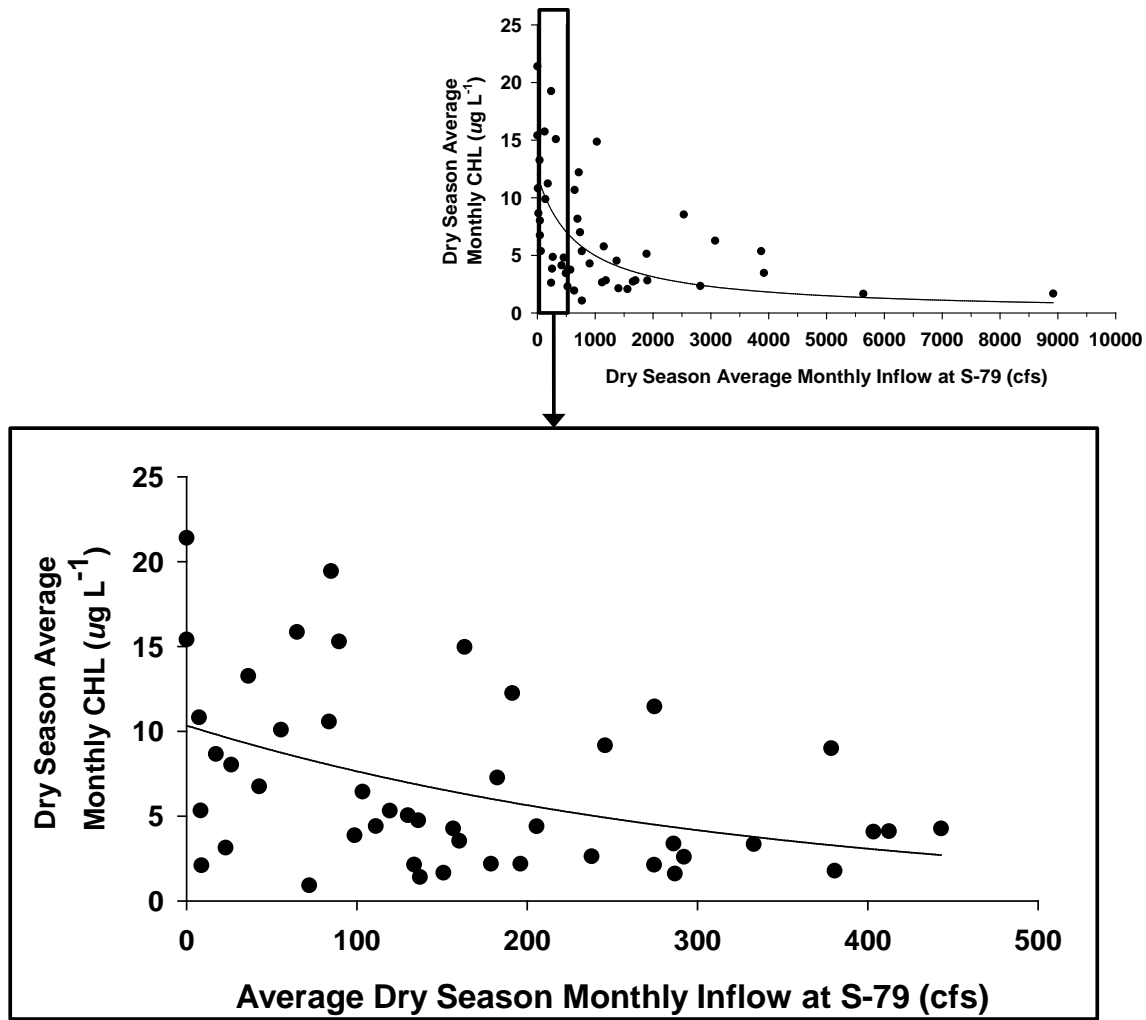


2261
 2262 **Figure 23.** Time series of water column CHL concentration predicted for the upper CRE (0–16
 2263 km downstream of S-79) using the simulation model. Data points represent the average CHL
 2264 concentration averaged among four stations in the upper CRE (S-79, CES01, CES02, and
 2265 CES03). Also shown are daily average flows from S-79.

2266
 2267 **Table 10.** Model calibration results to simulation CHL
 2268 concentration ($\mu\text{g L}^{-1}$) in the upper CRE (0–16 km from S-79)
 2269 from 2002 to 2009. Included are the average + standard
 2270 deviation for pooled monitoring data (CES01, CES02, CES03,
 2271 and S-79) and the model. The correlation coefficient (r) between
 2272 the data and the model was calculated using monthly average
 concentrations ($n = 96$ months).

Season	Data	Model	r
Dry	7.4 ± 4.5	6.8 ± 2.3	0.61
Wet	9.4 ± 3.9	14.2 ± 4.0	0.76

2273
 2274



2275
2276
2277
2278

Figure 24. Results from simulation model of the CRE. Average monthly inflow at S-79 (cfs) versus average monthly CHL concentration ($\mu\text{g L}^{-1}$) in upstream Segment 1. The zoomed scatterplot highlights inflows <500 cfs.

2279 An upper threshold of $11.0 \mu\text{g L}^{-1}$ was used as a critical criterion to query both the field
2280 and model CHL concentrations in the dry season (**Table 11**). There were 24 measurements
2281 of CHL at CES03 that were $>11.0 \mu\text{g L}^{-1}$ (19.5% of all dry season measurements). Daily
2282 average inflows at S-79 ranged from 0 to 2,270 cfs averaging 469 ± 689 cfs over these
2283 measurements. For the model, there were 265 daily predictions of CHL in the upper CRE
2284 that were $>11.0 \mu\text{g L}^{-1}$ (18.3% of dry season simulation days). Inflow at S-79 ranged from
2285 0 to 2,450 cfs averaging 269 ± 493 cfs for this subset of simulated days.

2286

2287 **Table 11.** Summary of daily average inflows at S-79 (cfs) when the CHL concentrations were >11
 2288 $\mu\text{g L}^{-1}$. Results from both field monitoring (top row) and the upper segment of the
 2289 Caloosahatchee River Estuary simulation model (bottom row; Buzzelli et al. 2014b). Water
 2290 column CHL concentrations were determined at station CES03 from April 1999 to April 2014 (n =
 2291 259). Using the model, water column CHL concentrations were predicted for the upper CRE (0 to
 2292 16 km from S-79) every day from 2002 to 2009 (n = 2,120 days). Values include the averages
 2293 and standard deviations (Avg \pm SD) for CHL and the freshwater inflows from S-79 (Q_{S79} ; cfs).
 2294 Results are for dry season days only (November – April) for both the field (n = 123) and model (n
 2295 = 1,450).

Source	Count	CHL $\geq 11 \mu\text{g L}^{-1}$ Avg \pm SD	Q_{S79} (cfs) Avg \pm SD
Data	24 (19.5%)	31.8 \pm 51.4	469 \pm 689
Model	265 (18.3%)	16.1 \pm 3.8	269 \pm 493

2296

2297 Discussion

2298 Reduced freshwater inflow has clear biogeochemical implications for shallow, micro-
 2299 tidal estuaries around the Gulf of Mexico (Murrell et al. 2007, Tolley et al. 2010). Internal
 2300 cycling of materials becomes more important with reduced inflow, overall biological
 2301 productivity can be severely inhibited as freshwater input declines (Livingston 2007).
 2302 These attributes can favor phytoplankton production in excess of transport and grazing and
 2303 the deposition of phyto-detritus in upstream sediments (Radabaugh and Peebles 2012,
 2304 Cloern et al. 2014). Decreased vertical mixing coupled with enhanced deposition of organic
 2305 matter can fuel hypoxia in the bottom water under reduced freshwater inflow (Doering et
 2306 al. 2006, Murrell et al. 2007, Tolley et al. 2010).

2307 Combined results suggested that daily inflows <500 cfs would result in the CHL_{max}
 2308 located less than ~13 km downstream of S-79. This sequence would position the CHL_{max}
 2309 above the deeper channel (~7 m) where bottom water DO concentrations $\leq 3 \text{ mg L}^{-1}$ occur.
 2310 Thus, diminished freshwater inflow could enhance both salinity stratification and the
 2311 deposition of phyto-detritus (Murrell et al. 2007, Radabaugh and Peebles 2012). The
 2312 possibility for hypoxia in the upper CRE is heightened given that both sediment organic
 2313 content and rates of sediment oxygen demand are greater in the upper CRE (Buzzelli et al.
 2314 2013b). Finally, at the estuary scale there is increased heterotrophy (e.g. the respiration of
 2315 organic matter) with reduced freshwater inflow (Buzzelli et al. 2013c).

2316 Previous studies of the CRE have established (1) that high CHL in surface waters is
 2317 correlated with low DO in bottom waters (2) hypoxia occurs most often in the upper estuary
 2318 and (3) that both the magnitude and position of the CHL_{max} depend on freshwater inflow
 2319 (Doering et al 2006, Wan et al 2013, Buzzelli et al. 2014a). Research into fine-scale
 2320 responses of water quality to variable freshwater inflow (APRS) has provided some
 2321 additional insight. While the APRS provides highly resolved spatial and temporal data,
 2322 there have been limited surveys at very low inflows. More cruises need to be conducted at
 2323 inflows of 0 to 500 cfs to better quantify the discharge required to mitigate the potential for
 2324 hypoxia in the upper CRE. These efforts will improve the predictions of CHL_{max} and permit
 2325 quantification of freshwater inflows required to avoid hypoxia in the upper CRE.

2326 The model and field results indicated that freshwater inflows of <269 and 469 cfs were
 2327 associated with CHL concentrations greater than the Impaired Waters Rule standard of
 2328 $11.0 \mu\text{g L}^{-1}$, annual average. Both the empirical and simulation estimates of the inflow

2329 magnitudes are valuable results of this study. Monthly monitoring of CHL concentrations
2330 at specific locations provides an indicator of water quality, but does not account for
2331 dynamic changes in phytoplankton assemblages on scales of hours-weeks. Whereas CHL
2332 is regularly monitored as a proxy for biomass, phytoplankton production is modulated by
2333 non-linear interactions among several environmental drivers (Cloern et al. 2014).
2334 Additionally, many of these biogeochemical interactions are lagged in time and space.

2335 In terms of water quality modeling, the many process-based parameters introduce
2336 uncertainty to the predictions. Confidence in model predictions is largely dependent upon
2337 the quality of both the experimental and calibration data (Buzzelli et al. 2014a).

2338 While this modeling effort has great utility to evaluate estuarine responses over a range
2339 of inflow and nutrient loading conditions, it was highly aggregated spatially (Buzzelli et
2340 al. 2014a, 2014b). The development and implementation of a hydrodynamic-water quality
2341 modeling framework with greater spatial resolution could greatly benefit quantification of
2342 the inflows required to support optimal levels of phytoplankton and other water column
2343 indicators (Wan et al. 2012, Condie et al. 2012, Funahashi et al. 2013, Azevedo et al. 2014).

DRAFT

2344 **Component Study 4: Zooplankton Response to Freshwater**
2345 **Inflow in the Caloosahatchee River Estuary**

2346 *Peter Doering*

2347 **Abstract**

2348 Freshwater inflow to some estuaries, including the CRE, is regulated through control
2349 structures. Zooplankton assemblages provide an essential food web link whose position in
2350 the estuary fluctuates with inflow. Unfortunately, zooplankton habitat can be both
2351 impinged and compressed due to the presence of a water control structure as inflow is
2352 reduced in the dry season. This study assessed impingement and habitat compression for
2353 zooplankton under reduced inflow. Data were from a study of the CRE conducted by
2354 Florida Gulf Coast University from 2008 to 2010. Zooplankton samples were collected
2355 monthly at each sampling site at night during a flood tide. The centers of abundance (COA)
2356 for the 13 taxa investigated migrated downstream and upstream as freshwater inflow
2357 increased and decreased, respectively. Both habitat compression and impingement were
2358 potentially harmful for zooplankton assemblages in the estuary. Impingement was possible
2359 if inflow from S-79 ranged and averaged 98 to 566 cfs and 412 ± 165 , respectively. Almost
2360 all taxa investigated (except *Menidia*) experienced habitat compression if the COA was
2361 <12 km downstream of S-79.

2362 **Introduction**

2363 Like many drowned river-valley type estuaries, the CRE is funnel shaped, being narrow
2364 near its head waters and wide at its mouth. Typically, this geomorphology results in a
2365 longitudinal volumetric gradient increasing from the head to the mouth of the estuary. The
2366 COA for planktonic organisms have been shown to move upstream and downstream as
2367 freshwater inflow decreases and increases, respectively (Peebles et al. 2007). This response
2368 to inflow coupled with the geomorphology of the estuary means that the volume of open
2369 water habitat available to planktonic populations varies with freshwater inflow (Peebles
2370 and Greenwood 2009). If the longitudinal dispersion of the population remains constant,
2371 the volume of water available for occupancy decreases with diminished inflow and the
2372 upstream movement of the organisms. The crowding of organisms into a relatively
2373 confined space (habitat compression; Crowder 1986, Copp 1992, Eby and Crowder 2002)
2374 may result in increased predation and competition for limited food resources. Some
2375 organisms may be forced to utilize habitat that is physiologically suboptimal and this may
2376 result in lower growth and survival (Petersen 2003). Many estuaries, including the CRE,
2377 have water control structures (e.g. dams) that regulate freshwater inflow (Franklin Lock
2378 and Dam or S-79). These structures block upstream movement of planktonic organisms
2379 with reduced inflow and serve as barriers to adult fish migration (impingement; Peebles
2380 and Greenwood 2009). Impingement against a water control structure such as S-79 in the
2381 upper CRE can exacerbate habitat compression.

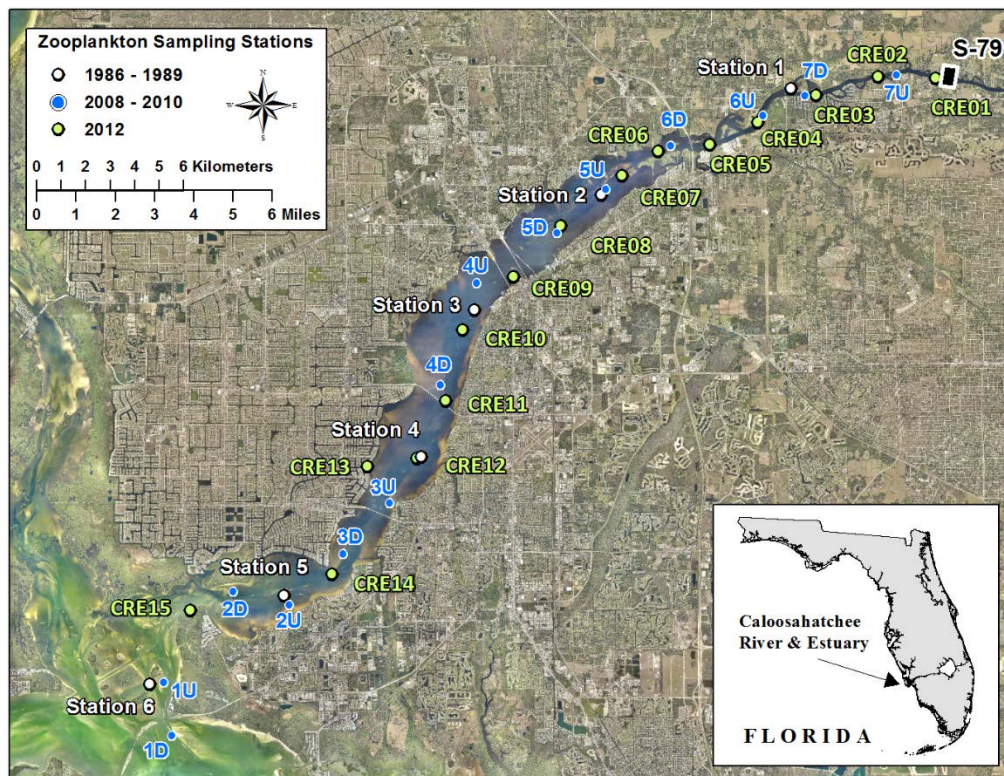
2382 The objectives of this study were to demonstrate the compression of the zooplankton
2383 community with upstream translation in the CRE, demonstrate the occurrence of
2384 impingement of zooplankton against S-79, and determine the discharges at S-79 that
2385 promote habitat compression and impingement.

2386 The source of data for the analysis was a 24-month study of plankton in the
 2387 Caloosahatchee Estuary conducted by Florida Gulf Coast University (May 2008–April
 2388 2010; Tolley et al. 2010). The overall goal of the project was to establish linkages between
 2389 variability in freshwater inflow and ecosystem condition by characterizing and quantifying
 2390 the responses of estuarine phytoplankton, zooplankton, and benthic microalgae. Major
 2391 details of the study design and sampling routine, extracted from Tolley et al. (2010), are
 2392 given below. The present analyses were conducted by SFWMD staff.

2393 Methods

2394 *Florida Gulf Coast University Plankton Surveys 2008–2010*

2395 This study used distance upstream from the estuary mouth to reference stations and
 2396 patterns. A total of seven zones were sampled from Point Ybel, Sanibel in San Carlos Bay
 2397 to S-79. There were two stations (downstream and upstream) within each zone for a total
 2398 of 14 stations per sampling (**Figure 25** and **Table 12**). The use of zones was not based on
 2399 the identification of strata along the estuarine gradient but simply facilitated station
 2400 location and sampling along the ~47-km transect. Zooplankton sampling sites were fixed
 2401 for all collections. The position of the collection vessel was recorded at the beginning of
 2402 each zooplankton tow using GPS. Mean distance between adjacent sampling sites was 3.26
 2403 ± 2.01 km. The system was sampled monthly for 24 months (May 2008–April 2010).



2404

2405 **Figure 25.** Zooplankton sampling stations. Distances in kilometers from Shell Point. The Franklin
 2406 Lock and Dam are located at about 43.5 km upstream of Shell Point. Data collected from 2008 to
 2407 2010 was used in this study.

2408 **Table 12.** Sampling stations for biological and water quality data (May 2008 to April 2010). Depth
 2409 represents the mean maximum water depth recorded at each station during biological sampling.
 2410 (Note: D = downstream and U = upstream stations within each zone, with zones as described
 2411 in text.)

Zone	Station	River (km)	Latitude	Longitude	Depth
1	D	-5.9	26.4776	82.01157	2.92
	U	-3.6	26.49721	82.01514	3.09
2	D	2.5	26.53089	81.98688	3.96
	U	5.2	26.52616	81.96375	2.91
3	D	7.6	26.54528	81.94169	4.06
	U	10.6	26.56413	81.92283	3.88
4	D	16.2	26.60805	81.9022	3.73
	U	20	26.64585	81.88743	2.53
5	D	24.2	26.66452	81.85461	1.97
	U	26.9	26.68076	81.83474	2.03
6	D	30.2	26.69704	81.808	2.97
	U	34.4	26.70864	81.77011	4.38
7	D	37.1	26.71587	81.75259	3.83
	U	41.0	26.72397	81.71516	1.64

2412

2413 Zooplankton samples were collected monthly at each sampling site at night during a
 2414 flood tide. Standard zooplankton collection gear consisted of a 500-micrometer Nitex
 2415 mesh, 0.5-m mouth diameter, conical (3:1 aspect ratio) plankton net, equipped with a three-
 2416 point bridle, 1-liter cod-end jar, 20 kilograms of weight suspended from the mouth ring,
 2417 and a General Oceanics model 2030R flowmeter suspended at the center of the net's mouth.
 2418 Deployment at each site consisted of a three-step oblique tow that divided fishing time
 2419 equally between bottom, mid-depth, and surface waters. Tow duration was 5 minutes with
 2420 tow speed estimated at 1.0–1.5 meters per second. Net position in the water column was
 2421 regulated using a gunwale-mounted winch with metered tow line. Flowmeter readings were
 2422 recorded before and after deployment to calculate the volume of water filtered during each
 2423 tow.

2424 **Data Analysis**

2425 Longitudinal variations in the volume of the CRE were determined using interpolated
 2426 bathymetry data and hypsometric assessment of distance downstream versus cumulative
 2427 volume (similar to Buzzelli et al. 2013b). Bathymetry data are available by request from
 2428 SFWMD. The volume of water contained in each 1-km segment of the estuary from S-79
 2429 to Shell Point was calculated.

2430 Organisms captured were identified to the lowest practical taxon. Quality control and
 2431 assurance procedures are described in Tolley et al. (2010). For each sampling event, the
 2432 density-weighted COA (rkm_U) within the sampling space was calculated following Peebles
 2433 et al. (2007) and Peebles and Greenwood (2009). The density weighted center of abundance
 2434 was calculated using **Equation 8:**

$$2435 \quad rkm_U = \sum (\text{km} \cdot U) / \sum U \quad (8)$$

2436 where U is the organism density (number per cubic meter [$\#/m^3$]) at a station and rkm is
 2437 the distance (km) of the station from Shell Point. $\sum U$ is the sum of organism density across
 2438 all stations for each sampling date. For each sampling date, the quantity ($km \cdot U$) is
 2439 calculated for each station. These are summed and divided by $\sum U$. rkm_U was correlated
 2440 with freshwater discharge (Q) at S79 averaged over the 1 to 120 days prior to sampling. A
 2441 linear regression of rkm_U on transformed freshwater inflow ($\ln(Q+1)$) was computed for
 2442 the “lagged inflow” with the highest correlation coefficient (Tolley et al 2010). Inflows
 2443 were calculated for lags of 60 days or less as these were considered most likely to be
 2444 achievable through management of inflows at S-79. Inflows were averaged over 0, 3, 7 14,
 2445 18, 20, 21, 30, 45, and 60 days prior to sampling.

2446 Taxa used for the evaluation of impingement and habitat compression were selected
 2447 from Tolley et al (2010). Tolley et al (2010) calculated regressions relating the location of
 2448 the COA to natural log transformed freshwater inflow at S-79 for over 60 taxa (see Table
 2449 3.7.1.1 in Tolley et al. 2010). The 11 marine species with intercepts occurring furthest
 2450 upstream (COA when inflow was 0 cfs) were evaluated for impingement and habitat
 2451 compression (**Table 13**). Based on the regression equations (see Table 3.7.1.1 in Tolley et
 2452 al., 2010), the calculated positions of these 11 species when inflow was 0.0 cfs was 67.3
 2453 km upstream of Shell Point or 24 km upstream of S-79. These responses made them good
 2454 candidates to experience habitat compression and impingement. Because of their high
 2455 relative abundance and importance in the food web (Tolley et al. 2010), adult (*Anchoa*
 2456 *mitchilli*) and juvenile (*Anchoa spp.*) anchovies were also included in the analysis.

2457
 2458

Table 13. List of organisms evaluated for potential habitat compression and impingement on S-79.

Taxon	Type
<i>Clytia</i> spp.	jellyfish
<i>Lironeca</i> spp.	isopod
<i>Edotia triloba</i>	isopod
<i>Bowmaniella brasilliensis</i>	mysid
<i>Americamysis almyra</i> adults	mysid
<i>Americamysis</i> spp. juveniles	mysid
<i>Psuedodiaptomus pelgicus</i>	copepod
<i>Gobiosoma</i> spp. postflexion larvae	fish
<i>Menidia</i> spp. preflexion larvae	fish
<i>Gobiidae</i> preflexion larvae	fish
<i>Microgobius</i> spp. postflexion larvae	fish
<i>Anchoa mitchilli</i> adult	fish
<i>Anchoa mitchilli</i> juveniles	fish

2459

2460 Potential habitat compression and impingement on S-79 were investigated using the
 2461 spatial abundance quantile approach outlined by Peebles and Greenwood (2009). This
 2462 approach utilizes the locations of the 10th and 90th deciles of cumulative abundance to
 2463 assess impingement and habitat compression. Abundance, represented as organism density
 2464 ($\# m^3$), was summed for each monthly survey to produce a total monthly value. Monthly
 2465 density at individual stations was then summed sequentially in the upstream direction, and
 2466 the resulting sums were expressed as a percentage of total monthly density. This process is
 2467 analogous to creating a cumulative distribution curve or function, except that it sums

2468 sequential density values from successive stations along a transect instead of summing
2469 data-class frequencies. The location (rkm) of the 10th (the lower decile) and 90th percentiles
2470 (the upper decile) of total monthly density were interpolated linearly. These linear
2471 interpolations were always made between the station with the highest percentile <10 or
2472 <90 and the next station upstream. The inter-decile range (IDR) is the distance in river km
2473 between the locations of the 10th and 90th abundance deciles. Monthly surveys were
2474 excluded from this analysis if >10% of the catch was encountered at the downstream-most
2475 station, or if there were fewer than three stations with non-zero densities (Peebles and
2476 Greenwood 2009).

2477 We tested the hypothesis that habitat volume decreases as the center of abundance
2478 translates upstream (habitat compression). For each taxon investigated, the relationship
2479 between rkm_U and the two deciles was modeled using linear least squares regression
2480 (Peebles and Greenwood 2009). The positions of the 10th and 90th deciles were calculated
2481 for a series of rkm_U ranging from river km 15 to river km 40. In addition the IDR was also
2482 calculated. For each rkm_U , the volume of water available for occupation (habitat volume)
2483 was calculated by combining estimates of estuarine segment volumes with the IDR. The
2484 segments containing the location of the upper and lower deciles were determined and the
2485 volumes of these and intervening segments summed to estimate the volume of water
2486 available for occupation. For each taxon investigated, this procedure yielded a series of
2487 rkm_U and potential habitat volumes occupied by 80% of the cumulative catch. This
2488 approach was used to determine if habitat volume decreases as rkm_U translates upstream
2489 or whether this decrease was offset by increased dispersion as measured by the IDR
2490 (Peebles and Greenwood 2009).

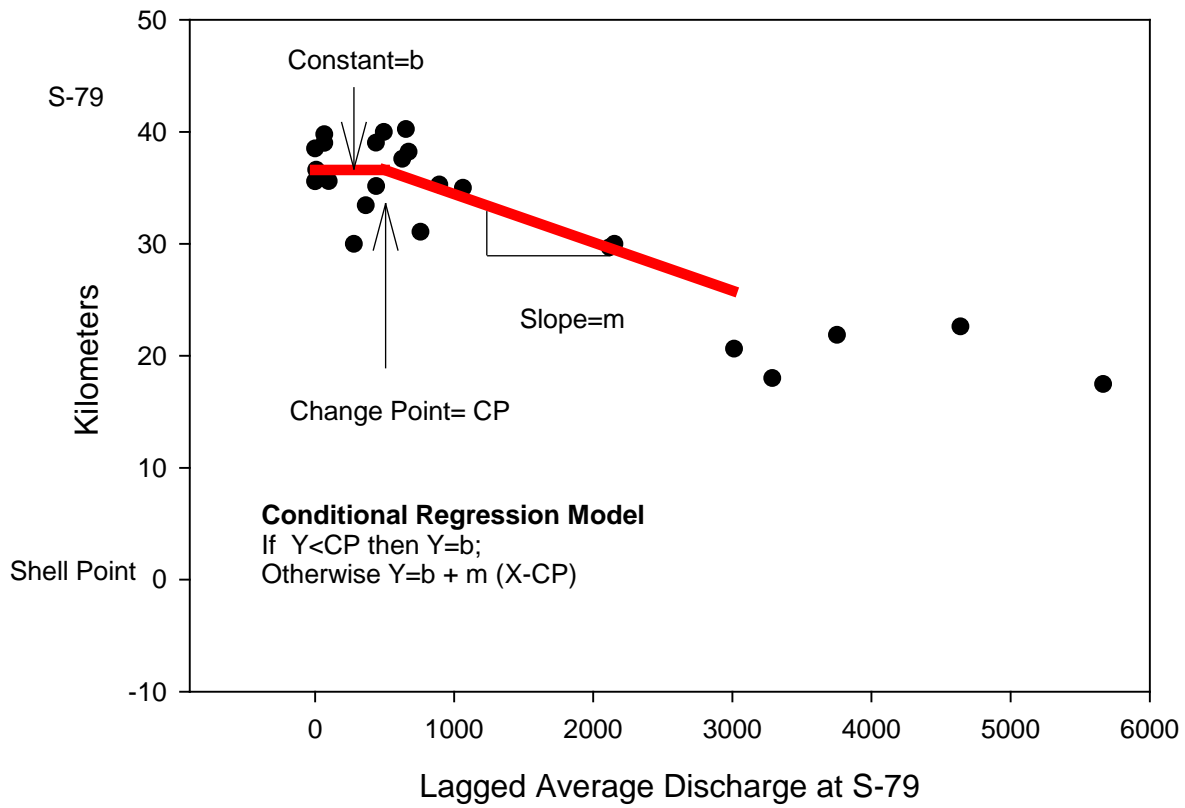
2491 Impingement was assessed by examining the location of the upper abundance
2492 percentile (90th percentile) as a function of lagged freshwater inflow at S-79. Inflows were
2493 calculated for lags of 60 days or less as these were considered most likely to be achievable
2494 through management of inflows at S-79. Inflows were averaged over 0, 3, 7, 14, 18, 20, 21,
2495 30, 45, and 60 days prior to sampling. For organisms whose location in the estuary moves
2496 upstream as freshwater inflow declines, impingement was indicated if a threshold inflow
2497 was reached at which the position of the 90th abundance decile ceases to change upon
2498 further reduction in inflow. Conversely, as inflows increased above this threshold
2499 impingement was relieved and the position of the 90th abundance decile moved
2500 downstream. This threshold inflow was determined by a change point analysis using the
2501 SAS NLIN procedure as described by Schwarz (2013). A conditional regression approach
2502 is employed (**Figure 26**):

$$2503 \quad \text{If } Y < \text{CP then } Y = b; \text{ otherwise } Y = b + m (X - \text{CP}) \quad (9)$$

2504 Where Y is the location of the 90th decile in the estuary, X is lagged inflow, CP is
2505 change point or threshold inflow, b is the constant or river kilometer where position of the
2506 90th decile becomes independent of inflow, and m is slope or the rate at which the position
2507 of the 90th decile changes as inflows increase above the threshold.

2508

Change Point Analysis using Conditional Regression



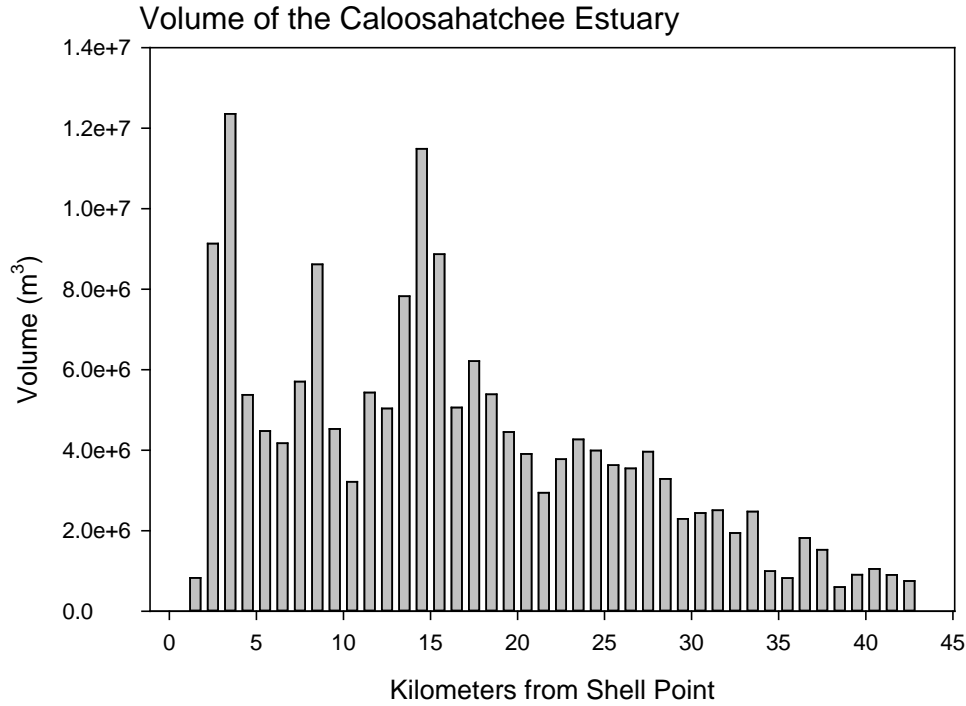
2509
2510
2511
2512

Figure 26. Change point analysis using conditional regression. The Y-axis is the position of the 90th abundance decile in the CRE. The x-axis is discharge averaged over a number of days before sampling, which ranged between 0 and 60.

2513 Results and Discussion

2514 Volume of 1-km increments ranged from $5.0 \times 10^5 \text{ m}^3$ to $1.3 \times 10^7 \text{ m}^3$ along the
2515 longitudinal gradient of the CRE (**Figure 27**). Volume was greatest ~2 to 3 km and 14 to
2516 16 km upstream of Shell Point. There is a major constriction and reduction in the volume
2517 of individual segments upstream of about kilometer 30 (Beautiful Island).

2518 The COA's for the 13 taxa investigated migrated downstream and upstream as
2519 freshwater inflow increased and decreased, respectively (**Table 14**). This response was
2520 revealed by the negative slope in regression relationships. Freshwater inflow at S-79
2521 explained from 15% to 50% of the variability in location of the COA's of the various taxa.
2522 Most taxa responded to inflows averaged over 45 or 60 days. This agrees with a previous
2523 analysis of the data by Tolley et al. (2010) that found most taxa responding to inflows
2524 averaged over ~50 days. For twelve of the thirteen taxa, COA's were sometimes located
2525 upstream of river km 30, in the narrow region of the estuary where habitat volume is greatly
2526 reduced indicating the potential for both habitat compression and impingement (**Figure**
2527 **28**). Inflows at S-79, required to locate the center of abundance of each taxon at river km
2528 30, ranged from 6.6 cfs to 1,362 cfs, and averaged (\pm standard deviation) 259 ± 378 cfs
2529 among the 13 taxa. The median was 128 cfs with 25th and 75th percentiles of 29.7 and
2530 289 cfs, respectively.



2531

2532

Figure 27. Volume of the CRE in 1-km increments. Shell Point (0 km) to the S-79 (43 km).

2533

2534

2535

2536

2537

2538

2539

Table 14. Regression relationships between freshwater inflow at S-79 (x) and the location of the center of abundance (rkmU; y) in the sampling space. n is the number of observations, a is the intercept, b is the slope, p is the level of statistical significance, r² is the coefficient of determination. Days are the number of days prior to each sampling date that inflow (Q) was averaged. In general regression equations were of the form $rkmU = a - b(\ln(Q+1))$ except where noted. Also given is the inflow required to locate the center of abundance at 30 km upstream of Shell Point where volume of the estuary begins to increase.

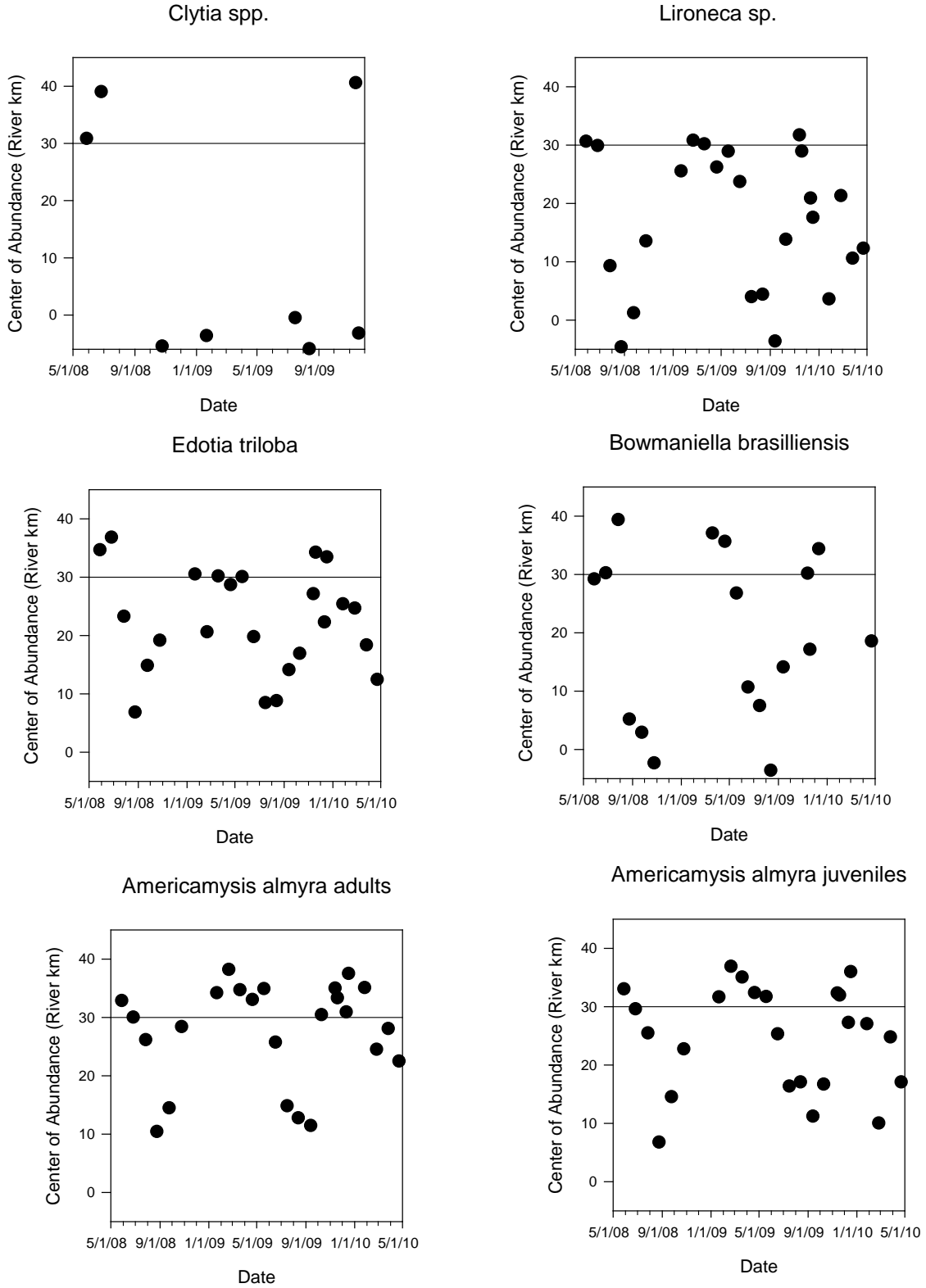
Taxon	n	a	b	p	r ²	Days	30 km (cfs)
<i>Lironeca</i> spp.	24	36.73	-3.31	0.001	0.43	14	6.6
<i>Edotia triloba</i>	24	47.31	-3.89	0.001	0.41	45	85.0
<i>Bowmaniensis brasilliensis</i>	24	44.76	-4.31	0.002	0.36	45	29.7
<i>Americamysis almyra</i> adults	24	49.90	-3.51	0.002	0.35	45	288.9
<i>Americamysis</i> spp. juveniles	24	46.72	-3.44	0.004	0.32	45	128.1
<i>Psuedodiapotomus pelagicus</i>	22	44.10	-5.37	0.001	0.46	60	12.8
<i>Gobiosoma</i> spp. postflexion larvae	20	51.85	-5.91	0.008	0.33	60	39.4
<i>Microgobius</i> spp. postflexion larvae	17	71.82	-7.88	0.001	0.54	60	200.8
<i>Gobiidae</i> preflexion larvae	24	45.72	-5.21	0.001	0.36	60	19.5
<i>Menidia</i> spp. preflexion larvae	17	76.31	-7.36	0.005	0.38	60	540.8
<i>Anchoa mitchilli</i> adults ^a	24	3.50	0.00	0.002	0.34	14	518.4
<i>Anchoa</i> spp. juveniles ^b	24	31.88	0.00	0.065	0.15	3	1,362.3

2540

2541

a. $\ln(rkmU) = a - b(Q)$

b. $rkmU = a - b(Q)$



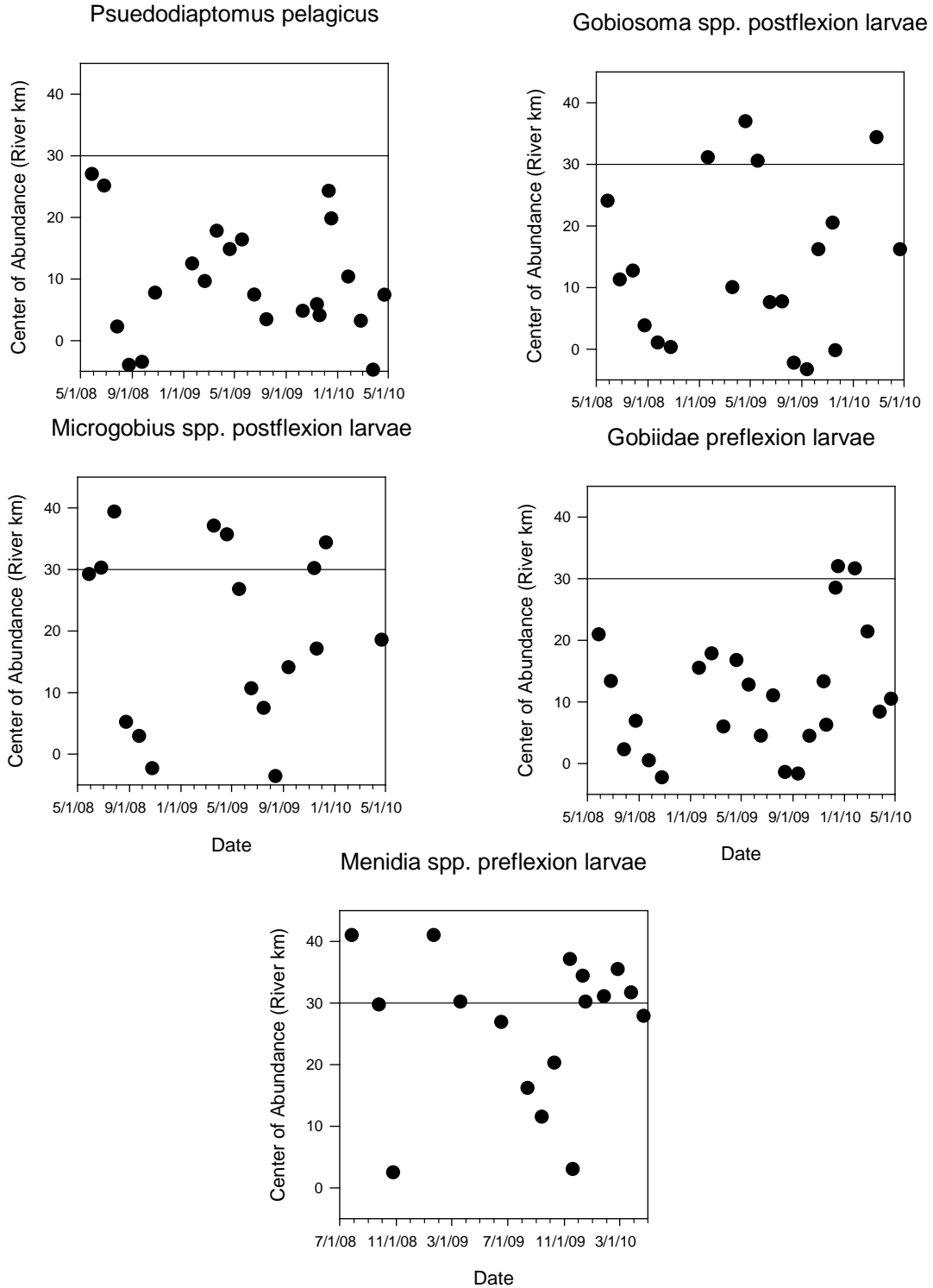
2542

2543

2544

Figure 28. COA for various taxa during the study period. Upstream of the reference line at 30 km, habitat volume is reduced.

2545

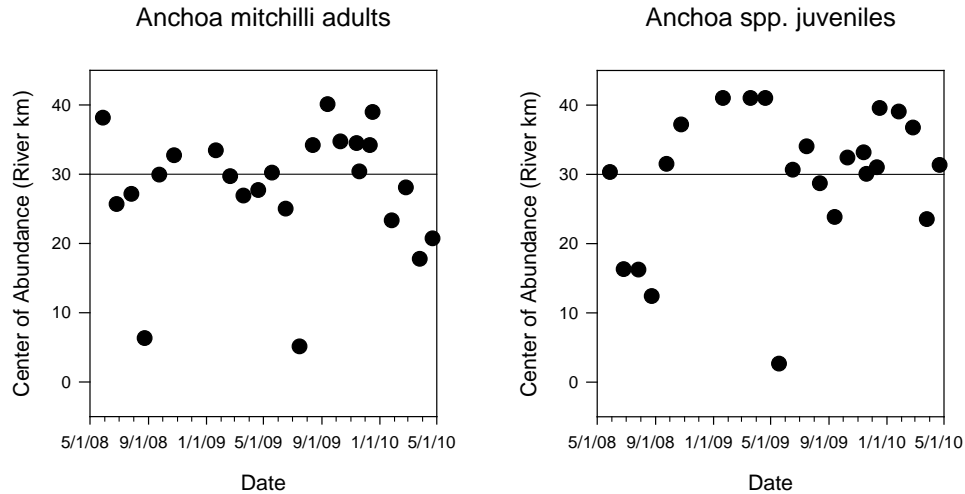


2546

2547

2548

Figure 28. Continued.



2549
2550

Figure 28. Continued.

2551 In general, the positions of the 10th and 90th abundance deciles were linearly related to
 2552 the location of *rkm_U* the distance-weighted center of abundance (see regressions in **Table**
 2553 **15**). For *Menidia*, the 10th abundance decile was unrelated to *rkm_U* so its average position
 2554 (12.9 km) was employed in calculations of habitat volume. The same situation obtained for
 2555 *Gobiidae preflexion* larvae but the average position of the 10th decile was -2.3 km and
 2556 outside the domain of the volume calculations. Neither decile was related to *rkm_U* for
 2557 *Clytia*. Habitat volumes were not calculated for these latter two taxa.

2558 **Table 15.** Linear regression relationships between the distance-weighted COA (x) and the
 2559 location (river km) of the 10th (KM_10) and 90th (KM_90) abundance deciles (y). n is the number
 2560 of observations, a is the intercept, b is the slope, and r² is the coefficient of determination. All
 2561 regression were statistically significant at p < 0.05 except where noted (ns = not significant and *
 2562 denotes p < 0.10).

Taxon	n	KM_10			KM_90		
		a	b	r ²	a	b	r ²
<i>Clytia</i> spp.	3			ns			ns
<i>Lironeca</i> spp.	16	-5.12	0.417	0.276	3.167	1.155	0.902
<i>Edotia triloba</i>	24	-4.27	0.81	0.759	0.7899	1.163	0.877
<i>Bowmaniensis brasilliensis</i>	23	-4.95	0.625	0.655	4.022	1.115	0.811
<i>Americamysis almyra</i> adults	24	12.32	1.07	0.796	11.48	0.764	0.828
<i>Americamysis</i> spp. juveniles	24	12.57	1.04	0.695	15.58	0.669	0.637
<i>Pseudodiapotomus pelagicus</i>	14	-5.73	0.681	0.604	1.099	1.026	0.762
<i>Gobiosoma</i> spp. postflexion larvae	10	-10.3	0.733	0.686	17.17	0.759	0.466
<i>Microgobius</i> spp. postflexion larvae	6	-9.05	0.739	0.554*	4.69	1.05	0.856
Gobiidae preflexion larvae	15			ns	19.8	0.71	0.461
<i>Menidia</i> spp. preflexion larvae	4			ns	4.64	1.05	0.958
<i>Anchoa mitchilli</i> -adults	17	13.34	1.018	0.489	13.8	0.732	0.833
<i>Anchoa</i> spp. -juveniles	17	-3.38	0.588	0.223	27.3	0.347	0.681

2563

2564 Habitat compression due to translation of rkm_U upstream was assessed graphically
2565 (**Figure 29**). Mysids (*Americamysis*, *Bowmaniella*) exhibited both a shrinking habitat
2566 volume and a contracting IDR as rkm_U progressed upstream. For these species a change in
2567 the habitat volume curve was evident between rkm_U of 25 and 30. By contrast, for the
2568 isopods (*Lironeca* and *Edotia*) and the copepod (*Pseudodiaptomus*), habitat volume
2569 showed curvature. For *Edotia* and *Pseudodiaptomus*, peak habitat volumes occurred when
2570 the COA was ~20 km and decreased further upstream despite monotonic expansion of the
2571 IDR (**Figure 29**). For *Lironeca* habitat, volume remained fairly constant to about 30 km
2572 where it began to decline with further upstream translation of the COA (**Figure 29**). The
2573 fish taxa exhibited various patterns. Like the mysids, both habitat volume and the IDR
2574 decreased as rkm_U moved upstream for the two *Anchoa* groups. The habitat volumes
2575 occupied by *Gobiosoma* and *Microgobius* decreased despite an increasing IDR. For both
2576 of these species, there is a distinct increase in the slope of the habitat volume curve at an
2577 rkm_U of 30 km.

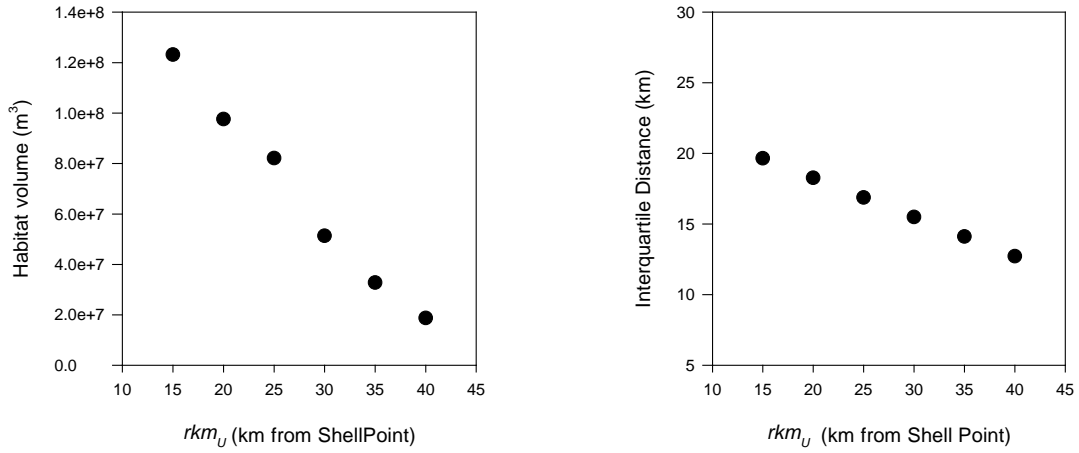
2578 It is noteworthy that taxa exhibiting downward curvature in their habitat volume plots
2579 also had monotonically increasing IDRs (*Gobiosoma*, *Microgobius*, *Lironeca*, *Edotia*, and
2580 *Pseudodiaptomus*). Such curvature may indicate that at least over part of the range
2581 examined (15 to 40 km) increases in dispersion compensated for loss of volume associated
2582 with upstream translation of the population. *Menidia* was the only taxon where both habitat
2583 volume and the IDR increased as rkm_U translated upstream. Increases in dispersion offset
2584 decreases in volume associated with geomorphology. The habitat volume plot was also
2585 curved indicating a progressive decline in the rate of increase. This decline in the rate of
2586 increase may have resulted from the interplay between a constant rate of IDR expansion
2587 and an increasing rate of decline in habitat volume associated with the funnel shape of the
2588 estuary. The incremental increases in IDR in the upper estuary were less effective at
2589 offsetting decreases in habitat volume than in the lower estuary.

2590 The conditional regression model used to evaluate impingement yielded a statistically
2591 significant demonstration of impingement for all taxa examined except *Clytia* (jellyfish)
2592 and *Menidia* spp. preflexion larvae. This result does not imply the absence of impingement
2593 for these two taxa, but more likely reflects the small number of observations that could be
2594 used in the analysis of deciles. The model explained between 40 and 89% of the variation
2595 in location of the 90th decile for the remaining taxa. Lagged inflows averaged 22.5 days
2596 and ranged between 3 and 60 days (**Table 16**). Impingement was evident following change
2597 point analysis of *Americamysis almyra* (adults) and *Edotia triloba* (**Figure 29**).

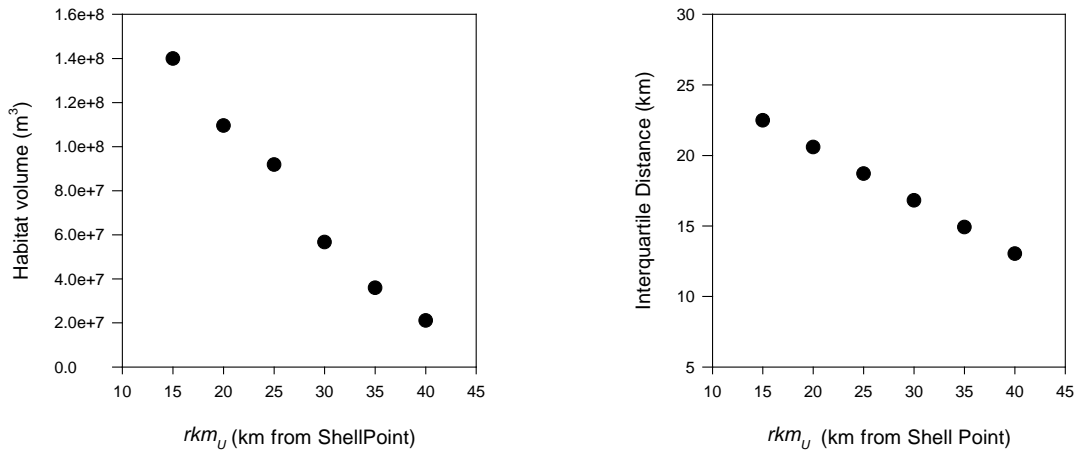
2598 Of the three parameters in the conditional regression model, estimates of threshold
2599 inflow had large errors compared to estimates of the constant and slope. In most cases, the
2600 95% confidence intervals bracketing the threshold inflow overlapped zero. Thus, for any
2601 one taxon, the river kilometer at which impingement occurs, where position of the 90th
2602 decile becomes independent of inflow, was estimated more robustly than the threshold
2603 inflow at which impingement begins to occur.

2604

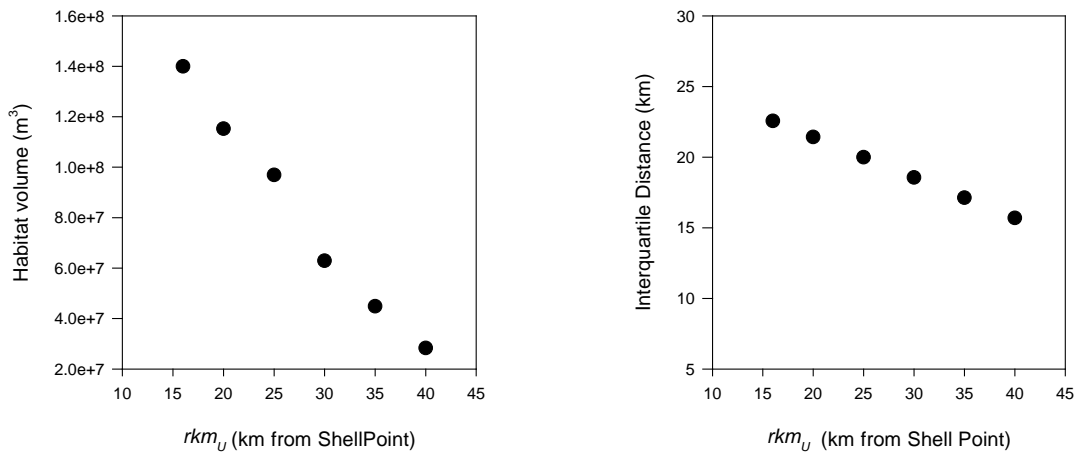
Americamysis almyra (adults)



Americamysis sp. (juveniles)



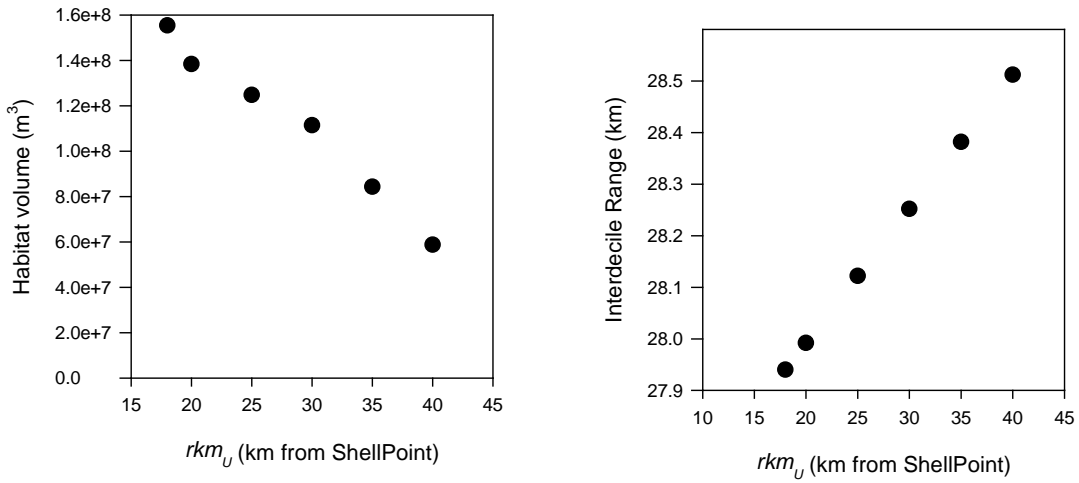
Bowmaniella brasiliensis



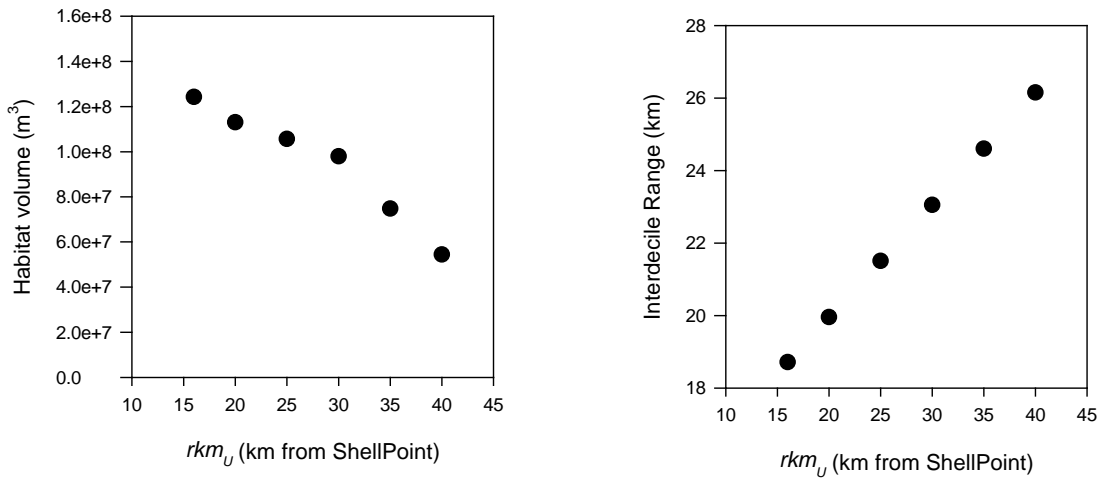
2605
2606
2607

Figure 29. Potential habitat volume as a function of the position of rkm_U (left) for different taxa. IDR as a function of the position of rkm_U (right).

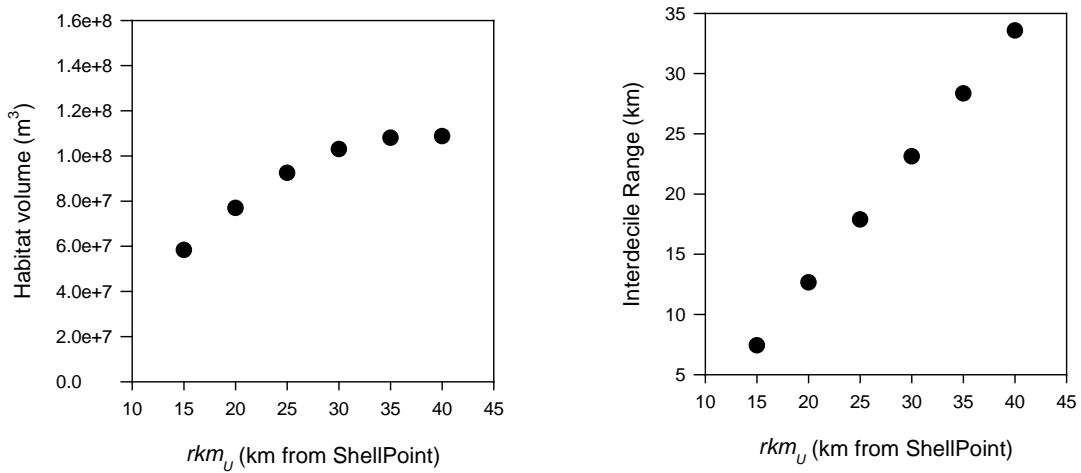
Gobiosoma sp. post flexion larvae



Microgobius spp. postflexion larvae



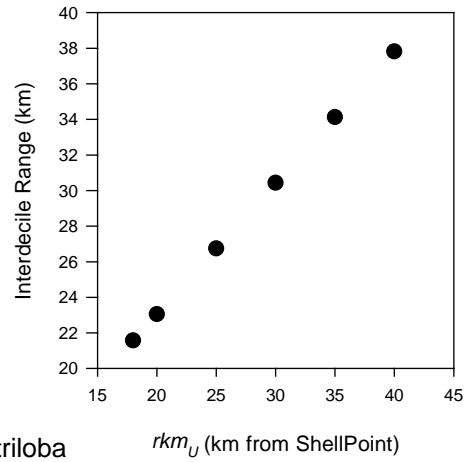
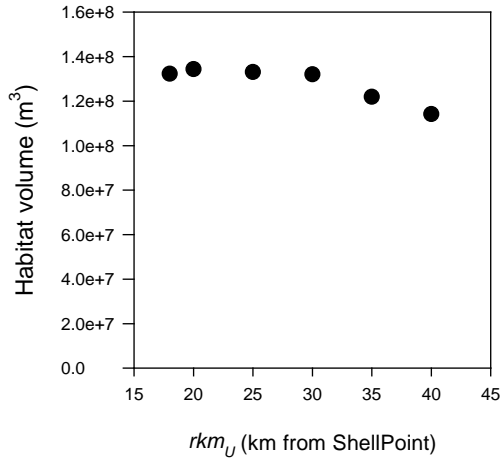
Menidia spp. preflexion larvae



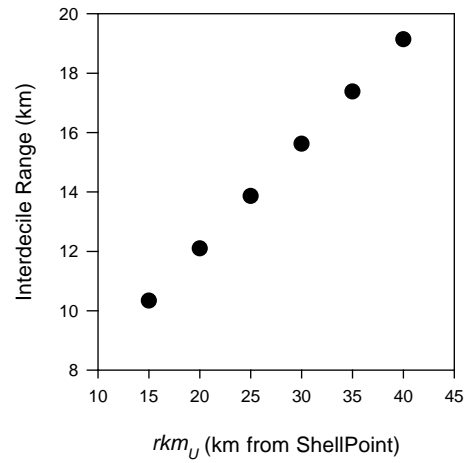
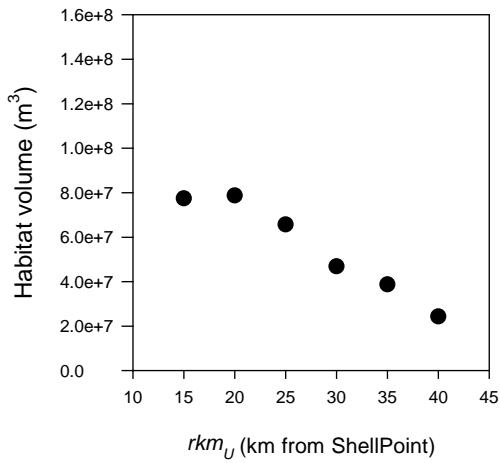
2608
2609
2610

Figure 29. Continued.

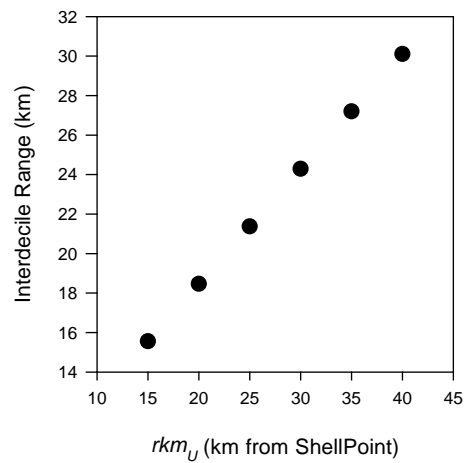
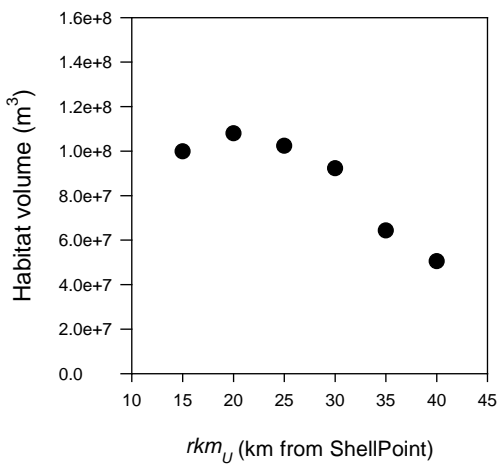
Lironeca sp. (isopod)



Edotia triloba



Psuedodiaptomus pelagicus



2611
2612

Figure 29. Continued.

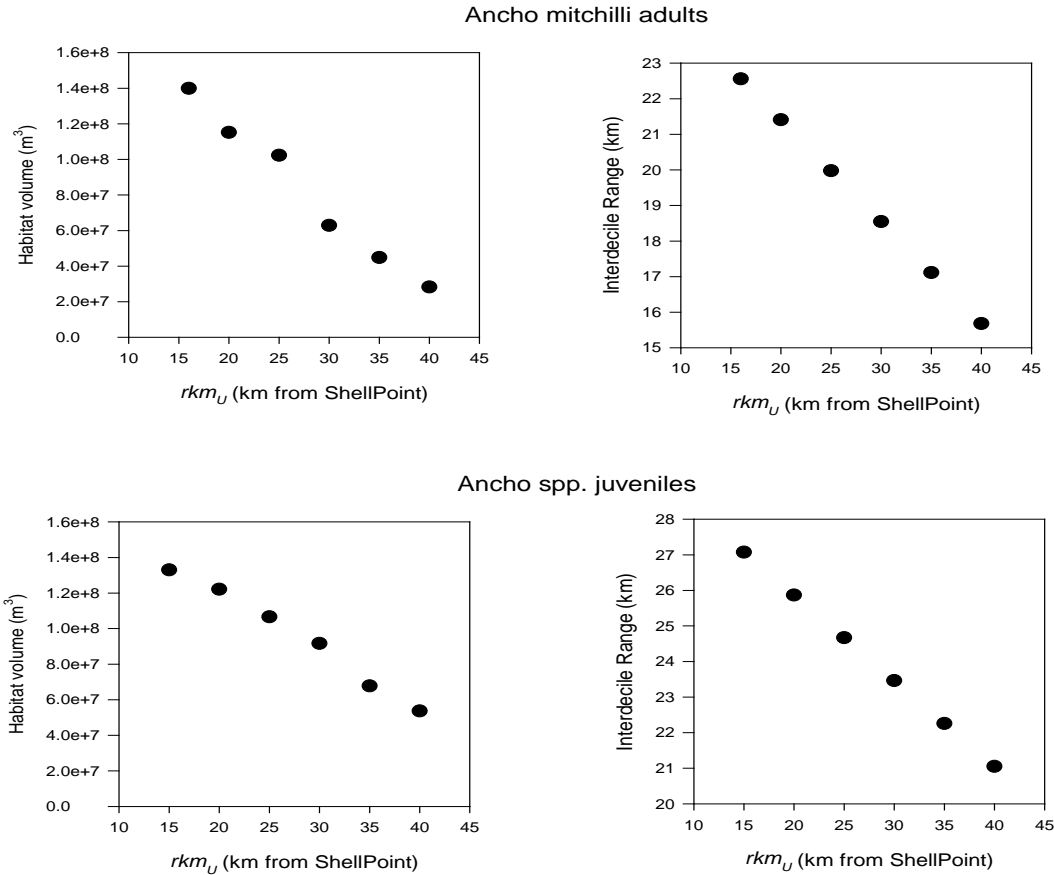


Figure 29. Continued.

2613
2614

2615 Estimates of threshold inflows for the two *Anchoa mitchilli* groups and Godiidae
2616 preflexion larvae were an order of magnitude higher than for other taxa. According to the
2617 equations given in Tolley et al (2010), inflows of these magnitudes (2,200–4,200 cfs over
2618 7–30 days) would position the COA for most marine zooplankton far downstream. Results
2619 for these taxa were not considered further. Despite the substantial error surrounding any
2620 single estimate of threshold inflow, the estimates for the remaining seven taxa were fairly
2621 consistent with a mean of 412 cfs ($\pm 40\%$), a median of 476 cfs and a range of 97.9–565.6
2622 cfs (**Table 16**). The location at which impingement occurred averaged 34.5 kilometers
2623 upstream of Shell Point or about 8 km downstream of S-79.

2624 Impingement was possible if inflow ranged and averaged 98–566 cfs and 412 ± 165 ,
2625 respectively. Inflows at which habitat compression occurred were less obvious. We do
2626 know that the volume of the estuary becomes very much smaller in the narrow region
2627 upstream of about river km 30. Almost all taxa investigated (except *Menidia*) experienced
2628 habitat compression if the COA was upstream of this point. This position in the river was
2629 associated with a clear increase in the rate of habitat compression (*Lironeca*, *Gobiosoma*,
2630 and *Microgobius*) or a distinct change in the habitat compression curve (e.g. *Americamysis*
2631 and *Bowmaniella*; **Figure 29**). Inflows associated with an rkm_U of 30 are 125 to 290 based
2632 on the median and 75th percentile and about 250 cfs based on the mean (**Table 14**).

2633
2634
2635
2636
2637

Table 16. Results of change point analysis to evaluate impingement on the Franklin Lock and Dam (S-79). Constant is the river km where the location of the 90th abundance quantile stops changing as inflows decrease, indicating impingement. CP is the inflow at which the 90th decile begins to move downstream as inflow increases. U and L indicate upper and lower limits of the 95% confidence interval. Decile data for *A. mitchelli* adults were natural log transformed for the analysis. Results for Anchoa and Gobiidae not included in calculation of means and standard deviations.

Taxon	n	Days	Constant (km)	95%L	95%U	CP (cfs)	95%L	95%U	beta2	Standard Error	R ²
<i>Clytia</i> spp.	3										
<i>Menidia</i> spp.	4										
<i>Anchoa mitchilli</i> adults (ln)	17	18	35.51	33.44	37.71	4277.0	4178	4377	-0.0026	0.0294	0.639
<i>Anchoa mitchilli</i> juveniles	19	7	37.79	36.1	39.5	3826.5	-1167	8820	-0.0017	0.000810	0.407
Gobiidae preflexion larvae	15	30	33.36	30.4	36.35	2219.7	-180	4620	-0.0189	0.0227	0.611
<i>Lironeca</i> spp.	16	3	32.18	24.5	39.86	476.3	-1323	2275	-0.0065	0.00188	0.516
<i>Edotia triloba</i>	24	60	31.8	25.7	38	452.1	-1286	2190	-0.0053	0.00168	0.404
<i>Bowmaniella brasiliensis</i>	23	14	29.13	23.3	34.91	512.2	-1041	2065	-0.0064	0.00197	0.454
<i>Americamysis almyra</i> adults	24	14	36.6	34.5	38.7	500.2	-322	1322	-0.0043	0.000572	0.805
<i>Americamysis</i> juveniles	24	14	36	33.5	38.5	565.6	-423	1554	-0.0042	0.000684	0.731
<i>Gobiosoma</i> postflexion larvae	10	45	37.6	23	52.2	97.9	-2615	2811	-0.0058	0.00109	0.783
<i>Microgobius</i> postflexion	6	20	38.1	28.6	47.6	280.2	-1763	2323	-0.0089	0.00209	0.895
			34.49			412.07					
			3.43			164.92					

2638

2639 **Component Study 5: Ichthyoplankton Response to Freshwater**
2640 **Inflow in the Caloosahatchee River Estuary**

2641 *Cassandra Thomas, Christopher Buzzelli and Peter Doering*

2642 **Abstract**

2643 Ichthyoplankton communities are key components of food webs in the upper,
2644 oligohaline reaches of most estuaries. This study analyzed historical (1986-1989) data to
2645 evaluate effects of salinity and freshwater inflow on ichthyoplankton communities in the
2646 Caloosahatchee estuary. Abundance of ichthyoplankton was greatest when 30-day inflows
2647 at S-79 averaged between 151 and 600 cfs. Juvenile fish appeared to prefer salinities <10
2648 and their abundance was centered just downstream of Station 2 near Beautiful Island.
2649 Flows at S-79 associated with a salinity of 10 in this region averaged 237.5 ± 255.5 cfs.
2650 Flows less than this could result in loss of favorable habitat.

2651 **Introduction**

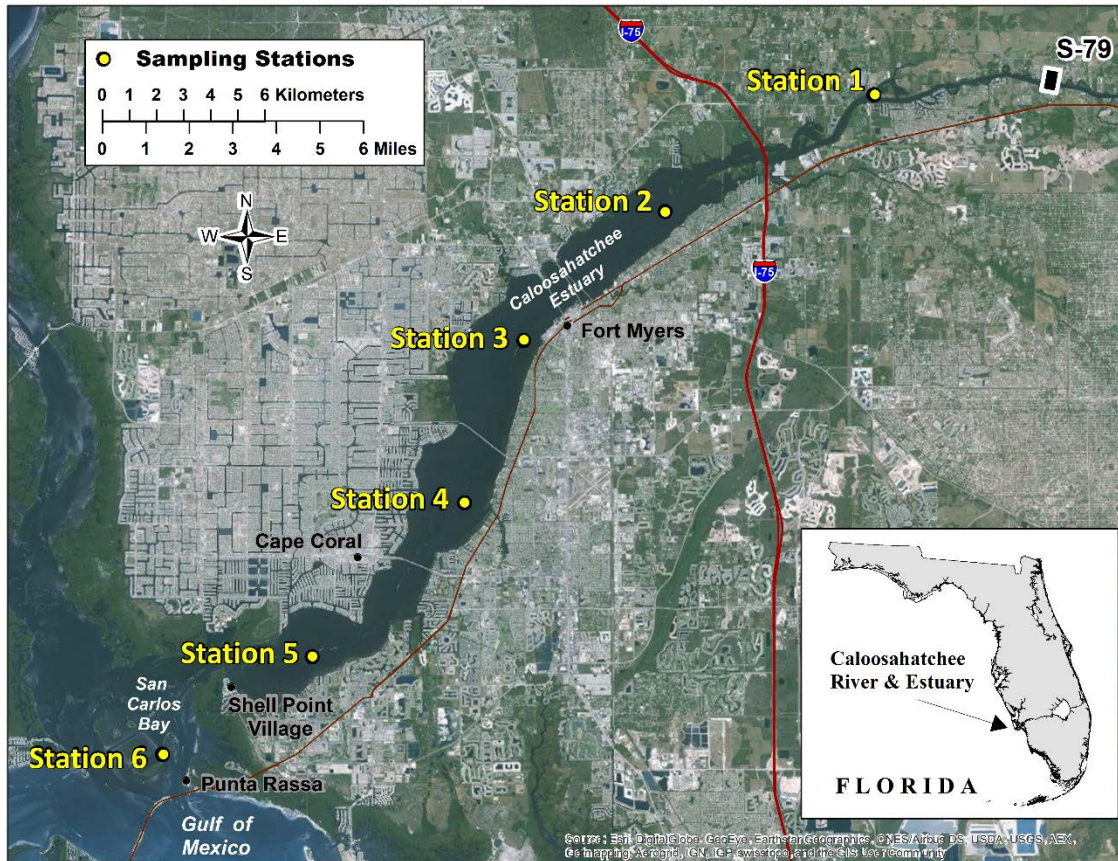
2652 Ichthyoplankton (e.g. larval fishes and decapods) are a relatively small but vital
2653 component of total zooplankton in estuaries (Able 2005, Sutherland et al. 2012). They feed
2654 on smaller plankton and serve as a food source for larger animals. Because they swim
2655 poorly or not at all they are sensitive to freshwater inflow (Gillson 2011). Ichthyoplankton
2656 assemblages can indicate the status and reproductive potential of adult fish populations in
2657 estuaries. This means that when fish such as anchovies and sardines are spawning,
2658 ichthyoplankton samples can provide a relative index of population size.

2659 It is important to understand the factors which influence fish populations in small,
2660 subtropical estuaries with managed freshwater inflow like the CRE in Southwest Florida
2661 (Stevens et al. 2013). Freshwater discharge influences ichthyoplankton location within an
2662 estuary and habitat overlap predators (Gillson 2011, Tolley et al. 2012). Additionally, the
2663 plankton food sources for fish and decapod larvae (phytoplankton and zooplankton) are
2664 also directly impacted by freshwater inflow in the CRE (Chamberlain et al. 2003).

2665 The objective of this research component was to assess the associations between
2666 freshwater inflow and ichthyoplankton abundance and community structure in the CRE.
2667 Ichthyoplankton data collected from a study conducted between 1986 and 1989 were used
2668 in this assessment.

2669 **Methods**

2670 Nocturnal samples were collected monthly from 1986 to 1989 at six stations within the
2671 CRE (**Figure 30**). Paired 0.5-millimeter conical zooplankton nets with a 505-micrometer
2672 mesh were towed obliquely with a flowmeter (meter per second) affixed to one net opening
2673 (m^2) to measure the water volume sampled (cubic meters per second). In the laboratory,
2674 the samples were sorted to the lowest possible taxonomic level and quantified. They were
2675 then grouped into the following categories for analysis: total, eggs, post-yolk sac larval,
2676 juvenile, by family, eggs by family, crab, and shrimp. Life stage categories were based on
2677 Hubbs (1943).



2678
2679 **Figure 30.** Map of ichthyoplankton sampling stations from 1986–1989 in the Caloosahatchee
2680 River Estuary.

2681 Freshwater inflow volume to the CRE was measured daily at S-79. Salinity values at
2682 each station were predicted using an auto-regressive approach that combined
2683 hydrodynamic and time series modeling (Qiu and Wan 2013). Salinities were averaged
2684 over 1-, 5-, 7-, 14-, 21-, and 30-day periods prior to the day of sampling. Freshwater inflow
2685 was averaged over the same temporal series and grouped into several categories: (1) 0–
2686 150 cfs, (2) 151–300 cfs, (3) 301–600 cfs, (4) 601–1,200 cfs, (5) 1,201–2,500 cfs, and
2687 (6) >2,500 cfs following Chamberlain et al. (2003). Due to infrequent sampling events in
2688 the second inflow category when averaged over 30 days, Categories 2 and 3
2689 were combined.

2690 The salinity envelop was assessed using the running median of abundance at different
2691 salinities. A running median is a smoothing technique that was used to determine the
2692 median value of abundance for a particular salinity, and then the median was graphed over
2693 all salinities in the data set. This approach removes the influence of outliers and is
2694 appropriate when the distribution around the mean is not normal.

2695 Untransformed data were evaluated a priori using principle components analysis and
2696 pairwise correlations. Additional statistical analyses included one- and two-way analysis
2697 of variance (ANOVA), analysis of covariance (ANCOVA), and nonlinear regressions were
2698 performed on $\log(x+1)$ transformed abundance data. Tukey's honestly significant
2699 difference was used to determine differences between groups. Essential independent

2700 variables included sampling station, month, season (dry season is November–April; wet
 2701 season is May–October), and freshwater inflow category. Interactions detected in two-way
 2702 ANOVAs were assessed for “clumping” of results (i.e., upper estuary versus lower estuary;
 2703 lower inflows versus higher inflows; continuous months). In addition, ANCOVAs were
 2704 run to test for significance of slope and intercept.

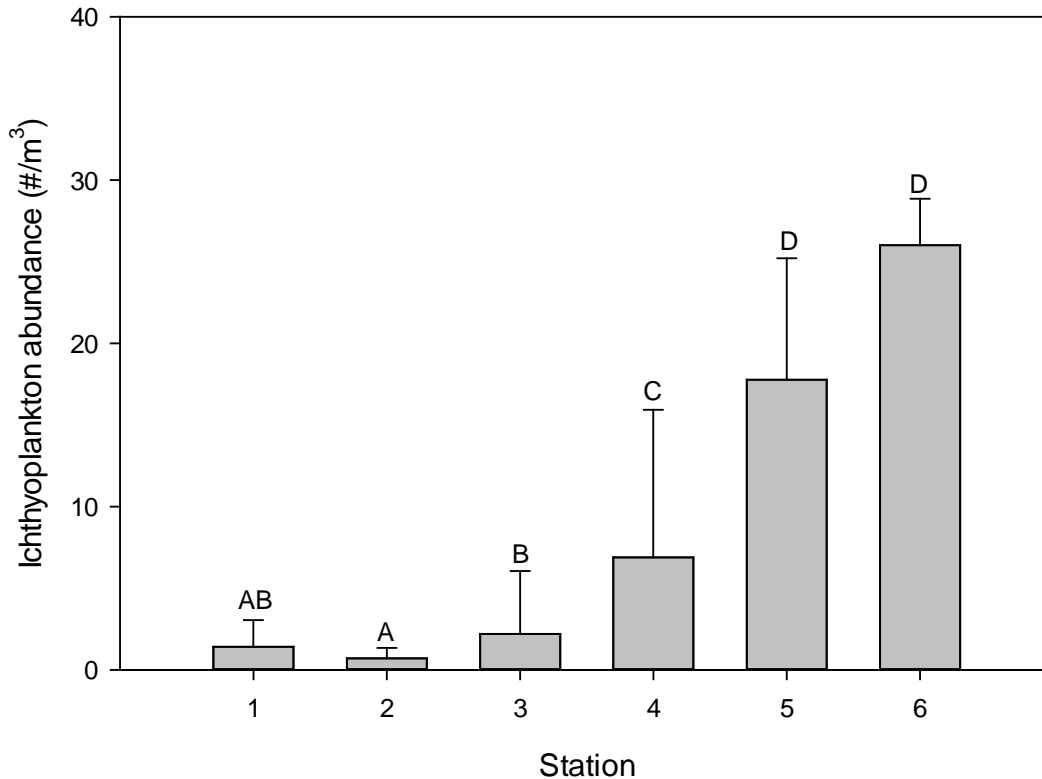
2705 The COA was calculated following Peebles et al. (2007) and Peebles and Greenwood
 2706 (2009) using **Equation 10**:

$$2707 \quad rkm_U = \Sigma(km * U) / \Sigma U \quad (10)$$

2708 where U is the organism’s density (# m³) at a station and rkm is the distance (km) of the
 2709 station from the S-79 structure. ΣU is the sum of organism density across all stations for
 2710 each sampling date. For each sampling date, the quantity (km * U) is calculated for each
 2711 station. These are summed and divided by ΣU .

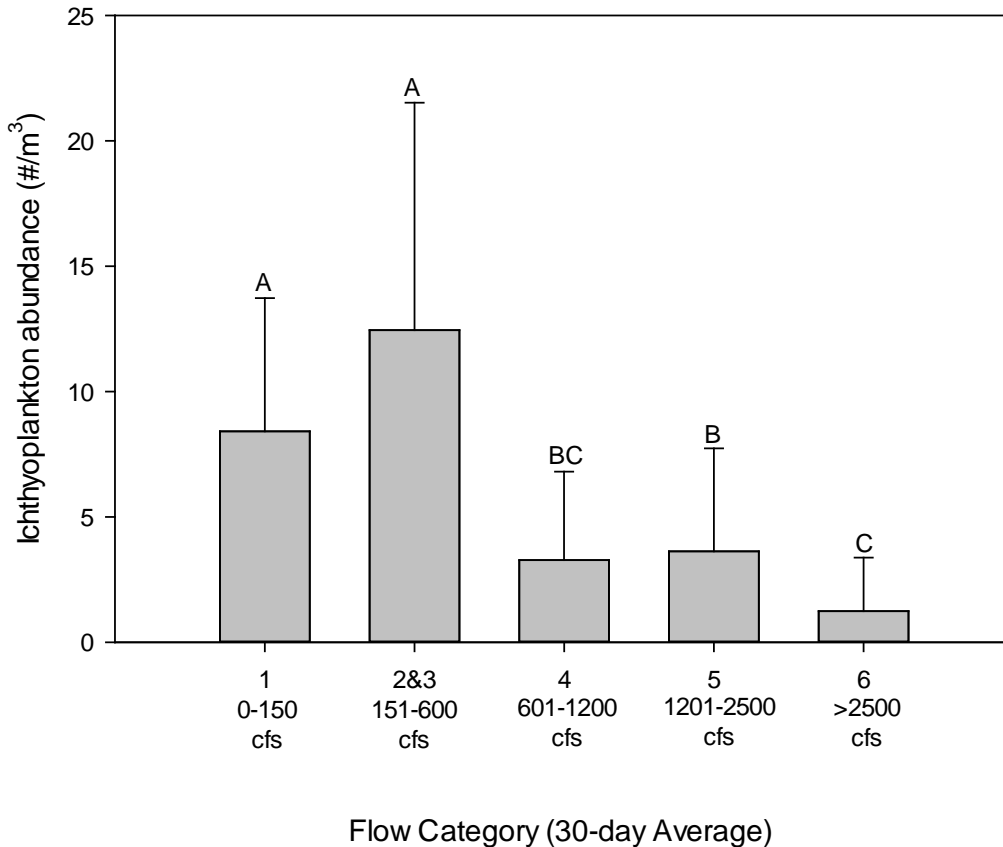
2712 Results and Discussion

2713 Total ichthyoplankton abundance most closely correlated to 30-day average inflow and
 2714 salinity ($p = 0.0002$ and $p < 0.0001$, respectively). Abundance was highest at Stations 5
 2715 and 6 ($p < 0.0001$, one-way ANOVA) favoring a more marine ichthyoplankton assemblage
 2716 (**Figure 31**). Abundances were greatest when inflows ranged from 151 to 600 cfs ($p <$
 2717 0.0001 , one-way ANOVA) and declined with increasing freshwater discharge (**Figure 32**).
 2718 There were no seasonal signals for total ichthyoplankton or individual taxa.



2719

2720 **Figure 31.** Ichthyoplankton abundance (number per cubic meter [# /m³]) across stations. Bars
 2721 with the same letters are not significantly different ($p > 0.05$). Data were retransformed from
 2722 $\log(x+1)$ transformed analysis.

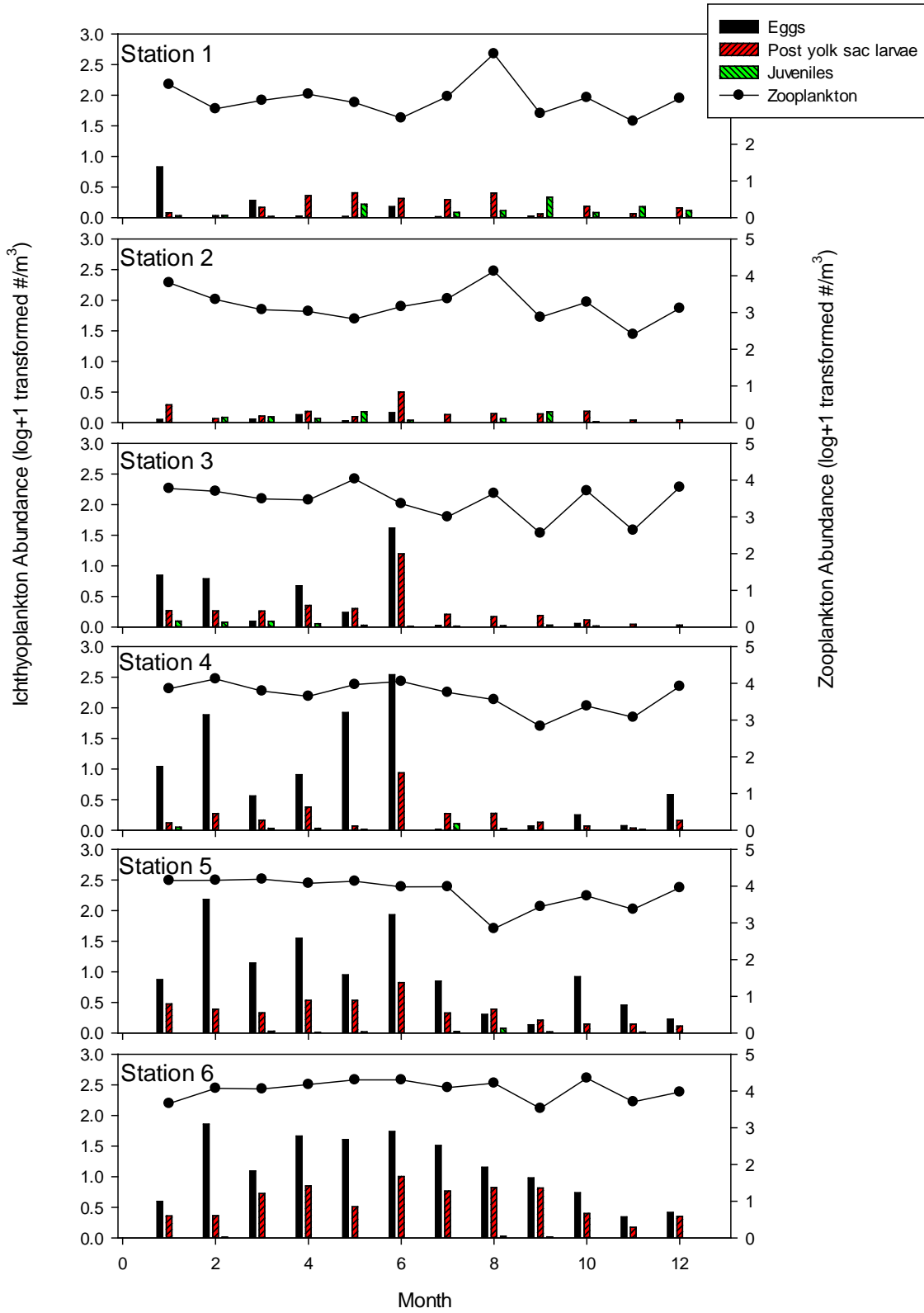


2723
2724
2725
2726
2727

Figure 32. Ichthyoplankton abundance (number per cubic meter [#/ m^3]) under different inflow regimes (1 = 0–150 cfs; 2 and 3 = 151–600 cfs; 4 = 601–1,200 cfs; 5 = 1,201–2,500 cfs; 6 = >2,500 cfs) (1986–1989 study). Bars with the same letters are not significantly different ($p > 0.05$). Data were retransformed from $\log(x+1)$ transformed analysis.

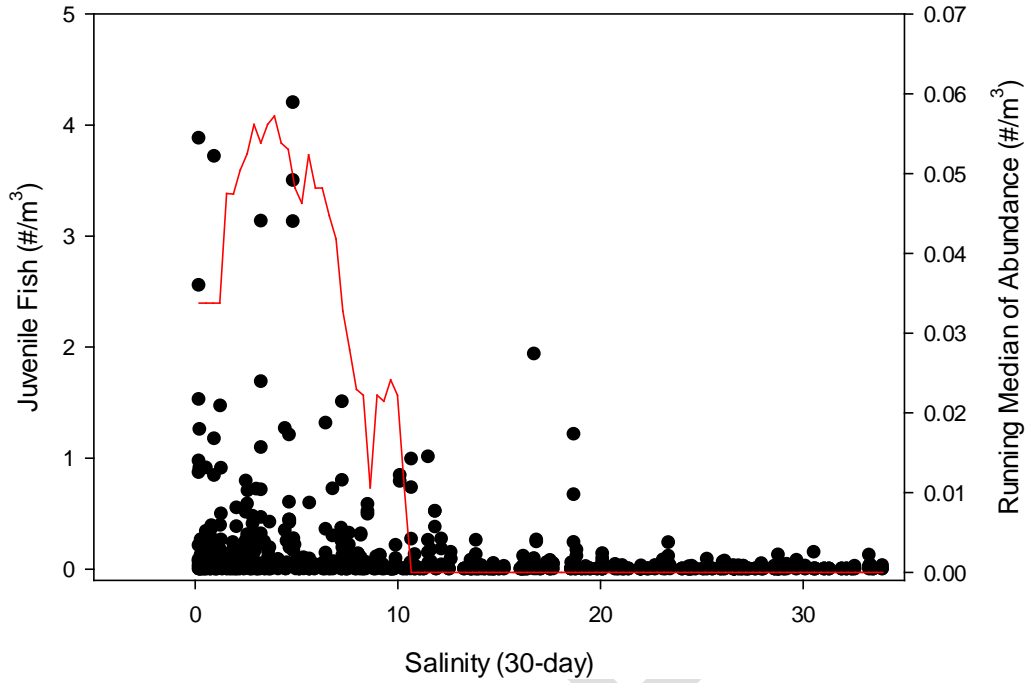
2728 Although eggs and post-yolk sac larva were primarily located in the lower estuary at
2729 high abundances, juvenile fishes were located in the upper estuary regardless of month
2730 (**Figure 33**). This assemblage was dominated by *Anchoa mitchilli* (bay anchovy), which
2731 Kimura et al. (2000) noted disperse up-estuary in the Chesapeake Bay to seek lower
2732 salinities if the timing of recruitment occurs when salinities are >18 in the lower estuary.
2733 It was likely that those remaining in the downstream estuary did not successfully recruit to
2734 the juvenile stage. Thus, the upper estuary is an important nursery for juvenile fish.

2735 Most juvenile fish were found associated with salinities ranging from 0 to 10 (**Figure**
2736 **34**). Juvenile fish are most abundant in the upper and mid-estuary. The COA of the juvenile
2737 fish ranged from 7 to 30 km downstream of S-79 and averaged 18.9 km (just downstream
2738 of Station 2) (**Figure 35**). Using the density-weighted salinity (S_U) as a covariate, higher
2739 inflows result in the COA being located further downstream ($p < 0.0001$, ANCOVA model,
2740 $p < 0.0001$ intercept, $p = 0.9024$ slope; **Figure 35**). These regressions can be used to locate
2741 the COA over a range of 30-day average salinity values for particular flow classes. For
2742 example, the COA ranged from 7 to 20 km downstream when the S-79 inflow rate was
2743 <600 cfs (lowest flow categories). This result suggested that hydrodynamics were
2744 important to the location of the COA, and that juvenile fish abundance could serve as an
2745 indicator for freshwater inflow.



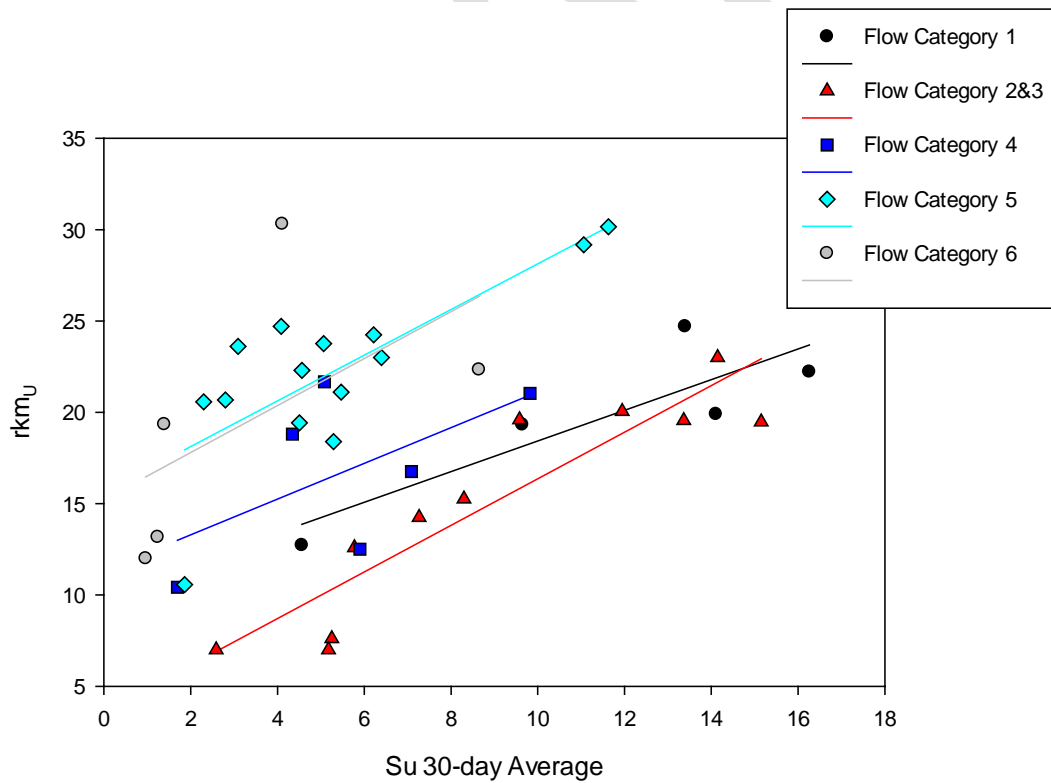
2746
2747
2748

Figure 33. Ichthyoplankton abundance of different life stages at each station over different months compared to abundance of zooplankton (1986–1989 study).



2749
2750
2751
2752

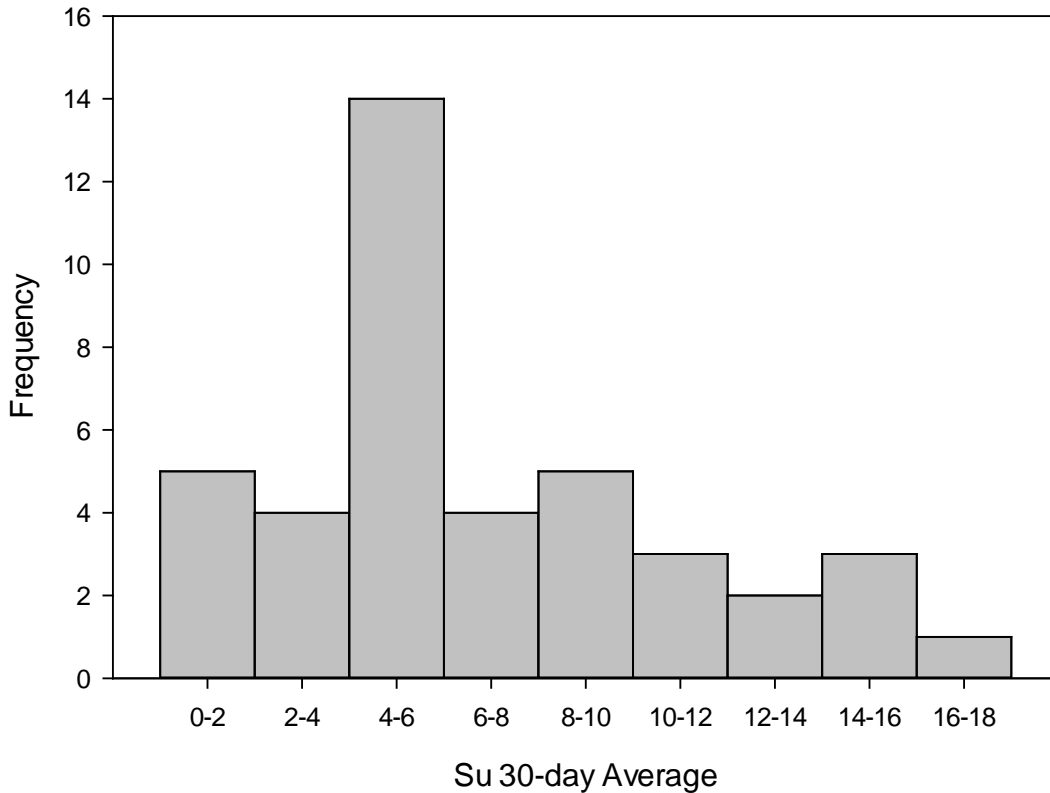
Figure 34. Juvenile fish abundance (number per cubic meter [$\#/m^3$]) relative to 30-day average salinity and the running median of abundance (right axis; red line) to establish a salinity envelope of preference.



2753
2754
2755
2756

Figure 35. COA for juvenile fish compared to density-weighted salinity at different inflow regimes (1 = 0–150 cfs; 2 and 3 = 151–600 cfs; 4 = 601–1,200 cfs; 5 = 1,201–2,500 cfs; 6 = >2,500 cfs) (1986–1989 study).

2757 Juvenile fish were most frequently found in salinities ranging from 4 to 6 with
 2758 frequency of occurrence declining at salinities that were >10 (**Figure 36**). Given that the
 2759 juvenile fish prefer salinity value <10 and had an average COA just downstream of Station
 2760 2, potential habitat loss was assessed by determining the flow at which salinity exceeded
 2761 10 at Station 2. Out of the five years of study, there were 11 months where the 30-day
 2762 average salinity was >10 at Station 2. The 30-day average inflows associated with these
 2763 salinity values ranged from 12.3 to 1,357 cfs and averaged 237.5 ± 255.5 cfs. Inflow rates
 2764 less than this average are likely to result in habitat loss for juvenile fish as the fish need to
 2765 move upstream toward the S-79 structure to seek their preferred salinity range.



2766
 2767
 2768

Figure 36. Frequency distribution of density-weighted salinity for juvenile fish.

2769 **Component Study 6: Summary and Interpretation of**
2770 **Macrobenthic Community Properties Relative to Salinity and**
2771 **Inflow in the Caloosahatchee River Estuary**

2772 *Christopher Buzzelli*

2773 **Abstract**

2774 The composition, distribution and density of benthic invertebrate communities
2775 (macrofauna) can be used as indicators of salinity and inflow for estuaries. The goal of this
2776 study component was to explore the relationships between inflow, salinity, and benthic
2777 macrofauna in the CRE. Benthic samples were collected every 2 to 4 months at seven
2778 stations during two periods (February 1986–April 1989 and October 1994–December
2779 1995). The abundance, diversity, and composition of the macrofaunal community were
2780 determined relative to observed fluctuations in salinity. Four distinct zones emerged based
2781 on salinity ranges and the composition of the macrobenthic community. Conditions
2782 conducive to maintain the characteristic community observed during the sampling periods
2783 in the most upstream zone (salinity = 0 to 4, 0 to 7 km from S-79) occurred on 54% of dry
2784 season days from 1993 to 2012. The indicator inflows (Q_i) ranged from 0 to 3,720 cfs and
2785 averaged 501 ± 525 cfs for the days where salinity was 3 to 4 ($n = 181$).

2786 **Introduction**

2787 Alterations to the quality, quantity, timing and distribution of inflows are extremely
2788 important to the health and function of an estuary (Montagna et al. 2013). Within the CRE,
2789 changes in freshwater inflows have altered salinity regimes and the ecology of the estuary
2790 (Chamberlain and Doering 1998a, Barnes 2005). Changes in freshwater inflows and
2791 salinity have been shown to change the distribution and dynamics of many taxa and
2792 communities in the CRE including submersed vegetation (Doering et al. 2001, Doering et
2793 al. 2002, Lauer et al. 2011), oysters and dermo disease (La Peyre et al. 2003, Barnes et al.
2794 2007, Volety et al. 2009), fauna inhabiting oyster reefs (Tolley et al. 2005, Tolley et al.
2795 2006), and fishes (Collins et al. 2008, Heupel and Simpfendorfer 2008, Stevens et al. 2010,
2796 Simpfendorfer et al. 2011, Poulakis et al. 2013).

2797 Benthic organisms are ideal biological indicators of changes in water quality because
2798 they have limited mobility, long lifespans relative to plankton, and sensitivity to changes
2799 in water and sediment quality (Montagna et al. 2013). Many studies have used benthic
2800 communities as indicators of freshwater inflow and estuarine status (for a summary see
2801 Montagna et al. 2013). Macrobenthic communities have been used as indicators in Rincon
2802 Bayou, Texas (Montagna et al. 2002b) and other Texas estuaries (Palmer et al. 2011),
2803 Southwest Florida (Montagna et al. 2008, Palmer et al. 2011), and the St. Johns River
2804 Estuary in northeastern Florida (Mattson et al. 2012).

2805 The goal of this research component was to explore the relationships between
2806 freshwater inflow, salinity patterns, and the distribution, density, and composition of
2807 benthic macrofaunal communities in the CRE (Montagna and Palmer 2014). This
2808 assessment was based on a more comprehensive analysis of macrofaunal communities and
2809 salinity patterns in the CRE (Montagna and Palmer 2014). Specifically, this effort
2810 emphasized the potential effects of reduced dry season inflow on salinity patterns in the
2811 upper CRE.

2812 **Methods**

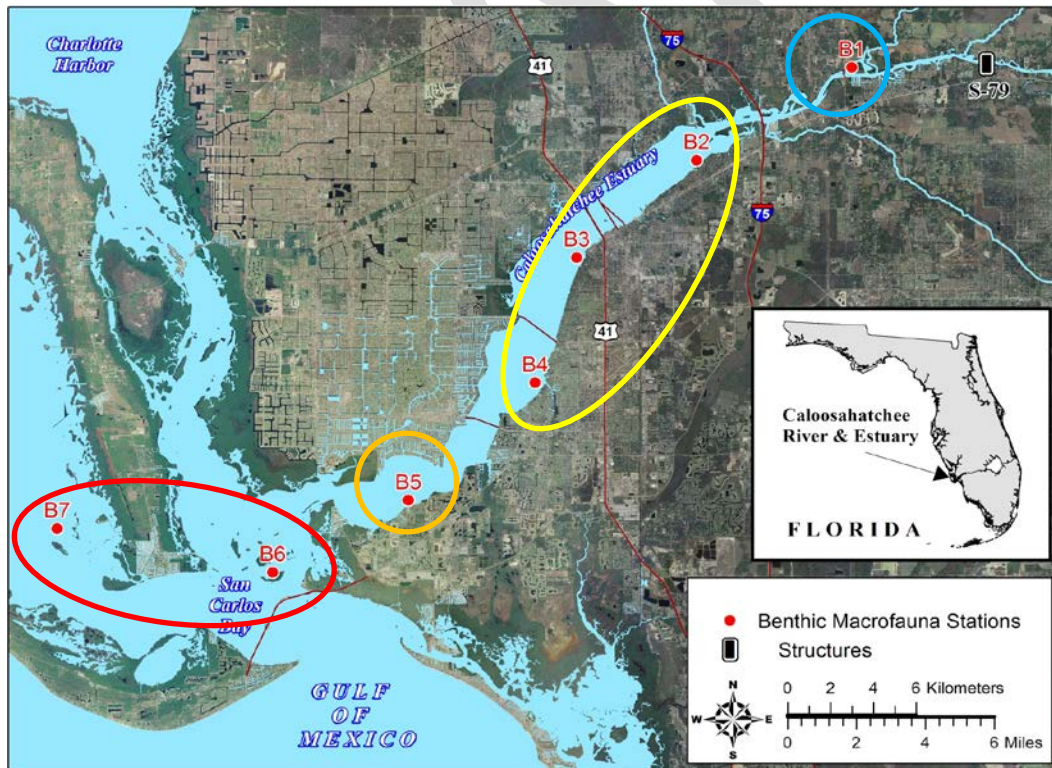
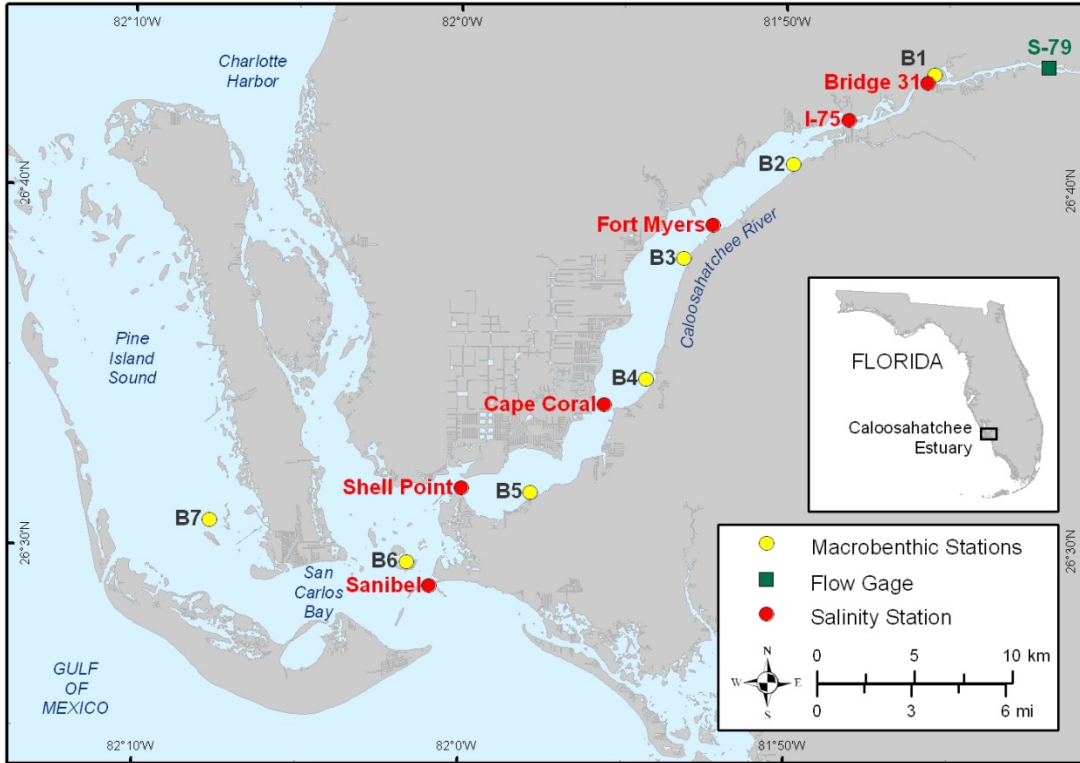
2813 The study was designed by Robert Chamberlain, SFWMD, to investigate benthic
2814 macrofauna distributions as a function of salinity and to compare variability between dry
2815 (November–April) and wet (May–October) seasons. Benthic samples were collected at
2816 seven stations (B1–B7; **Figure 37A**) during two periods; from February 1986 to April 1989
2817 (Period 1) and from October 1994 to December 1995 (Period 2). Sampling occurred every
2818 two months at Stations 1 through 6 and every four months at Station 7 during Period 1.
2819 Four stations (2, 4, 5, and 6) were sampled in Period 2 for 12 of 15 months. The
2820 environmental conditions were different between the two sampling periods. While
2821 relatively low inflow rates characterized Period 1, extremely high inflow rates occurred
2822 during Period 2.

2823 Benthic samples were collected using a Wildco® petite ponar grab (0.02323 m²). Five
2824 replicates were collected at each station within a 30–50 m diameter. The sediment at each
2825 station consisted of predominantly sand and shell hash. Samples were sieved in the field
2826 on a 500–micrometer screen, preserved in formalin buffered by Epsom salt, and stained
2827 with Rose Bengal. Invertebrates were separated from the sieved substrate by either
2828 SFWMD (Period 1) or Mote Marine Laboratory (Period 2) and stored in ethanol. Staff from
2829 Mote Marine Lab identified the dominant taxa (95% of organisms) to the species level and
2830 the remaining taxa to genera or higher taxa groups.

2831 Salinity values along the length of the CRE from 1980 to 2000 were estimated using a
2832 time series modeling technique that accounted for spatial distribution of salinity in the
2833 estuary and driving factors such as freshwater inflows, rainfall, and tide (Qiu and Wan
2834 2013). This model output has been calibrated to local salinities and uses a linear reservoir
2835 model to simulate Tidal Basin flows (Wan and Konyha 2015).

2836 Macrofaunal diversity was calculated using Hill's N1 diversity index because it has
2837 units of number of dominant species (Hill 1973). Differences in macrofauna characteristics
2838 among stations were tested on two subsets of the data because the sampling design was
2839 uneven. The first subset included all seven stations for ten months in Period 1 (dry season
2840 only). The second subset included four stations (2, 4, 5, and 6) across all months (except
2841 November 1987) and encompassed both sampling periods. Differences in macrofauna
2842 characteristics among stations were determined using two-way ANOVA with station and
2843 month-year as treatments. A linear contrast was added to the ANOVA on the second subset
2844 (four stations, all dates) to test for differences among sampling periods. Post-hoc Tukey
2845 tests were run to test for differences among stations and station-period interactions.

2846 Macrofaunal community structure was analyzed using non-metric multi-dimensional
2847 scaling (MDS) using a Bray-Curtis similarity matrix among stations to create a MDS plot
2848 (Clarke 1993, Clarke and Warwick 2001). Relationships within each MDS were
2849 highlighted through cluster analysis using the group average method. Significant
2850 differences between each cluster were tested with the SIMPROF permutation procedure
2851 with a significance level of 5% ($p = 0.05$). Where stations were sampled in both time
2852 periods, differences in community structure and species assemblages between periods and
2853 among zones were tested using ANOSIM and SIMPER in Primer (Clarke 1993). Data were
2854 $\log_e(x + 1)$ transformed prior to multivariate analysis to decrease the effect of numerically
2855 dominant species on community composition (Clarke and Gorley 2006). This information
2856 was used to help characterize salinity zones for the CRE in both dry and wet seasons.



2857
 2858
 2859
 2860
 2861

Figure 37. (A) Location map for macrobenthic sampling in the CRE. Included are sampling macrobenthic stations (B1 through B7; yellow), the long-term salinity stations (red), and the upstream location of freshwater inflow (S-79; green). **(B)** Map of the CRE with the macrobenthic sampling stations (B1 through B7; red) and four estuarine zones determined in this study.

2862 The benthic community in the uppermost CRE (0–7 km from S-79) should be most
2863 sensitive to reduced freshwater inflow. Salinity responds quickly to changes in discharge
2864 in this part of the estuary. Changes in the number of low salinity species indicate a change
2865 in hydrologic conditions. The MDS analysis provided a target salinity range of 0–4 for the
2866 macrobenthic communities in the upper CRE (Montagna and Palmer 2014). Thus, salinities
2867 >4 may lead to changes in the oligohaline benthic community.

2868 Long-term salinity data collected at Bridge 31 (BR31) in the upper CRE was used to
2869 assess estuarine conditions for macrofauna communities in the most upstream portion of
2870 the estuary (**Figure 37A**). Average daily salinity at this location from January 22, 1992, to
2871 August 16, 2012, was merged with average daily freshwater inflow at S-79. These data
2872 were categorized by water year and season (dry versus wet) with analyses focused on the
2873 dry season days throughout the POR. The number and percentage of dry season days where
2874 salinity values ranged from 0 to 1, 1 to 2, 2 to 3, and 3 to 4, and >4 were calculated along
2875 with the averages and standard deviations for salinity and freshwater inflow associated with
2876 each of these salinity classes. The freshwater inflows on the days where salinity was
2877 assumed to be the highest level tolerated by the expected macrofauna species (salinity = 3
2878 to 4) were queried from the data set. The range and average and standard deviation of
2879 associated freshwater inflows were calculated from these selected days.

2880 **Results and Discussion**

2881 There was clear zonation of benthic communities along the salinity gradient in the CRE
2882 (**Figure 37B**). This zonation was evident when comparing N1 diversity and multivariate
2883 community structure of the communities along the length of the CRE. The positive
2884 relationship between salinity and diversity on a spatial salinity gradient is common in many
2885 estuaries due to the increasing abundance of marine species in downstream locations
2886 (Whitfield et al. 2012).

2887 In the current study, 34 taxa were identified as being indicators of salinity (**Table 17**).
2888 Two taxa served as indicators of limnetic conditions (salinity <0.5), 6 taxa indicated
2889 oligohaline conditions (salinity 0.5 to 5), 11 indicated mesohaline conditions (salinity 5 to
2890 18), 10 indicated polyhaline conditions (salinity 18 to 30), and 5 provided an indication of
2891 euhaline conditions (salinity 30 to 40) according to the Venice salinity classification system
2892 (**Table 17**; Anon 1958, Cowardin et al. 1979).

2893

2894

Table 17. Summary of dominant macrobenthic taxa and relationship with salinity in the CRE (Montagna and Palmer 2014).

Taxa name	Higher Taxa group ¹	Lower Taxa Group ²	Parameters					p Value
			a (Peak Abundance)	b (Skewness)	c (Salinity)			
					Estimate	90% Low	90% High	
<i>Ceratopogonidae</i> sp.	Insecta	Diptera	29	3.93	0.0	-1.7	1.8	0.0364
<i>Amphicteis floridus</i>	Polychaeta	Ampharetidae	137	2.10	0.4	-0.3	1.0	< 0.0001
<i>Edotia</i> sp. 1	Crustacea	Isopoda	546	1.16	0.8	0.5	1.2	0.0008
<i>Edotia</i> spp.	Crustacea	Isopoda	253	1.53	1.0	0.2	1.7	0.0016
<i>Tellina texana</i>	Bivalvia	Veneroida	1139	-1.38	1.6	0.5	2.7	0.0002
Tubificidae w/o cap. setae	Clitellata	Oligochaeta	1034	1.94	1.9	0.6	3.2	< 0.0001
<i>Neanthes succinea</i>	Polychaeta	Nereididae	109	1.26	2.2	0.0	4.3	0.0131
<i>Streblospio benedicti</i>	Polychaeta	Spionidae	970	1.48	2.7	1.0	4.4	< 0.0001
<i>Eteone heteropoda</i>	Polychaeta	Phyllodocidae	128	0.68	5.2	3.2	7.2	0.0022
<i>Assiminea succinea</i>	Gastropoda	Neotaenioglossa	6.2 x 10 ¹⁰	-0.04	5.9	5.1	6.8	< 0.0001
<i>Mulinia lateralis</i>	Bivalvia	Veneroida	1347	-0.65	6.8	0.6	13.0	0.0772
<i>Tellina versicolor</i>	Bivalvia	Veneroida	16711	-0.09	7.0	6.7	7.2	< 0.0001
<i>Stylochus</i> sp.	Platyhelminthes	Polycladida	51	0.77	8.8	5.7	11.8	< 0.0001
<i>Tagelus plebeius</i>	Bivalvia	Veneroida	57497727	-0.04	10.1	9.9	10.2	< 0.0001
<i>Ischadium recurvum</i>	Bivalvia	Mytiloidea	1016692	0.05	10.1	9.7	10.5	< 0.0001
<i>Lucina nassula</i>	Bivalvia	Veneroida	36	-0.63	13.0	-3.1	29.1	0.0075
<i>Ampelisca</i> spp.	Crustacea	Amphipoda	3469	0.36	15.0	12.1	17.9	0.0003
<i>Paraprionospio pinnata</i>	Polychaeta	Spionidae	290	0.95	15.8	9.5	22.1	< 0.0001
<i>Mysella</i> sp. A	Bivalvia	Veneroida	1828	-0.04	17.0	16.7	17.4	0.0063
<i>Odostomia</i> sp.	Gastropoda	Heterostropha	220	0.11	20.4	19.9	21.0	0.0032

2895

2896

Table 17. Continued.

Taxa name	Higher Taxa group ¹	Lower Taxa Group ²	Parameters					p Value
			a (Peak Abundance)	b (Skewness)	c (Salinity)			
					Estimate	90% Low	90% High	
<i>Mysella planulata</i>	Bivalvia	Veneroidea	115	0.35	21.5	14.2	28.7	0.0302
<i>Caecum pulchellum</i>	Gastropoda	Neotaenioglossa	124	0.10	21.7	20.2	23.1	0.0067
<i>Aglaophamus verrilli</i>	Polychaeta	Nephtyidae	22	0.58	23.5	8.7	38.4	0.001
<i>Phascolion strombus</i>	Sipuncula	Golfingiiformes	119	0.15	24.8	22.7	26.9	0.0211
<i>Listriella barnardi</i>	Crustacea	Amphipoda	864	-0.04	26.0	24.1	27.2	0.0005
<i>Parvilucina multilineata</i>	Bivalvia	Veneroidea	51	0.24	26.1	23.8	28.4	< 0.0001
<i>Ampelisca</i> sp. 3	Crustacea	Amphipoda	153	0.15	26.5	23.7	29.3	0.004
<i>Sthenelais</i> sp. A (or spp.)	Polychaeta	Sigalionidae	72	0.23	26.9	22.4	31.3	0.0015
<i>Kalliapseudes</i> sp. 1	Crustacea	Tanaidacea	188	0.12	27.6	26.4	28.9	0.0012
<i>Schistomeringos rudolphi</i>	Polychaeta	Dorvilleidae	103	0.03	30.1	29.7	30.4	0.0041
<i>Spiochaetopterus oculatus</i>	Polychaeta	Chaetopteridae	425	0.01	30.7	30.3	31.1	0.001
<i>Molgula occidentalis</i>	Asciacea	Pleurogona	519	-0.03	31.4	31.1	31.8	0.0006
<i>Eusarsiella texana</i>	Crustacea	Ostracoda	310	-0.03	31.6	31.2	32.1	< 0.0001
<i>Grubeulepis mexicana</i>	Polychaeta	Eulepethidae	110	0.04	32.1	31.8	32.5	0.027

2897

2898

2899

2900 While the Venice system is widely used to divide an estuary into salinity-based zones,
 2901 it is not biologically relevant in all cases. It is often more practical to divide an estuary into
 2902 several overlapping zones that are based on the abundances of organisms along a salinity
 2903 gradient (Bulger et al. 1993). This study applied a combination of these two classification
 2904 schemes to specify four zones to describe the distribution and composition of macrobenthic
 2905 communities in the CRE (**Table 18**). These zones, based on dry season salinities, were
 2906 designated Bulger Zone 1 (salinity of 0.2–4.2), oligohaline zone 2 (2.6–12.5), mesohaline
 2907 zone 3 (15.1–24.9), and polyhaline zone 4 (28.0–34.7).

2908 **Table 18.** Seasonal ranges for salinity zones in the CRE based
 2909 on classifications provided by Bulger et al. 1993.

Zone	Dry	Wet
Bulger Zone 1	0.2–4.2	0.2–0.2
Oligohaline	2.6–12.5	0.2–3.1
Mesohaline	15.1–24.9	7.9–13.9
Polyhaline	28.0–34.7	21.0–30.5

2910

2911 Despite the loss of several macrobenthic species in high flow relative to low flow
 2912 periods, the abundance of several mobile invertebrates and fish have been documented to
 2913 decrease during low flow periods in Southwest Florida estuaries (Flannery et al. 2002).
 2914 Mobile species with decreases during low flow periods include bay anchovy and sand
 2915 seatrout juveniles, mysids, and grass shrimp. A previous study on fish and mobile aquatic
 2916 invertebrates (blue crab [*Callinectes sapidus*] and pink shrimp [*Farfantepenaeus*
 2917 *duorarum*]) separated the CRE into three zones, with the lower, middle and upper zones
 2918 incorporating the reach of the benthic stations in the current study of stations 4 and 5, 2
 2919 and 3, and 1, respectively (Stevens et al. 2010).

2920 Salinity observations at BR31 from WY1993–WY2012 provided a platform to explore
 2921 long-term, dry season variations in inflow and salinity conditions in the Bulger Zone (0.2
 2922 to 4.2; **Table 19**; **Figure 38A**). Average dry season salinity varied from 0.3 (WY1995) to
 2923 13.3 (WY2001) averaging 4.5 ± 4.8 over all dry season days ($n = 3,591$). Periods of reduced
 2924 salinity coincided with increased inflows in the dry seasons of WY1994–WY1996,
 2925 WY1998, and WY2003–WY2006. The percentage of dry season days where salinity was
 2926 within the desired range indicative of the Bulger Zone as defined for macrobenthic
 2927 communities ranged from 0.0% (WY1997, WY2001, WY2007, and WY2008) to 96–99%
 2928 (WY1995 and WY2003–WY2006; **Figure 38B**). Salinity was within the desired 0 to 4
 2929 range on ~54% of dry season days at BR31 with percentages of 38.7%, 5.8%, 4.6%, and
 2930 5.0% for the 0 to 1, 1 to 2, 2 to 3, and 3 to 4 salinity categories, respectively (**Table 19**).
 2931 This means that salinity values were in excess of 4 on ~46% of the dry season days. The
 2932 inflow rate ranged from 0 to 3,720 cfs and averaged 501 ± 525 cfs for the days where
 2933 salinity was 3 to 4 ($n = 181$).

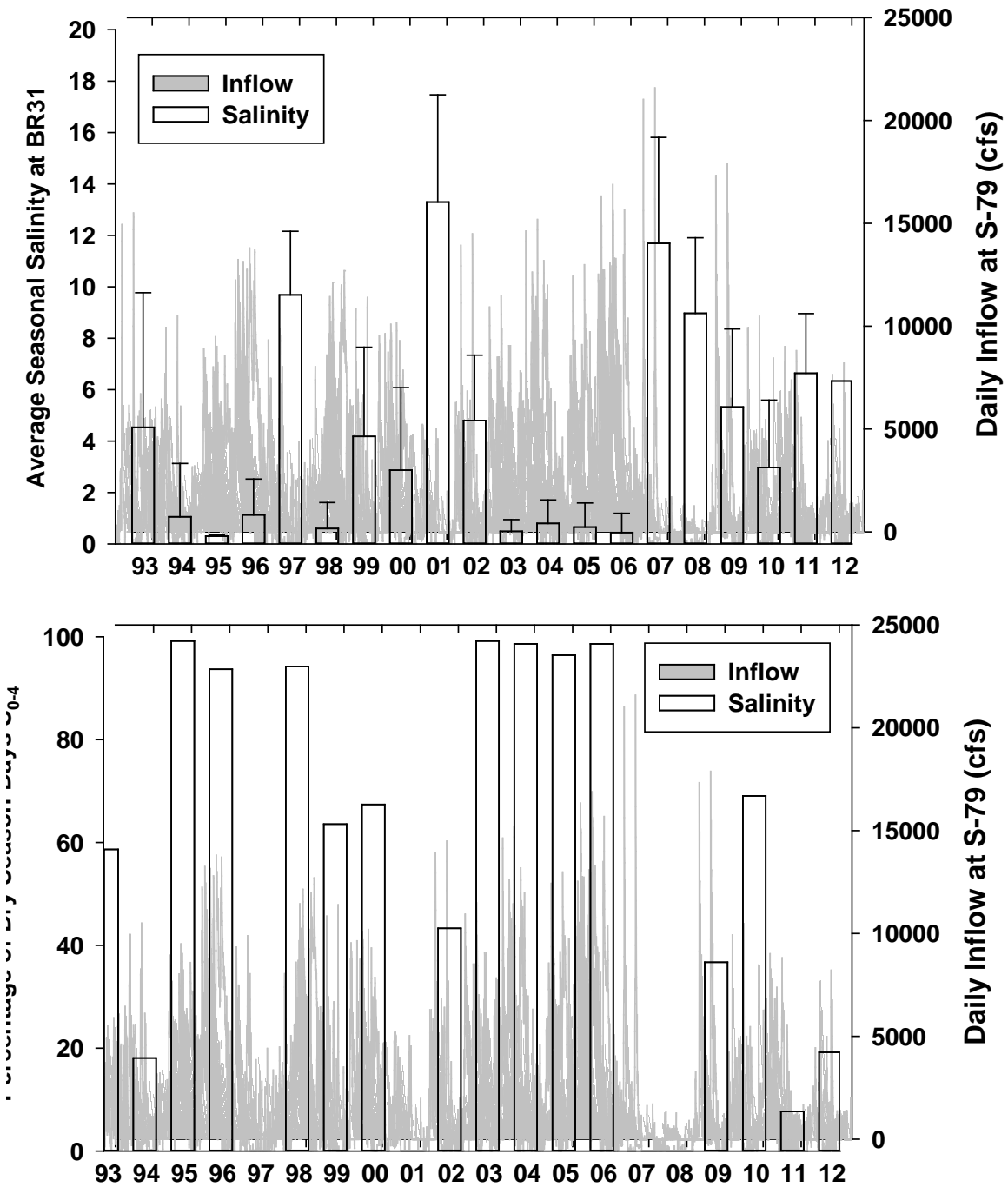
2934 Benthic communities are not only indicators of a salinity gradient, but are part of the
 2935 food chain for many mobile aquatic species. Providing sufficient inflows to the CRE
 2936 promotes spatial salinity gradients that are favorable for a wide range of benthic and water
 2937 column communities. Reduced dry season freshwater inflows can cause freshwater and
 2938 low salinity species and habitats in the upper CRE to be lost or reduced in size as these

2939 habitats are destroyed or relocated upstream (Chamberlain and Doering 1998a).
 2940 Maintaining low salinity habitat is integral for at least part of the life cycle of mobile
 2941 species such as *Callinectes sapidus* (blue crab), *Carcharhinus leucas* (bull shark), and
 2942 *Pristis pectinata* (smalltooth sawfish; Hunt and Doering 2013) and many other species in
 2943 the Caloosahatchee Estuary (Stevens et al. 2010).

2944 **Table 19.** The number and percentages of dry season days for average daily salinity values at
 2945 BR31 over a series of salinity class criteria (0 to 1, 1 to 2, 2 to 3, 3 to 4, >4, and all dry season
 2946 days) from WY1993 to WY2012.

Salinity Class	Number	Percentage (%)	Salinity	Inflow S-79 (cfs)	
			Avg ± SD	Range	Avg ± SD
0 to 1	1,388	38.7	0.3 ± 0.2	0 to 15,700	3,074 ± 2,777
1 to 2	208	5.8	1.5 ± 0.3	0 to 6,990	782 ± 980
2 to 3	165	4.6	2.5 ± 0.3	0 to 4,260	596 ± 782
3 to 4	181	5.0	3.5 ± 0.3	0 to 3,720	501 ± 525
>4	1,649	45.9	9.0 ± 3.6	0 to 4,410	239 ± 465
All Dry Season Days	3,591	100.0	4.5 ± 4.8	0 to 15,700	1,366 ± 2,201

2947
 2948



2949

2950

2951

2952

2953

Figure 38. (A) Long-term average salinity in the dry season at Bridge 31 in the upper CRE (open bars; left axis) superimposed on daily freshwater inflow at S-79 (grey fill; right axis). **(B)** The percentage of dry season days where salinity ranged from 0 to 4 (S₀₋₄) at Bridge 31 in the upper CRE (open bars; left axis) superimposed on daily freshwater inflow at S-79 (grey fill; right axis).

2954

2955 **Component Study 7: Relationships between Salinity and the**
2956 **Survival of *Vallisneria americana* in the Caloosahatchee**
2957 **River Estuary**

2958 *Christopher Buzzelli, Peter Doering, Zhiqiang Chen, and Yongshan Wan*

2959 **Abstract**

2960 *Vallisneria americana* is sensitive to increased salinity in many estuaries, including the
2961 CRE. Much of the historical *Vallisneria* observed from 1993 to 1999 in the CRE has been
2962 lost since droughts in 2001 and 2007–2008. This study examined relationships between
2963 *Vallisneria* and salinity through change-point analysis, assessment of long-term patterns of
2964 abundance, and exploration of the effects of salinity exposure time. Change-point analysis
2965 revealed salinity thresholds of 4, 9, and 15. Dry season average daily salinity was ~5 and
2966 rarely exceeded 10 when *Vallisneria* was abundant from 1993 to 1999. Indicator inflows
2967 (Q_I) ranging and averaging 0 to 3,160 and 545 ± 774 , respectively, were associated with
2968 dry season salinity values of 9 to 10 ($n = 63$) at Fort Myers from 1993 to 1999. In contrast,
2969 *Vallisneria* was virtually absent from 2007 to 2013 as dry season average daily salinity
2970 exceeded 10. Negative changes in shoot density can be rapid as ~50 to 60% of the
2971 aboveground material was lost if salinity was >10 for two to three weeks. These results
2972 highlight the effects of both the magnitude and duration of environmental conditions that
2973 can inhibit *Vallisneria* survival in the CRE.

2974 **Introduction**

2975 *Vallisneria* is a freshwater species of SAV commonly found in many lakes, rivers, and
2976 upper reaches of estuaries (Kraemer et al. 1999, Bortone and Turpin 2000, McFarland
2977 2006). *Vallisneria* is dioecious, perennial, and capable of extensive clonal growth through
2978 the formation of belowground stolons (Lovett-Doust and LaPorte 1991). Northern
2979 populations overwinter as a dormant winter bud buried in the sediments (Titus and Hoover
2980 1991). In South Florida, populations do not completely die back in winter as plants actively
2981 grow year round (Dawes and Lawrence 1989, Doering et al. 1999).

2982 *Vallisneria* habitats are ecologically and economic important components in many
2983 estuaries (Wigand et al. 2000, Rozas and Minello 2006, Hauxwell et al. 2007). However,
2984 the survival of *Vallisneria* in estuaries can be modulated by interactions among salinity
2985 intolerance, submarine light limitation, and grazing by herbivores (Kraemer et al. 1999,
2986 Hauxwell et al. 2004, Dobberfuhl 2007, Moore et al. 2010). In particular, there have been
2987 many laboratory experiments to evaluate the responses of *Vallisneria* to altered salinity
2988 (**Table 20**). Bourn (1932, 1943) reported that growth stopped at 8.4, while Boustany et al.
2989 (2010) found limited growth at 8.0. Haller (1974) reported growth at 10.0 but death at 13.3.
2990 While growth was minimal or zero when salinities ranged from 10.0 to 15.0, values >15.0
2991 caused mortality (Haller 1974, Doering et al. 2001, Doering et al. 2002, French and Moore
2992 2003, Frazier et al. 2006, Boustany et al. 2010, Lauer et al. 2011). It is widely accepted that
2993 salinity >10.0 can be damaging to the survival of *Vallisneria*.

2994

Table 20. Summary of *Vallisneria* salinity tolerances from a variety of studies in different locations.

REFERENCE	LOCATION	CONDITIONS	RESPONSE
PLANTS			
Bourn 1932, 1943	Back Bay, VA	Static, acute 2-month exposure, outdoors, 11 salinity treatments	Growth stopped at a salinity of 8.4 in both winter and summer.
Haller 1974	Fort Lauderdale, FL	Static, acute 4-week exposure in greenhouse, 6 salinity treatments	Growth lower at salinities of 6.66 and 10 than at 0.17 and 3.33. Death at salinities of 13.32 and 16.65.
Twilley and Barko 1990	Potomac River, VA	Static, 5-week exposure outdoors, slowly raise salinity to treatment levels, 5 salinity (maximum 12) and 2 light treatments	No effect on growth at salinities of 0 to 12 regardless of light.
Doering et al. 1999	Caloosahatchee Estuary, FL	Flow through mesocosms, 6-week exposure, artificial light, indoors, slowly raise salinity. 5 salinity treatments (maximum 15)	Growth declined with increasing salinity, nil or very slow at a salinity of 15.
Doering et al. 2002	Caloosahatchee Estuary, FL	Flow through mesocosms, 5–6-week exposures, artificial light, indoors, slowly raise salinity. 10 salinity treatments (maximum 30)	Growth low or ceased at salinities of 10 and 15, mortality at salinities >15.
French and Moore 2003	Maryland	Static, outdoor mesocosms exposure 7-month growing season, 4 salinity treatments (maximum 15), 3 light levels	Growth minimal at salinities of 10 and 15.
Boustany et al. 2010	St. Johns River, FL	Static, greenhouse, 10 week exposure, 10 week recovery, 3 salinity treatments (maximum 18), 3 light levels	Survived a salinity of 8, but growth was limited. Aboveground biomass perished after 10 weeks at a salinity of 18, 20% of these plants recovered after 10 weeks.
DURATION			
Doering et al. 2001	Caloosahatchee Estuary, FL	Flow through mesocosms, 0- to 70-day exposure to 18, 30-day recovery, artificial light, indoors, slowly raise salinity.	Declines in blades and shoots observed after 5-day exposure. Statistically significant declines at 20- to 70-day exposures. Viable plants after 70 days.
Frazier et al. 2006	Kings Bay, Florida	Static, acute, 4 salinity treatments (maximum 25), 3 durations of exposure, 28-day recovery	100% mortality at a salinity of 25 after 1-, 2-, or 7-day exposure. 75% mortality at a salinity of 15 after a 7-day exposure. Exposure to a salinity of 5 had no effect on growth.
FLOWERING			
French and Moore 2003	Maryland	See French and Moore 2003 above	No flowering at salinities of 10 or 15 regardless of light level.
Doering et al. unpublished	Caloosahatchee Estuary, FL	See Doering et al. 1999 above	Female structures at salinities of 0 and 3. Male structures at salinities of 0, 3, and 9. Neither structures at salinities of 12 or 15.
SEEDS			
Nosach 2007	Caloosahatchee Estuary, FL	Petri dishes, laboratory incubator, 3 temperature, 2 light, and 4 salinity (maximum 15) treatments.	Seeds germinated at all salinities although rate declined as salinity increased. Temperature had the greatest effect with highest germination at 30° C.
Jarvis and Moore 2008	Tidal tributary of the Potomac River, MD	Field characterization and laboratory experiments. A. Salinity at 4 levels 1 to 15 in petri dishes; B. temperature at 4 levels 13 to 29 ° C in petri dishes; C. dark and light for oxygenated and hypoxic in 250 milliliter serum bottles; and D. 4 treatments of varying sediment composition and 6 burial depths.	Increased salinity had significant negative effect on germination with the threshold between salinities of 5 and 10. Seed viability was maintained at salinity >10. Temperature exhibited a strong influence on germination with the highest germination occurring at >22° C. Oxygenation enhanced germination while light and burial depth (0.2 to 10 centimeter) had no effect.

2995

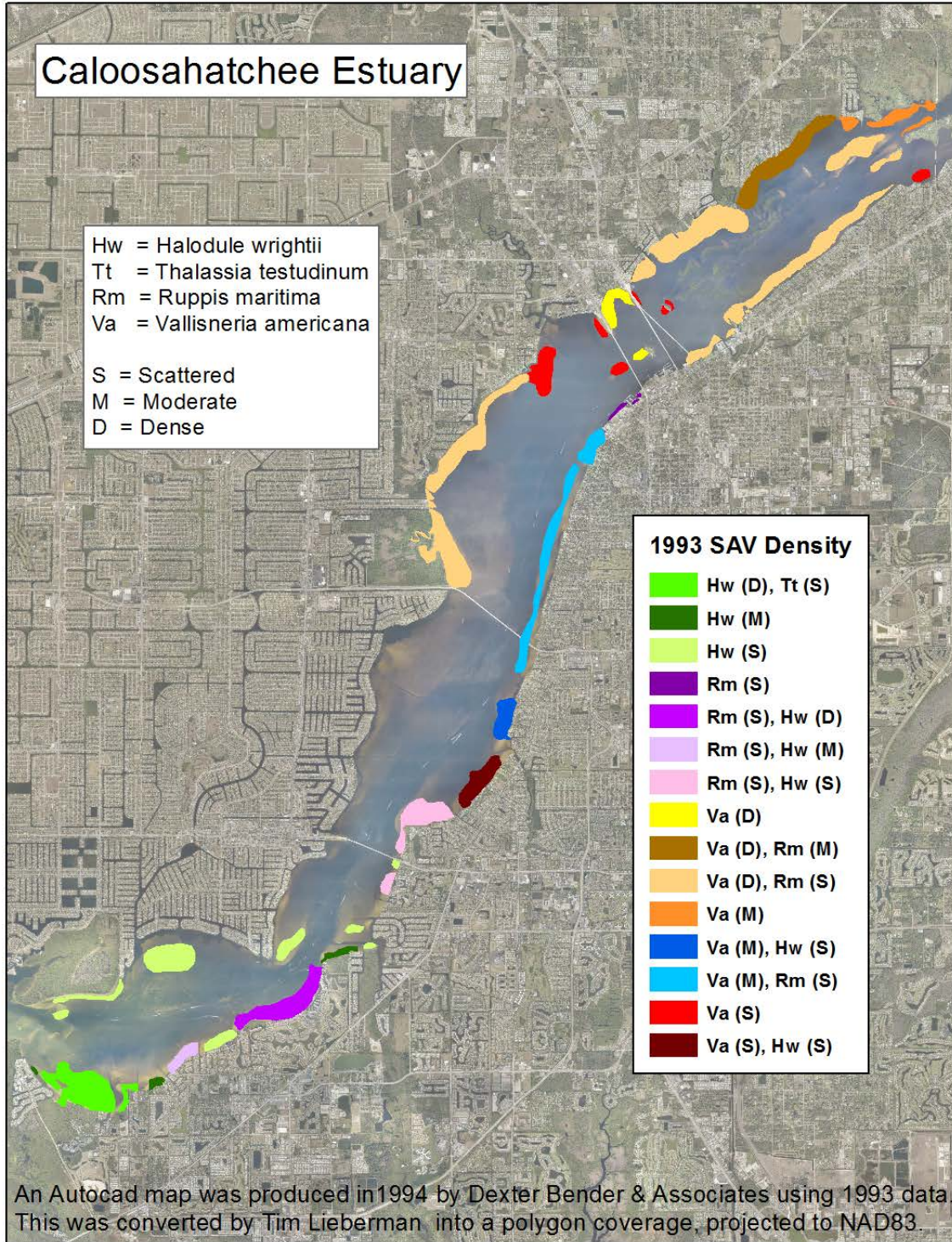
2996 Salinity also influences flowering and seed production in the life history of estuarine
2997 *Vallisneria* populations. French and Moore (2003) noted that flowering did not occur in
2998 salinity treatments of 10 and 15. Although the data were not included in Doering et al.
2999 (1999), they observed female flowers at 0 and 3, but not at 9 or above. Male flowers
3000 occurred at salinity values of 0, 3, and 9 but not when salinity was 12 or 15. Nosach (2007)
3001 examined the effects of temperature, light, and salinity on germination of *Vallisneria* seeds.
3002 Although seeds germinated across all salinities in this study (0 to 15), the best conditions
3003 for seed germination occurred at a temperature of 30 degrees Celsius (° C) and salinities
3004 <5. Jarvis and Moore (2008) found that *Vallisneria* germination occurred best at
3005 temperatures >22° C and was significantly greater in salinity treatments of <1 and 5
3006 compared to the 10 and 15 treatments. Non-germinated seeds provide a pathway for
3007 revegetation by remaining viable throughout most environmental conditions.

3008 The growing season for *Vallisneria* in the CRE in Southwest Florida lasts from March
3009 to September, with peak shoot density occurring in June or July (Bortone and Turpin 2000).
3010 Shoot density begins to decline in late summer as the production of male and female
3011 flowers is greatest in September or October. Blade length increases from March to
3012 September or October, sometimes to over a meter, and declines into the winter.
3013 Overwintering rosettes have short blades, 10 centimeters or less in length (Bortone and
3014 Turpin 2000).

3015 Historically, there was abundant *Vallisneria* habitat in the upper CRE (Kraemer et al.
3016 1999, Bortone and Turpin 2000, Doering et al. 2002, Bartleson et al. 2014). Published
3017 qualitative observations supported the presence of *Vallisneria* in the early 1960s (Gunter
3018 and Hall 1962, Phillips and Springer 1960). *Vallisneria* was present in the CRE from the
3019 mid-1980s until quantitative monitoring began in January 1998 (Bortone and Turpin 2000).
3020 Hoffacker (1994) conducted a visual census from July to October 1993 characterizing
3021 coverage as dense, moderate, or scattered. *Vallisneria* coverage was dense in the upper
3022 estuary between the Railroad Trestle near Beautiful Island and the Edison Bridge at Fort.
3023 Myers (**Figure 39**). The maximum downstream extent (Whiskey Creek) was documented
3024 in the Hoffacker map. When considered along with quantitative monitoring, it appears that
3025 there were dense beds of *Vallisneria* in the upper CRE from 1993 to 1999.

3026 The management of freshwater inflow through the Franklin Lock and Dam at the head
3027 of the CRE (S-79; **Figure 40**) is an important influence on circulation and transport in the
3028 CRE. Reduced freshwater inflow during the dry season (November–April) permits
3029 upstream encroachment of salt water (Wan et al. 2013, Buzzelli et al. 2014a).
3030 Superimposed on intra-annual variations and water management are droughts such as the
3031 one in 2000–2001 when increased salinity led to widespread loss of *Vallisneria*. Rainfall
3032 for the CRE MFL Watershed (**Figure 1A**) averages 51.1 inches annually. In 2001, the
3033 rainfall was only 35.8 inches, which was representative of a 1-in-25 year drought event.
3034 Another drought event occurred in 2007 that was equivalent to a 1-in-10 year drought.
3035 Additionally, for many years since 2000, dry season rainfall has been well below normal.
3036 As a result of multiple drought events and deficits in dry season rainfall, freshwater inflows
3037 in the CRE have been reduced.

3038



3039
 3040
 3041

Figure 39. 1993 map of SAV habitat density in the CRE from Hoffaker (1994).

3042 Based on accumulated knowledge, this study assumed that salinity is the dominant
3043 driver for *Vallisneria* survival. This phenomenon was explored through local observations
3044 and data to assess survival of *Vallisneria* with fluctuating salinity using three separate
3045 approaches. The first was a statistical approach that applied Bayesian change-point analysis
3046 to determine the critical salinity values for *Vallisneria* (Beckage et al. 2007). This method
3047 uses piecewise regression to identify abrupt changes in sequential data (e.g. time series).
3048 The second was an assessment of long-term patterns of *Vallisneria* shoot densities and
3049 salinity. This approach provided an historical perspective that could help explain the
3050 present status of the resource. The relationship between the duration of super critical
3051 salinity and the proportional mortality of *Vallisneria* shoots was examined in the
3052 third approach.

3053 **Methods**

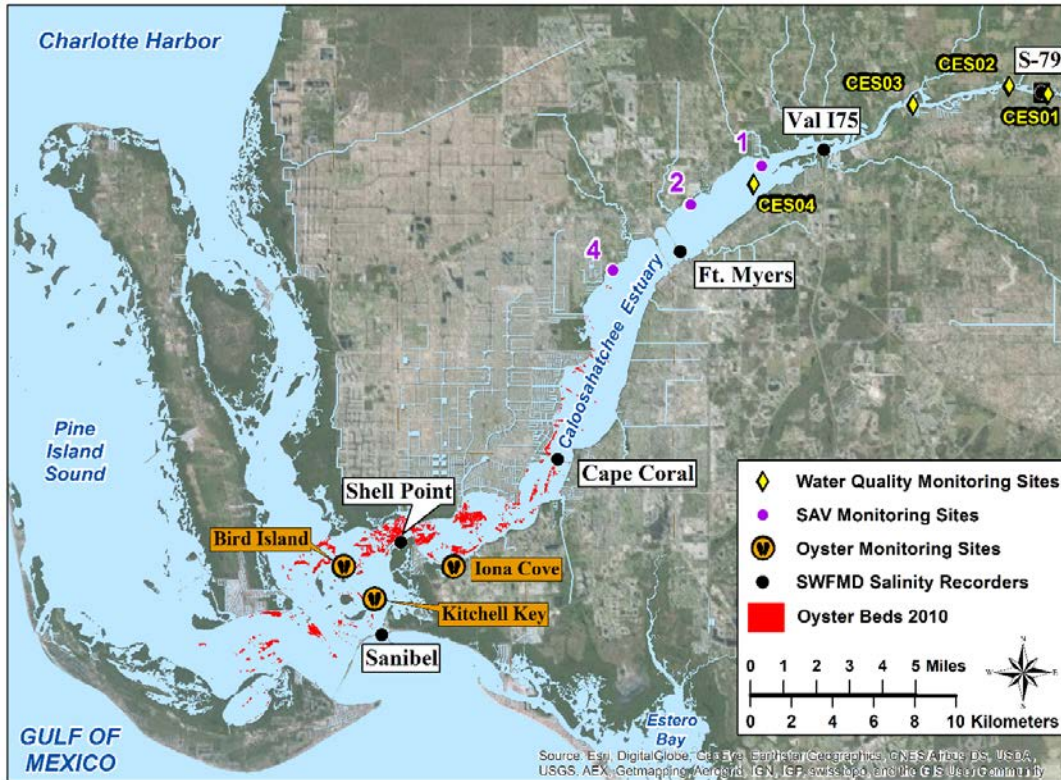
3054 ***Vallisneria* Monitoring in the Caloosahatchee River Estuary**

3055 Quantitative monitoring of *Vallisneria* started in 1998 at Sites 1 through 4 (**Figure 40**).
3056 Researchers established paired, perpendicular 100-m transects at each site. On each
3057 sampling date, the number of blades, shoots, and flowers were counted in five separate,
3058 random 0.1-m² quadrats along each transect (n = 10 = 5 quadrats x 2 transects; Bortone and
3059 Turpin 2000; Doering et al. 2002). Blade length and width were also determined in each
3060 quadrat. Field monitoring methods were changed in 2008 to a gridded presence/absence
3061 method where the number of cells containing shoots within a 1-m² quadrat was counted at
3062 multiple, randomly distributed sites. Because Site 3 was discontinued in 2003, there are
3063 three sites (1, 2, and 4) where shoot densities were monitored at approximately monthly
3064 intervals from 1998 to 2007. Data from Sites 1 and 2 were used in this study. Site 4 was
3065 omitted because *Vallisneria* presence was extremely variable at this most
3066 downstream station.

3067 **Salinity Monitoring in the CRE**

3068 Since 1992, SFWMD has monitored salinity at several locations in the CRE at 15-
3069 minute intervals (**Figure 40**). Salinity is determined at two depths (20% and 80% of depth
3070 relative to mean sea level) using in situ data recorders. Daily average surface salinity
3071 recorded at Fort Myers from May 1, 1992 to April 30, 2014 was obtained from the
3072 DBHYDRO (http://www.sfwmd.gov/dbhydroplsql/show_dbkey_info.main_menu).
3073 Missing daily salinity values (1,058 of 8,035 days) were estimated using an autoregressive
3074 model (Qiu and Wan 2013).

3075



3076

3077

3078

3079

Figure 40. Location map for the CRE including the S-79 water control structure, water quality monitoring sites, SAV monitoring sites (upper CRE), and the location of continuous salinity recorders.

3080

Data Analyses

3081

3082

3083

3084

Both salinity and *Vallisneria* shoot count data were expressed as a time series of water years. A water year spans May 1 to April 30 to include both wet (May–October) and dry (November–April) seasons representative of the subtropical climate of South Florida. There were a few different approaches to assess *Vallisneria*-salinity relationships.

3085

3086

3087

3088

3089

3090

3091

3092

3093

3094

3095

3096

3097

3098

First, salinity thresholds were quantified by applying Bayesian change-point analyses to the merged salinity-*Vallisneria* data (Qian et al. 2004, Ruggieri 2012). Change-point analyses successively split the data into two groups. At each split, the statistical properties (e.g., posterior means) of the two groups are evaluated to determine the likelihood (probability) that each group is statistically similar unto itself and at the same time statistically distinct from the opposing group. The most probable change point was considered to represent a change point threshold of salinity with uncertainty quantified by constructing a high density credible interval around this threshold. The Bayesian change point package in “R” was used (<http://cran.r-project.org/web/packages/bcp/>; Erdman and Emerson 2007). Shoot density data were log transformed to normalize the distribution. In addition, shoot density data were binned based on integer salinity values from 1 to the maximum salinity observed. The procedure results in posterior means and a probability distribution over salinity groups. Change points of salinity were chosen as salinities where there was maximum probability of difference among adjacent data groups at each split.

3099 Second, historical differences in indicators of *Vallisneria* abundance and salinity were
3100 assessed to better understand the conditions that either promote or inhibit *Vallisneria*. This
3101 was accomplished by defining two equivalent time periods each containing seven wet and
3102 six dry seasons for analysis of salinity patterns. The two periods were May 1, 1993–
3103 October 31, 1999 (WY1994 to wet season of WY2000), and, May 1, 2007–October 31,
3104 2013 (WY2008 to wet season WY2014). Salinity patterns during these time periods were
3105 qualitatively compared to shoot densities from Site 2. Data from the first period (WY1993–
3106 WY1999) were queried to extract the dry season days where salinity at Fort Myers was 9
3107 to 10. These inflows were assumed to be below the desirable limit to maintain favorable
3108 salinity conditions.

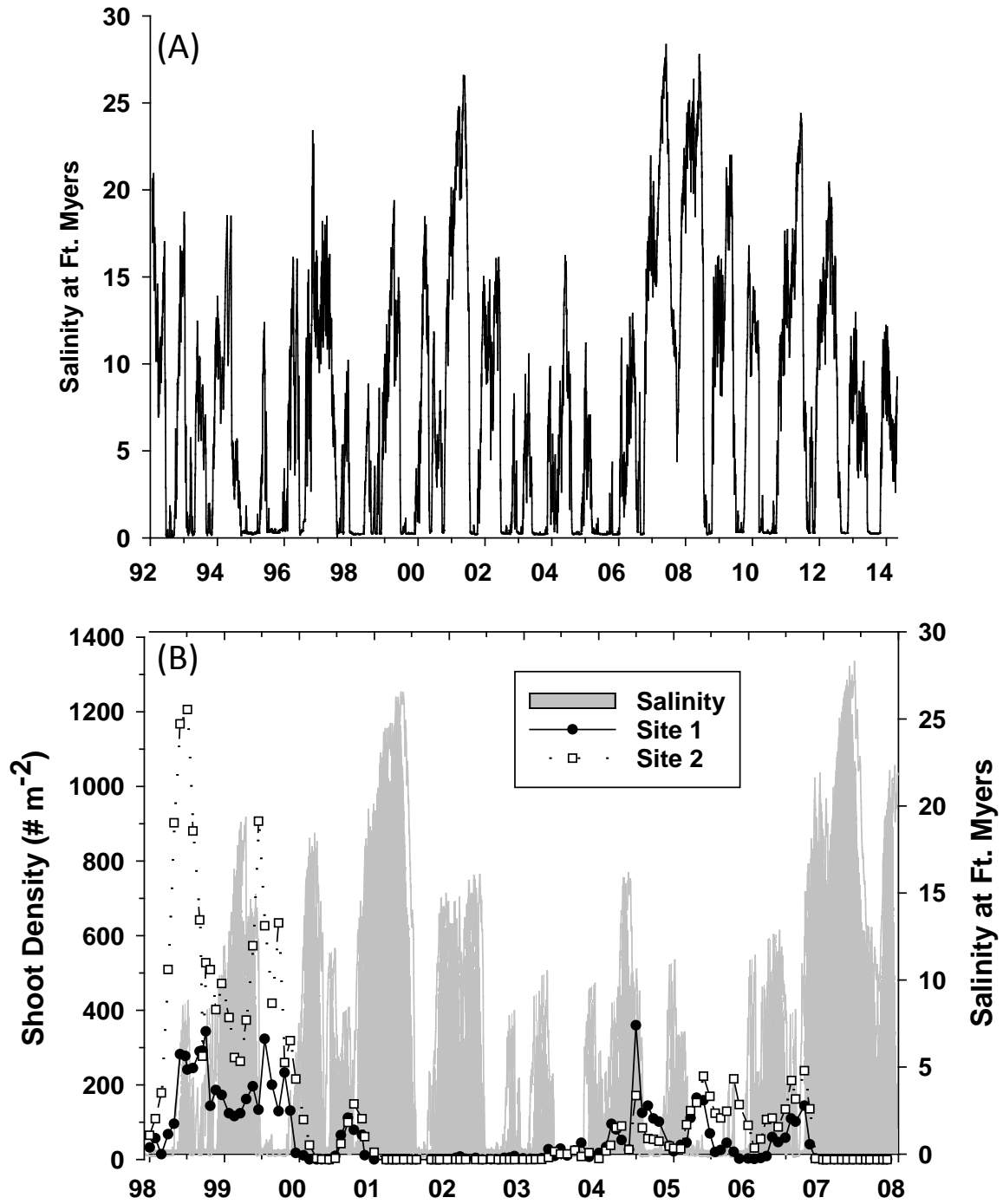
3109 Finally, the effects of exposure time on the survival of *Vallisneria* were examined using
3110 the observed shoot densities at Sites 1 and 2 and the Fort Myers salinity record. The 30-
3111 day moving average salinity was calculated. Four time periods among the two sites were
3112 selected to assess decreases in shoot density with critical salinity values. Not all high
3113 salinity (30-day average salinity >10) events were included in the data set. Two episodes
3114 occurring between March and June 2002 were excluded because initial shoot density was
3115 too low (≤ 11 shoots per m^2) to quantify a decline. An episode that occurred in 1999 also
3116 was not included. While plants did decline, the decline itself began well before salinity at
3117 Fort Myers reached 10 and other factors either singly or in combination with salinity may
3118 have been responsible. For the remaining intervals, the shoot density on the first day was
3119 used as the initial condition. The number of days where the 30-day moving average salinity
3120 exceeded 10 (x) was paired with the percent of shoots remaining relative to the initial
3121 conditions (y) and modeled using a negative exponential curve.

3122 Results

3123 Salinity at Fort Myers varied on seasonal, annual, and multi-annual time scales (**Figure**
3124 **41A**). It was greatest in the dry season peaking at ~26 and 27 in 2001, 2007, and 2008.
3125 Values were generally lowest from 2003 to 2006. Average shoot densities ranged from 0
3126 to 370 and 0 to 1,200 shoots per m^2 at Sites 1 and 2 (**Figure 41B**). Shoots were abundant
3127 from 1998 to 2000 with densities at Site 2 much greater than those observed at Site 1. Shoot
3128 densities were much reduced and similar between the two sites in 2000 before dropping to
3129 near zero from 2001 to 2004. Density increased slightly to 0 to 200 shoots per m^2 from
3130 2004 to 2006 before again falling to zero in 2007.

3131 The Bayesian change-point analysis resulted in clear salinity thresholds of 4, 9, and 15
3132 (**Figure 42**). These values reinforce previous findings where salinity values that were ≥ 5
3133 impaired growth, those ≥ 10 stopped growth, and salinity values ≥ 15 caused mortality. The
3134 first threshold (4) was associated with the highest shoot densities. The most pronounced
3135 change point of salinity was around 9 (posterior probability of 86%) with the 95%
3136 credibility limit from 8 to 10. Salinity values >9 were associated with decreased densities
3137 from 200 to 100 shoots per m^2 . The inflection point around a salinity of 15 had a probability
3138 of 0.6 and a 95% credibility limit of 14 to 16. Salinity values >15 were associated with
3139 decreased densities to <40 shoots per m^2 .

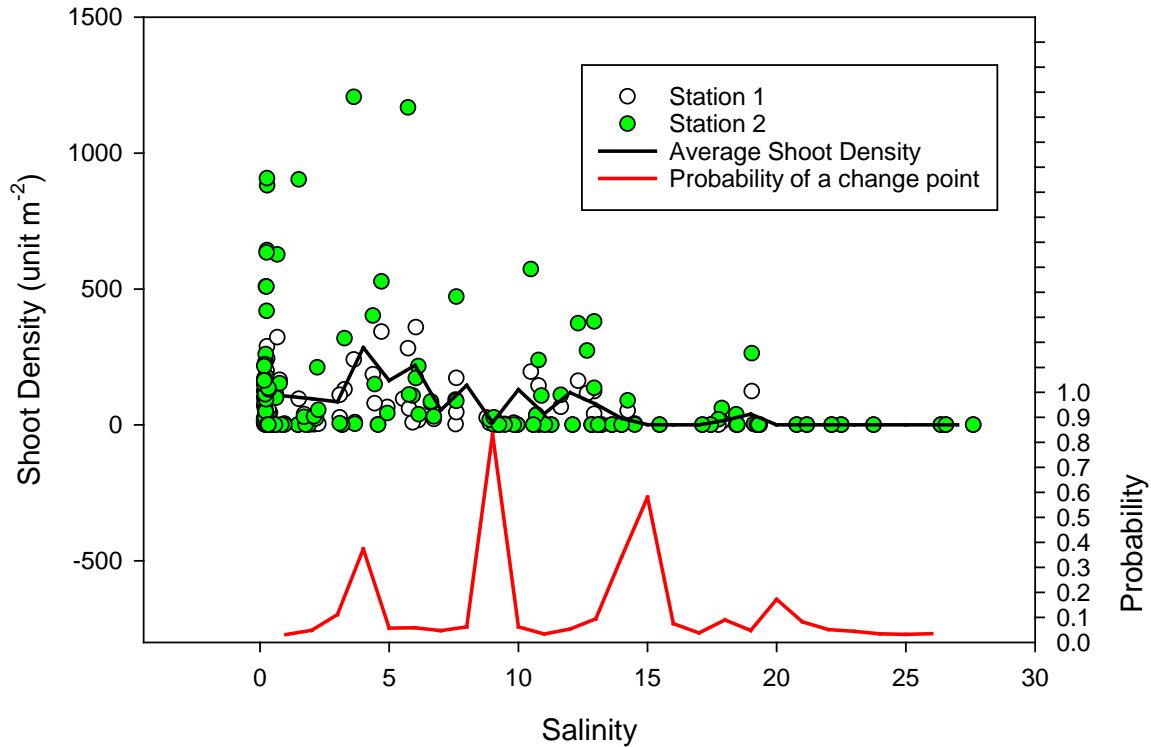
3140



3141
 3142
 3143
 3144
 3145

Figure 41. (A) Time series of daily average surface water salinity at Fort Myers from January 1992 to April 2014. (B) Time series of average *Vallisneria* shoot densities (# m⁻²) at Sites 1 (filled circle) and 2 (open square) in the CRE from 1998 to 2007. Average daily surface salinity at Fort Myers is shown as the grey filled time series (right axis).

3146



3147
3148
3149
3150
3151

Figure 42. Combination plot showing *Vallisneria* shoot densities (unit per m² [unit m⁻²]; left axis) from monitoring Sites 1 and 2 as a function of the 30-day moving average salinity at Ft. Myers. The red line depicts the probabilities of break points in the relationship between shoot density and salinity.

3152 Anecdotal, observational, and quantitative information indicated large differences in
3153 *Vallisneria* distribution and density between the two time periods (WY1993–WY1999 and
3154 WY2007–WY2013; **Figure 42**). The Hoffaker map (1994; **Figure 39**) revealed extensive
3155 *Vallisneria* habitat throughout the upper half of the CRE. Personal observations by
3156 SFWMD staff (P. Doering and R. Chamberlain) confirmed dense beds of *Vallisneria*
3157 from the WY1995–WY1997 period. Shoot densities derived from in situ counts ranged from
3158 200 to 900 shoots per m² from WY1998 to WY2000 across the habitat area. Both the
3159 distribution and abundance declined through 2001 reaching ~0.0 from 2002 to 2003. There
3160 were small observable increases in shoot density from WY2004 to WY2007. However,
3161 monitoring conducted since WY2008 indicated that *Vallisneria* has been mostly absent
3162 except for a minor appearance in WY2011.

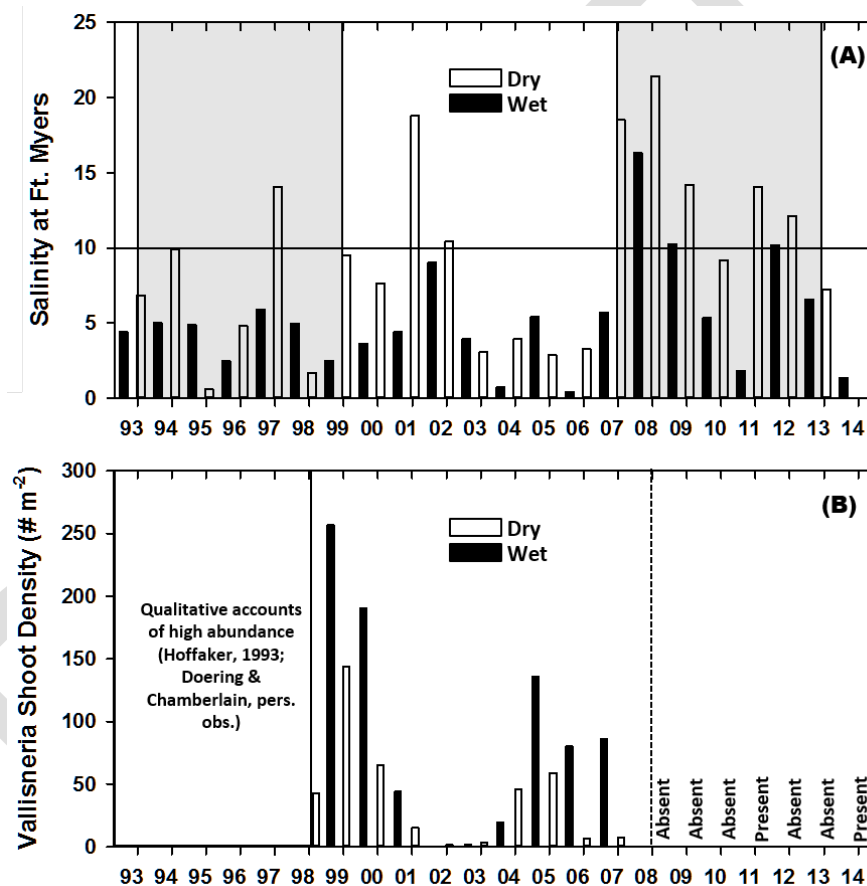
3163 Daily surface salinity at Fort Myers over the entire period of record (May 1, 1993–
3164 April 30, 2014) averaged 7.17 ± 7.09 ($n = 8,035$). During the period when *Vallisneria* beds
3165 were likely extensive and dense (WY1993–WY1999), daily salinity averaged 5.4 ± 5.4
3166 ($n = 2,375$; **Table 21**). In contrast, salinity during the period when *Vallisneria* was virtually
3167 absent (WY2007–WY2013) averaged 10.0 ± 8.0 ($n = 2,376$). One-way ANOVA showed
3168 these averages to be significantly different ($p < 0.001$). In general, *Vallisneria* requires
3169 salinities below 10 for a sustainable population (French and Moore 2003). Average
3170 seasonal salinity exceeded this value only once during the first period when *Vallisneria*
3171 was abundant (dry season 1997; **Figure 43**). During the more recent period when
3172 *Vallisneria* was sparse or absent, average salinity exceeded this threshold in five of six dry

3173 seasons and three of six wet seasons. Freshwater inflows ranging and averaging 0 to 3,160
 3174 and 545 ± 774 , respectively, were associated with dry season salinity values of 9 to 10 (n
 3175 = 63) at Fort Myers in Period 1 when *Vallisneria* was abundant (WY1993–WY1999).

3176 **Table 21.** Descriptive statistics for salinity values at Fort Myers. Two equal subsets of data were
 3177 extracted from the long-term (1992–2014) time series. Period 1 was from May 1, 1993 to
 3178 October 31, 1999. Period 2 was from May 1, 2007 to October 31, 2013.

Salinity	Period 1	Period 2
Number	2,375	2,376
Range	0.03–23.4	0.15–28.3
Average + Standard Deviation	5.4 ± 5.4	10.0 ± 8.0
Median	3.6	10.3

3179



3180

3181 **Figure 43.** (A) Time series of average seasonal salinity at Fort Myers from 1993 to 2014. The
 3182 shaded areas mark two separate seven-year periods (1993–1999; 2007–2014). (B) Time series
 3183 of average seasonal shoot density from 1998 to 2007. Data before this period were qualitative.
 3184 Monitoring methods changed to detect presence versus absence since 2008.

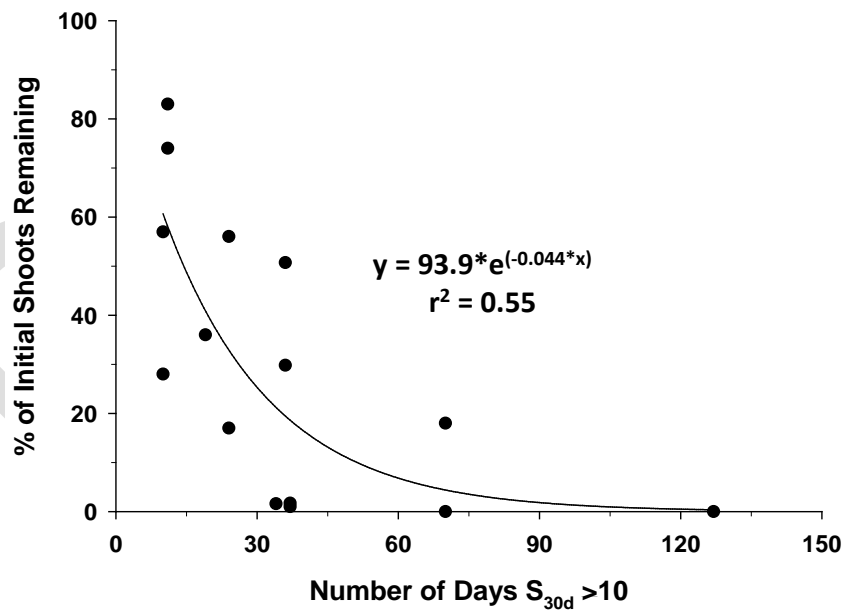
3185 *Vallisneria* shoot density decreased precipitously with increased duration of 30-day
 3186 average salinity values in excess of 10 at Fort Myers (**Table 22** and **Figure 44**). The
 3187 negative exponential relationship suggests that a 50% reduction in plant density would
 3188 occur after 14 days, an 85% reduction after 42 days, and a 95% reduction after 63 days.

3189 Examination of the upper confidence limit on the mean prediction of the equation revealed
 3190 that significant mortality occurred after 4 days (95% confidence interval no longer overlaps
 3191 100% remaining).

3192 **Table 22.** Time periods and data used to calculate percent change in *Vallisneria* shoot densities
 3193 relative to salinity criteria at Fort Myers. See text and **Figure 44** for details and results.

Station 1 Start	End	Initial Shoots	Days	% Remaining	Comment
2/27/2000	3/16/2000	10.5	19	0	Not used
11/18/2000	3/26/2001	79	11	83	
			24	17	
			70	0	
5/20/2004	6/23/2004	52	36	50.7	
11/12/2006	1/24/2007	143.9	10	28	
			37	1.7	

Station 2 Start	End	Initial Shoots	Days	% Remaining	Comment
2/27/2000	4/20/2000	107	19	36	
			34	1.6	
11/18/2000	3/26/2001	149	11	74	
			24	56	
			70	18	
			127	0	
5/20/2004	6/23/2000	90	36	29.78	
11/12/2006	1/24/2007	238.3	10	56.95	
			37	1.0	



3194 **Figure 44.** Proportional mortality plot showing the number of days where salinity at Fort Myers
 3195 was >10 versus the percent of initial shoots remaining. See text and **Table 22** for details
 3196 of analysis.

3197 **Discussion**

3198 This study represents an important step towards an improved understanding of the
 3199 survival of *Vallisneria americana* in the CRE in Southwest Florida. This understanding

3200 builds upon a foundation of original accounts, local surveys, quantitative monitoring,
3201 mesocosm experiments, statistical analyses, and simulation modeling (Hoffaker 1994,
3202 Doering et al. 1999, Bortone and Turpin 2000, Doering et al. 2002, Bartleson et al. 2014;
3203 Buzzelli et al. 2015). While estuarine *Vallisneria* is sensitive to multiple environmental
3204 factors (e.g. light, grazing, and temperature), it appears that the dominant driver is salinity
3205 (French and Moore 2003, Dobberfuhr 2007, Boustany et al. 2010, Lauer et al. 2011).

3206 Salinity is a conservative property of estuaries that, while uninfluenced by
3207 biogeochemical processes, varies over many time scales through complex hydrodynamic
3208 processes. These processes integrate rainfall, surface inflows, groundwater discharge, wind
3209 events, and tidal exchanges to establish salinity conditions (Zheng and Weisberg 2004) and
3210 modulate biological processes (Jassby et al. 1995, Livingston et al. 1997, Whitfield et al.
3211 2012). Thus, estuaries are very sensitive to anthropogenic changes in freshwater inflow
3212 (Alber 2002). Physical alterations such as dredging and dams change natural inflows,
3213 impact mixing with the coastal ocean, and dramatically affect salinity and water quality in
3214 the estuary (Day et al. 1989, Zhu et al. 2015). Discharge, salinity gradients, biogeochemical
3215 properties, and biological attributes of the CRE are greatly influenced by a combination of
3216 subtropical climatic variability and landscape-scale water management (Tolley et al. 2005,
3217 Volety et al. 2009, Buzzelli et al. 2013c, Wan et al. 2013).

3218 The location of particular isohalines in estuaries can be used as an indicator of
3219 ecological conditions (Jassby et al. 1995). In the case of the CRE, a salinity of 10 at Fort
3220 Myers has been established as a benchmark for water management (SFWMD 2012). The
3221 long-term salinity record at Fort Myers provides an excellent indication of the
3222 environmental suitability for *Vallisneria* in the upper CRE. Increasing salinity thresholds
3223 of 4 to 5, 8 to 10, and >15 serve to slow growth, inhibit survival, and cause mortality in
3224 estuarine populations of *Vallisneria*, respectively (Bourn 1932, 1943, Haller 1974, Doering
3225 et al. 2001, Doering et al. 2002, French and Moore 2003, Frazier et al. 2006; Boustany et
3226 al. 2010, Lauer et al. 2011).

3227 This study demonstrated that differences in salinity between two time periods (1993–
3228 1999 and 2007–2013) may have contributed to observed differences in density and spatial
3229 extent of *Vallisneria* in the upper CRE. During the initial period when *Vallisneria* beds
3230 were dense and widespread, salinity was ~5 and seasonally averaged salinity rarely
3231 exceeded 10 for a sustainable population. There was a 40% reduction in freshwater inflow
3232 to the upstream estuary during the second seven-year period. Reduced freshwater inflow is
3233 an important driver leading to increased salinity in the CRE. When *Vallisneria* was
3234 virtually absent in the second period, salinity was ~10 with multiple wet and dry seasonal
3235 exceedances of this threshold.

3236 It is not surprising that the *Vallisneria* habitat in the CRE has trouble recovering from
3237 repeated, severe drought-induced stress in 2001 and 2007–2008. Salinity in the CRE has
3238 been much higher since 2007 as compared to the last known period of *Vallisneria*
3239 abundance (WY1993–WY1999). Additionally, approximately half of the standing stock
3240 could be lost if salinity at Fort Myers is greater than 10 for 14 consecutive days. Loss of
3241 mature shoots inhibits the potential to reestablish viable habitat through vegetative and
3242 reproductive growth. The cumulative impacts of anthropogenic changes, increased salinity,
3243 decreased shoot density, and shrunken habitat extent have created circumstances that
3244 greatly inhibit the recovery of *Vallisneria* habitat in the CRE.

3245 **Component Study 8: Development and Application of a**
3246 **Simulation Model for *Vallisneria americana* in the**
3247 **Caloosahatchee River Estuary**

3248 *Christopher Buzzelli, Peter Doering, Yongshan Wan, and Teresa Coley*

3249 **Abstract**

3250 Monitoring of *Vallisneria americana* densities in the upper CRE from 1998 to 2007
3251 was accompanied by mesocosm experiments to determine relationships between salinity
3252 and growth. This study built upon these efforts by developing a simulation model to
3253 examine the effects of temperature, salinity, and light on *Vallisneria* survival and biomass
3254 in the upper CRE from 1998 to 2014. The effects of salinity on *Vallisneria* mortality were
3255 explored through using an eight-year experimental model based on favorable conditions
3256 from 1998 to 1999. Using the experimental model, the dry season salinity was
3257 systematically increased in 5% increments until the net annual biomass accumulation of
3258 *Vallisneria* was negative. A five-fold increase in grazing was required to stabilize model
3259 biomass under optimal conditions. A 55% salinity increase to 12 promoted shoot mortality
3260 in the experimental model. Annual inflow-salinity relationships for Fort Myers were used
3261 to estimate that dry season inflows ranging from 15.2 to 629.0 cfs and averaging 342 ± 180
3262 cfs were associated with a salinity of 12 at Fort Myers. Model results suggested that an
3263 estimated 85.4% and 86.7% of the shoots were lost in the dry seasons of 2001 and
3264 2007, respectively.

3265 **Introduction**

3266 *Vallisneria* is a freshwater species of SAV commonly found in many lakes, rivers, and
3267 upper reaches of estuaries (Bortone and Turpin 2000, McFarland 2006). *Vallisneria* habitat
3268 in estuaries is desirable since it supports a variety of ecologically and commercially
3269 important fauna (Wigand et al. 2000, Hauxwell et al. 2004, Rozas and Minello 2006).
3270 Because it is a freshwater organism that can extend into oligohaline estuarine areas,
3271 *Vallisneria* is very responsive to fluctuations in salinity (Doering et al. 2002,
3272 Boustany et al. 2010).

3273 There have been many laboratory experiments to evaluate the responses of *Vallisneria*
3274 to altered salinity. Salinity values in excess of 8 to 15 can be stressful and result in net
3275 mortality depending upon exposure time (Doering et al. 1999, Doering et al. 2001, French
3276 and Moore 2003, Boustany et al. 2010, Lauer et al. 2011). Bourn (1932, 1943) reported
3277 that growth stopped at 8.4, while Boustany et al (2010) found limited growth at 8.0. Haller
3278 (1974) reported growth at 10.0 but death at 13.3. While growth was minimal or zero when
3279 salinities ranged from 10.0 to 15.0, values >15.0 caused mortality in several studies (Haller
3280 1974, Doering et al. 2001, French and Moore 2003, Frazier et al. 2006, Boustany et al.
3281 2010, Lauer et al. 2011). It is generally accepted that salinity >10.0 is detrimental to
3282 *Vallisneria*.

3283 Water clarity is a complicating factor that can affect the survival and growth of
3284 *Vallisneria* in estuaries. Submarine light penetration in the upper part of estuaries is
3285 affected by colored dissolved organic matter, which is directly proportional to freshwater
3286 inflow (McPherson and Miller 1994, Bowers and Brett 2008, Buzzelli et al. 2014b).
3287 *Vallisneria* requires ~9 to 14% of surface irradiance with total light extinction coefficients

3288 of 3 to 4 per m being most favorable (French and Moore 2003, Dobberfuhl, 2007, Boustany
3289 et al. 2010, Moore et al. 2010). The obvious implication is that the low salinity necessary
3290 for *Vallisneria* survival in oligohaline estuarine areas is usually accompanied by decreased
3291 light levels.

3292 The growing season for *Vallisneria* in Southwest Florida lasts from March to
3293 September, with maximum shoot density and biomass occurring in July–August (Bortone
3294 and Turpin 2000). Published qualitative observations supported the presence of *Vallisneria*
3295 in the early 1960s (Gunter and Hall 1962, Phillips and Springer 1960) and the 1980s
3296 (Bortone and Turpin 2000). Hoffacker (1994) conducted a visual census from July to
3297 October 1993 that documented widespread coverage with variable density. The negative
3298 response of *Vallisneria* to increased salinity makes it an excellent ecological indicator for
3299 freshwater management (Doering et al. 2002). It provides a useful indicator because its
3300 sensitivity provides insight into environmental conditions that trigger problems at the
3301 habitat scale (Dale and Beyeler 2001).

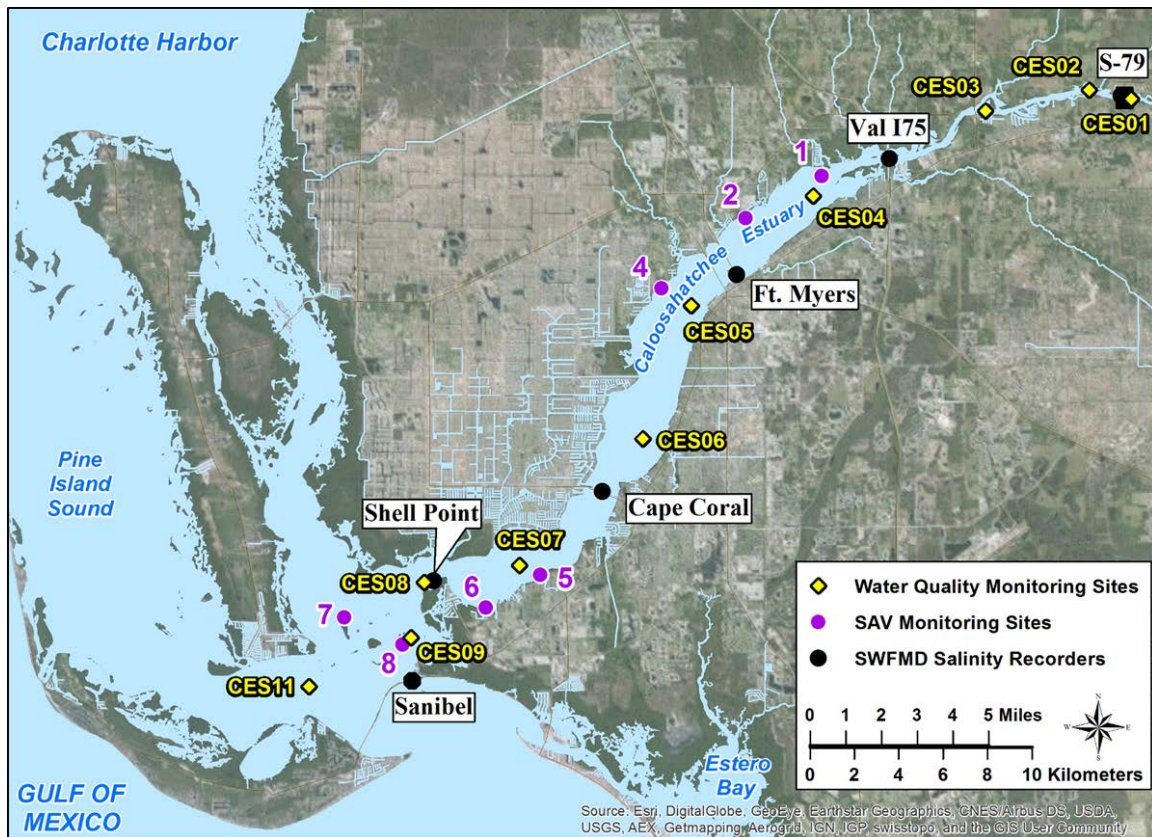
3302 The distribution and density of *Vallisneria* habitat is variable in the upper CRE in
3303 Southwest Florida (Kraemer et al. 1999, Bortone and Turpin 2000, Doering et al. 2002,
3304 Bartleson et al. 2014). The decreased availability of fresh water in the dry season
3305 (November–April) can lead to reduced freshwater inflow and the upstream encroachment
3306 of saline water (Wan et al. 2013, Buzzelli et al. 2014a). These attributes were particularly
3307 acute during droughts in 2001 and 2007–2008 when salinity increases in the upper CRE
3308 led to widespread loss of *Vallisneria*.

3309 The goal of this study was to develop a simulation model for *Vallisneria* in the CRE
3310 (Buzzelli et al. 2012, Buzzelli et al. 2014b). There has been much environmental
3311 monitoring since initial efforts to use *Vallisneria* as an indicator of freshwater inputs over
3312 a decade ago. These data provide an empirical foundation for ongoing management, and,
3313 the creation of a mathematical model to forecast potential responses to proposed
3314 management actions. The objectives were to develop and test a simulation model of
3315 *Vallisneria* responses to environmental variables (temperature, salinity, and light) and
3316 evaluate the salinity and inflow conditions that support viable oligohaline (0–10) SAV
3317 habitat in the upper CRE.

3318 **Methods**

3319 **Study Site**

3320 The CRE is bounded upstream by S-79 and extends ~42 km downstream to the mouth
3321 near the Sanibel Bridge (**Figure 45**). The surface area of the CRE is 67.6 km² (6764
3322 hectares = 16,715 acres) with an average depth of 2.7 m (Buzzelli et al. 2013b). Average
3323 flushing time ranges from 5 to 60 days (Wan et al. 2013; Buzzelli et al. 2013c). A variety
3324 of physical, chemical, and biological variables are regularly monitored by SFWMD and
3325 other organizations. Discharge from S-79 has been recorded since 1966 and is reported
3326 here as the daily mean average inflow rate in cfs. Salinity has been monitored at multiple
3327 locations since the 1990s (S-79, Val I75, Fort Myers, Cape Coral, Shell Point, and Sanibel;
3328 **Figure 45**). The distribution and density of SAV have been determined at the upper stations
3329 (1, 2, and 4) since 1998 and the in the lower estuary (5, 6, 7, and 8) every two months since
3330 2004. This study focused on SAV Site 1 because of its upstream location near Beautiful
3331 Island and proximity to the Fort Myers salinity monitoring location.



3332

3333

3334

Figure 45. Location map for the CRE including the S-79 water control structure, water quality monitoring sites, SAV monitoring sites, and the location of continuous salinity recorders.

3335

Empirical Data

3336

3337

3338

3339

3340

Daily average surface salinity recorded at Fort Myers from May 1, 1992, to April 30, 2014, was obtained from the DBHYDRO, which is accessible from the following link: http://www.sfwmd.gov/dbhydroplsql/show_dbkey_info.main_menu). Missing daily salinity values (1,058 of 8,035 days) were estimated using an autoregressive model (Qiu and Wan 2013).

3341

3342

3343

3344

3345

3346

3347

Researchers established paired, perpendicular 100-m transects at the beginning of the SAV monitoring period for each site. On each sampling date the number of blades, shoots, and flowers were counted in five separate, random 0.1-m² quadrats along each transect (n = 10 = 5 quadrats x 2 transects; Bortone and Turpin 2000, Doering et al. 2002). Blade length and width were also determined in each quadrat. SAV shoot counts, length, width, and dry weight biomass were monitored approximately bi-monthly at Site 1 from 1998 to 2007.

3348

3349

3350

3351

3352

3353

3354

Both salinity and *Vallisneria* shoot count data were expressed as a time series of water years. Each water year includes wet (May–October) and dry (November–April) seasons representative of the subtropical climate of South Florida. Mesocosm experiments provided data used to generate a linear regression between shoot densities and aboveground biomass (Doering et al. 1999, 2001). This relationship was used to convert shoot densities (number per square meter [# m⁻²]) observed at Site 1 to biomass (grams dry weight per square meter [gdw m⁻²]) and generate a time series of shoot biomass from 1998 to 2007.

3355 This time series was used to calibrate model predictions of shoot biomass. The regression
3356 relationship also was used to convert predicted shoot biomass back to shoot density for
3357 various applications.

3358 **Model Boundaries**

3359 *Vallisneria* habitat near Beautiful Island in the upper CRE provided the spatial
3360 reference for the model (Doering et al. 2001). The model was developed to represent
3361 changes in biomass at Site 1 over an 18-year period from 1997 to 2014 (6,574 days or 216
3362 months). The integration interval was 0.75 hours (0.03125 day; Buzzelli et al. 2012,
3363 2014b). The first year of simulation time (1997) was used to stabilize the model and was
3364 not included in reporting and interpretation. The model output (1998–2014) was summed
3365 or averaged to depict daily, monthly, seasonal, and annual (calendar and water year)
3366 time scales.

3367 **Model Mathematical Structure**

3368 Water temperature (T_w), submarine light (I_z), and salinity (S) were the important
3369 environmental drivers for the *Vallisneria* model (**Figure 46**). A daily time series of T_w at
3370 Fort Myers from 1998 to 2012 was derived from continuous monitoring (**Figure 47A**).
3371 Missing temperature data were estimated using an interpolation method (Baldwin and Hunt
3372 2014). Temperature influences both the photosynthesis-irradiance relationship (fT_{shoot}) and
3373 the effective rate of respiration (**Table 23** and **Table 24**; **Figure 47B**).

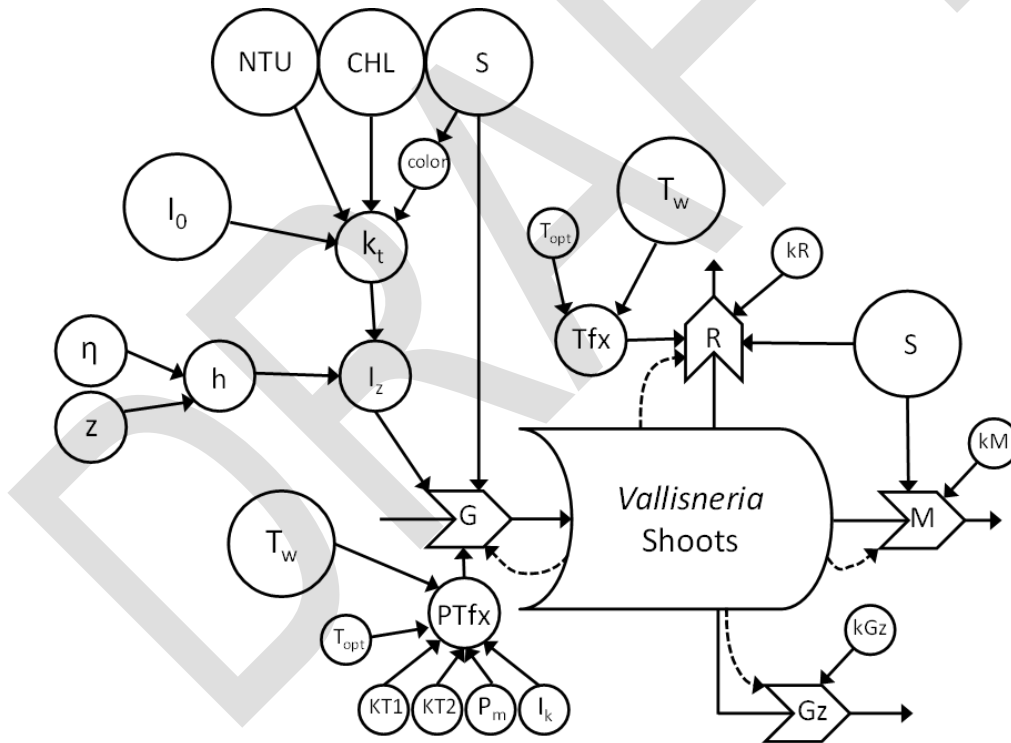
3374 Daily salinity at SAV monitoring Site 1 (S_{val}) was predicted using a method derived
3375 through integrated hydrodynamic and time series modeling (**Figure 48A**; Qiu and Wan
3376 2013). The method combines empirically derived freshwater inflow through S-79,
3377 estimated freshwater input through combined tributaries and groundwater inflows from the
3378 downstream Tidal Basin, and daily salinity data observations from the I-75 Bridge in the
3379 upper CRE to generate a continuous time series of salinities at Site 1 (Qiu and Wan 2013).
3380 S_{val} was used to influence rates of *Vallisneria* gross production and loss. A salinity range
3381 of 0 to 10 decreased and increased the model rates of gross production and mortality,
3382 respectively (**Figure 48B**).

3383 Irradiance at the water surface (I_0) and photoperiod (P_{photo}) were necessary to simulate
3384 variations in light (**Table 23** and **Table 24**). Surface light was attenuated by water depth
3385 and the total attenuation coefficient to derive irradiance at the bottom (I_z). Variable water
3386 level (η) was calculated hourly based on the amplitude (AM2), period (TM2), and phase
3387 of the M2 tide (PhM2) determined for Fort Myers, Florida (**Table 23** and **Table 24**). Depth
3388 (h) was calculated as the difference between η and the base elevation of the habitat (z). The
3389 total attenuation coefficient for submarine light (k_t) contained contributions from pure
3390 water (k_w), color, turbidity (NTU), and CHL (Christian and Sheng 2003). Attenuation due
3391 to color (k_{color}) was estimated using a negative exponential relationship with salinity (**Table**
3392 **23** and **Table 24**; McPherson and Miller 1994, Buzzelli et al. 2012). Time series for
3393 monthly average NTU and CHL were derived from monitoring data at station CES04
3394 (**Figure 49A** and **49B**). These data are available through DBHYDRO
3395 (http://www.sfwmd.gov/dbhydroplsql/show_dbkey_info.main_menu). There were
3396 specific coefficients for each of the attenuation components (k_w , attenuation factor for
3397 turbidity [a_{NTU}], attenuation factor for chlorophyll a [a_{CHL}], and constants for salinity-color
3398 relationship [a_{color} and b_{color}]; **Table 24**). I_z ($\mu\text{moles per square meter per second}$ [μmoles

3399 $\text{m}^{-2} \text{s}^{-1}$) was calculated as an exponential decline with h depending upon k_t (**Table 23** and
 3400 **Table 24**). The percentage of surface irradiance at the bottom ($\%I_0$) is simply a ratio
 3401 between the half-saturation irradiance value (I_k) and I_0 multiplied by 100 (**Table 23** and
 3402 **Table 24**).

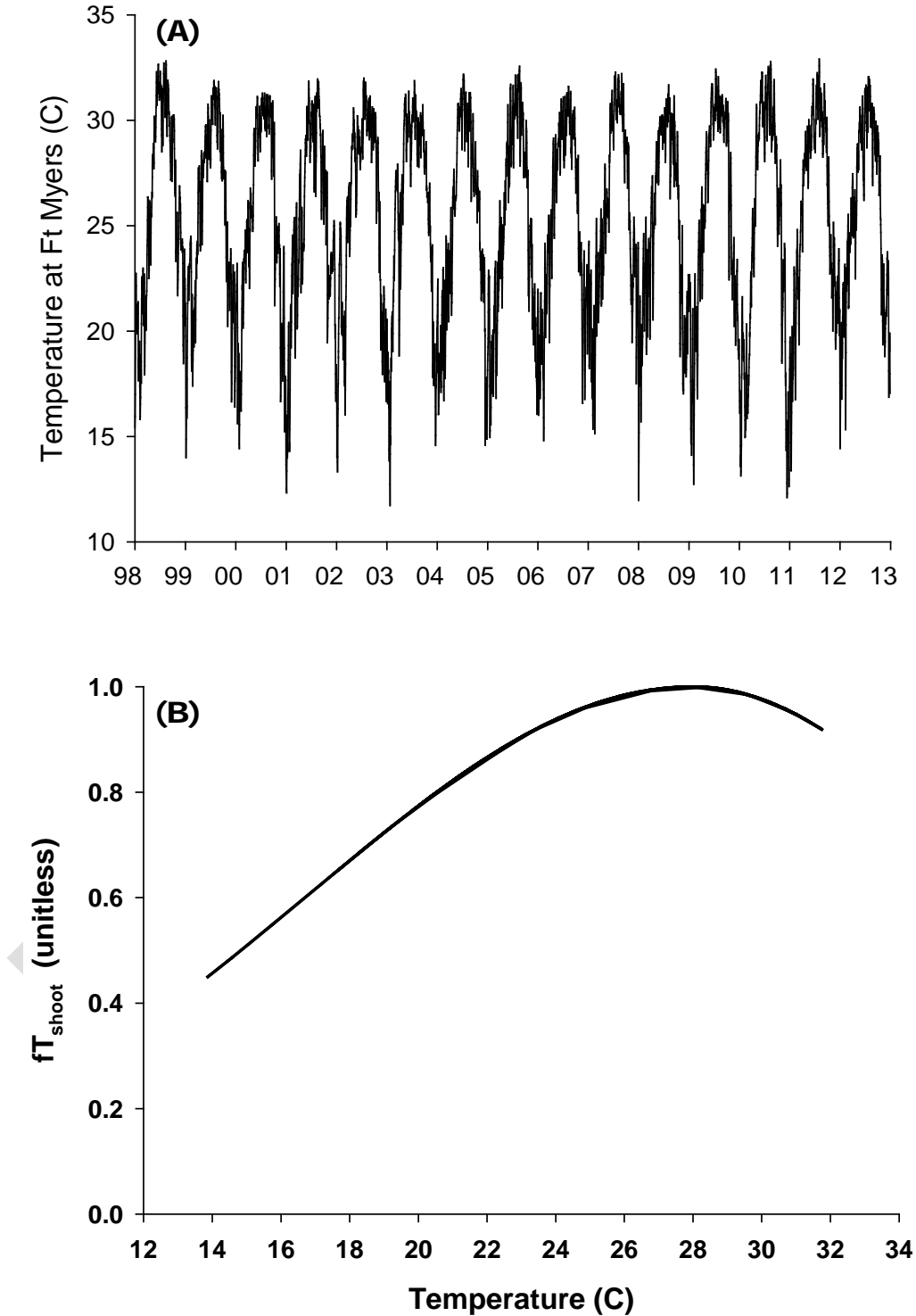
3403 The equations for *Vallisneria* were similar to those used in modeling of seagrass
 3404 communities in the Southern Indian River Lagoon and the lower CRE (Buzzelli et al. 2012,
 3405 2014b). Changes in the aboveground biomass of *Vallisneria* (C_{shoot}) resulted from gross
 3406 production (G_{shoot}), respiration (R_{shoot}), salinity-based mortality (M_{shoot}), and herbivorous
 3407 grazing (Gz_{shoot} ; **Table 23**). G_{shoot} included terms for the maximum rate of photosynthesis
 3408 (P_m), light limitation using I_k , fS_{gross} (**Figure 48B**), fT_{shoot} , and C_{shoot} (Buzzelli et al. 2012,
 3409 2014b). The rate was also scaled using the maximum biomass ($C_{\text{shoot}}/C_{\text{max}}$). P_m and I_k were
 3410 set at 0.02 per day and $56 \mu\text{moles m}^{-2} \text{s}^{-1}$, respectively (**Table 24**; Blanch et al. 1998). R_{shoot}
 3411 included a basal rate of respiration (kR) and an exponential increase with T_w (**Table 24**).
 3412 M_{shoot} was calculated using the basal rate of mortality (kM) combined with fS_{loss} (**Figure**
 3413 **48B**). Finally, the Gz_{shoot} was the product of a basal grazing rate (kGz) and the square of
 3414 C_{shoot} (**Table 23** and **Table 24**).

3415



3416

3417 **Figure 46.** Conceptual model for response of *Vallisneria* shoots to variable temperature (T_w),
 3418 irradiance at the bottom (I_z), and salinity (S). See Tables 1 and 2 for model equations and
 3419 coefficients, respectively. Surface irradiance (I_0), turbidity (NTU), chlorophyll a (CHL), and color
 3420 were used to calculate I_z . S was used as a term to estimate color. Depth (h) was calculated using
 3421 water level (η) and sediment elevation (z). A suite of coefficients— optimum temperature (T_{opt}),
 3422 *Vallisneria* constants for photosynthesis (KT_1) and (KT_2), maximum rate of photosynthesis (P_m),
 3423 and the half-saturation irradiance value (I_k)—are combined with T_w and shoot biomass to
 3424 calculate gross production (G). Respiration (R) is influenced by a temperature effect (T_{fx}) and S .
 3425 S also influences the rate of shoot mortality (M). Loss due to grazing (Gz) is a function of the
 3426 shoot biomass and the basal grazing rate (kGz).



3427

3428

3429

3430

Figure 47. (A) Time series of daily water temperature in °C (C) at Fort Myers from 1998 to 2012.
(B) Relationship between water temperature in °C (C) and the shoot gross production rate (fT_{shoot}).

3431

3432
3433**Table 23.** List of equations to simulate dynamics of *Vallisneria americana* shoot biomass. See Buzzelli et al. (2012, 2014b) for mathematical details.

Description	Equations
(1) Photoperiod (P_{photo} ; hrs)	$P_{photo} = 12 - 2 * \cos\left(\frac{2 * \pi * day}{365}\right)$
(2) Surface irradiance (I_0 ; $\mu\text{mole m}^{-2} \text{s}^{-1}$)	$I_0 = \text{MAX}\left[\left(I_{amp} * \cos\left(\frac{2 * \pi * (hour - 12)}{2 * P_{photo}}\right)\right), 0.0\right]$
(3) M_2 water level (η ; m)	$\eta = \text{MSL} + (\text{AM} * 2 * \cos(2 * \pi * \left(\frac{hour - \text{PhM} * 2}{\text{TM} * 2}\right)))$
(4) Water Depth (h ; m)	$h = \eta - z$
(5) Light extinction coefficient (k_t ; m^{-1})	$k_t = k_w + [k_{color}] + [a_{NTU} * \text{NTU}] + [a_{CHL} * \text{CHL}]$
(6) Light extinction color (k_{color} ; m^{-1})	$k_{color} = a_{color} * e^{(-b_{color} * S)}$
(7) Light at bottom (I_z ; $\mu\text{mole m}^{-2} \text{s}^{-1}$)	$I_z = I_0 * e^{(-k_t * h)}$
(8) Percentage of surface light at bottom ($\%I_z$)	$\%I_z = \left(\frac{I_z}{I_0}\right) * 100$
(9) <i>Vallisneria</i> shoot (C_{shoot} ; gC m^{-2})	$\frac{dC_{shoot}}{dt} = G_{shoot} + N_{shoot} - R_{shoot} - M_{shoot} - Gz_{shoot}$
(10) <i>Vallisneria</i> shoot growth (G_{shoot})	$G_{shoot} = P_m * \left[\frac{I_z}{(I_k + I_z)}\right] * fS_{gross} * fT_{shoot} * \left[\frac{C_{shoot}}{C_{max}}\right] * C_{shoot}$
(11) <i>Vallisneria</i> photosynthesis T effect (fT_{shoot})	$fT_{shoot} = IF(T \leq T_{opt}) e^{-kT^{1/4}(T - T_{opt})^2}$ $fT_{shoot} = IF(T > T_{opt}) e^{-kT^{2/3}(T_{opt} - T)^2}$
(12) <i>Vallisneria</i> new shoots (N_{shoot} ; $\text{gC m}^{-2} \text{d}^{-1}$)	$N_{shoot} = C_{shoot} * kN$
(13) <i>Vallisneria</i> shoot respiration (R_{shoot} ; $\text{gC m}^{-2} \text{d}^{-1}$)	$R_{shoot} = C_{shoot} * [kR * e^{KtB(T - T_{opt})}]$
(14) <i>Vallisneria</i> shoot mortality (M_{shoot} ; $\text{gC m}^{-2} \text{d}^{-1}$)	$M_{shoot} = C_{shoot} * kS_{loss} * fS_{loss}$
(15) <i>Vallisneria</i> shoot grazing (Gz_{shoot} ; $\text{gC m}^{-2} \text{d}^{-1}$)	$Gz_{shoot} = kGz * C_{shoot}^2$

3434
3435
3436

Key to units: $\mu\text{mole m}^{-2} \text{s}^{-1}$ – micromoles per square meter per second; gC m^{-2} – grams shoots per square meter; $\text{gC m}^{-2} \text{d}^{-1}$ – grams shoots per square meter per day; hrs – hours; m – meters; and m^{-1} – per meter.

3437

Table 24. List of *Vallisneria* model coefficients. See Buzzelli et al. (2012, 2014b) for mathematical details.

Parameter	Value	Unit	Description	Source
I_{amp}	1000	$\mu\text{mole m}^{-2} \text{d}^{-1}$	Amplitude of surface irradiance	local data
MSL	0.0	m	Mean sea level	***
TM2	12.42	hours	Period of M2 tide	NOAA Ft. Myers
AM2	0.111	m	Amplitude of M2 tide	NOAA Ft. Myers
PhM2	1.43	radians	Phase angle of M2 tide	NOAA Ft. Myers
z	-0.75	m	Sediment elevation of habitat	USGS bathymetry data
k_w	0.15	m^{-1}	Attenuation due to water	Calculated from Gallegos 2001
a_{NTU}	0.062	NTU^{-1}	Attenuation factor for turbidity	McPherson and Miller 1987
a_{CHL}	0.058	$\text{m}^3 \text{mg}^{-1}$	Attenuation factor for chlorophyll a	McPherson and Miller 1987
a_{color}	2.89	m^{-1}	Constant for salinity-color relationship	McPherson and Miller 1987
b_{color}	0.096	m^{-1}	Constant for salinity-color relationship	McPherson and Miller 1987
T_{opt}	28	$^{\circ}\text{C}$	Optimum temperature for rate processes	Bartleson et al. 2014
KtB	0.069	$^{\circ}\text{C}^{-1}$	Rate constant for temperature effect	Buzzelli et al. 1999
P_m	0.02	d^{-1}	<i>Vallisneria</i> max photosynthetic rate	Blanch et al. 1998
I_k	56	$\mu\text{mole m}^{-2} \text{d}^{-1}$	<i>Vallisneria</i> light constant	Blanch et al. 1998
kT1	0.004	unitless	<i>Vallisneria</i> temperature constant for photosynthesis	Buzzelli et al. 1999
kT2	0.006	unitless	<i>Vallisneria</i> temperature constant for photosynthesis	Buzzelli et al. 1999
kN	0.01	unitless	<i>Vallisneria</i> source of new shoots	Calibration
kR	0.001	d^{-1}	<i>Vallisneria</i> shoot respiration rate	Calibration
kS_{los}	0.01	d^{-1}	<i>Vallisneria</i> loss rate with salinity	Calibration
kGz	0.0002	$\text{m}^2 \text{gdw}^{-1}$	<i>Vallisneria</i> shoot grazing rate	Calibration
C_{init}	15	gdw m^{-2}	<i>Vallisneria</i> initial shoot biomass	Calibration - CRE data
C_{max}	100	gdw m^{-2}	<i>Vallisneria</i> maximum shoot biomass	Calibration - CRE data

3438

3439

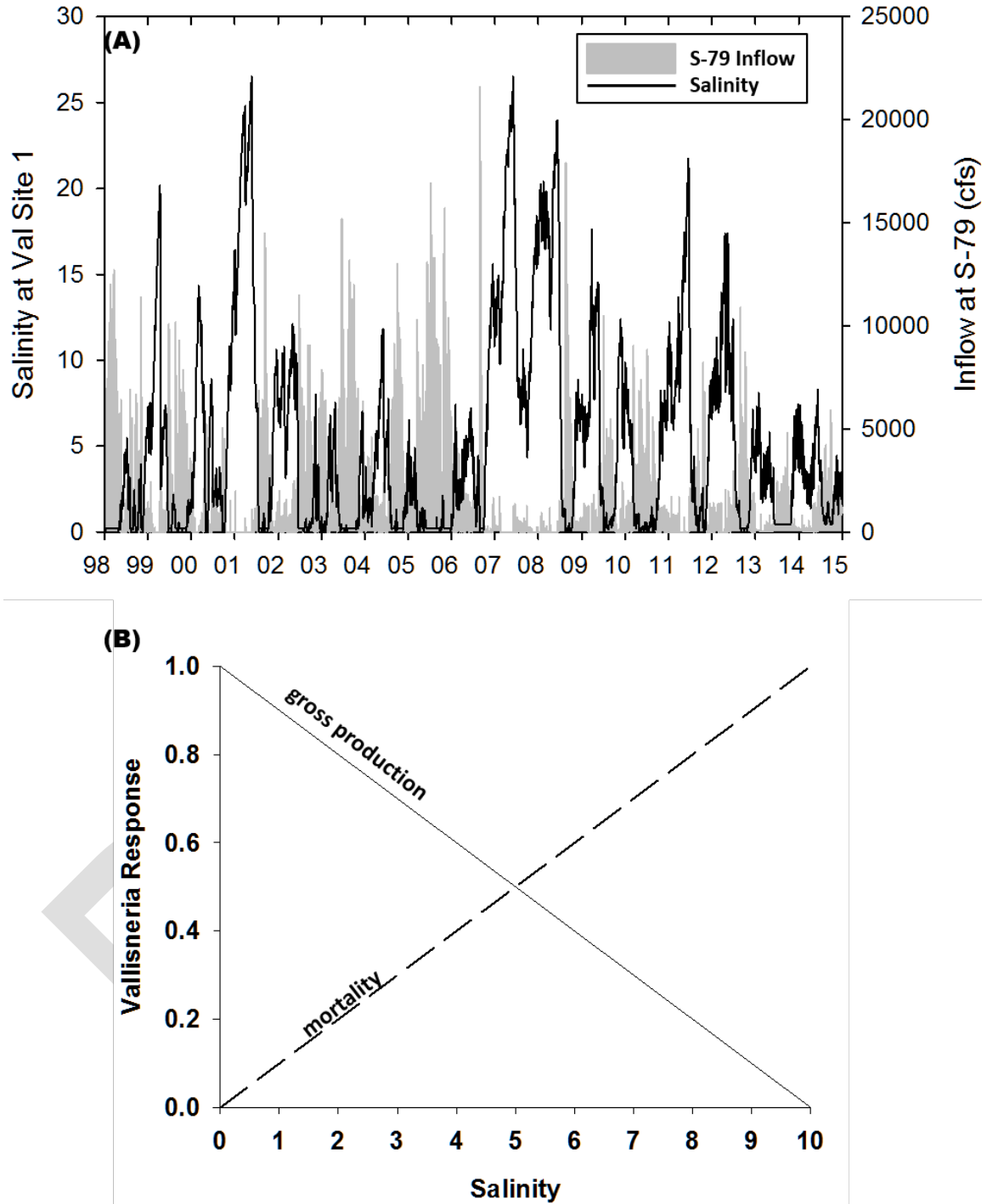
3440

3441

3442

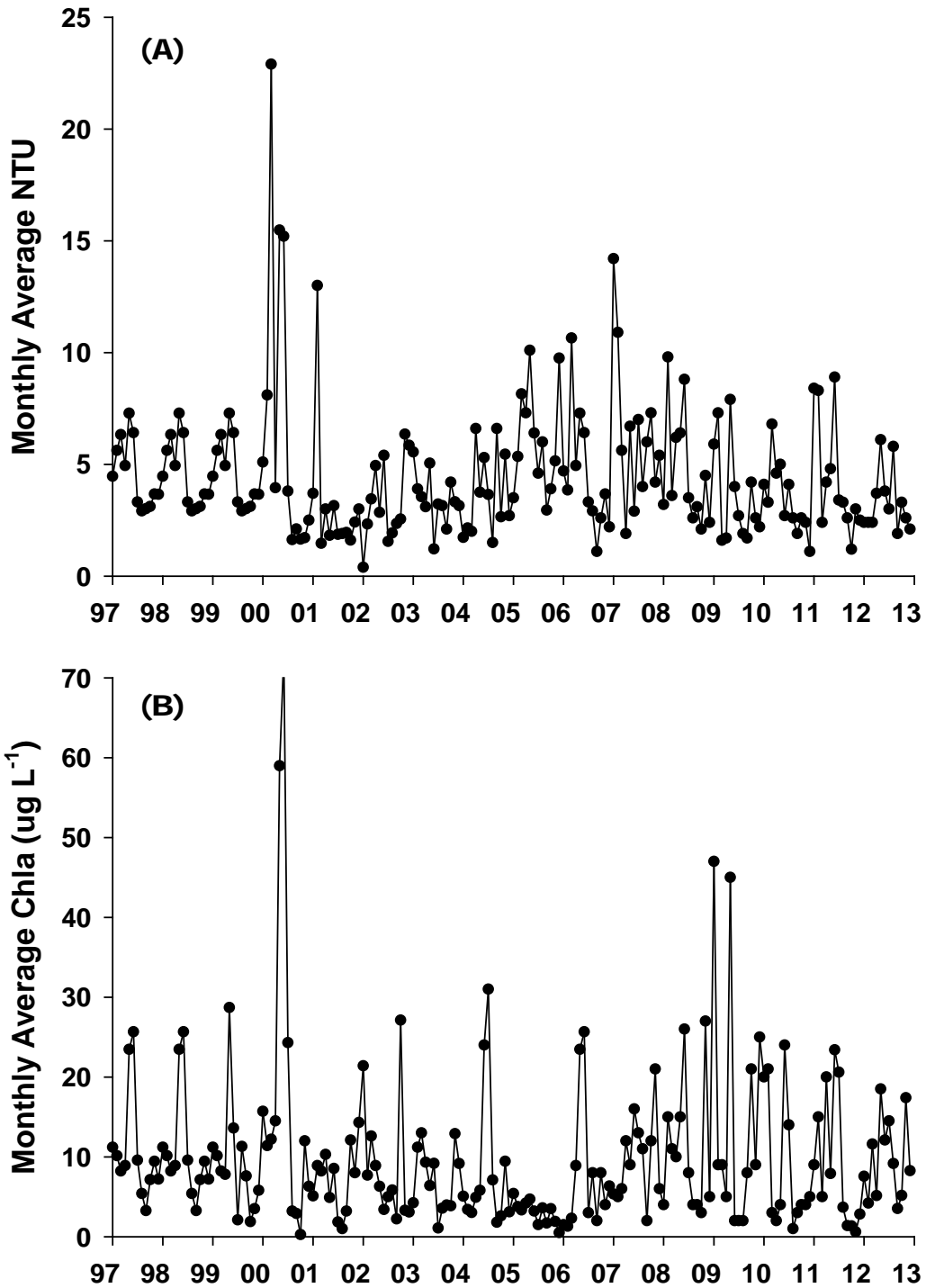
Key to units: $^{\circ}\text{C}$ – degrees Celsius; $^{\circ}\text{C}^{-1}$ – per degrees Celsius; $\mu\text{mole m}^{-2} \text{d}^{-1}$ – micromoles per square meter per day; $\mu\text{mole m}^{-2} \text{s}^{-1}$ – micromoles per square meter per second; d^{-1} – per day; gdw m^{-2} – grams dry weight per square meter; m – meters; m^{-1} – per meter; $\text{m}^2 \text{gdw}^{-1}$ – square meters per grams dry weight; $\text{m}^3 \text{mg}^{-1}$ – cubic meters per milligram; and NTU^{-1} – per turbidity.

Key to agencies: NOAA – National Oceanic and Atmospheric Administration and USGS – United States Geological Survey.



3443
 3444
 3445
 3446
 3447
 3448

Figure 48. (A) Time series of daily salinity predicted for SAV monitoring Site 1 from 1998 to 2014 (black line; left axis) and freshwater inflow at S-79 (cubic meters per second [$m^3 s^{-1}$]; grey fill; right axis). (B) Scalar multiplier for the negative effects of salinity on gross photosynthesis (fS_{gross} ; solid) and positive effects on shoot mortality (fS_{loss} ; dashed).



3449
3450
3451
3452

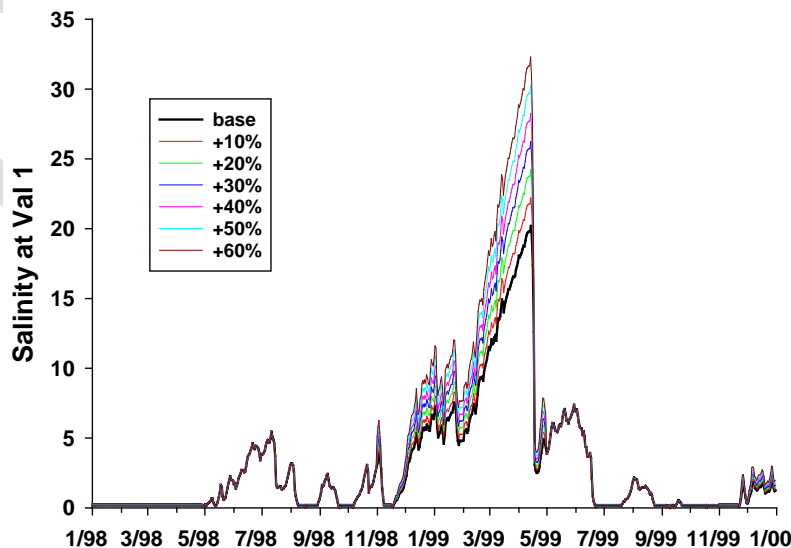
Figure 49. Monthly time series at CES04 monitoring site in the Caloosahatchee Estuary for (A) turbidity (NTU) and (B) CHL.

3453 **Model Calibration, Sensitivity, and Application**

3454 *Vallisneria* occurs naturally in a wide range of freshwater and estuarine environments
 3455 from Maine to Texas and inland to the Mississippi River (McFarland 2006). Despite its
 3456 prevalence, there have been few physiological studies through which to obtain essential
 3457 rate constants for model development. Calibration exercises were mindful of the spatial
 3458 variations in patch densities inherent in the natural community, unavoidable sampling bias
 3459 during routine monitoring, variability in the mesocosm-derived relationship between shoot
 3460 densities and biomass, and the lack of information on rates of mortality and grazing specific
 3461 to the CRE.

3462 The goal of calibration was to provide the best approximation of the biomass time series
 3463 derived for Site 1 near Beautiful Island in the upper CRE. The simulation of *Vallisneria*
 3464 shoot biomass was calibrated by adjusting initial biomass values (C_{init}), the salinity-specific
 3465 loss rate (kS_{loss}), and kGz . C_{init} , P_m , kR , kS_{loss} , and kGz were varied by $\pm 10\%$ and $\pm 50\%$
 3466 relative to the base model values in a series of sensitivity tests.

3467 In order to help describe the conditions that account for *Vallisneria* survival versus loss,
 3468 the environmental variables (inflow, temperature, salinity, and light) and *Vallisneria* shoot
 3469 biomass were evaluated for each dry season from 1998 to 2014. An eight-year experimental
 3470 model was generated by looping the favorable environmental conditions (salinity,
 3471 turbidity, and CHL) from the 1998–1999 calendar years (2 year x 4 loops = 8 year
 3472 simulations). Salinity values for each day in the dry season were systematically increased
 3473 by 5% to 75% at 5% intervals over 16 model runs (base model + 15 separate simulations;
 3474 7 of which are shown in **Figure 50**). In order to identify the S-79 inflows associated with
 3475 net mortality of *Vallisneria*, the daily dry season salinity was systematically increased until
 3476 shoot biomass at the end of the simulation was less than that at the beginning (i.e. net
 3477 mortality). The resulting dry season salinity increase that led to net mortality was used to
 3478 estimate the freshwater inflows using the annual regression equations from Component
 3479 Study 2. Finally, the model was used to calculate the percentage of shoots lost based on the
 3480 number of consecutive days where salinity was ≥ 10 in multiple dry seasons.



3481

3482 **Figure 50.** Time series of altered daily salinity in the dry season as input to the 1998–1999
 3483 loop model.

3484 **Results**

3485 The model output was sensitive to changes in C_{init} , P_m , kR , kS_{loss} , and kGz . Predicted
3486 shoot biomass declined by -19.5% and -69.2% when P_m was decreased by -10% and -50%,
3487 respectively (**Table 25**). The effects of increasing P_m by +10% and +50% were
3488 comparatively greater as model shoot biomass increased by +25.1% and +201.0%.
3489 Predicted shoot biomass increased by +8.6% and +52.9% when kR was decreased by -10%
3490 and -50%, respectively (**Table 25**). The effects of increasing kR by 10% and 50% led to
3491 shoot biomass decreases of -7.7% and -32.0%. Adjustments in C_{init} had diminished effects
3492 on predicted shoot biomass relative to the other parameters. Decreased values for kS_{loss}
3493 resulted in the greatest relative increase in predicted biomass (72.7% and 861.5%). The
3494 effect of increasing kS_{loss} was less dramatic (-36.0% and -81.9%). Finally, decreasing kGz
3495 by -10% and -50% increased shoot biomass by 8.9% and 70.9%, respectively. Increasing
3496 kGz had a reduced negative effect (-7.5% and -28.5% for +10% and +50% increase
3497 in kGz).

3498 The average inflow rate through S-79 over all dry seasons averaged 1,172 cfs ranging
3499 from 52 ± 151 cfs (2008) to $5,596 \pm 3,655$ cfs (1998; **Table 26**). S_{val1} averaged 6.9 ± 2.9
3500 ranging from 1.2 (1998) to ~16.5 (2001 and 2008). An average of ~7% of surface irradiance
3501 reached the bottom including a minimum of 3.3% under the greatest inflows (1998) and a
3502 maximum of 15.7% when inflow was low (2001). Submarine light extinction ranged from
3503 a maximum of ~8.0 per meter (m^{-1}) (~0% surface irradiance) in 2000 to $<1.0 m^{-1}$ (>30%
3504 surface irradiance) in 2001, 2008, and 2011 (**Figure 51**). Light availability for *Vallisneria*
3505 was generally inversely related to freshwater inflow due to the dominant role of color
3506 (McPherson and Miller 1994, Buzzelli et al. 2014b, Chen et al. 2015). The exception
3507 occurred in May–June 2000 when the relative influences of both CHL and turbidity
3508 enhanced light extinction (**Figure 49**).

3509 Average *Vallisneria* shoot density at Site 1 was variable ranging from 0.0 to 325 shoots
3510 m^{-2} from 1998 to 2007 (**Figure 52A**). Average density peaked in the wet seasons of 1998–
3511 1999 (200–300 shoots per square meter [m^{-2}]) and 2005–2006 (100–200 shoots m^{-2}). There
3512 was a decline approaching 0.0 in the 2000 dry season followed by an increase (~100
3513 shoots m^{-2}) in the wet season before minimal shoots were observed from 2001 to 2003.
3514 Shoot density increased in the subsequent wet seasons before dry conditions in 2007 and
3515 into 2008 triggered widespread loss of shoots. The relationship between shoot density and
3516 biomass was used to generate the time series of aboveground biomass used to calibrate the
3517 model ($gdw m^{-2}$; $r^2 = 0.82$; **Figure 52B and C**).

3518 The model provided a reasonable approximation of the shoot biomass converted from
3519 the observed densities (**Figure 53**). Although the model was sensitive to parameter values
3520 and over-predicted the biomass for the 2006 dry season, it was a responsive indicator of
3521 changes in salinity. This was evident throughout the simulation period culminating in a
3522 slight increase in shoot biomass as conditions improved from 2013 to 2014.

3523

3524

3525 **Table 25.** Results of sensitivity tests for the effects of physiological coefficients on predicted
 3526 *Vallisneria* shoot biomass. The maximum rate of photosynthesis (P_m ; per day), the basal rate of
 3527 respiration (kR ; per day), the initial shoot biomass (C_{init} ; $gdw\ m^{-2}$), the shoot loss rate due to
 3528 salinity (kS_{loss} ; per day), and the basal grazing rate (kGz ; square meter per grams dry weight [m^2
 3529 gdw^{-1}]) were varied by +10% and +50% in independent model simulations. Simulations spanned
 3530 18 years (1997–2014 = 6,574 days). Provided are the coefficient values, the predicted biomass
 3531 ranges (C_{shoot} ; $gdw\ m^{-2}$), the average and standard deviations ($Avg \pm SD$) of predicted biomass
 3532 ($gdw\ m^{-2}$), and the percent difference between the base model values (base) and each sensitivity
 3533 test averaged over all simulation days ($\%Difference = ((observed - expected)/expected) * 100$).

Coefficient	Sensitivity Test	Coefficient Value	Range	Avg \pm SD	%Difference
P_m	Base	0.020			
	-10%	0.018	0.1–32.0	5.0 \pm 5.8	-19.5%
	-50%	0.010	0.0–14.9	2.2 \pm 2.7	-69.2%
	+10%	0.022	0.15–38.1	6.7 \pm 7.2	25.1%
	+50%	0.030	0.2–45.8	10.5 \pm 9.7	201.0%
kR	Base	0.001			
	-10%	0.0009	0.1–36.1	6.1 \pm 6.7	8.6%
	-50%	0.0005	0.2–38.8	7.2 \pm 7.4	52.9%
	+10%	0.0011	0.1–34.6	5.6 \pm 6.4	-7.7%
	+50%	0.0015	0.1–31.1	4.6 \pm 5.6	-32.0%
C_{init}	Base	15.0			
	-10%	13.5	0.1–35.3	5.7 \pm 6.5	-0.9%
	-50%	7.5	0.1–35.3	5.3 \pm 6.3	-5.6%
	+10%	16.5	0.1–35.3	5.9 \pm 6.6	0.8%
	+50%	22.5	0.1–35.3	6.1 \pm 6.7	3.4%
kS_{loss}	Base	0.01			
	-10%	0.009	0.2–36.6	7.1 \pm 6.9	72.7%
	-50%	0.005	1.9–39.3	14.0 \pm 7.5	861.5%
	+10%	0.011	0.0–33.5	4.8 \pm 6.0	-36.0%
	+50%	0.015	0.0–14.9	1.8 \pm 2.8	-81.9%
kGz	Base	0.0002			
	-10%	0.00018	0.1–38.6	6.3 \pm 7.1	8.9%
	-50%	0.0001	0.2–60.9	9.6 \pm 11.0	70.9%
	+10%	0.00022	0.1–32.6	5.4 \pm 6.1	-7.5%
	+50%	0.0003	0.1–24.9	4.2 \pm 4.7	-28.5%

3534

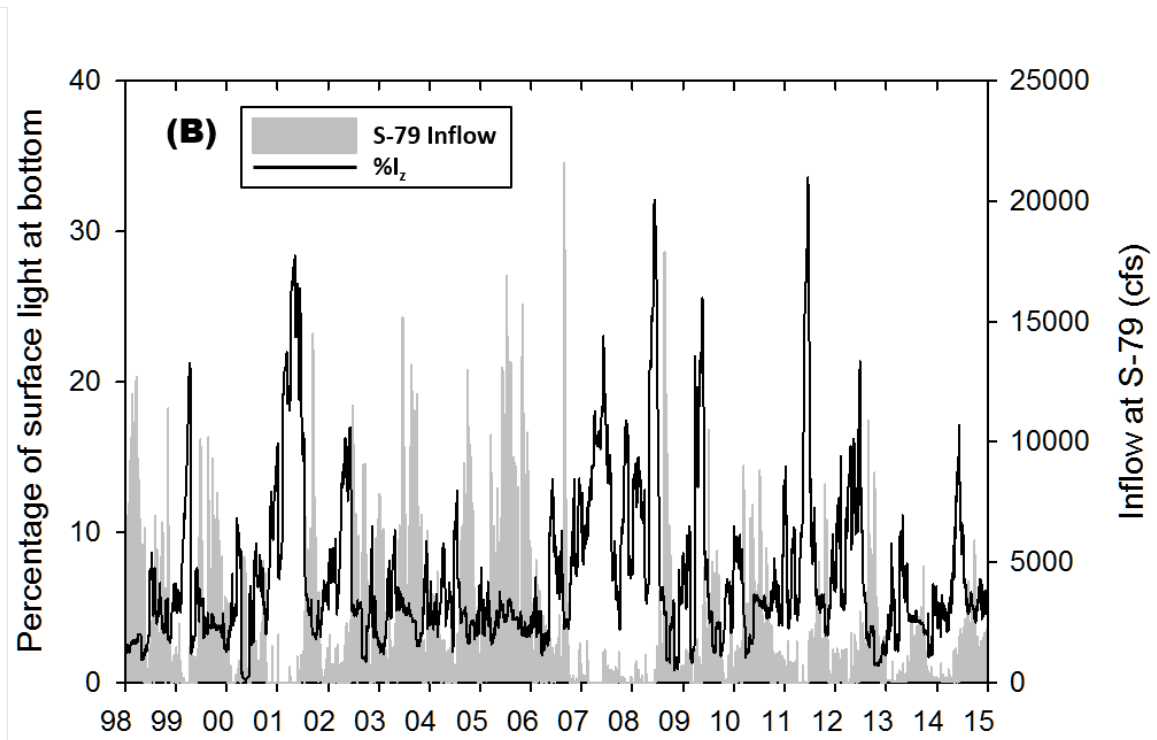
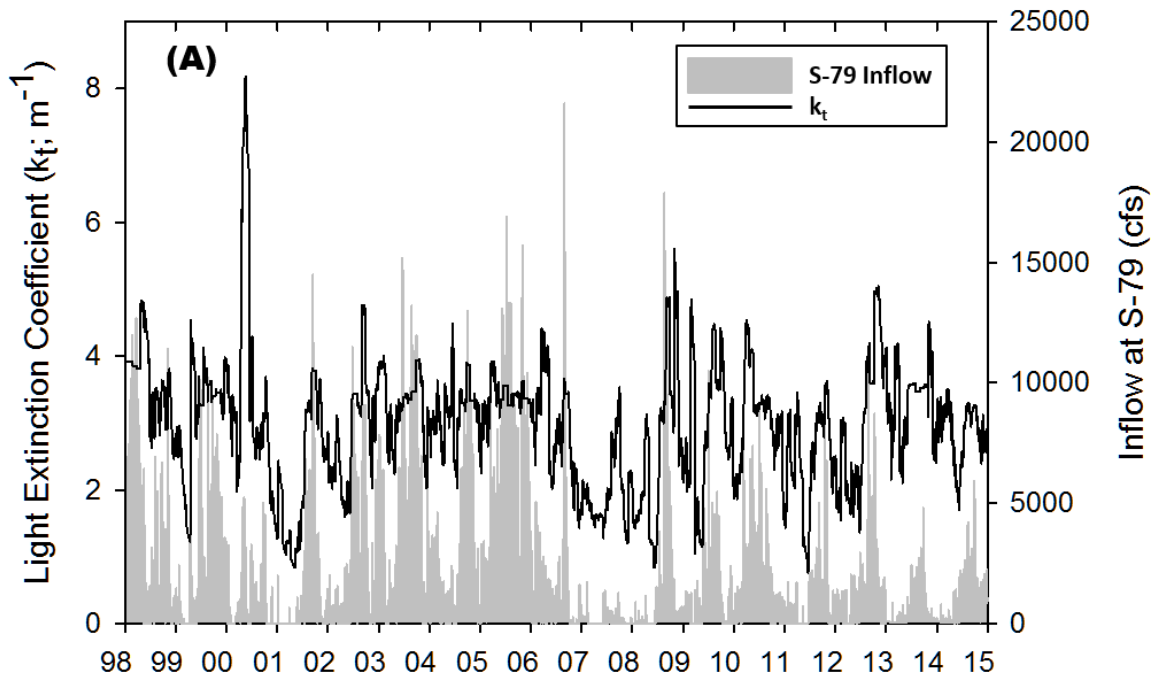
3535
3536
3537
3538
3539

Table 26. Dry season (November–April) average and standard deviations (Avg \pm SD) for model variables from WY1998–WY2014. Variables include freshwater inflow at S-79 (Q_{S79}) and the tidal basin (Q_{TB} ; cfs), salinity at *Vallisneria* monitoring site 1 (S_{val1}), temperature at Ft. Myers (T; °C), total light extinction coefficient (k_t ; m^{-1}), the percentage of surface light at the bottom ($\%I_0$; unitless), and model *Vallisneria* shoot biomass (C_{shoot} ; $gdw\ m^{-2}$). The range of model *Vallisneria* shoot biomass for each dry season is also provided. See text for description of model input and response variables.

WY	Q_{S79} (cfs) Avg \pm SD	Q_{TB} (cfs) Avg \pm SD	S_{val1} Avg \pm SD	T Avg \pm SD	k_t Avg \pm SD	$\%I_0$ Avg \pm SD	Range	C_{shoot} Avg \pm SD
1998	5596 \pm 3655	1024 \pm 679	1.2 \pm 1.9	21.3 \pm 2.5	3.6 \pm 0.5	3.3 \pm 1.4	7.8-12.2	9.2 \pm 2.8
1999	737 \pm 1606	344 \pm 460	7.7 \pm 5.6	22.8 \pm 3.0	2.6 \pm 0.8	8.0 \pm 5.4	7.8-17.5	14.1 \pm 3.1
2000	1412 \pm 1766	147 \pm 135	5.5 \pm 4.6	21.7 \pm 2.9	3.5 \pm 1.0	4.3 \pm 2.5	7.6-18.5	13.5 \pm 3.4
2001	61 \pm 269	146 \pm 148	16.6 \pm 5.3	21.1 \pm 3.9	1.5 \pm 0.5	15.7 \pm 6.2	2.5-7.5	5.8 \pm 1.7
2002	440 \pm 462	125 \pm 110	7.4 \pm 2.4	22.5 \pm 3.5	2.5 \pm 0.4	7.6 \pm 2.9	1.5-3.0	2.5 \pm 0.4
2003	1809 \pm 1948	306 \pm 271	2.7 \pm 2.4	21.7 \pm 3.9	3.2 \pm 0.6	4.9 \pm 2.4	2.2-4.9	3.9 \pm 0.9
2004	1358 \pm 1360	198 \pm 190	2.8 \pm 2.0	21.1 \pm 2.9	2.9 \pm 0.4	5.3 \pm 1.7	9.8-16.4	13.6 \pm 1.7
2005	2212 \pm 1991	185 \pm 209	1.8 \pm 1.5	21.1 \pm 3.0	3.2 \pm 0.4	4.2 \pm 1.0	11.3-18.7	15.5 \pm 1.8
2006	3273 \pm 3552	185 \pm 220	2.0 \pm 1.8	21.7 \pm 3.1	3.5 \pm 0.4	3.5 \pm 1.0	17.2-35.3	26.6 \pm 5.3
2007	128 \pm 262	120 \pm 102	14.7 \pm 3.9	21.5 \pm 2.4	1.8 \pm 0.3	11.9 \pm 2.9	3.5-17.1	10.3 \pm 4.6
2008	52 \pm 151	148 \pm 132	16.5 \pm 2.2	22.2 \pm 2.7	1.9 \pm 0.5	11.4 \pm 3.5	0.3-1.1	0.8 \pm 0.3
2009	426 \pm 340	130 \pm 121	8.1 \pm 3.1	20.9 \pm 3.0	2.9 \pm 1.2	7.5 \pm 5.9	0.2-0.4	0.3 \pm 0.1
2010	1117 \pm 1448	344 \pm 401	5.6 \pm 3.7	20.4 \pm 3.3	2.9 \pm 0.8	5.9 \pm 2.6	0.2-0.4	0.3 \pm 0.1
2011	268 \pm 371	164 \pm 171	8.7 \pm 2.2	21.2 \pm 4.4	2.6 \pm 0.5	7.0 \pm 2.8	0.4-1.3	0.9 \pm 0.3
2012	488 \pm 695	256 \pm 304	8.2 \pm 3.9	22.4 \pm 2.5	2.4 \pm 0.5	8.4 \pm 3.3	0.2-0.8	0.5 \pm 0.2
2013	371 \pm 534	162 \pm 141	4.0 \pm 1.6	21.7 \pm 2.6	3.5 \pm 0.8	4.0 \pm 2.6	0.3-0.5	0.4 \pm 0.1
2014	168 \pm 145	168 \pm 145	4.0 \pm 1.5	22.2 \pm 2.8	3.2 \pm 0.5	4.6 \pm 1.4	1.4-2.0	1.6 \pm 0.2
Total	1172 \pm 1117	244 \pm 154	6.9 \pm 2.9	21.6 \pm 3.1	2.8 \pm 0.6	6.9 \pm 2.9		7.1 \pm 1.6

3540

3541



3542

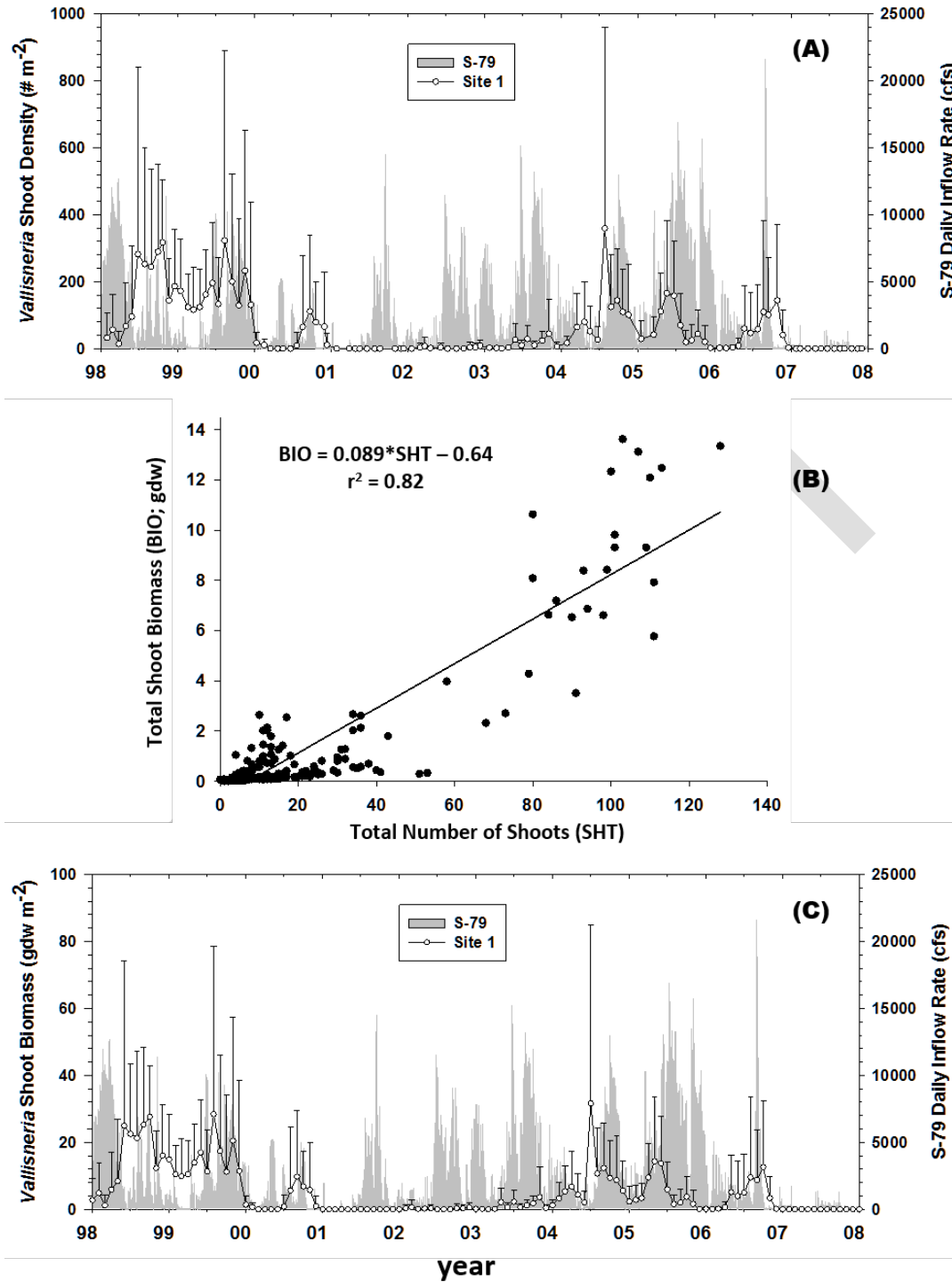
3543

3544

3545

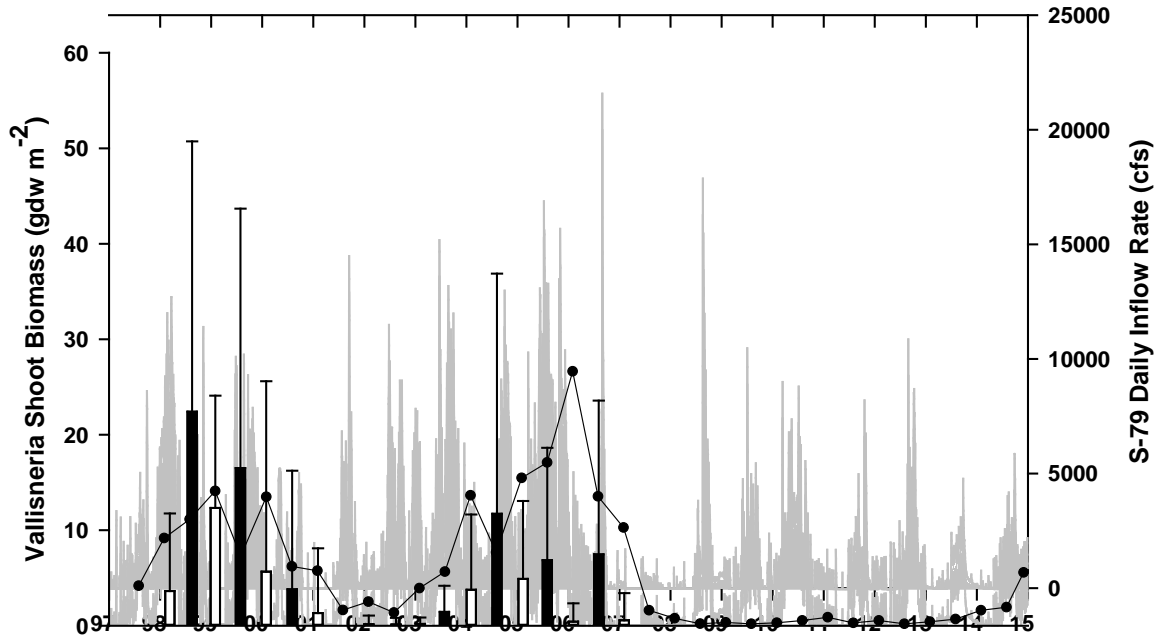
Figure 51. (A) Time series of the submarine light extinction coefficient (k_t ; m^{-1} ; left axis) and daily freshwater inflow at S-79 (cfs; right axis). (B) Time series of the percent of light at the bottom ($\%I_0$; left axis) and daily freshwater inflow at S-79 (cfs; right axis).

3546



3547
 3548
 3549
 3550
 3551
 3552

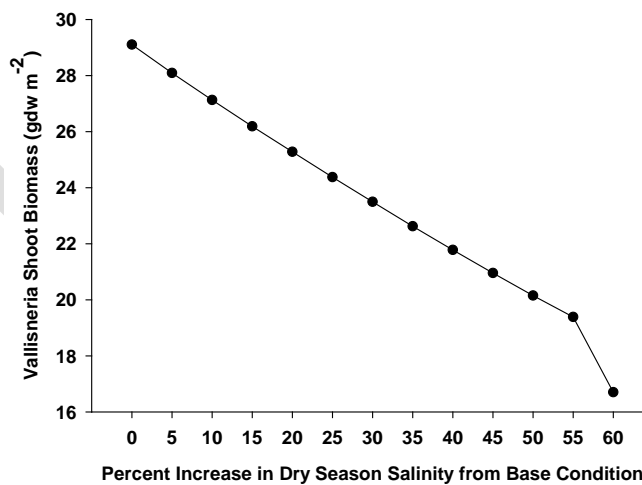
Figure 52. (A) Time series of *Vallisneria* shoot density (average + standard deviation) from Site 1 near Beautiful Island in the CRE. (B) Linear regression between total number of *Vallisneria* shoots and total dry weight biomass of shoots (grams dry weight [gdw]) from controlled mesocosm experiments. (C) Time series of Site 1 *Vallisneria* shoot biomass (average + standard deviation) derived by converted shoot density using the regression equation.



3553
3554
3555
3556

Figure 53. Time series (1998–2014) of average seasonal *Vallisneria* shoot biomass from the model superimposed on average seasonal values at Site 1 (1998–2008). Daily inflow at S-79 shown as shaded area with right axis.

3557 Conditions from 1998 to 1999 were conducive for survival and growth of *Vallisneria*
3558 in the upper CRE (**Table 26**). Salinity increases of 5% per trial led to a linear reduction in
3559 model biomass over the eight-year experimental simulations (**Figure 54**). A 55% increase
3560 in dry season salinities resulted in a net decrease in shoot biomass at the end of the
3561 experimental simulation. The model experiment predicted that an average dry season
3562 salinity of 12 will result in net mortality of *Vallisneria* in the CRE. This value was used to
3563 estimate the associated freshwater inflows from the annual inflow-salinity relationships
3564 derived in Component Study 2. Estimated inflows associated with *Vallisneria* mortality
3565 ranged from 15 to 629 cfs (n = 14) averaging 342 ± 180 cfs.



3566
3567
3568

Figure 54. Plot of % increase in dry season salinity versus average shoot biomass. A 55% increase in dry season salinity values resulted in net mortality of *Vallisneria*.

3569 The number of consecutive days where S_{val1} was ≥ 10 ranged among 10 days (2002),
 3570 40–48 days (1999, 2000, 2009, and 2012), and 145–182 days (2001, 2007, and 2008; **Table**
 3571 **27**). Model results suggested that an estimated 17.6% of the *Vallisneria* shoots were lost
 3572 when salinity was ≥ 10 for 10 consecutive days. This value increased to 85.4% (2001) and
 3573 86.7% (2007) when salinity was elevated for a majority of the dry season. Due to the losses
 3574 in 2007, initial shoot density was not great enough to calculate changes with extended times
 3575 of increased salinity in 2008–2012.

3576 **Table 27.** Results from simulation model of *Vallisneria*. Shown are dry seasons with average
 3577 daily salinities ≥ 10 at Monitoring Site 1 in the CRE from WY1999 to WY2012. All values based on
 3578 daily salinity ≥ 10 including the total number of days in the dry season, the average and standard
 3579 deviation (Avg \pm SD) of salinity for those days, the initial and final dates bracketing consecutive
 3580 days where salinity ≥ 10 , the initial shoot density, and the percentage of initial shoots lost during
 3581 the consecutive days. The model biomass reaches a minimum of 0.1 gdw m^{-2} , which converts to
 3582 ~ 8 shoots m^{-2} .

Water Year	Total Number of Days $S_{\text{val1}} \geq 10$	Salinity Avg \pm SD	Initial Date	Final Date	Consecutive Days $S_{\text{val1}} \geq 10$	Initial Shoot Density (# m^{-2})	% Shoots Lost
1999	53	15.4 \pm 3.0	3/1/99	4/17/99	48	283	54.8%
2000	42	12.3 \pm 1.2	2/17/00	3/29/00	42	222	47.3%
2001	150	18.3 \pm 4.2	12/6/00	4/30/01	145	110	86.7%
2002	19	10.5 \pm 0.4	4/21/02	4/30/02	10	11	17.6%
2007	174	14.9 \pm 3.8	11/7/06	4/30/07	174	72	85.4%
2008	182	16.5 \pm 2.2	11/1/07	4/30/08	182	9	5.4%
2009	46	12.8 \pm 1.7	3/10/09	4/30/09	46	-	-
2010	26	11.1 \pm 0.6	11/10/09	12/5/09	26	-	-
2011	47	11.7 \pm 1.3	4/12/11	4/30/11	18	-	-
2012	50	12.9 \pm 2.1	3/16/12	4/24/12	40	-	-

3583 Discussion

3584 The incorporation of the environmental requirements of *Vallisneria* into a resource-
 3585 based approach to estuary and water management is very unique in estuarine science
 3586 (Doering et al. 2002). This uniqueness emerges because (1) freshwater inflow from S-79
 3587 has been regulated since 1966; (2) low freshwater inflow in the dry season can lead to
 3588 increased salinity throughout the estuary; (3) historically, *Vallisneria* habitat has been an
 3589 important ecological resource in the upper CRE; and (4) *Vallisneria* sensitivity to salinity
 3590 at weekly-annual time scales makes it an excellent indicator of managed freshwater
 3591 inflows. This study built upon existing information to derive a model to simulate the
 3592 responses of *Vallisneria* to environmental drivers (i.e. temperature, salinity, and light;
 3593 Doering et al 1999, 2002, French and Moore 2003, Bartleson et al. 2014). Ecological
 3594 modeling provides a pathway to incorporate the effects of multiple non-linear variables,
 3595 evaluate different management alternatives, and build consensus among a variety of
 3596 stakeholders (Costanza and Ruth 1998, Urban 2006, Buzzelli et al. 2015).

3597 The *Vallisneria* model exhibited greater sensitivity to changes in parameter values than
 3598 equivalent models of seagrasses in South Florida (Buzzelli et al. 2012, 2014b). The
 3599 enhanced sensitivity of the *Vallisneria* model resulted because small changes in salinity
 3600 (i.e., 4 to 5) triggered large changes in photosynthesis and mortality ($>10\%$). By
 3601 comparison, the same salinity change would alter these rates by $<3\%$ in the model of the
 3602 seagrass *Syringodium filiforme* (Buzzelli et al. 2012). Since the P_m was determined

3603 experimentally (Blanch et al. 1998), calibration focused on adjusting the basal loss rates of
3604 mortality (kSloss) and grazing (kGz) to best approximate the observed shoot attributes. The
3605 present model calibration provides a suitable representation of the responses of *Vallisneria*
3606 to fluctuations in salinity from 1998 to 2014.

3607 The combination of the environmental drivers, field monitoring data, and the calibrated
3608 model indicated that salinity was indeed the key variable affecting the survival and growth
3609 of *Vallisneria*. Although only 3 to 8% of submarine light reached the bottom, dry season
3610 salinity conditions in 1998–2000 and 2004–2006 promoted the production of shoot
3611 biomass. In contrast, an average of 11 to 15% of submarine light was available in the
3612 drought years of 2001 and 2007–2008 when *Vallisneria* declined. There were intra- and
3613 inter-annual patterns between inflow, salinity, and *Vallisneria*. Periods where *Vallisneria*
3614 biomass increased generally spanned 4 to 6 months indicative of wet season conditions
3615 with increasing freshwater inflow and decreasing salinity. Each of these periods of
3616 favorable conditions started in June or July with salinity values ranging from ~1.0 to 2.0.
3617 Periods where *Vallisneria* biomass decreased generally spanned 6 to 8 months indicative
3618 of dry season conditions that extended into May–July of the following calendar year.

3619 The model provided an effective tool to explore and quantify both freshwater inflow
3620 and the duration of high salinity conditions that contribute to the mortality of *Vallisneria*
3621 in the CRE. While the field monitoring and Fort Myers salinity data were used to estimate
3622 that inflows of at least 545 ± 774 cfs were associated with *Vallisneria* survival from 1993
3623 to 1999 (Component 7), the model was used to specify the freshwater inflow associated
3624 with net mortality (342 ± 180 cfs). Furthermore, the model results demonstrated that ~50%
3625 of the *Vallisneria* shoots were lost when salinity in the *Vallisneria* habitat near Beautiful
3626 Island was greater than 10 for ~1 month. These results provide a quantitative base to assess
3627 freshwater inflow requirements for the CRE.

3628 **Component Study 9: Assessment of Dry Season Salinity and**
3629 **Freshwater Inflow Relevant for Oyster Habitat in the**
3630 **Caloosahatchee River Estuary**

3631 *Christopher Buzzelli, Cassondra Thomas, and Peter Doering*

3632 **Abstract**

3633 Short- and long-term alteration of salinity distributions in estuaries with variable
3634 freshwater inflow affects the survival, abundance, and extent of oyster habitat. The
3635 objective of this study was to evaluate salinity conditions at two locations (Cape Coral and
3636 Shell Point) in the CRE. Salinity data from the 2006–2014 dry seasons (November–April)
3637 were categorized relative to oyster habitat criteria and related to freshwater inflow. Daily
3638 salinity was within the appropriate range for oysters (10 to 25) on 70.1% of the
3639 observations. Daily inflow ranged from 0 to 2,000 cfs and averaged 296 ± 410 cfs when
3640 salinity ranged from 20 to 25 at Cape Coral in the dry season. The influence of the marine
3641 parasite *Perkinsus marinus* (Dermo) is limited due to the subtropical climate where
3642 temperature is low when salinity is high (dry season) and temperature is high when salinity
3643 is low (wet season). Overall salinity patterns were favorable for oyster survival at the
3644 upstream extent of oyster habitat in the CRE.

3645 **Introduction**

3646 The distribution and abundance of eastern oyster (*Crassostrea virginica*) habitat
3647 provides an ecosystem-scale indication of estuarine status (Kemp et al. 2005). Oysters filter
3648 suspended solids coupling the benthos to the water column while providing habitat for a
3649 variety of fauna (Tolley et al. 2006, Coen et al. 2007). The survival and growth of oysters
3650 are influenced by covariations in temperature, salinity, food supply and mortality (Stanley
3651 and Sellers 1986, Bataller et al. 1999). Oyster habitat is declining worldwide through
3652 multiple interactive factors including over-harvesting, disease, sedimentation, and altered
3653 salinity patterns (Beck et al. 2011).

3654 Salinity is a primary environmental factor affecting the eastern oyster in the Gulf of
3655 Mexico estuaries with optimal values varying from 10 to 30 (Shumway 1996, Livingston
3656 et al. 2000, Barnes et al. 2007, Wang et al. 2008; **Table 28**). A functioning oyster habitat
3657 is composed of the population cohorts (larvae, juvenile, and adults), protistan parasites (e.g.
3658 *Perkinsus marinus* or Dermo), the epibiotic community, and resident and transient
3659 consumers each with particular life histories and salinity tolerances (Dekshenieks et al.
3660 2000, Tolley et al. 2006). Because the oyster life cycle is sensitive to both the timing and
3661 magnitude of variations in salinity, evaluating potential responses of oyster habitat to
3662 variable freshwater inflow offers a biotic tool for water management (Chamberlain and
3663 Doering 1998b, Volety et al. 2009).

3664

3665

Table 28. Summary of salinity tolerances for different oyster life stages.

Life Stage	Salinity Ranges			Citation
	Optimal	Sub-Optimal	Lethal	
Spawning	≥12		0–10,40	Woodward-Clyde 1999, RECOVER 2014
Egg Development	23–29	5–32		Clark 1935
Larvae	23–27	12–32	<12	Kennedy 1991, Dekshenieks et al. 1993, 1996
Spat				
Survival	10–27.5	5–32	<5	Loosanoff 1953, RECOVER 2014
Setting	16–18	9–29		Loosanoff 1965, Kennedy 1991
Juvenile				
Survival	10–20	5–32		Woodward-Clyde 1999
Predation Avoidance	<20		20–25	Butler 1954, Wells 1961, Mackin and Hopkins 1962, Galtsoff 1964, Zachary and Haven 1973
Adult				
Survival	10–30	5–40	<7	Loosanoff 1953, Mackin and Hopkins 1962, Brown and Hartwick 1988, Fisher et al. 1996
Disease avoidance	<5			La Peyre et al. 2009

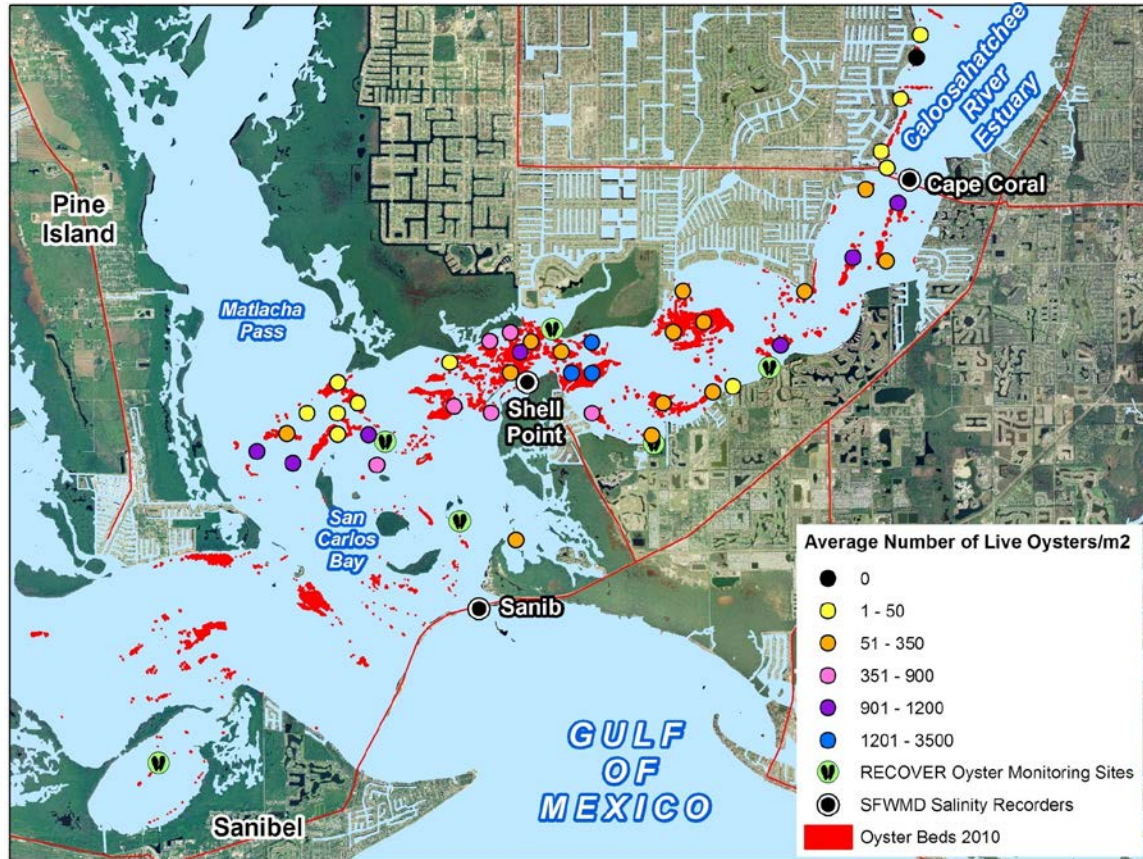
3666

3667 Conventional wisdom suggests reduced freshwater inflow leads to increased salinity,
 3668 which negatively impacts oyster populations (Powell et al. 2003, Turner 2006). The
 3669 introduction of marine parasites and predators is assumed to account for oyster losses
 3670 (Stanley and Sellers 1986, Livingston et al. 2000, Powell et al. 2003, LaPeyre et al. 2003,
 3671 Buzan et al. 2009, Petes et al. 2012). However, while episodic freshwater inputs reduce
 3672 parasite activity, oyster filtration rates also can be suppressed by decreased salinity (Pollack
 3673 et al. 2011). The ability of oysters to close their shells and alter pumping rates allows them
 3674 to survive under fluctuating salinities (Loosanoff 1953, Davis 1958, Andrews et al. 1959).
 3675 Patterns can be complicated as both oyster condition and long-term harvests around the
 3676 Gulf of Mexico are positively correlated to salinity (Turner 2006, Guillian and Aguirre-
 3677 Macedo 2009).

3678 Turner (2006) hypothesized that the effects of salinity on oyster yields depend upon
 3679 both the historical conditions and current trajectory for salinity in a particular estuary. It
 3680 has been suggested that increasing total freshwater input to the Gulf of Mexico estuaries
 3681 for natural resource protection probably would not increase estuarine oyster harvests
 3682 (Hofstetter 1977, Turner 2006). Therefore, short- and long-term alteration of salinity
 3683 distributions in Gulf of Mexico estuaries with variable inflow can have implications for
 3684 oyster survival, abundance, and habitat extent (Chamberlain and Doering 1998a, Wang et
 3685 al. 2008, Volety et al. 2009, Pollack et al. 2011).

3686 The objective of this research component was to evaluate salinity conditions at two
 3687 locations with oyster habitat in the CRE. The two locations are Cape Coral and Shell Point
 3688 near the mouth of the CRE (**Figure 55**). Salinity data from the 2006–2014 dry seasons
 3689 (November–April) were categorized relative to oyster habitat criteria and related to
 3690 freshwater inflow at S-79 at the head of the CRE.

3691



3692

3693

3694

Figure 55. Location map for Cape Coral and Shell Point sampling sites, oyster habitat derived from side-scan mapping (red), and average densities (colored circles) in the lower CRE.

3695

Methods

3696

3697

3698

3699

3700

3701

3702

3703

3704

3705

3706

Oyster habitat in the CRE was mapped in 2010 using side-scan sonar as part of CERP (RECOVER 2012). This effort resulted in estimates of the extent and magnitude of oyster habitat. The benthic sampling effort used a four-prong approach: (1) calibration of the side-scan sonar and Quester Tangent Sideview Classification software in known oyster reef areas with varying substrate types, (2) remote sensing, (3) field intensive ground truth data to classify benthic habitat types, and (4) extensive mapping and quantitative assessment of live and dead reefs and oyster shell lengths of live oyster reefs. The mapping effort resulted in an estimated 847 acres (3.7%) of bottom classified as “oyster” habitat in the lower CRE. Although there were isolated patches located in the middle estuary, the upstream limit for mapped oyster habitat was near Cape Coral. Oyster habitat was denser and more widespread near Shell Point (**Figure 55**).

3707

3708

3709

3710

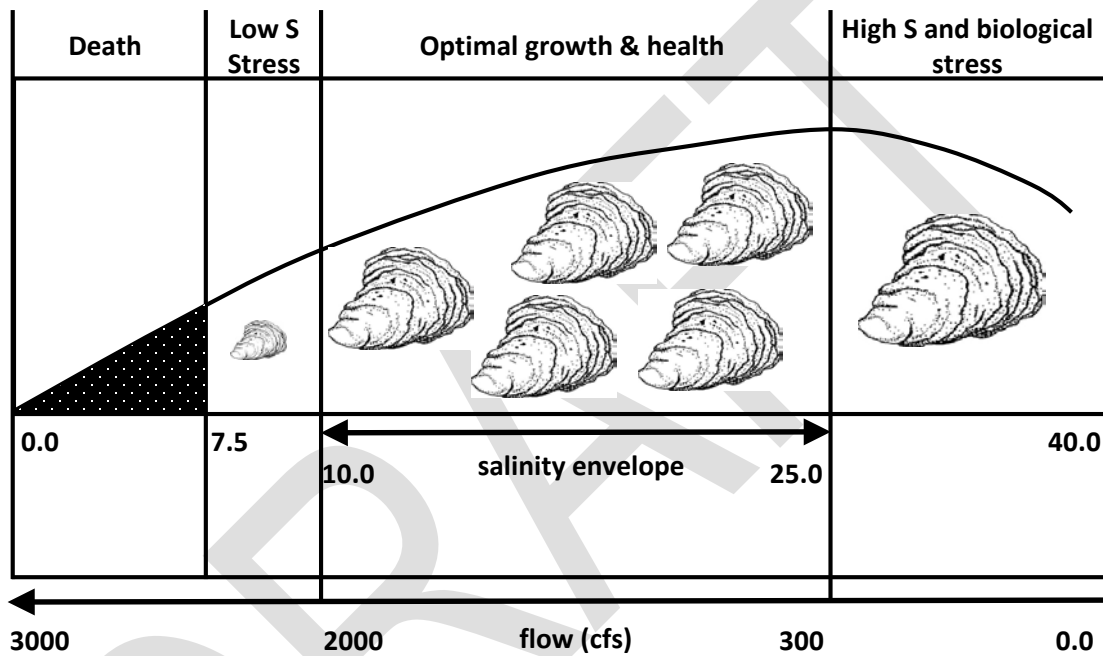
3711

3712

3713

Salinity data collected at Cape Coral and Shell Point were used to assess estuarine conditions for oyster habitat. The POR for salinity data matched that for the monitoring of oyster population attributes in the CRE (2005–2014). Average daily salinity values at these locations were merged with average daily freshwater inflow at S-79. These data were used to generate time series (daily) and regressions between inflow and salinity at each station (monthly). Additionally, the data were categorized by water year and season (dry versus wet) with analyses focused on the dry season days.

3714 In general, oyster growth and survival are maximized if salinity varies from 10 to 25
 3715 (**Table 28**; Loosanoff 1958, Shumway 1996, Dekshenieks et al. 2000, Barnes et al. 2007).
 3716 A conceptual model of oyster responses to salinity and freshwater inflow was developed
 3717 for the CRE (**Figure 56**; Buzzelli et al. 2013d). Based on this conceptualization, salinity
 3718 data at Cape Coral and Shell Point were split into five categories: <10, 10–15, 15–20, 20–
 3719 25, and >25. The number and percentage of dry season days where salinity values were
 3720 within each of these categories were calculated. The averages and standard deviations for
 3721 salinity and freshwater inflow associated with each of these salinity classes were also
 3722 calculated for each of the downstream locations. The freshwater inflow associated with dry
 3723 season salinity values of 20 to 25 at the upstream extent of oyster habitat (e.g. Cape Coral)
 3724 was quantified.

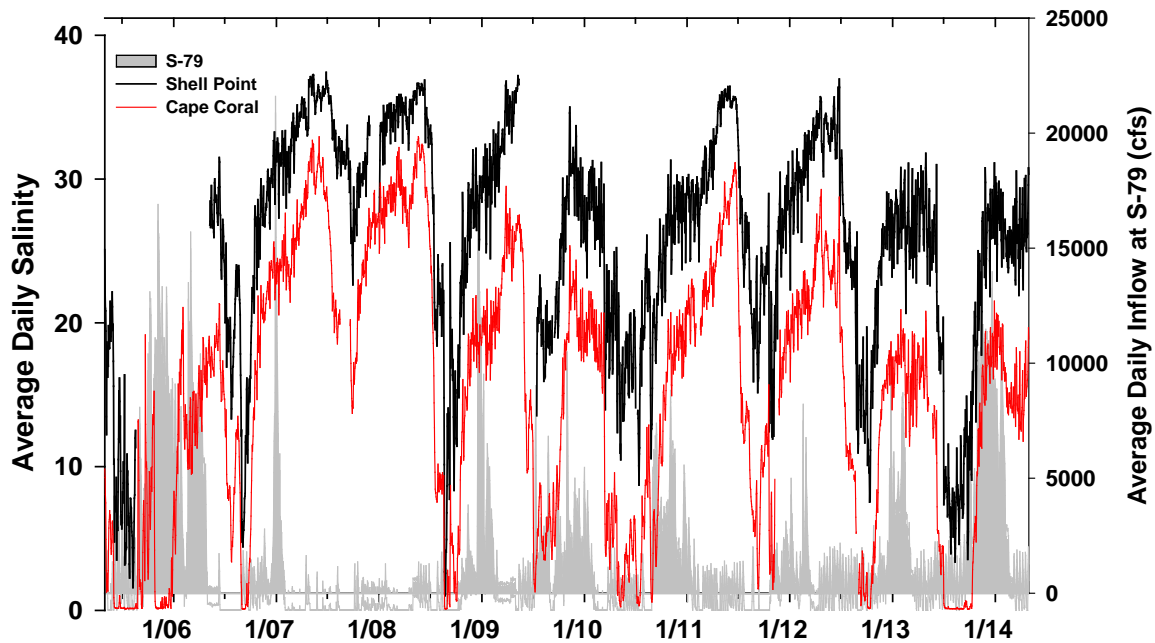


3725
 3726 **Figure 56.** Conceptual model of the effects of salinity (S) on oyster survival and growth.
 3727 Generalized freshwater inflows that could account for the target salinity range are shown at
 3728 the bottom.

3729 **Results**

3730 Freshwater inflow ranged from near zero to >20,000 cfs throughout the POR (**Figure**
 3731 **57**). Salinity at both locations increased with decreased inflow as the highest values were
 3732 observed from January 2007 to August/September 2008. On average, salinity at Shell Point
 3733 was ~1.5 times greater than at Cape Coral. Dry season salinity ranged from 1.1 to 32.2 and
 3734 averaged 19.8 ± 5.7 at Cape Coral (**Table 29**). Wet season salinity at Cape Coral ranged
 3735 from 0.1 to 33.0 and averaged 12.6 ± 9.9 . At Shell Point, salinity ranged from 12.0 to 36.9
 3736 and averaged 29.1 ± 4.1 in the dry season and 1.0 to 37.4 and 23.4 ± 8.6 in the wet season.

3737



3738

3739

3740

Figure 57. Time series of average daily freshwater inflow at S-79 (cfs; right axis; shaded fill) and salinities at Cape Coral (red) and Shell Point (black) from May 1, 2005, to April 30, 2014.

3741

3742

3743

Table 29. Seasonal ranges, averages (Avg), and standard deviations (SD) for salinity values recorded at Cape Coral and Shell Point from 2005 to 2014.

Station	Season	Range	Avg ± SD
CC	Dry	1.1–32.2	19.8 ± 5.7
	Wet	0.1–33.0	12.6 ± 9.9
SP	Dry	12.0–36.9	29.1 ± 4.1
	Wet	1.0–37.4	23.4 ± 8.6

3744

3745

3746

3747

3748

3749

3750

3751

3752

3753

Salinity was <10 at Cape Coral for 234 or 13% of dry season days from 2005 to 2014 (Table 30). By contrast, there were 299 days (16.8%) where salinity was >25 at this location. The average and standard deviation for freshwater inflow were 90 ± 273 cfs when dry season salinity was >25. Daily salinity was within the desired range for oyster survival (10 to 25) on 70.1% of the observations. Daily inflow ranged from 0 to 2,000 cfs and averaged 296 ± 410 cfs when salinity ranged from 20 to 25 at Cape Coral in the dry season. While, dry season salinity was never <10 at Shell Point, it exceeded 25 for 1,266 or 83.3% of the days (Table 31). Salinity at Shell Point was within the 10 to 25 range on 16.8% of the days within the period of record.

3754

3755 **Table 30.** The number (n) and percentages (%) of dry season days with measured average (Avg)
 3756 daily salinity values (\pm standard deviation [SD]) at Cape Coral that were <10, 10 to 15, 15 to 20,
 3757 20 to 25, and > 25 from 2005 to 2014. Included are descriptive statistics (range; Avg \pm SD) for
 3758 salinity and freshwater inflow at S-79 (cfs) for each salinity class.

Salinity Class	n	%	Salinity		Inflow at S-79	
			Range	Avg \pm SD	Range	Avg \pm SD
<10	234	13.1	0.15-10.0	4.5 \pm 3.3	0-15,700	4,002 \pm 2,984
10-15	221	12.4	10.1-15.0	13.2 \pm 1.4	0-9,030	1,068 \pm 981
15-20	606	34.0	15.0-20.0	17.6 \pm 1.4	0-6,990	670 \pm 693
20-25	422	23.7	20.0-25.0	22.3 \pm 1.4	0-2,000	296 \pm 410
>25	299	16.8	25.0-32.2	27.7 \pm 1.6	0-2,030	90 \pm 273
Total	1782	100.0	0.15-32.2	18.1 \pm 7.1	0-15,700	967 \pm 1,721

3759

3760 **Table 31.** The number (n) and percentages (%) of dry season days with measured average (Avg)
 3761 daily salinity values (\pm standard deviation [SD]) at Shell Point that were <10, 10 to 15, 15 to 20,
 3762 20 to 25, and > 25 from 2005 to 2014. Included are descriptive statistics (range; Avg \pm SD) for
 3763 salinity and freshwater inflow at S-79 (cfs) for each salinity class. (Note: NA – not applicable.)

Salinity Class	n	%	Salinity		Inflow at S-79	
			Range	Avg \pm SD	Range	Avg \pm SD
<10	0	0.0	NA	NA	NA	NA
10-15	13	0.9	10.3-14.9	13.1 \pm 1.4	264-10,030	4,696 \pm 2,760
15-20	62	4.1	15.1-20.0	17.9 \pm 1.4	256-5,990	2,537 \pm 1,449
20-25	179	11.8	20.1-25.0	23.2 \pm 1.3	0-9,030	1,243 \pm 1,203
>25	1266	83.3	25.0-36.9	30.0 \pm 3.0	0-6,990	428 \pm 567
Total	1520	100.0	10.3-36.9	28.6 \pm 4.4	0-15,700	967 \pm 1,721

3764

3765 Discussion

3766 Overall salinity patterns were favorable for oyster survival at the upstream extent of
 3767 oyster habitat in the CRE (i.e., Cape Coral). Dry season salinity averaged 19.8 and was
 3768 within the 10 to 25 range ~70% of the time. Oyster habitat is more widespread with average
 3769 densities of ~1,000 oysters m⁻² in the lower CRE around Shell Point. This is despite the
 3770 fact that salinity exceeded 25 for >80% of the time in this location. Thus, the assertion that
 3771 salinity values >25 are potentially detrimental to oysters in the lower CRE was difficult
 3772 to support.

3773 The historical contention that increased salinity can negatively affect oyster
 3774 populations may not be relevant for oyster habitat in the CRE. This contention is supported
 3775 by studies in the northern Gulf of Mexico that demonstrated that an upper salinity threshold
 3776 of 17 to 25 could damage oysters in Apalachicola Bay (Petes et al. 2012). Damage occurs
 3777 through the increased activity and prevalence of the marine, oyster-specific disease Dermo
 3778 as an impediment to the health, distribution, and density of oysters. However, this may be
 3779 limited in the CRE due to the subtropical climate where temperature is low when salinity
 3780 is high (dry season), and temperature is high when salinity is low (wet season). This
 3781 contrast greatly inhibits the impact of Dermo. In fact, laboratory experiments, field studies,
 3782 and simulation models support this understanding (LaPeyre et al. 2003, Buzzelli et al.
 3783 2013d). While Dermo can be detected in large percentage of individual oysters from the
 3784 monitoring locations in the lower CRE, infection intensity levels are generally very low
 3785 (RECOVER 2014).

3786 Using oyster habitat properties as indicators of inflow and salinity in the CRE might be
3787 limited. First, the influence of freshwater inflow on salinity is reduced in polyhaline (18 to
3788 30) areas of estuaries including the CRE (Qiu and Wan 2013). This is due to the effects of
3789 tidal exchange and wind on patterns of circulation. Most of the oyster habitat is located
3790 ~40 km downstream from the dominant source of freshwater inflow (S-79). Second, the
3791 effects of the marine parasite Dermo on oyster populations are muted. Third, the role of
3792 predators with increased salinity in the CRE is largely unknown.

DRAFT

3793 **Component Study 10: Ecohydrological Controls on Blue Crab**
3794 **Landings and Minimum Freshwater Inflow to the**
3795 **Caloosahatchee River Estuary**

3796 *Peter H. Doering and Yongshan Wan*

3797 **Abstract**

3798 A long-term record (28 years) was used for blue crab (*Callinectes sapidus*) landings in
3799 the CRE to establish relationships between (1) changes in hydrology and changes in water
3800 resource function and (2) the magnitude of the functional loss and time to recover. Annual
3801 CPUE, computed from monthly landings of crabs and measures of fishing effort,
3802 represented the resource function. Annual landings expressed as both unadjusted and de-
3803 trended CPUE were found to be significantly correlated with hydrologic variables—
3804 rainfall and freshwater inflow during the previous year's dry season. Increases in CPUE
3805 from one year to the next were also positively related to dry season rainfall in the first of
3806 the two years. Geometric mean functional regressions and Monte Carlo simulations were
3807 used to identify the dry season rainfall associated with losses of water resource function
3808 (CPUE) that required 1, 2, or 3 years of average dry season rainfall to recover. A spectral
3809 analysis indicated that time series of both dry season rainfall and blue crab catch had
3810 periodicities of 5.6 years. A Monte Carlo analysis revealed that the rainfall associated with
3811 two and three year recoveries had return intervals of 5.8 and 8.2 years, respectively.

3812 **Introduction**

3813 Estuaries are among the most productive (Nixon et al. 1986) and economically
3814 important ecosystems on earth, supporting both commercial and recreational fisheries
3815 (Copeland 1966, Seaman 1988). The critical role of freshwater inflow in supporting
3816 estuarine productivity is well recognized (Copeland 1966, Nixon 1981, Nixon et al. 2004,
3817 Wetz et al. 2011, Montagna et al. 2013). In the early 1970s, Sutcliffe (1972, 1973)
3818 presented correlations between discharge from the St. Lawrence River and lagged landings
3819 of lobster, halibut, haddock, and soft shell clams from the Gulf of St. Lawrence. These
3820 relationships established a link between freshwater discharge and production at higher
3821 trophic levels.

3822 Since that time, numerous studies have found similar correlations between river
3823 discharge or rainfall and recruitment or catch of fish and shell fish (Drinkwater and Frank
3824 1994, Robins et al. 2005); including in Florida for pink shrimp (Browder 1985), blue crabs
3825 and oysters (Meeter et al. 1979, Wilber 1992, 1994). Reductions in freshwater inflow from
3826 droughts (Dolbeth et al. 2008, Wetz et al. 2011) and the construction of dams (Aleem 1972,
3827 Baisre and Arboleya 2006) have been associated with reduced fisheries landings. These
3828 studies suggest that correlations between river flow and rainfall and fish catch are real
3829 rather than spurious. While the underlying mechanisms accounting for these correlations
3830 are not clearly understood, Robins et al. (2005) reviewed the literature and identified the
3831 following three hypotheses: (1) The food chain hypothesis is basically an agricultural
3832 argument whereby nutrients in freshwater discharge enhance food supplies resulting in
3833 better growth and survival (e.g. Loneragan and Bunn 1999); (2) a hydrodynamically-based
3834 alternative argues that freshwater discharge and the associated circulation may increase the
3835 size of retention areas and enhance recruitment (Gillanders and Kingsford 2002); and

3836 (3) inflows may change spatial distribution and influence catchability (Loneragan and
3837 Bunn 1999).

3838 In the State of Florida water resource protection rules are often based on harm
3839 standards. An MFL protects a waterbody from “significant harm” caused by further
3840 withdrawals. “Significant harm” means the temporary loss of water resource functions,
3841 which result from a change in surface or ground water hydrology, which takes more than
3842 two years to recover” (Subsection 40E-8.021(24), Florida Administrative Code).
3843 Establishing a water resource protection rule requires quantitative relationships between
3844 (1) changes in hydrology and changes in resource function and (2) the magnitude of
3845 resource loss and time to recover. Most of the MFLs that SFWMD has established contain
3846 a “return frequency” (SFWMD 2014). This concept recognizes that “significant harm” may
3847 happen naturally, at a frequency associated with the occurrence of a particular level
3848 of drought.

3849 Most approaches to establishing freshwater inflow requirements are ultimately
3850 resource based by quantifying the relationships between freshwater inflow, estuarine
3851 conditions, and biological resources (Chamberlain and Doering 1998b, Alber 2002, Palmer
3852 et al. 2011). The freshwater requirements of estuarine fisheries are often included in the
3853 planning, allocation, and management of water resources (Robins et al. 2005). The fisheries
3854 themselves can be economically important. Their dependence on freshwater inflow is
3855 comprehensible to a wide variety of stakeholders (Alber 2002) and illustrates both the
3856 ecological and economic importance of freshwater supplies to estuaries (Copeland 1966).

3857 In this component, we established quantitative relationships between hydrologic
3858 variables (rainfall and freshwater inflow) and commercial blue crab landings in Lee
3859 County, Florida. Secondly, we related reductions in catch to recovery time under average
3860 hydrologic conditions. Lastly, we analyzed periodicity in the time series of hydrologic and
3861 crab catch data to investigate return frequency.

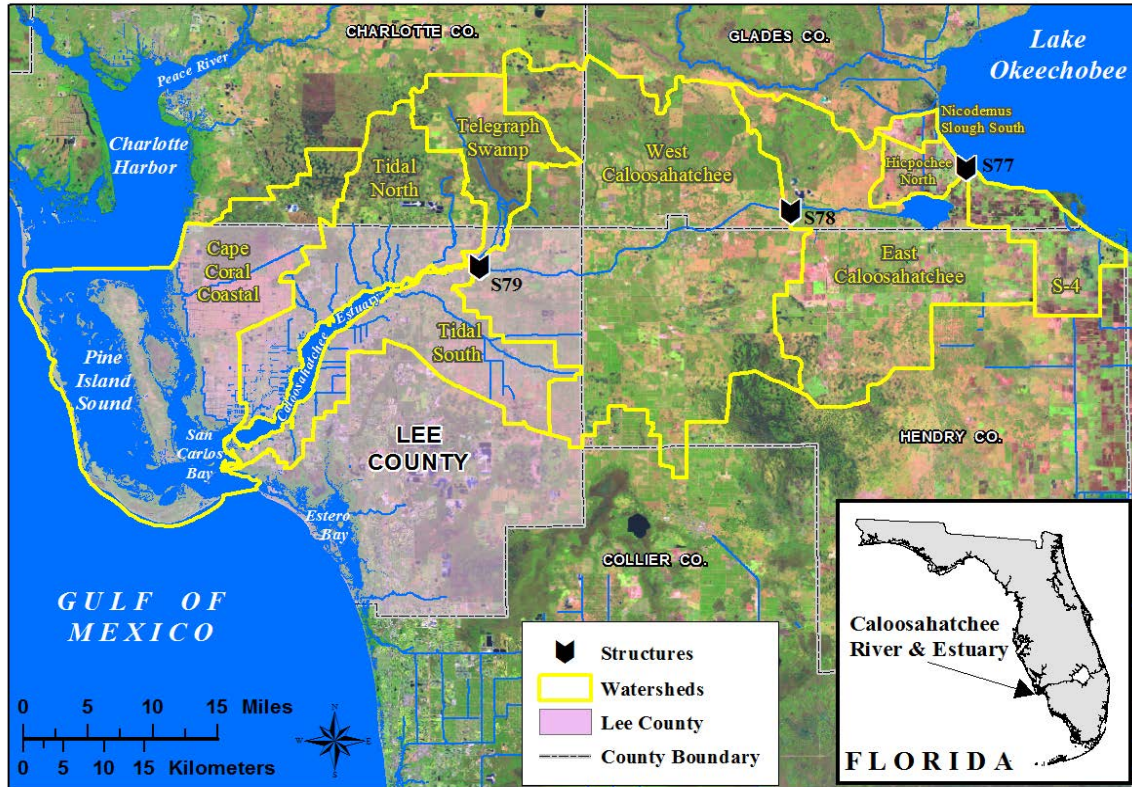
3862 The blue crab is an estuarine dependent macroinvertebrate that supports valuable
3863 recreational and commercial fisheries along the Atlantic and Gulf coasts (Guillory 2000,
3864 Mazzotti et al. 2006, Murphy et al. 2007). Blue crab, common in the crab trap fishery in
3865 the CRE, has historically had large and consistent landings within the estuary (Mazotti et
3866 al. 2006). It is classified as “highly abundant” by the NOAA’s Estuarine Living Marine
3867 Resources program (Nelson 1992). In 2003, licensed crab fishers in Lee County numbered
3868 183 and the number of licensed crab traps was over 63,000 (FWRI 2003). This fishery
3869 expends a large effort and yields large numbers of crabs for local and distant consumers
3870 while supporting a valuable local economic employment opportunity.

3871 **Methods**

3872 **Study Area**

3873 The Caloosahatchee River and Estuary, a portion of the C-43 Canal (upstream of S-79)
3874 and Lee County are located on the southwest coast of Florida (**Figure 58**). The C-43 Canal
3875 runs 67 km from Lake Okeechobee to the Franklin Lock and Dam (S-79). S-79 separates
3876 the freshwater from the CRE, which terminates 42 km further downstream at Shell Point.
3877 The system has been altered to provide for navigation, water supply, and flood control on
3878 both a local and regional scale (Chamberlain and Doering 1998a, Doering et al. 2006). The
3879 river has been straightened and deepened and three water control structures (S-77, S-78

3880 and S-79) have been added (Antonini et al. 2002). The Franklin Lock and Dam (S-79) was
 3881 added in part to act as a salinity barrier at the head of the estuary (Flaig and Capece 1998).
 3882 The historic river (now C-43 Canal) has also been artificially connected to Lake
 3883 Okeechobee to convey releases of water to tide for the purpose of regulating water levels
 3884 in the lake. The estuarine portion of the system has also been modified: a navigation
 3885 channel has been dredged (Antonini et al. 2002) and a causeway built across the mouth of
 3886 San Carlos Bay.



3887
 3888 **Figure 58.** Location of Lee County and the Caloosahatchee River and CRE. Over 60% of land
 3889 area in Lee County drains into the CRE and San Carlos Bay.

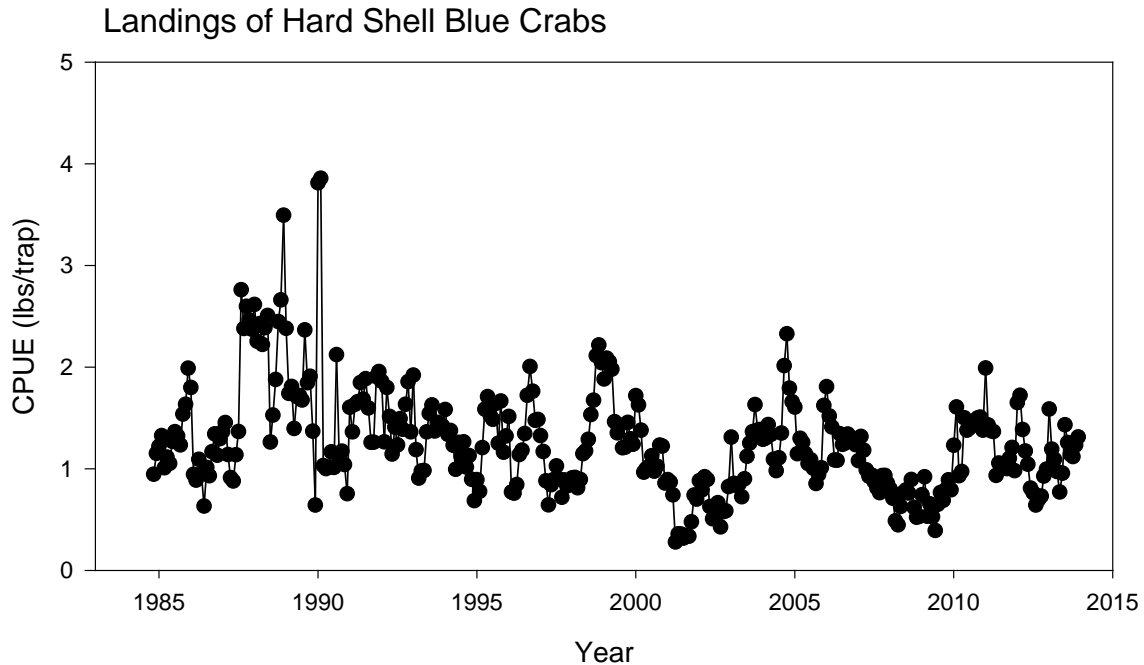
3890 **Inflow Characteristics**

3891 Major surface water inflows to the estuary come from Lake Okeechobee, the C-43
 3892 Basin upstream of S-79 (S-4 Basin, and East and West Caloosahatchee subbasins) and the
 3893 Tidal Basin (i.e. the Telegraph Swamp, Tidal North, and Tidal South subbasins) located
 3894 between S-79 and Shell point (**Figure 58**). Over the long term (1997–2014) the annual total
 3895 surface water inflow from these three sources averages 1.8×10^6 ac-ft with 31.6% coming
 3896 from Lake Okeechobee, 47.6 % from the Caloosahatchee Basin, and 21% from the Tidal
 3897 Basin (SFWMD 2015).

3898 **Data Sources**

3899 Monthly landings of blue crabs in Lee County for the period of November 1984 through
 3900 December 2013 were obtained from the Florida Fish and Wildlife Conservation
 3901 Commission's Florida Wildlife Research Institute in St. Petersburg, Florida (**Figure 59**).
 3902 Fisherman are asked to report the weight of hard and soft shell crabs caught and the number

3903 of traps pulled on a per trip basis. The number of traps pulled is not always reported and is
 3904 estimated when missing (Murphy et al. 2007). Daily rainfall (inches) for Lee County and
 3905 daily discharge (cfs) at S-79 were obtained from the SFWMD's database DBHYDRO
 3906 (http://www.sfwmd.gov/dbhydroplsql/show_dbkey_info.main_menu). Inflows from the
 3907 tidal basin were predicted using a rainfall-runoff model calibrated to five years of measured
 3908 discharge data from tidal creeks (Wan and Konya 2015). Total discharge to the estuary was
 3909 taken as the sum of discharge at S-79 and inflows from the tidal basin.



3910
 3911 **Figure 59.** Monthly landings of hard shell blue crabs in Lee County Florida. Data from the Florida
 3912 Fish and Wildlife Conservation Commission's Florida Wildlife Research Institute.
 3913 (Note: lbs/trap – pounds per trap.)

3914 ***Relationships between Hydrologic Variables and Blue Crab Catch***

3915 All time series were expressed in terms of water years. The advantage of defining the
 3916 time series on the basis of water year is that each 12-month period contains one full wet
 3917 season (May–October) and one full dry season (November–April). The period of record
 3918 for analysis was 28 years (WY1986–WY2013). Monthly landings of crabs (pounds [lbs]
 3919 hard, lbs soft) and measures of fishing effort (number of trips and number of traps pulled)
 3920 were summed to produce annual totals. From these, annual estimates of CPUE were
 3921 computed. CPUE was defined as lbs of crab (hard or soft) per trap (e.g. lbs of hard shell
 3922 crabs per total number of traps pulled). Rainfall in Lee County, discharge at S-79, and total
 3923 discharge (Tidal Basin + S-79) were also expressed on both an annual and seasonal (dry
 3924 and wet) basis. To allow for examining the effects of previous years of rainfall and
 3925 discharge on a current year's CPUE, the POR for hydrologic variables ran from WY1981
 3926 to WY2013.

3927 ***Statistical Analyses***

3928 Statistical analyses were conducted using SAS version 9.3. Following Wilber (1994),
 3929 annual estimates of CPUE for hard and soft shelled crabs were tested for association with

3930 rainfall in Lee County and discharge (at S-79 and total discharge) at annual lags of zero to
3931 five years by calculating the Pearson Correlation coefficient. A lag of 0 indicates that the
3932 current year's CPUE was paired with the current year's rainfall or discharge. At a lag of 1,
3933 CPUE was correlated with the previous water year's rainfall or discharge.

3934 When a correlation using unadjusted data was statistically significant, each time series
3935 involved was tested for long-term trend (linear increase or decrease over time) using least
3936 squares linear regression. If significant, a de-trended time series was obtained from the
3937 residuals of the least squares regression of CPUE on rainfall or flow. This procedure
3938 yielded a time series of deviations from the long-term mean (de-trended residuals). The
3939 time series were also tested for autocorrelation at a lag of one year. If statistically
3940 significant, autocorrelation was removed by subtracting the previous year's value from the
3941 value of a variable for a given year. Correlations between CPUE and hydrologic factors
3942 were reevaluated using the corrected time series.

3943 Relationships between CPUE and hydrologic factors (rainfall and discharge) were
3944 quantified using a geometric mean functional regression (Ricker 1973), which provides an
3945 estimate of central tendency. This approach is appropriate when there is error in both X
3946 and Y. In order to evaluate periodicity, a spectral analysis (Proc Spectral in SAS) was
3947 conducted. Following Chatfield (1989), any trend (monotonic increase or decrease over
3948 time) was removed before analysis using least squares linear regression.

3949 ***Loss of Water Resource Function and Recovery in Relation to Rainfall***

3950 In order to estimate the rate of recovery of CPUE, we developed a relationship between
3951 magnitude of the loss of resource function and recovery time. In the case of the blue crab
3952 fishery, the water resource function was expressed as CPUE. Loss of resource function was
3953 therefore a decrease in CPUE. In quantifying the relationship between loss of resource
3954 function and recovery time, three assumptions were made: (1) loss of resource function
3955 occurred when CPUE fell below the long-term annual mean of 1.26 pounds per trap
3956 (lbs/trap) (2) recovery occurred under average hydrologic conditions; and, (3) recovery
3957 was achieved when CPUE returned to the long-term annual mean.

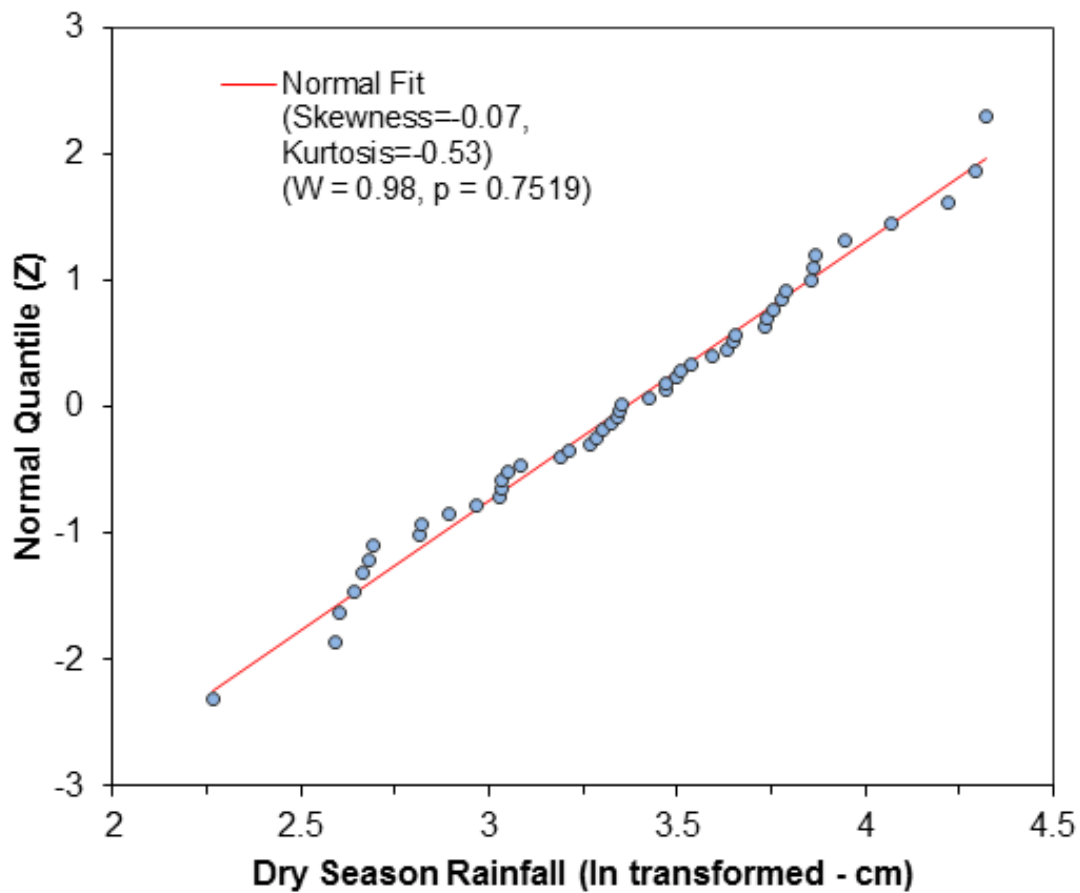
3958 To determine rate of recovery, instances from the POR (WY1986–WY2013) in which
3959 CPUE increased from one year to the next were extracted, expressed as an annual rate of
3960 increase in CPUE, and regressed on rainfall occurring during the first of the two years. This
3961 relationship was then used to estimate the change in CPUE associated with one year of
3962 average rainfall.

3963 The loss in resource function or deviation from the long-term mean that can be
3964 recovered in one year was the estimated change in CPUE associated with one year of
3965 average rainfall. The loss that can be recovered in two years was twice the change in CPUE
3966 associated with one year of average rainfall, and so on.

3967 The actual value of the CPUE that takes one year to recover to the long-term mean was
3968 the long-term mean minus the change in CPUE associated with one year of average rainfall.
3969 For a two-year recovery, the value of the CPUE was the long-term mean minus twice the
3970 change in CPUE associated with one year of average rainfall.

3971 The above analysis of the rainfall associated with loss of blue crab CPUE and recovery
3972 was, to a certain extent, limited by the quantity of data within the POR. The time series did
3973 not include a sufficient number of events to quantify these relationships simply by

3974 examining the record itself. As an alternative, we conducted Monte Carlo simulations, to
 3975 acquire the frequency or probability of rainfall associated with CPUE recovery times of
 3976 two and three years. Monte Carlo simulations have been used widely in fishery and
 3977 hydrological research for assessing a model's outputs with different types and levels of
 3978 variability or uncertainty in the model's inputs (e.g. Restrepo et al. 1992, Punt 2003, and
 3979 Petrie and Brunsell 2011). In order to conduct a Monte Carlo simulation, an underlying
 3980 probability distribution was specified. A normality test (Shapiro-Wilk's test (W) along with
 3981 the normal quantile plot) of the Lee County dry season rainfall data from 1965 to 2013
 3982 indicated that the variability of the dry season rainfall can be well described by a log-
 3983 normal distribution (**Figure 60**; $W = 0.98$, $p = 0.752$, and $\alpha = 0.05$). Monte Carlo
 3984 simulations were conducted based on this dry season rainfall probability distribution to
 3985 generate ten sets of 10,000 years of dry season rainfall.



3986

3987

3988

Figure 60. Normality test of natural log-transformed dry season rainfall during WY1966–WY2013.
 (Note: cm – centimeters.)

3989

3990 The functional regression equation relating annual CPUE and Lee County rainfall was
 3991 used to predict blue crab CPUE with the generated rainfall data as inputs. The years with
 3992 CPUE lower than the long-term (WY1986–WY2013) mean CPUE followed by successive
 3993 two or three years of recovery back to normal were identified, respectively. The average
 3994 dry season rainfall for these years and associated average return interval and probability of
 3995 occurrence at least once in ten years were calculated.

3996 **Determination of Flow Associated with Rainfall**

3997 To convert estimates of rainfall associated with various recovery times to discharge
 3998 (S-79 or total), regression analysis was performed. To maximize the probability of
 3999 detecting a statistically significant relationship between discharge and rainfall, a longer
 4000 POR (WY1967–WY2013) was used in this analysis.

4001 **Results**

4002 **Relationships between Hydrologic Variables and Blue Crab Catch**

4003 Annual rainfall in Lee County averaged about 55 inches and ranged from a low of 41
 4004 inches in WY1981 to a high of 81.5 inches in WY1983. About 76% of the total annual
 4005 rainfall occurred in the wet season and 24% in the dry season (**Table 32**). Dry season
 4006 rainfall ranged from a low of 3.8 inches in WY2009 to a high of 29.6 inches in WY1998
 4007 (Fig. A10-4A). Annual discharge at S-79 averaged 1,764 cfs (**Table 32**) ranging from a
 4008 low of 113 cfs in WY2008 to a high of 5,044 cfs in WY2006. Daily average discharge at
 4009 S-79 during the wet season (2,294 cfs) was nearly twice the average dry season discharge
 4010 (1,238 cfs). Dry season discharge at S-79 ranged from a low of 52 cfs in WY2008 to a high
 4011 of 5,616 cfs in WY1998. Total discharge averaged 2,267 cfs on an annual basis with tidal
 4012 basin inflows adding about 500 cfs to the discharge at S-79. Daily total discharge averaged
 4013 3,055 cfs in the wet season and 1,480 cfs in the dry season, with Tidal Basin inflows
 4014 contributing 760 and 245 cfs in the wet and dry seasons, respectively (**Table 32**).

4015 **Table 32.** Annual and seasonal (wet versus dry) rainfall (inches) in Lee County and discharge
 4016 (cfs) at the Franklin Lock and Dam and total discharge to the estuary (sum of S-79 and Tidal
 4017 Basin). Values are average (standard deviation). POR was WY1981–WY2013.

	Annual	Wet Season	Dry Season
Lee County Rainfall	55.2 (9.2)	42.3 (7.7)	12.8(5.9)
Discharge at S-79	1,764 (1208)	2,294 (1413)	1,235 (1445)
Total Discharge	2,267(1332)	3,055(1586)	1,480 (1599)

4018

4019 Annual landings in Lee County were dominated by hard shelled crabs with soft shelled
 4020 crabs averaging only 3% of the total catch in lbs (**Figure 60**). The CPUE for hard shelled
 4021 crabs was also higher than for soft shelled crabs. On an annual basis, CPUE for hard shelled
 4022 crabs averaged 1.26 lb/trap and ranging from a high of 2.1 lb/trap in 1989 to a low of
 4023 0.70 lb/trap in 2002 (**Figure 61B**). For soft shelled crabs, CPUE averaged 0.75 lb/trap
 4024 (**Figure 60**), ranging from a high of 1.58 lb /trap in 1989 to a low of 0.05 lb/trap in 2004.

4025

4026

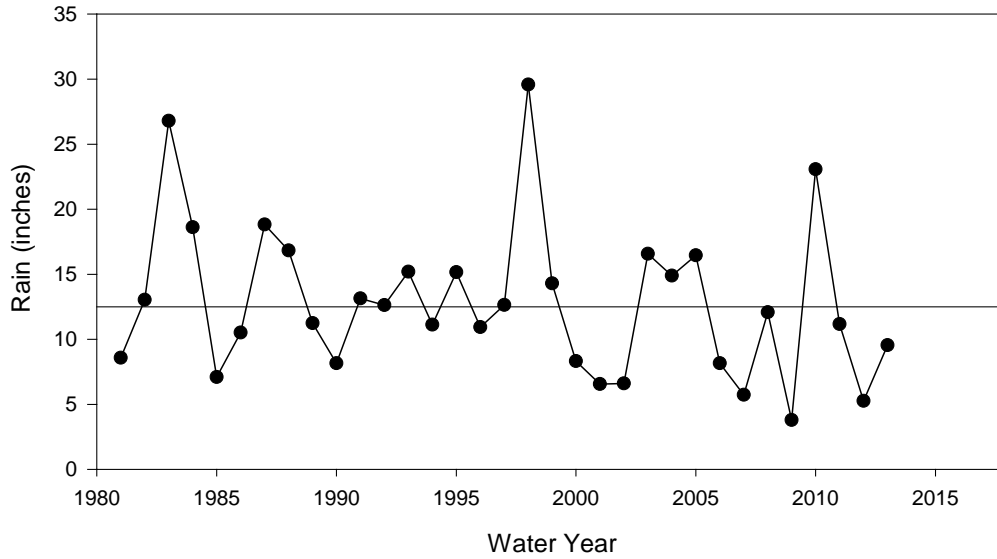
4027
4028
4029

Table 33. Mean annual landings in pounds per year (lbs/yr) of hard and soft shell blue crabs for WY1986–WY2013. Values are average (standard deviation).

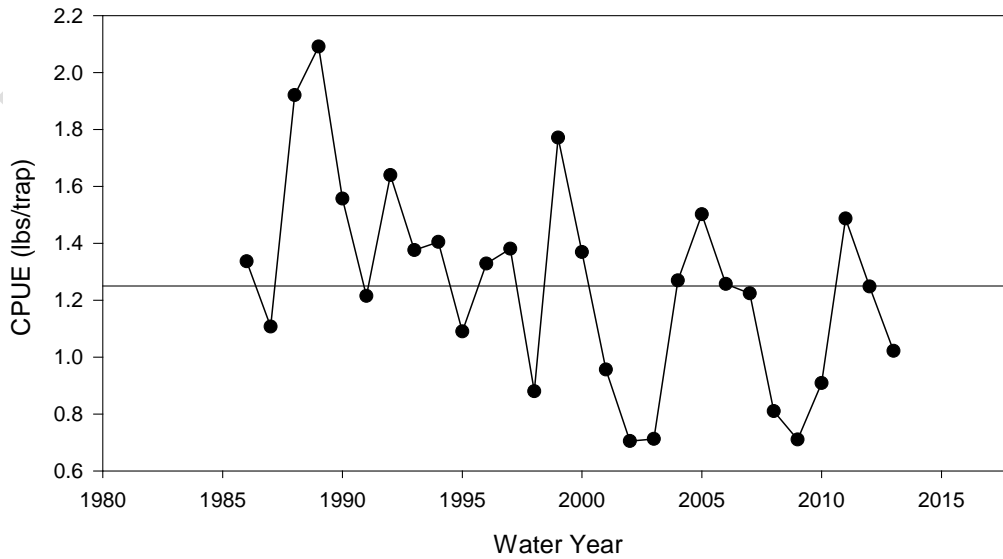
	Landings lbs/yr	CPUE lbs/trap
Hard Shell	1,315,808 (711,508)	1.26 (0.35)
Soft Shell	36,515 (38465)	0.75 (0.43)

4030

Dry Season Rainfall Lee County



Lee County Hard Shell Blue Crab Landings



4031
4032
4033

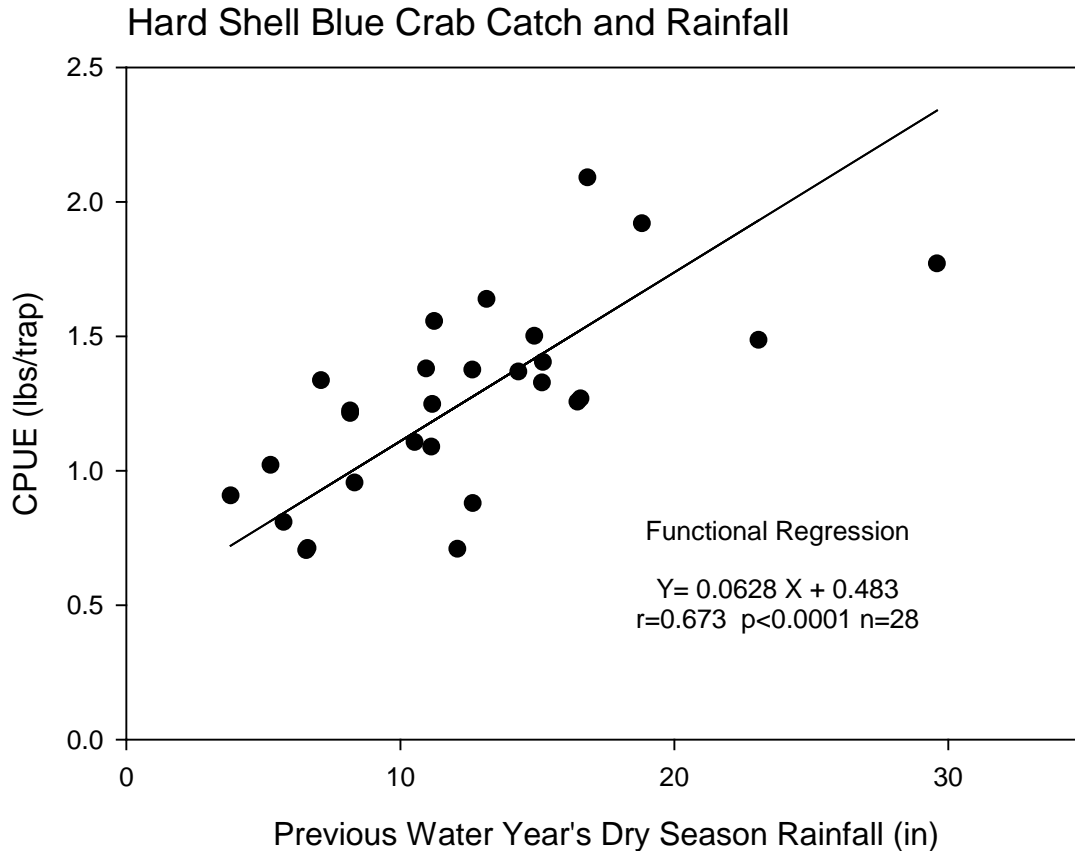
Figure 61. (A) Dry season (November–April) rainfall in Lee County. (B) Annual landings of hard shell blue crabs.

4034 CPUE for hard and soft shelled crabs were tested for association with rainfall and
 4035 discharge (S-79 and total) at annual lags of 0 to 5 years. Statistically significant ($p < 0.05$)
 4036 correlations between CPUE and rainfall or discharge were found only when hydrologic
 4037 variables were lagged by one year. Further, only correlations with dry season rainfall or
 4038 discharge, lagged by one year, were statistically significant (**Table 34**). Therefore, the
 4039 CPUE during the current year was positively associated with rainfall or discharge during
 4040 the previous year's dry season. Of the three hydrologic variables tested, dry season rainfall
 4041 explained the most variance in CPUE. A linear functional regression indicated that dry
 4042 season rainfall explained about 45% of the variability in CPUE of hard shelled crabs, with
 4043 CPUE increasing at a rate of 0.063 lbs/trap per inch (lbs/trap/inch) of rain (**Figure 62**). The
 4044 95% confidence interval (Ricker 1975) for the slope was 0.046 to 0.084 lbs/trap/inch
 4045 of rain.

4046 **Table 34.** Correlation of unadjusted hydrologic variables with unadjusted estimates of CPUE.
 4047 $n=28$ in all cases. Statistical significance: * $p < 0.10$, ** $p < 0.05$, and *** $p < 0.01$.

Variable	Annual CPUE	
	Hard (lbs/trap)	Soft (lbs/trap)
Lee County Rainfall		
Water Year (Lag 1)	0.216	-0.085
Wet Season (Lag 1)	-0.251	-0.309
Dry Season (Lag 1)	0.673***	0.399**
Discharge at S-79		
Mean Water Year (Lag 1)	0.289	0.091
Mean Wet Season (Lag 1)	0.083	-0.161
Mean Dry Season (Lag 1)	0.424**	0.345*
Total Discharge = S-79 + Tidal Basin		
Mean Water Year (Lag 1)	0.293	0.094
Mean Wet Season (Lag 1)	0.058	-0.177
Mean Dry Season (Lag 1)	0.450**	0.369*

4048



4049
 4050
 4051

Figure 62. Functional regression of hard shell blue crab landings on the previous year's dry season rainfall (unadjusted data).

4052 Long-term trend and autocorrelation may lead to spurious correlations between two
 4053 time series (Chatfield 1989). For example, two variables that are both decreasing over time
 4054 may appear correlated even though decreasing trends may have different causes. Linear
 4055 regressions of dry season rainfall, total discharge and discharge at S-79 on water year were
 4056 not statistically significant indicating that these time series showed no long-term trends.
 4057 CPUE for both hard and soft shelled crabs exhibited significant, declining trends over time.
 4058 Only CPUE for soft shelled crabs had significant autocorrelation at a lag of one year. In
 4059 other words, for this variable, the current year's CPUE appeared dependent on the previous
 4060 year's CPUE. When corrections for long-term trend and autocorrelation at lag 1 were made
 4061 as appropriate, CPUE for both hard and soft shelled crabs were still correlated with dry
 4062 season rainfall or discharge at a lag of 1 year (**Table 35**). Because soft-shelled crabs
 4063 accounted for a small percentage of the total catch and because correlations between
 4064 discharge and CPUE were relatively weak, further analysis focused on hard-shelled crabs
 4065 and dry season rainfall.

4066

4067
4068
4069
4070
4071

Table 35. Correlations between hydrologic variables and CPUE after adjustment for long-term trend (de-trended) and autocorrelation (corrected) as appropriate. Included are correlations lagged by one year for dry (November–May) season Lee County rainfall, freshwater discharge through S-79, and total discharge calculated as the sum of S-79 and the Tidal Basin.
* $p < 0.10$, ** $p < 0.05$, and *** $p < 0.01$.

Variable	Annual CPUE	
	Hard (lbs/trap) (de-trended)	Soft (lbs/trap) (de-trended corrected)
Lee County Rainfall Dry Season (Lag 1)	0.696 ***	0.495***
Discharge at S-79 Mean Dry Season (Lag 1)	0.468 **	0.426**
Total Discharge = S-79 + Tidal Basin Mean Dry Season (Lag 1)	0.497***	0.447**

4072

4073

Loss of Water Resource Function and Recovery in Relation to Rainfall

4074

4075

4076

4077

4078

4079

4080

4081

4082

4083

4084

4085

4086

4087

Year-to-year increases in unadjusted (not de-trended) CPUE for hard shelled crabs ($n = 12$) over the period WY1986–WY2013 were expressed as an annual rate of increase in CPUE and associated with dry season rainfall occurring in the first of the two years (**Figure 63**). The functional regression of annual rate of increase in CPUE on dry season rainfall was statistically significant (**Figure 63**, $p < 0.005$, $R^2 = 0.570$). For the average dry season rainfall (WY1986–WY2013) of 12.45 inches per year, this relationship yielded an annual increase of 0.22 CPUE per year. The deviation from the long-term mean that would be recovered after one year of average rainfall was therefore 0.22 CPUE. For two and three year recoveries, the deviations were 0.44 CPUE and 0.66 CPUE, respectively (**Table 36**.) Given a long-term (WY1986–WY2013) average of 1.26 CPUE, the actual CPUE associated with a one, two, or three year recovery are given in **Table 36**. Using the equation in **Table 34**, the previous year's dry season rainfall associated with these CPUE was calculated. The rainfall corresponding to recoveries of one to three years ranged from 8.9 in (1 year) to 1.9 in (3 years).

4088

4089

4090

4091

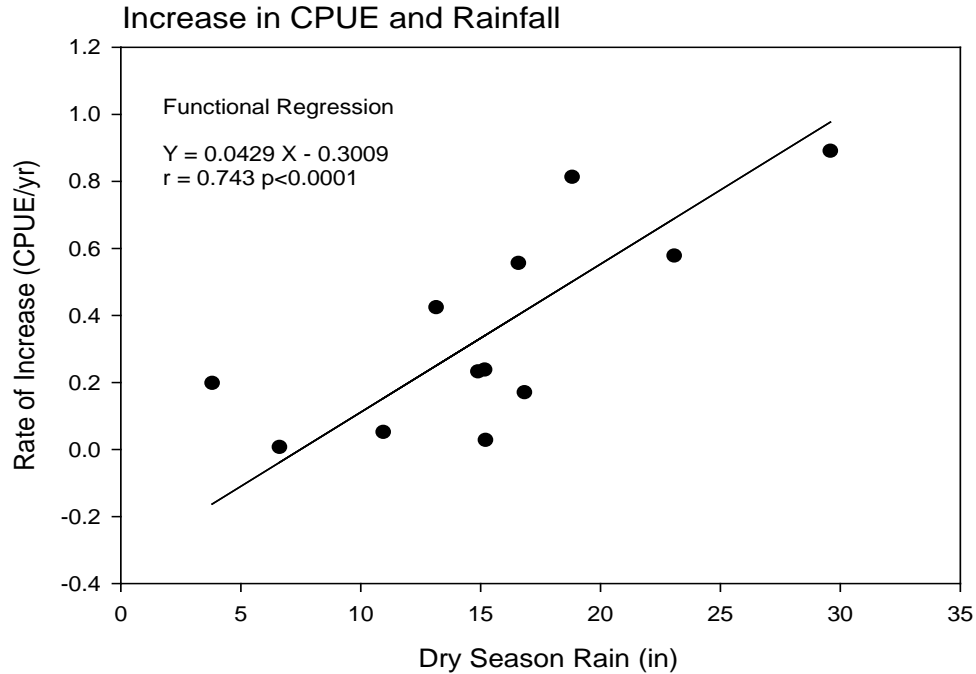
4092

4093

4094

With the Monte Carlo analysis, recovery periods of two and three years back to the average CPUE (1.26 lb/trap) were considered to estimate the dry season rainfall associated with each. Results, summarized in **Table 35**, were based on about 750 observations of recoveries requiring two to three years in each of the ten Monte Carlo runs. Average dry season rainfall associated with a deviation below the long-term average CPUE that took two years to recover was 7.1 inches. The average dry season rainfall associated with a deviation requiring three years to recover was 6.4 inches (**Table 35**).

4095



4096
4097
4098

Figure 63. Functional regression of the increase in CPUE from one year to the next on the dry season rainfall occurring during the first of the two years. Data from **Figure 61**.

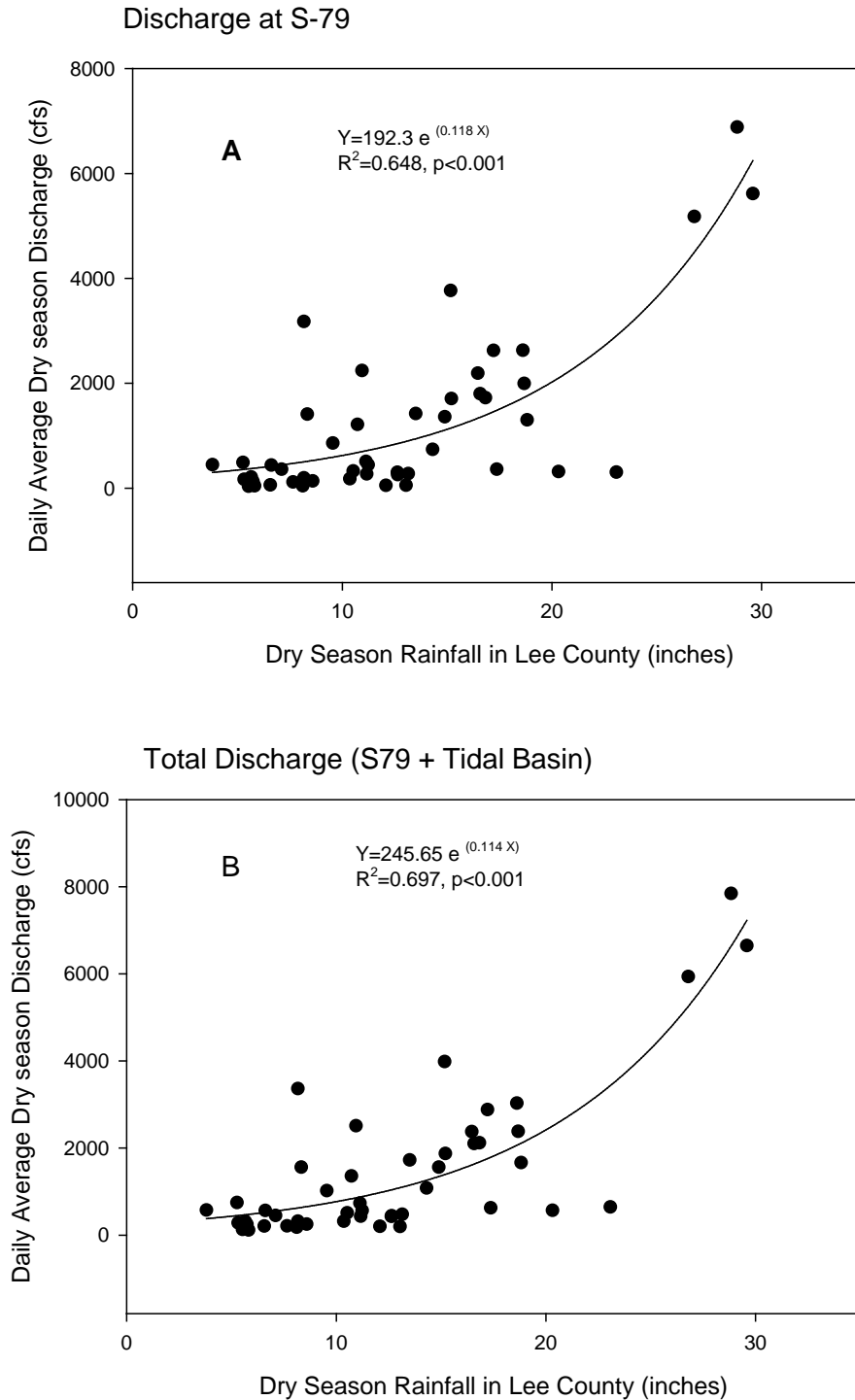
4099
4100
4101
4102
4103
4104

Table 36. Estimates of the preceding water year’s dry season rainfall (Lee County) that produce annual catches of hard shelled crabs that will return to the long-term mean CPUE (1.26 lbs/trap) after one to three years of average dry season rainfall (12.45 inches). Estimates were made using a regression technique and a probabilistic Monte Carlo approach. Also given are the dry season discharge at S-79 and total discharge (S-79 + Tidal Basin) associated with the dry season rainfall in Lee County.

Method	Rainfall (inches)	CPUE (lbs/trap)	Years to Recover	Discharge S-79 (cfs)	Discharge Total (cfs)
Regression	8.9	1.04	1	543	675
	5.4	0.82	2	360	453
	1.9	0.66	3	239	304
Monte Carlo	7.1	0.97	2	440	552
	6.4	0.93	3	407	512

4105
4106
4107
4108
4109
4110
4111
4112

It is important to note that lagged (by 1 year) total dry season discharge and lagged dry season discharge at S-79 were also significantly related to CPUE for hard shelled crabs (**Table 35**). However, neither of these variables was related to year to year increases in CPUE as was the case for dry season rainfall (**Figure 63**). Thus a parallel analysis employing flow instead of rainfall could not be accomplished. Both flow variables were related to dry season rainfall in the current year. The data could be described by non-linear, exponential relationships that explained more than 60% of the variance (**Figure 64**).



4113

4114

4115

Figure 64. Exponential relationships between dry season rainfall in Lee County and discharge to the CRE at S-79 (top panel) or total discharge (bottom panel).

4116

4117

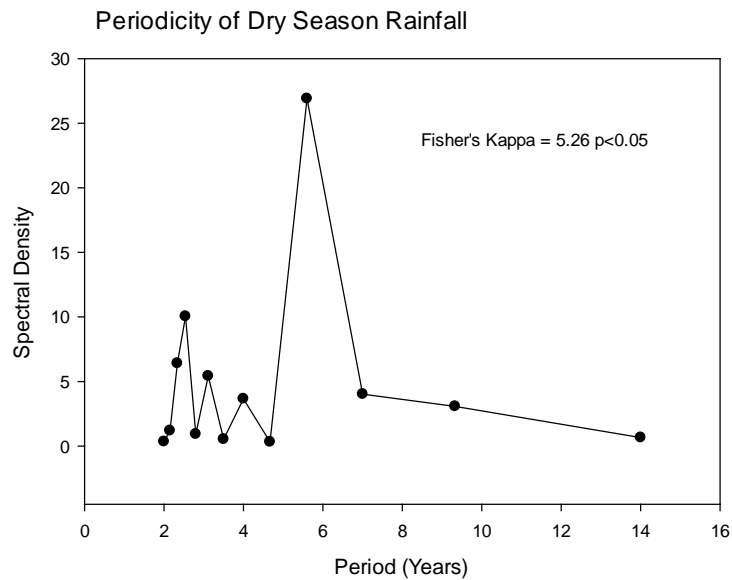
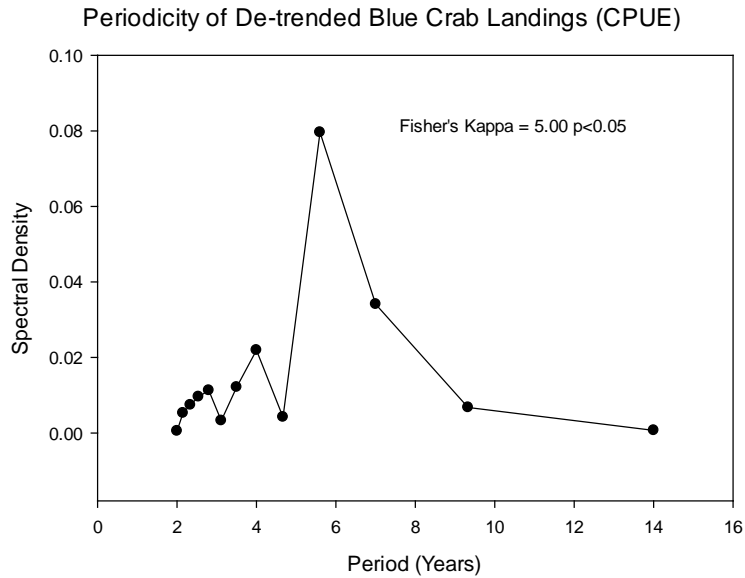
4118

4119

The exponential relationships were used to convert the estimates of dry season rainfall to inflow. The average daily dry season discharge at S-79 associated with one-, two-, or three-year recoveries ranged from 239 to 543 cfs (**Table 36**). Accounting for additional inflow from the tidal basin resulted in flows ranging from 304 to 675 cfs (**Table 36**).

4120 **Return Frequency**

4121 Results of the spectral analysis indicated that both dry season rainfall and CPUE
 4122 showed statistically significant fluctuations with a period of 5.6 years (**Figure 65**).
 4123 Analysis of the results of the Monte Carlo simulations indicated that the average rainfall
 4124 with a two-year recovery of 7.1 inches has a return interval of 5.8 years, very close to the
 4125 results of the spectral analysis (**Table 37**). The average rainfall with a three-year recovery
 4126 was 6.4 in with a return interval of 8.2 years (**Table 37**). The probability for such dry season
 4127 rainfall <6.4 inches to occur at least once in ten years is still high (73%).



4128
 4129 **Figure 65.** Results of spectral analysis. Periodicity of de-trended blue crab landings (top panel)
 4130 and dry season rainfall (bottom panel) in Lee County for WY1986–WY2013. Results indicate that
 4131 both time series show major fluctuation with a period of about six years.

4132

4133
4134**Table 37.** Average dry season rainfall for potential significant harm and associated return interval and probability of occurrences from Monte Carlo simulations.

Simulation	1	2	3	4	5	6	7	8	9	10	Mean
Dry Season Rainfall with 2-year Recovery (inches)	7.1	7.1	7.1	7.1	7.2	7.2	7.1	7.1	7.1	7.0	7.1
Average Return Interval (year)	5.8	5.5	5.9	5.8	5.7	5.5	6.0	5.9	5.8	6.0	5.8
Probability of 1-in-10 Year Occurrence (%)	85	87	84	85	86	87	84	85	85	84	85
Dry Season Rainfall with 3-year Recovery (inches)	6.4	6.1	6.2	6.7	6.6	6.5	6.0	6.5	6.5	6.4	6.4
Average Return Interval (years)	8.3	9	9.4	7.4	7.6	7.7	8.9	7.9	7.9	8.2	8.2
Probability of One in Ten Years Occurrence (%)	72	69	68	77	76	75	70	74	74	73	73

4135

4136

Discussion

4137 The blue crab is an estuarine dependent species that utilizes the full range of salinity
4138 from oligohaline conditions to >30 during its life time (Perry and McIlwain 1986, Longley
4139 et al. 1994). Salinities >20 are required for successful reproduction and larval development
4140 (Perry and McIlwain 1986, Sandoz and Rogers 1944). Juveniles may use low salinity (<15)
4141 regions of estuaries as nurseries (Van Engel 1958, Posey et al. 2005). During a three-year
4142 monitoring program in the CRE, Stevens et al (2008) observed recruitment of juvenile
4143 crabs (< 40 millimeter carapace width) primarily between November and April, with
4144 highest numbers in February, March, and April. Most of these were caught in low salinity
4145 conditions (0.5 to 5). There is also partitioning of the estuarine salinity gradient according
4146 to sex, with adult males remaining in low salinity waters, while mature females prefer the
4147 higher salinities found in lower estuarine and coastal regions (Perry and McIlwain 1986).

4148 Given the dependence on a wide range of salinity for successful completion of its life
4149 cycle, it is not surprising that the productivity of blue crabs in an estuary may be influenced
4150 by freshwater inflow. Lower abundances of blue crabs have been associated with drought
4151 conditions in South Carolina (Childress 2010) and several Texas estuaries (Palmer et al.
4152 2011). Commercial landings provide a convenient measure of productivity (Wilber 1994).
4153 Results from this study agreed with previous investigations that have reported positive
4154 relationships between freshwater inflow and landings of blue crabs (Meeter et al. 1979,
4155 Rogers et al. 1990, Wilber 1994, Guillory 2000). Wilber (1994) suggested three possible
4156 explanations for such relationships: (1) increased freshwater will reduce estuarine salinity
4157 and provide more low salinity habitat for juvenile crabs; (2) increased flows may further
4158 broadcast cues that may attract females from offshore, thus increasing the brood stock; and
4159 (3) higher inflows increase nutrient and detrital loading and thus directly or indirectly
4160 enhance food supply.

4161 The long-term and inter-annual patterns that we observed for Lee County landings
4162 agree well with those observed statewide in Florida. In their recent assessment of the blue
4163 crab fishery in Florida, Murphy et al (2007) characterized the fishery as follows:

4164 Commercial landings in Florida have shown a general decreasing trend since the
4165 mid 1980's. Superimposed on this pattern are large oscillations often related to
4166 extended years of drought when blue crab production is apparently low and wet
4167 years when blue crab production is apparently high.

4168 The period of record analyzed here (WY1986–WY2013) exhibited a decreasing long-
4169 term trend with much of the inter-annual variability (45%) explained by rainfall. The lower
4170 the rainfall and inflow during the dry season, the lower the following year's production of
4171 blue crabs. A similar lagged relationship between annual crab landings and the previous
4172 year's inflow from the Apalachicola River was observed by Wilber (1994). Blue crabs in
4173 the Gulf of Mexico reach harvestable size within a year of age (Perry 1984 as cited in
4174 Wilber 1994). The positive correlations between crab landings and river flows lagged by
4175 one year may reflect a positive influence of fresh water on juvenile crabs that reach
4176 harvestable size the following year (Wilber 1994). In this study, current annual landings
4177 were correlated with the previous year's dry season rainfall and inflow. The recruitment of
4178 juvenile blue crabs during the dry season (November–April) in the CRE may explain this
4179 correlation (Stevens et al. 2008).

4180 Two key relationships are required to establish resource protection criteria:
4181 relationships between (1) changes in hydrology and changes in water resource function and
4182 (2) the magnitude of the functional loss and time to recover. In this component we have
4183 established a relationship between CPUE, which is the resource function, and dry season
4184 rainfall during the preceding water year, which represents the hydrology of the system.
4185 Since rainfall and freshwater flow were also related, changes in CPUE can also be related
4186 to a flow variable (e.g. discharge at S-79 and total discharge). We have also related the loss
4187 of water resource function to recovery time. Functional loss is defined as a negative
4188 deviation from the long-term mean CPUE. Recovery is achieved when the CPUE returns
4189 to the long-term mean. We have identified the CPUE that should recover to the long-term
4190 mean with one, two, or three years of average rainfall. Lastly, we have examined return
4191 frequency using spectral analysis and a Monte Carlo analysis.

4192 **Component Study 11: Relationships between Freshwater Inflow,**
4193 **Salinity, and Potential Habitat for Sawfish (*Pristis pectinata*) in**
4194 **the Caloosahatchee River Estuary**

4195 *Christopher Buzzelli, Peter Doering, Yongshan Wan, and Detong Sun*

4196 **Abstract**

4197 The smalltooth sawfish (*Pristis pectinata*) is an endangered species that historically
4198 ranged from Texas to North Carolina. The distribution and abundance of sawfish have
4199 declined due to over-fishing and habitat loss. Presently, the CRE is an important sawfish
4200 nursery. Juvenile sawfish habitat can be characterized as nearshore environments <1 meter
4201 in depth, where salinities range from 12 (S₁₂) to 27 (S₂₇). This study quantified sawfish
4202 habitat with variable inflow to the CRE in the dry season using a combination of
4203 bathymetric analyses and hydrodynamic modeling. Inflows of 150 to 300 cfs positioned
4204 the S₁₂ and S₂₇ in the shallowest part of the estuary (10 to 30 km downstream). Specifically,
4205 the area of sawfish habitat (A_{saw}) was greatest (5.7 km²) when inflow through the Franklin
4206 Lock and Dam (S-79) was 270 cfs in the dry season. Under reduced inflow the habitat
4207 migrated into the channel above Beautiful Island where it was compressed against S-79.
4208 Higher inflows pushed S₂₇ out of the estuary.

4209 **Introduction**

4210 Fluctuations in freshwater inflows over time scales ranging from weeks to years have
4211 altered salinity regimes and impacted the ecological integrity of the CRE (Chamberlain
4212 and Doering 1998a, Barnes 2005). Changes in freshwater inflows and salinity have been
4213 shown to affect the distribution and dynamics of many taxa and communities including
4214 phytoplankton and zooplankton (Tolley et al. 2010, Radabaugh and Peebles 2012), SAV
4215 (Doering et al. 2001, 2002, Lauer et al. 2011), oysters and pathogens (La Peyre et al. 2003,
4216 Barnes et al. 2007, Volety et al. 2009), fauna inhabiting oyster reefs (Tolley et al. 2005,
4217 2006), and fishes (Collins et al. 2008, Heupel and Simpfendorfer 2008, Stevens et al. 2010,
4218 Simpfendorfer et al. 2011, Poulakis et al. 2013).

4219 The balance between downstream transport of fresh water and the upstream
4220 encroachment of salinity creates gradients that influence all biogeochemical and biological
4221 processes and patterns. The gradient can be represented by lines of equal salinity (e.g.
4222 isohalines) whose positions fluctuate up and down the estuary with freshwater inflow(s),
4223 tidal cycles, and meteorological phenomena (e.g. fronts, winds, and storms). Particular
4224 isohalines provide indications of desirable (or undesirable) salinity conditions for sentinel
4225 organisms or communities (Jassby et al. 1995).

4226 The smalltooth sawfish (*Pristis pectinata*) is an endangered species that historically
4227 ranged from Texas to North Carolina in the eastern United States (Simpfendorfer et al.
4228 2011, Norton et al. 2012). The distribution and abundance of sawfish have declined due to
4229 over-fishing and widespread habitat loss. The patterns of decline in the largemouth sawfish
4230 (*P. pristis*) are similar to smalltooth sawfish (Fernandez-Carvalho et al. 2014). Presently,
4231 sawfish populations are limited to habitats in southwest Florida from Charlotte Harbor to
4232 the Dry Tortugas, including the CRE (NOAA 2009).

4233 Little was known about sawfish feeding, reproduction, or habitat usage prior to
4234 designation as an endangered species in 2003 (Norton et al. 2012). More recently the CRE
4235 has been recognized as an essential nursery for neonates and juvenile sawfish
4236 (Simpfendorfer et al. 2011, Carlson et al. 2014). A suite of research studies was conducted
4237 to examine the distribution, location, and activity of juvenile sawfish in southwestern
4238 Florida and improve the existing understanding of the relationships between population
4239 dynamics, environmental conditions, and management actions (Poulakis et al. 2014).

4240 Sawfish, cownose rays (*Rhinoptera bonasus*), and bull sharks (*Carcharhinus leucas*)
4241 are important components of the elasmobranch community in the CRE (Collins et al. 2008,
4242 Ortega et al. 2009, Heupel et al. 2010, Poulakis et al. 2011). Like many estuarine
4243 organisms, salinity is a key driver for these fish populations (Jassby et al. 1995, Collins et
4244 al. 2008, Heupel and Simpfendorfer 2008, Ortega et al. 2009). Migration within the estuary
4245 is modulated through a combination of osmotic regulation and the availability of prey
4246 resources (Poulakis et al. 2013). Individual cownose rays followed their preferred salinity
4247 range further upstream with decreasing freshwater discharge (Collins et al. 2008). A similar
4248 situation exists for bull sharks, which utilize the CRE as a nursery for at least 18 months,
4249 prefer salinities of 7 to 20, and move upstream with reduced inflow (Heupel and
4250 Simpfendorfer 2008).

4251 Smalltooth sawfish generally prefer salinities of 12 to 27 but can survive and grow over
4252 a wider range (Poulakis et al. 2013). The desirable habitat for sawfish has been described
4253 as adjacent to red mangroves where nearshore depths are ≤ 0.9 m (Poulakis et al. 2011,
4254 Norton et al. 2012, Carlson et al. 2014). Sawfish spend their first few years of life in the
4255 CRE. Recent studies have shown that small sawfish (< 1 m) grow very fast over the full
4256 range of salinity conditions. While medium-sized fish (< 1.5 m) respond to changes in
4257 salinity lagged on a 90 day time scale, the largest fish (> 1.5 m) with the widest home range
4258 are more likely to be influenced by prey availability (Poulakis et al. 2013). Additionally,
4259 the average daily activity space (0 to 4 km) is correlated to sawfish body length (60 to 260
4260 centimeters) as larger individuals can tolerate greater variations in salinity
4261 (Carlson et al. 2014).

4262 Similar to cownose rays and bull sharks, increased salinity promotes upstream
4263 migration of juvenile sawfish away from downstream hot spots (Poulakis et al. 2013).
4264 Whereas juvenile sawfish can be found throughout the CRE, there are documented hotspots
4265 for smalltooth sawfish: Iona Cove, Glover Bight, the Cape Coral Causeway, and the US 41
4266 Bridges near Fort Myers (Poulakis et al. 2014). Many sawfish are located in the lower
4267 estuary (Iona Cove and Glover Bight) when salinity is favorable, but migrate further
4268 upstream (US 41 Bridges) as salinity increases. This is potentially problematic for two
4269 reasons. First, the upper CRE from S-79 to Beautiful Island is much deeper and narrower
4270 with greatly reduced nearshore shallow habitat. Second, upstream migration into a
4271 bathymetrically compressed habitat potentially places juvenile sawfish in closer proximity
4272 to larger predators such as bull sharks (Poulakis et al. 2011).

4273 It is possible that environmental factors other than salinity (i.e., temperature, DO,
4274 depth, shoreline attributes, and food availability) influence the distribution of juvenile
4275 sawfish (Poulakis et al. 2014). Although the endangered status of sawfish inhibits
4276 traditional dietary assessments, anecdotal evidence points to pink shrimp, blue crabs, fishes
4277 (clupeids, carangids, mullet, pinfish, mojarras, and kingfish), and stingrays as prey items.
4278 As opposed to stationary organisms such as oysters and benthic macrofauna, identification

4279 of essential habitat based on bathymetric and salinity attributes can be tenuous for mobile
4280 fish populations (Norton et al. 2012). This study recognizes the inherent complexity in
4281 linking freshwater discharge, salinity distributions, and sawfish habitat requirements. Thus,
4282 the objective of this effort was to quantify the extent of the nearshore habitat potentially
4283 available to sawfish under reduced inflow to the CRE.

4284 Based on knowledge of the CRE morphology and inflow-salinity relationships this
4285 study hypothesized that there would be a dry season inflow that would maximize the area
4286 where salinity ranged from 12 to 27 in shallow environments ≤ 1.0 m (**Figure 66A**). While
4287 inflows less than the critical value allows salinity to encroach upstream where there is less
4288 shallow habitat, higher inflows may narrow the available habitat within the CRE (Fig.
4289 **Figure 66B**). This study combined sawfish salinity requirements, bathymetric data for the
4290 CRE, and low inflow salinity distributions predicted using a three-dimensional
4291 hydrodynamic model, CH3D (**Figure 67**).

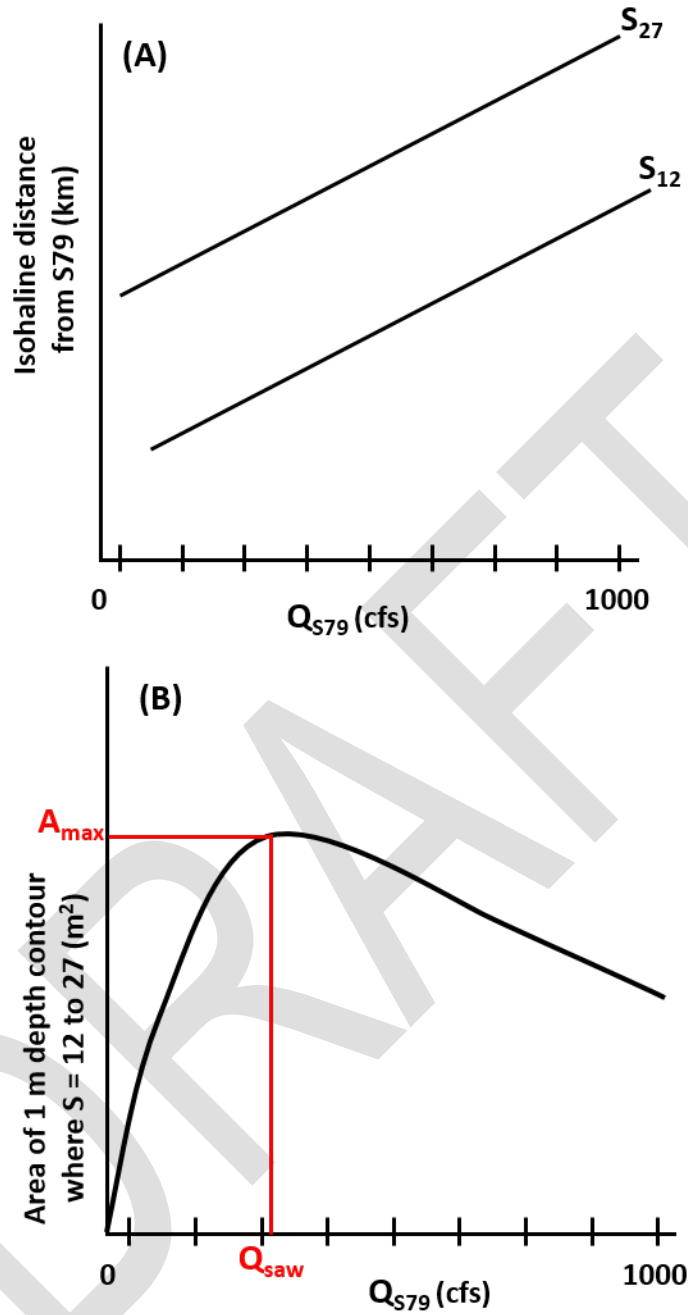
4292 **Methods**

4293 ***Bathymetric Analyses***

4294 Three separate bathymetric data sets were merged to create a digital elevation model
4295 of the CRE (Fig. A11-2). Data collected in the estuary between Beautiful Island and Shell
4296 Point by the USACE (2000) and the United States Geological Survey (2002) were
4297 combined with data collected between S-79 and Beautiful Island by SFWMD (2014).
4298 Aerial photography was digitized to provide a shoreline boundary for the digital elevation
4299 model. The digital elevation model was divided into 42 1-km segments between S-79 and
4300 Shell Point. The area and volume of the 0- to 1-m depth contour was quantified for each of
4301 the 42 segments.

4302 ***Hydrodynamic Modeling***

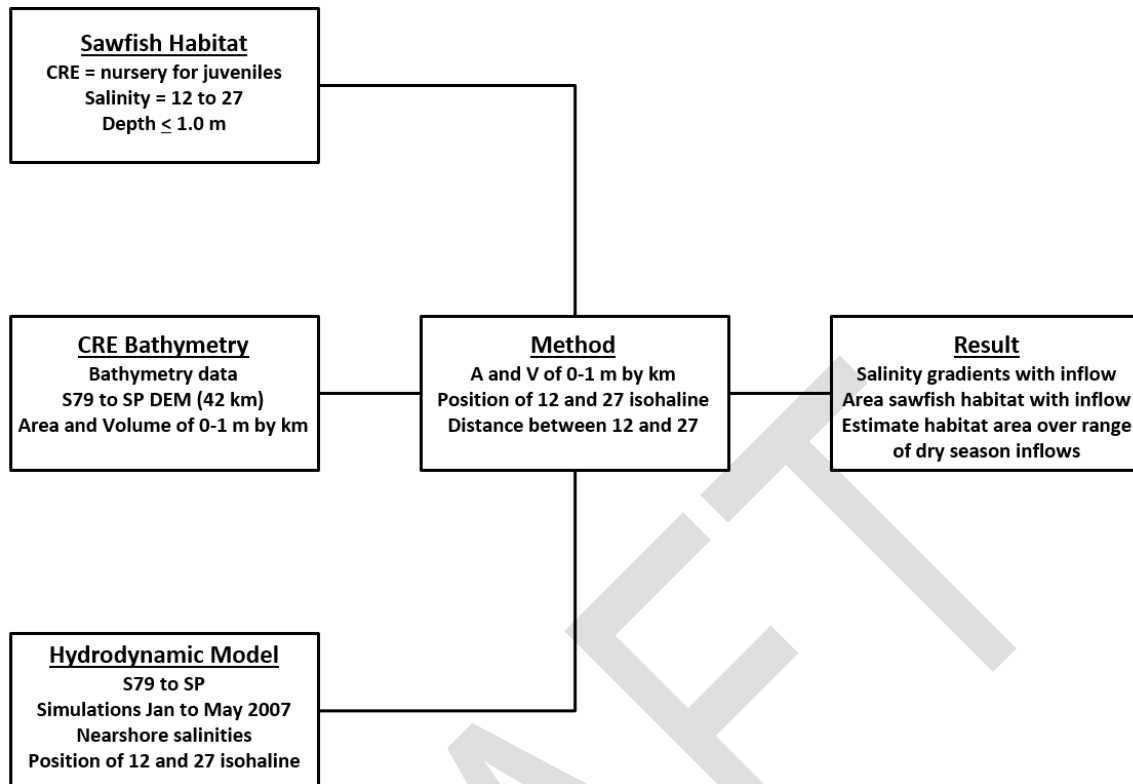
4303 The CH3D model, originally developed by Sheng (1986), is a non-orthogonal
4304 curvilinear grid model capable of simulating complicated hydrodynamic processes
4305 including wind-driven, density-driven, and tidal circulation. The model has a robust
4306 turbulence closure scheme for accurate simulation of stratified flows in estuaries and
4307 coastal waters (Sheng 1986, 1987). The non-orthogonal nature of the model enables it to
4308 represent the complex geometry of a tidal estuary such as the CRE. The model includes a
4309 circulation model to simulate 3-D hydrodynamics and a salinity model to simulate salt
4310 transport. The model is driven by external forcing prescribed at the boundaries including
4311 tidal forcing at the ocean boundary, freshwater inflow from the watershed, and
4312 meteorological forcing including wind and rainfall. The CH3D model has been
4313 successfully developed for many waterbodies including east coast Florida estuaries such
4314 as the Indian River Lagoon, St. Lucie Estuary (Sun 2009, Wan et al. 2012) and Loxahatchee
4315 River Estuary (Sun 2004).



4316
 4317
 4318
 4319
 4320
 4321

Figure 66. (A) Hypothetical relationship between inflow at S-79 (Q_{S79} ; cfs) and the downstream locations of the S_{12} and S_{27} . (B) Hypothetical relationship between inflow at S-79 and the area for sawfish in the CRE.

(Note: A_{max} – maximum area; Q_{saw} – inflow that maximizes habitat area; and S – salinity.)



4322

4323

4324

4325

4326

Figure 67. Schematic of method used to combine sawfish habitat requirements, the bathymetry of the CRE, and the hydrodynamic model (CH3D) to estimate A_{saw} . (Note: A and V – A_{saw} and habitat volume [V_{saw}]; DEM – digital elevation model; and SP – Shell Point.)

4327

4328

4329

4330

4331

4332

4333

4334

4335

4336

4337

4338

4339

The CRE CH3D model was developed from the Charlotte Harbor CH3D model (Sheng 2002). The original Charlotte Harbor model was calibrated using two months of hydrodynamic and salinity data collected during summer 1986 at six stations located in and around Pine Island Sound and the Peace River. SFWMD extended the model to the CRE using 16 months of continuous salinity monitoring data (Qiu 2002, SFWMD 2003). The CRE CH3D model was further calibrated with three years of salinity observations (October 2001–December 2004) at five stations in the estuary for the evaluation of various alternative plans of the Southwest Florida Feasibility Study and the C-43 West Basin Reservoir Project (Sheng and Zhang 2006, Qiu et al. 2006, USACE and SFWMD 2010). An external peer review of the CH3D model was conducted in 2006 for this application (Qiu 2006). The latest calibration of the model was conducted with data collected up to 2010 at seven locations in the estuary to support the development of the Lake Okeechobee Adaptive Protocols (SFWMD 2010, Wan et al. 2013).

4340

4341

4342

4343

4344

4345

The CRE CH3D model domain covers the entire estuarine system, including CRE, Charlotte Harbor, Pine Island Sound, San Carlos Bay, Estero Bay, and the major tributaries, as well as about 30 km offshore in the Gulf of Mexico. In the horizontal dimension, the grid has 166 x 128 elements allowing fine enough resolution to represent the numerous islands, including the islands of the Sanibel Causeway. The higher resolution within the CRE and San Carlos Bay (50 to 100 m) provides a more detailed representation of the

4346 complex shoreline and the navigation channel. Five vertical layers evenly spaced over the
4347 water column enable simulation of density stratification within the estuary.

4348 The hydrodynamic model was applied in a test mode to generate salinity distributions
4349 over a range of S-79 inflows indicative of the dry season. Sawfish habitat was defined as
4350 the area (A_{saw}) (or habitat volume [V_{saw}]) of the estuary where depth was ≤ 1 m and surface
4351 water salinity ranged from 12 to 27 (**Figure 67**). WY2007 was selected as the test case
4352 because it is within the POR for which the model has been calibrated and freshwater inflow
4353 was near the long-term minima. Simulations were from January 1, 2007, to May 31, 2007.
4354 The existing boundary conditions included empirical inputs for water level at the ocean
4355 boundary, rainfall, and wind at the surface, and estimated Tidal Basin runoff. These
4356 boundary conditions were applied over the entire simulation period. While observed S-79
4357 freshwater inflows were applied from January 1, 2007 to February 28, 2007, a constant
4358 inflow was applied for the remaining time for each model simulation. This method was
4359 used because the model dynamics had to be established before the inflows could be
4360 manipulated. A total of seven simulations were performed for constant flow at S-79 of 0,
4361 150, 300, 450, 650, 800, and 1,000 cfs. Based on long-term inflow records from WY1966
4362 to WY2014, May has the lowest average rate of discharge through S-79 (761 ± 569 cfs).
4363 Thus, salinities from May 2007 from each of the simulations were used in sawfish
4364 habitat calculations.

4365 **Data Analyses**

4366 Surface salinities predicted for the nearshore areas using the hydrodynamic model
4367 along the northern and southern shorelines were averaged between S-79 and Shell Point.
4368 The average nearshore surface salinity then was plotted versus distance downstream of
4369 S-79 to visualize the salinity gradient for each of the seven constant inflows. Similarly, the
4370 area and volume of 0- to 1-m depth contour from the bathymetric analysis were plotted
4371 versus distance. The downstream positions of the 12 and 27 isohalines (S_{12} and S_{27}) were
4372 plotted versus the series of constant inflows. A_{saw} was derived by summing the area of
4373 bottom ≤ 1 m between S_{12} and S_{27} (millions of $\text{m}^2 = 10^6 \text{ m}^2 = 1 \text{ km}^2$). V_{saw} (millions of m^3
4374 $= 10^6 \text{ m}^3$) was calculated similarly as the volume of the 0- to 1-m depth contour for each
4375 km of estuary located between S_{12} and S_{27} was summed. A_{saw} and V_{saw} were plotted versus
4376 each of the constant inflows. A polynomial curve was fit to the scatterplot between A_{saw}
4377 and inflow at S-79 (Q_{S79} ; cfs) as a tool to predict the A_{saw} as a function of dry
4378 season inflows.

4379 **Results**

4380 Depth ranges from 0.5 to 6.5 m in the CRE (**Figure 68A**). Approximately 58% of the
4381 CRE is <1.0 -m depth (**Figure 68B**; Buzzelli et al. 2013b). The area of the 0- to 1-m depth
4382 contour within each 1 km segment ranged from 0.01×10^6 to $0.53 \times 10^6 \text{ m}^2$ (**Figure 69**).
4383 These shallow depths were more prevalent from ~ 10 to 20 km downstream of S-79.
4384 Although the values increased with decreasing discharge, salinity was stable and nearly
4385 constant from S-79 and ~ 10 km downstream (**Figure 70**; Buzzelli et al. 2014a). When there
4386 was no inflow, salinity was >20 from 0 to 10 km before increasing to 35 near Shell Point.
4387 Similarly, salinity was >14 in the upper CRE with 150 cfs of inflow. Because salinity was
4388 >12 at S-79 for both of these inflow classes, the potential area of sawfish habitat was
4389 estimated to extend from the water control structure to the downstream location of S_{27} .

4390 Conversely, salinities were <27 throughout the CRE for the 1,000-cfs inflow class. Thus,
4391 A_{saw} could not be estimated for the highest inflow tested since S_{27} was located outside of
4392 the estuary domain.

4393 The distance between the S_{12} and S_{27} ranged from ~ 19 km when inflow was 0 cfs to
4394 26.7 km when inflow was 150 cfs (**Figure 71A**). This finding led to maximum values for
4395 A_{saw} (5.7 km^2) and V_{saw} ($2.8 \times 10^6 \text{ m}^3$; **Figure 71B**). A polynomial curve was fit to the
4396 relationship between A_{saw} and inflow at S-79 to estimate sawfish habitat area over a full
4397 range of inflows indicative of the dry season (**Figure 71C**). A_{saw} was maximized when
4398 inflow was 270 cfs.

4399 Discussion

4400 An estimated 95% of the historical smalltooth sawfish population from Texas to North
4401 Carolina has been lost (Heupel et al. 2007, Norton et al. 2012). Salinity tolerance, food
4402 availability, and protection from predators are among the variables that characterize
4403 sawfish habitat. Although they can have widespread distribution depending upon age,
4404 *Pristis pectinata* can be found across a wide range of salinity values though they generally
4405 prefer 12 to 27 (Poulakis et al. 2013). This study connected knowledge of sawfish habitat
4406 requirements with spatial analyses of the bathymetry and a three-dimensional
4407 hydrodynamic model to estimate changes in sawfish habitat area in the CRE with inflow
4408 in the dry season.

4409 Combined bathymetric and modeling results suggested that the maximum A_{saw}
4410 occurred when the inflow was 270 cfs in May 2007. May 2007 was selected because there
4411 was no freshwater input through S-79 and occurred in one of the driest years on record.
4412 This inflow (270 cfs) would position the 12 to 27 salinity range ~ 10 to 30 km downstream
4413 of S-79 (above Beautiful Island to Cape Coral). Sawfish habitat area between S-79 and
4414 Shell Point would be greatest under these conditions ($\sim 5.5 \text{ km}^2$). Less than 270 cfs could
4415 confine the sawfish habitat to the deeper upper CRE where there is much less shoal area,
4416 and, lead to habitat compression against the structure. Upstream migration into a
4417 bathymetrically compressed habitat potentially places juvenile sawfish in closer proximity
4418 to larger predators such as bull sharks (Poulakis et al. 2011). At the other end, dry season
4419 inflows >800 cfs should push the S_{27} out of the CRE and extend the sawfish habitat into
4420 San Carlos Bay.

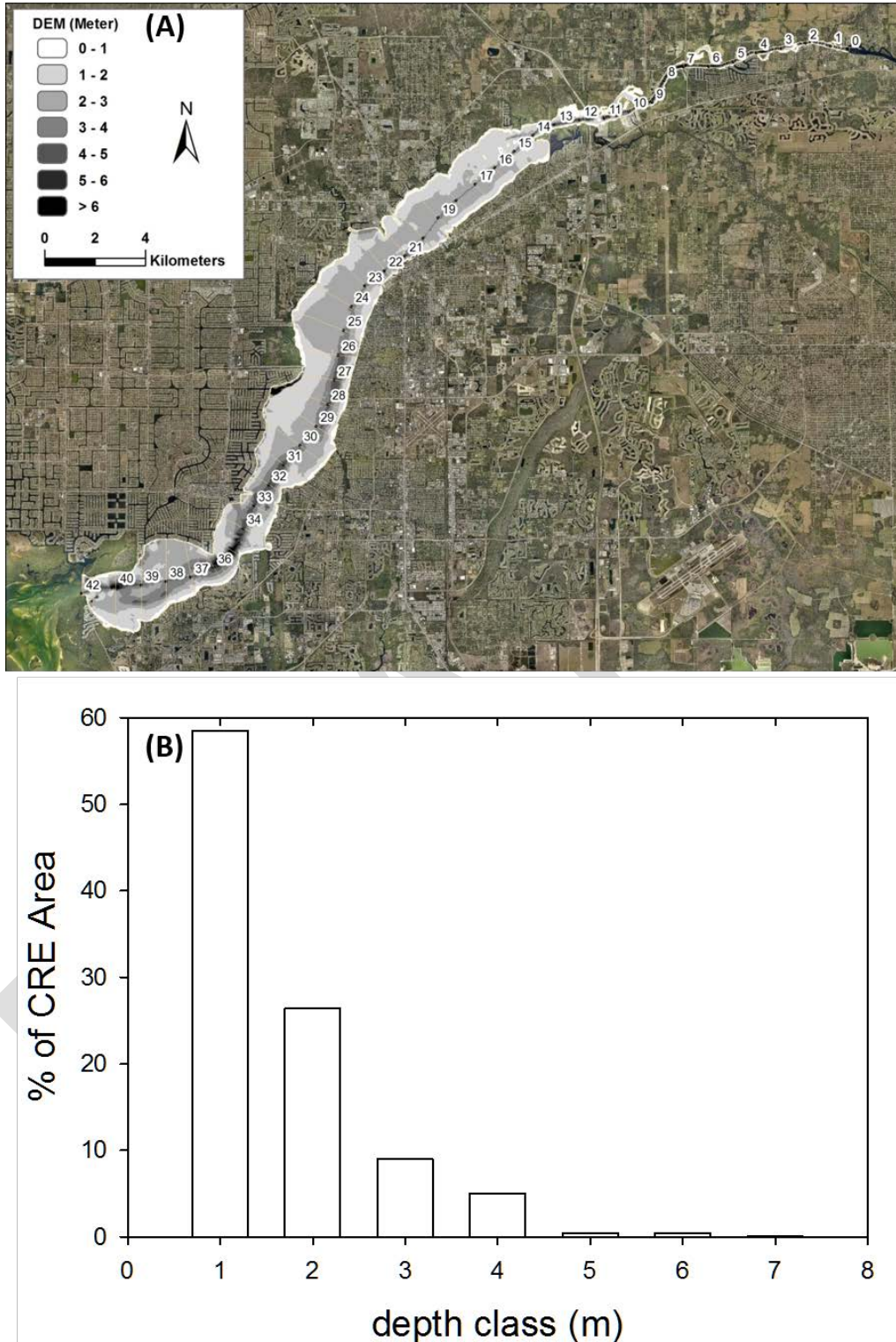


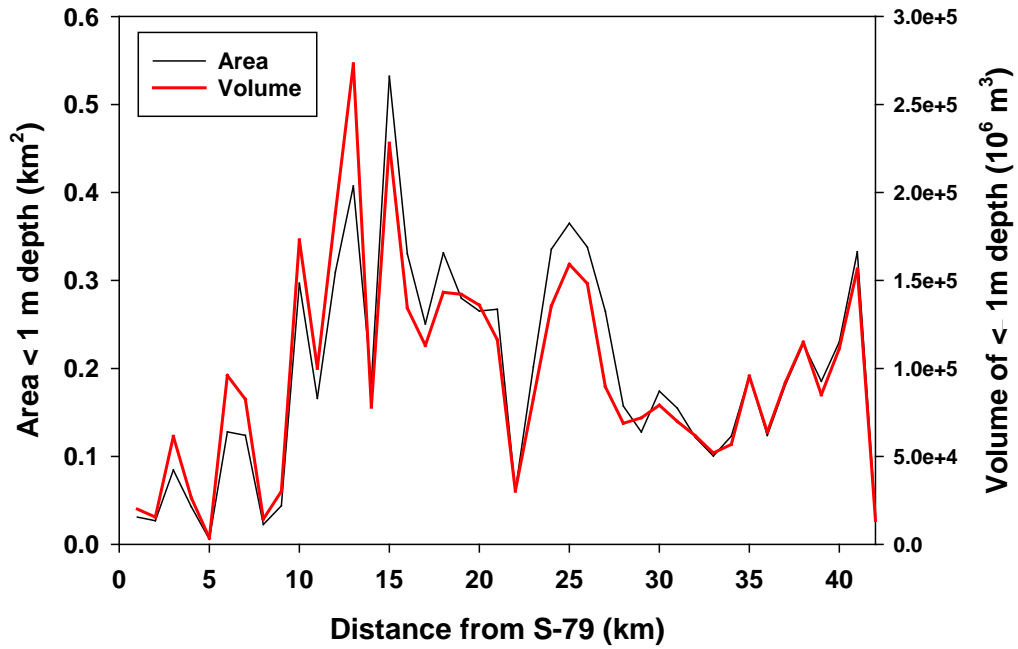
Figure 68. (A) Bathymetric contour map for the CRE. (B) Frequency histogram depicting the bottom area for each of several CRE depth classes.

4421

4422

4423

4424



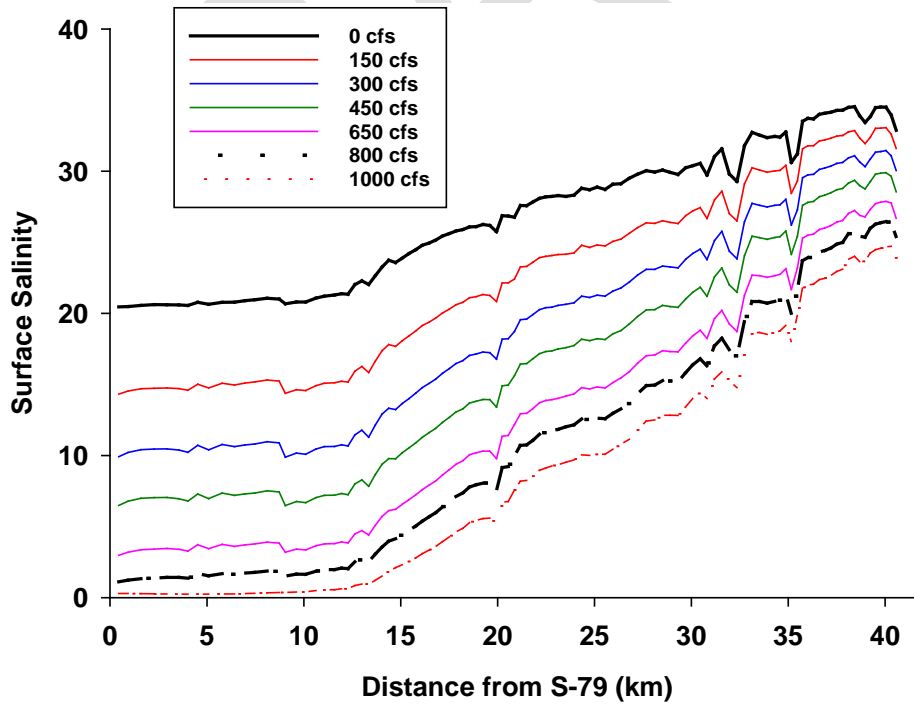
4425

4426

4427

Figure 69. Results of bathymetric analyses depicting the area (km²) and volume (10⁶ m³) of the 0- to 1-m depth contour relative to distance downstream of S-79.

4428

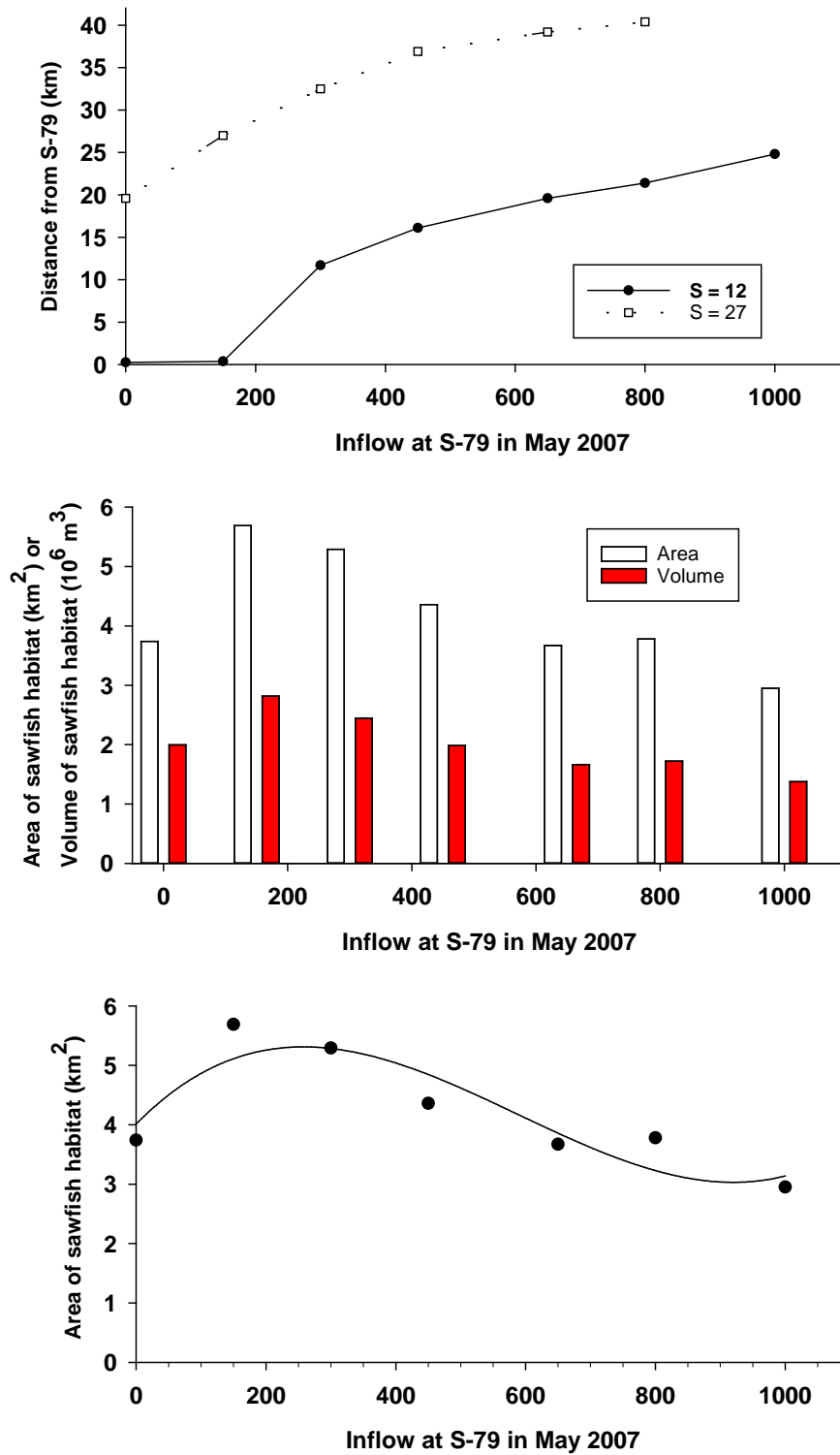


4429

4430

4431

Figure 70. The gradient in average salinities in nearshore environments predicted over a range of inflows (0, 150, 300, 450, 650, 800, and 1,000 cfs) from May 2007.



4432
 4433
 4434
 4435

Figure 71. (A) The position of the S₁₂ and S₂₇ salinity isohalines as a function of dry season inflow. (B) The A_{saw} and V_{saw} as a function of dry season inflow. (C) Scatterplot and polynomial curve fit between inflow at S-79 and the A_{saw}.

REFERENCES

4436

4437 Able, K.W. 2005. A re-examination of fish estuarine dependence: Evidence for
4438 connectivity between estuarine and ocean habitats. *Estuarine, Coastal, and Shelf*
4439 *Science* 64:5-17.

4440 Adams, J.B., G.C. Bate, T.D. Harrison, P. Huizinga, S. Taljaard, L. van Niekerk, E.E.
4441 Plumstead, A.K. Whitfield and T.H. Wooldridge. 2002. A method to assess the
4442 freshwater inflow requirements of estuaries and application to the Mtata Estuary, South
4443 Africa. *Estuaries* 25(6B):1382-1393.

4444 Ahn, H. and R.T. James. 2001. Variability, uncertainty, and sensitivity of phosphorus
4445 deposition load estimates in South Florida. *Water, Air, and Soil Pollution* 126:37-51.

4446 Alber, M. 2002. A conceptual model of estuarine freshwater inflow management. *Estuaries*
4447 25:1246-1261.

4448 Aleem, A.A. 1972. Effect of river outflow management on marine life. *Marine Biology*
4449 15:200-208.

4450 Andrews, J.D., D. Haven and D.B. Quayle. 1959. Freshwater kill of oysters (*Crassostrea*
4451 *virginica*) in James River, Virginia, 1958. *Proceedings of the National Shellfish*
4452 *Association* 49:29-49.

4453 Anon. 1958. The Venice system for the classification of marine waters according to
4454 salinity. *Limnology and Oceanography* 3:346-347.

4455 Antonini, G.A., D.A. Fann and P. Roat. 2002. A Historical Geography of Southwest
4456 Florida Waterways. *Volume Two: Placida Harbor to Marco Island*, National Seagrant
4457 College Program. Silver Spring, MD.

4458 Austin, J.A. 2004. Estimating effective longitudinal dispersion in the Chesapeake Bay.
4459 *Estuarine, Coastal, and Shelf Science* 60:359-368.

4460 Azevedo, I.C., A.A. Bordalo and P. Duarte. 2014. Influence of freshwater inflow variability
4461 on the Douro estuary primary productivity: A modeling study. *Ecological Modelling*
4462 272:1-15.

4463 Baisre, J.A. and Z. Arboleya. 2006. Going against the flow: Effects of river damming in
4464 Cuban fisheries. *Fisheries Research* 81:283-292.

4465 Baldwin, L. and M.J. Hunt. 2014. Daily Water Temperature Time Series for the Upper
4466 Caloosahatchee Estuary. Publication WR-2014-003, South Florida Water Management
4467 District, West Palm Beach, FL.

4468 Barnes, T.K. 2005. Caloosahatchee Estuary Conceptual Ecological Model. *Wetlands*
4469 25(4):884-897.

4470 Barnes, T.K., A.K. Volety, K. Chartier, F.J. Mazzotti and L. Pearlstine. 2007. A habitat
4471 suitability index model for the eastern oyster (*Crassostrea virginica*), a tool for
4472 restoration of the Caloosahatchee Estuary, Florida. *Journal of Shellfish Research*
4473 26(4):949-959.

4474 Barras, J., S. Beville, D. Britsch, S. Hartley, S. Hawes, J. Johnston, P. Kemp, Q. Kinler,
4475 A. Martucci, J. Porthouse, D. Reed, K. Roy, S. Sapktoa and J. Suhayda. 2004.

- 4476 Historical and Projected Coastal Louisiana Land Changes: 1978–2050. Open File
4477 Report 03-334, United States Geologic Survey, Washington, DC.
- 4478 Bartleson, R.D., M.J. Hunt and P.H. Doering. 2014. Effects of temperature on growth of
4479 *Vallisneria americana* in a sub-tropical estuarine environment. *Wetlands Ecology and*
4480 *Management* DOI 10.1007/s1 1273-014-9354-6.
- 4481 Bataller, E.E., A.D. Boghen and M.D.B. Burt. 1999. Comparative growth of the eastern
4482 oyster *Crassostrea virginica* (Gmelin) reared at low and high salinities in New
4483 Brunswick, Canada. *Journal of Shellfish Research* 18:107-114.
- 4484 Beck, M.W., R.D. Brumbaugh, L. Airoidi, A. Carranza, L.D. Coen, C. Crawford, O. Defeo,
4485 G. J. Edgar, B. Hancock, M.C. Kay, H.S. Lenihan, M.W. Luckenback, C.L. Toropova,
4486 G. Zhang and X. Guo. 2011. Oyster reefs at risk and recommendations for
4487 conservation, restoration, and management. *Bioscience* 61:107-116.
- 4488 Beckage, B., L. Joseph, P. Belisle, D.B. Wolfson and W.J. Platt. 2007. Bayesian change-
4489 point analyses in ecology. *New Phytologist* 174:456-467.
- 4490 Black, W.M. 1887. Condition of Caloosahatchee Basin. Letter to Chief of Engineers. File
4491 Copy 1155(2). Federal Records Center, Southeast Region, United States Army,
4492 Washington, DC. Pages 126–129 and 214–217.
- 4493 Blanch, S.J., G.G. Ganf and K.F. Walker. 1998. Growth and recruitment in *Vallisneria*
4494 *americana* as related to average irradiance in the water column. *Aquatic Botany*
4495 61:181-205.
- 4496 Bortone, S.A. and R.K. Turpin. 2000. Tapegrass life history metrics associated with
4497 environmental variables in a controlled estuary. Pages 65-79 in: Bortone S.A. (ed),
4498 *Seagrass Monitoring, Ecology, Physiology, and Management*, CRC Press, Boca Raton,
4499 FL.
- 4500 Bourn, W.S. 1932. Ecological and physiological studies on certain aquatic angiosperms.
4501 *Contributions from Boyce Thompson Institute* 4:425-496.
- 4502 Bourn, W.S. 1943. Seawater tolerance of *Vallisneria spiralis* L. and *Potamogeton foliosus*
4503 Raf. *Contributions from Boyce Thompson Institute* 6:303-308.
- 4504 Boustany, R.G., T.C. Michot and R.F. Moss. 2010. Effects of salinity and light on biomass
4505 and growth of *Vallisneria americana* from lower St. Johns River, FL, USA. *Wetlands*
4506 *Ecology and Management* 18:203-217.
- 4507 Bowers, D.G. and H.L. Brett. 2008. The relationship between CDOM and salinity in
4508 estuaries: An analytical and graphical solution. *Journal of Marine Systems* 73:1-7.
- 4509 Breitburg, D. 2002. Effects of hypoxia, and the balance between hypoxia and enrichment,
4510 on coastal fishes and fisheries. *Estuaries* 25(4B):767-781.
- 4511 Browder, J. 1985. Relationship between pink shrimp production in the Tortugas and water
4512 flow patterns in the Florida Everglades. *Bulletin of Marine Science* 37: 839-856.
- 4513 Brown, J.R. and E.B. Hartwick. 1988. Influences of temperature, salinity and available
4514 food upon suspended culture of the Pacific oyster, *Crassostrea gigas*. 1. Absolute and
4515 allometric growth. *Aquaculture* 70:231-251.

- 4516 Butler, J.P. 1954. The southern oyster drill. Proceedings of the National Shellfisheries
4517 Association. 44:67-75.
- 4518 Bulger, A.J., B.P. Hayden, M.E. Monaco, D.M. Nelson and M.G. McCormick-Ray. 1993.
4519 Biologically-based estuarine salinity zones derived from a multivariate analysis.
4520 *Estuaries* 16:311-322.
- 4521 Burnett, W.C., P.K. Aggarwal, A. Aureli, H. Bokuniewicz, J.E. Cable, M.A. Charette,
4522 E. Kontar, S. Krupa, K.M. Kulkarni, A. Loveless, W.S. Moore, J.A. Oberdorfer,
4523 J. Oliveira, N. Ozyurt, P. Povinec, A.M.G. Privitera, R. Rajar, R.T. Ramessur,
4524 J.Scholten, T. Stieglitz, M. Taniguchi and J.V. Turner. 2006. Quantifying submarine
4525 groundwater discharge in a coastal zone via multiple methods. *Science of the Total*
4526 *Environment* 367:498-543.
- 4527 Buzan, D., W. Lee, J. Culbertson, N. Kuhn and L. Robinson. 2009. Positive relationship
4528 between freshwater inflow and oyster abundance in Galveston Bay, Texas. *Estuaries*
4529 *& Coasts* 32:206-212.
- 4530 Buzzelli, C., R.L. Wetzel and M.B. Meyers. 1999. A linked physical and biological
4531 framework to assess biogeochemical dynamics in a shallow estuarine ecosystem.
4532 *Estuarine, Coastal, and Shelf Science* 49:829-851.
- 4533 Buzzelli, C. 2011. Ecosystem modeling in small sub-tropical estuaries and embayments.
4534 Pages 331–353, Volume 9, in: Wolanski, E. and D.S. McLusky (eds), *Treatise on*
4535 *Estuarine and Coastal Science*, Academic Press, Waltham, MA.
- 4536 Buzzelli, C., R. Robbins, P. Doering, Z. Chen, D. Sun, Y. Wan, B. Welch and
4537 A. Schwarzhild. 2012. Monitoring and modeling of *Syringodium filiforme* (manatee
4538 grass) in the southern Indian River Lagoon. *Estuaries and Coasts* 35:1401-1415.
- 4539 Buzzelli, C., P. Doering, Y. Wan, P. Gorman and A. Volety. 2013a. Simulation of potential
4540 oyster density with variable freshwater inflow (1965–2000) to the Caloosahatchee
4541 River Estuary, Southwest Florida, USA. *Environmental Management* 52(4):981-994.
- 4542 Buzzelli, C., Z. Chen, T. Coley, P. Doering, R. Samimy, D. Schlezinger and B. Howes.
4543 2013b. Dry season sediment-water exchanges of nutrients and oxygen in two Florida
4544 estuaries: Patterns, comparisons, and internal loading. *Florida Scientist* 76(1):54-79.
- 4545 Buzzelli, C., Y. Wan, P. Doering and J.N. Boyer. 2013c. Seasonal dissolved inorganic
4546 nitrogen and phosphorus budgets for two sub-tropical estuaries in South Florida, USA.
4547 *Biogeosciences* 10:6721-6736.
- 4548 Buzzelli, C, M. Parker, S. Geiger, Y. Wan, P. Doering and D. Haurert. 2013d. Predicting
4549 system-scale impacts of oyster clearance on phytoplankton productivity in a small sub-
4550 tropical estuary. *Environmental Modeling & Assessment* 18(2):185-198.
- 4551 Buzzelli, C., B. Boutin, M. Ashton, B. Welch, P. Gorman, Y. Wan and P. Doering. 2014a.
4552 Fine-scale detection of estuarine water quality with managed freshwater releases.
4553 *Estuaries and Coasts* 37:1134-1144.
- 4554 Buzzelli, C., P. Doering, Y. Wan, D. Sun and D. Fugate. 2014b. Modeling ecosystem
4555 processes with variable freshwater inflow to the Caloosahatchee River Estuary,
4556 Southwest Florida. I. Model development. *Estuarine, Coastal, and Shelf Science*
4557 151:256-271.

- 4558 Buzzelli, C., P. Doering, Y. Wan, D. Sun and D. Fugate. 2014c. Modeling ecosystem
4559 processes with variable freshwater inflow to the Caloosahatchee River Estuary,
4560 Southwest Florida. II. Nutrient loading, submarine light, and seagrass. *Estuarine,
4561 Coastal, and Shelf Science* 151:272-284.
- 4562 Buzzelli, C., P. Gorman, P.H. Doering, Z. Chen and Y. Wan. 2015. The application of
4563 oyster and seagrass models to evaluate alternative inflow scenarios related to
4564 Everglades restoration. *Ecological Modelling* 297:154-170.
- 4565 Carlson, J.K., S.J.B. Gulak, C.A. Simpfendorfer, R.D. Grubbs, J.G. Romine and G.H.
4566 Burgess. 2014. Movement patterns and habitat use of smalltooth sawfish, *Pristis
4567 pectinata*, determined using pop-up satellite archival tags. *Aquatic Conservation:
4568 Marine and Freshwater Ecosystems* 24:104-117.
- 4569 Chamberlain, R.H. and P.H. Doering. 1998a. Freshwater inflow to the Caloosahatchee
4570 Estuary and the resource-based method for evaluation. In: S.F. Treat (ed.), *Proceedings
4571 of the Charlotte Harbor Public Conference and Technical Symposium*, South Florida
4572 Water Management District, Punta Gorda, Florida.
- 4573 Chamberlain, R.H. and P.H. Doering. 1998b. Preliminary estimate of optimum freshwater
4574 inflow to the Caloosahatchee Estuary: A resource based approach. In: S.F. Treat (ed.),
4575 *Proceedings of the Charlotte Harbor Public Conference and Technical Symposium*.
4576 South Florida Water Management District, Punta Gorda, Florida.
- 4577 Chamberlain, R.H., P.H. Doering, K.M. Haunert and D. Crean. 2003. Appendix C: Impacts
4578 of Freshwater Inflows on the Distribution of Zooplankton and Ichthyoplankton in the
4579 Caloosahatchee Estuary, Florida. *Technical Documentation to Support Development of
4580 Minimum Flows and Levels for the Caloosahatchee River and Estuary*, South Florida
4581 Water Management District, West Palm Beach, FL.
- 4582 Chatfield, C. 1989. *The Analysis of Time Series: An Introduction, Fourth Edition*. Chapman
4583 and Hall, New York, NY.
- 4584 Chen, Z., P.H. Doering, M. Ashton and B.A. Orlando. 2015. Mixing behavior of colored
4585 dissolved organic matter and its potential ecological implication in the Caloosahatchee
4586 River Estuary, Florida. *Estuaries and Coasts* DOI 10.1007/s/12237-014-9916-0.
- 4587 Childers, D.L., J.N. Boyer, S.E. Davis, C.J. Madden, D.T. Rudnick and F. Sklar. 2006.
4588 Relating precipitation and water management to nutrient concentrations in the
4589 oligotrophic "upside-down" estuaries of the Florida Everglades. *Limnology and
4590 Oceanography* 51:602-616.
- 4591 Childress, M.J. 2010. Modeling the impact of drought on South Carolina blue crabs using
4592 a spatially explicit individual-based population model. *Proceedings of the 2010 South
4593 Carolina Water Resources Conference*, Institute of Computational Ecology, Clemson
4594 University, Clemson, SC.
- 4595 Christian, D. and Y.P. Sheng. 2003. Relative influence of various water quality parameters
4596 on light attenuation in Indian River Lagoon. *Estuarine, Coastal, and Shelf Science*
4597 57:961-971.
- 4598 Clark, A.E. 1935. Effects of temperature and salinity on early development of the oyster.
4599 16:10, *Progress Report of the Atlantic Biological Station*, St. Andrews, New
4600 Brunswick.

- 4601 Clarke K.R. 1993. Non-parametric multivariate analyses of changes in community
4602 structure. *Australian Journal of Ecology* 18:117-143.
- 4603 Clarke, K.R. and M. Ainsworth. 1993. A method of linking multivariate community
4604 structure to environmental variables. *Marine Ecology Progress Series* 92:205-219.
- 4605 Clarke, K.R. and R.N. Gorley. 2006. *PRIMER v6: User Manual/Tutorial*. PRIMER-E,
4606 Plymouth, United Kingdom.
- 4607 Clarke, K.R. and R.M Warwick. 2001. *Change in Marine Communities: An Approach to*
4608 *Statistical Analysis and Interpretation, 2nd Edition*. PRIMER-E, Plymouth, United
4609 Kingdom.
- 4610 Cloern, J.E. and A.D. Jassby. 2009. Patterns and scales of phytoplankton variability in
4611 estuarine-coastal ecosystems. *Estuaries and Coasts* 33:230-241.
- 4612 Cloern, J.E. and A.D. Jassby. 2012. Drivers of change in estuarine-coastal ecosystems:
4613 Discoveries from four decades of study in San Francisco Bay. *Review of Geophysics*
4614 50(RG4001):1-33.
- 4615 Cloern, J.E., S.Q. Foster and A.E. Kleckner. 2014. Phytoplankton primary production in
4616 the world's estuarine-coastal ecosystems. *Biogeosciences* 11:2477-2501.
- 4617 Coen, L.D., R.D. Brumbaugh, D. Bushek, R.E. Grizzle, M.W. Luckenbach, M. H. Posey,
4618 S.P. Powers and S.G. Tolley. 2007. Ecosystem services related to oyster restoration.
4619 *Marine Ecology Progress Series* 341:303-307.
- 4620 Collins A.B., M.R. Heupel and C.A. Simpfendorfer. 2008. Spatial distribution and long-
4621 term movement patterns of cownose rays *Rhinoptera bonasus* within an estuarine river.
4622 *Estuaries and Coasts* 31:1174–1183.
- 4623 Committee on Environment and Natural Resources. 2010. *Scientific Assessment of*
4624 *Hypoxia in U.S. Coastal Waters*. Interagency Working Group on Harmful Algal
4625 Blooms, Hypoxia, and Human Health of the Joint Subcommittee on Ocean Science and
4626 Technology, Washington, DC.
- 4627 Condie, S.A., D. Hayes, E.A. Fulton and M. Savina. 2012. Modelling ecological change
4628 over a half a century in a subtropical estuary: Impacts of climate change, land-use,
4629 urbanization, and freshwater extraction. *Marine Ecology Progress Series* 457:43-66.
- 4630 Copeland, B.J. 1966. Effects of decreased river flow on estuarine ecology. *Journal of the*
4631 *Water Pollution Control Federation* 38:1831-1839.
- 4632 Copp, G.H. 1992. Comparative microhabitat use of cyprinid larvae and juveniles in a lotic
4633 floodplain channel. *Environmental Biology of Fishes* 33:181-193.
- 4634 Costanza, R and M. Ruth. 1998. Using dynamic modeling to scope environmental
4635 problems and build consensus. *Environmental Management* 22(2):183-195.
- 4636 Cowardin, L.M., V. Carter, F.C. Golet and E.T. LaRoe. 1979. Classification of Wetlands
4637 and Deepwater Habitats of the United States. Fish and Wildlife Service, United States
4638 Department of the Interior, Jamestown, ND. December 4, 1998.
- 4639 Crowder, L.B. 1986. Ecological and morphological shifts in Lake Michigan fishes:
4640 Glimpses of the ghost of competition past. *Environmental Biology of Fishes*
4641 16:147-157.

- 4642 Dale, V.H. and S.C. Beyeler. 2001. Challenges in the development and use of ecological
4643 indicators. *Ecological Indicators* 1:3-10.
- 4644 Davis, H.C. 1958. Survival and growth of clam and oyster larvae at different salinities.
4645 *Biological Bulletin* 114:296-307
- 4646 Dawes, C.J. and J.M. Lawrence. 1989. Allocation of energy resources in the freshwater
4647 angiosperms *Vallisneria americana* Michx. and *Potamogeton pectinatus* L. in Florida.
4648 *Florida Scientist* 52:59-63.
- 4649 Day, J. W., C.A.S. Hall, W.M. Kemp and A. Yanez-Arancibia. 1989. Estuarine Ecology.
4650 John Wiley & Sons, Inc., New York, NY.
- 4651 Day, J.W., J. Barras, E. Clarain, J. Johnston, D. Justic, G.P. Kemp, J.-Y. Ko, R. Lane,
4652 W.J. Mitsch, G. Steyer, P. Templet and A. Yanez-Arancibia. 2005. Implications of
4653 global climate change and energy cost and availability for the restoration of the
4654 Mississippi delta. *Ecological Engineering* 24:253-265.
- 4655 Deegan, L., H. Kennedy and C. Neil. 1984. Natural factors and human modifications
4656 contributing to marsh loss in Louisiana's Mississippi River deltaic plain.
4657 *Environmental Management* 3:133-144.
- 4658 Deksheniaks, M.M., E.E. Hofmann and E.N. Powell. 1993. Environmental effects on the
4659 growth and development of eastern oyster, *Crassostrea virginica* (Gmelin, 1791),
4660 larvae: a modeling study. *Journal of Shellfish Research* 12:241-254.
- 4661 Deksheniaks, M.M., E.E. Hofmann, J.M. Klinck and E.N. Powell. 1996. Modeling the
4662 vertical distribution of oyster larvae in response to environmental conditions. *Marine*
4663 *Ecology Progress Series* 136:97-110.
- 4664 Deksheniaks, M.M., E.E. Hofmann, J.M. Klinck and E.N. Powell. 2000. Quantifying the
4665 effects of environmental change on an oyster population: A modeling study. *Estuaries*
4666 23:593-610.
- 4667 Diaz, R.J. and R. Rosenberg. 2008. Spreading dead zones and consequences for marine
4668 ecosystems. *Science* 321:926-929.
- 4669 Dobberfuhl, D.R. 2007. Light limiting thresholds for submerged aquatic vegetation in a
4670 blackwater river. *Aquatic Botany* 86:346-352.
- 4671 Doering, P.H., R.H. Chamberlain, K.M. Donohue and A.D. Steinman. 1999. Effect of
4672 salinity on the growth of *Vallisneria americana* Michx. from the Caloosahatchee
4673 Estuary, Florida. *Florida Scientist* 62(2):89-105.
- 4674 Doering, P.H., R.H. Chamberlain and J.M. McMunigal. 2001. Effects of simulated
4675 saltwater intrusions on the growth and survival of wild celery, *Vallisneria americana*,
4676 from the Caloosahatchee Estuary (South Florida). *Estuaries* 24(6A):894-903.
- 4677 Doering, P.H., R.H. Chamberlain, and D. Haurert. 2002. Using submersed aquatic
4678 vegetation to establish minimum and maximum freshwater inflows to the
4679 Caloosahatchee Estuary, Florida. *Estuaries* 25:1343-1354.
- 4680 Doering, P. H., R.H. Chamberlain and K. M. Haurert. 2006. Chlorophyll *a* and its use as
4681 an indicator of eutrophication in the Caloosahatchee Estuary, Florida. *Florida Scientist*
4682 69:51-72.

- 4683 Dolbeth, M., F. Martinho, I. Viegas, H. Cabral and M.A. Pardal. 2008. Estuarine
4684 production of resident and nursery fish species: Conditioning by drought events?
4685 *Estuarine and Coastal Shelf Science* 78:51-60.
- 4686 Drinkwater, K.F. and K.T. Frank. 1994. Effects of river regulation and diversion on marine
4687 fish and invertebrates. *Aquatic Conservation: Freshwater and Marine Ecosystems*
4688 4:135-151.
- 4689 Dyer, K.R. and R.J. Orth (eds.). 1994. *Changes in Fluxes in Estuaries*. Olsen & Olsen,
4690 Fredensborg, Denmark.
- 4691 Eby, L.A. and L.B. Crowder. 2002. Hypoxia-based habitat compression in the Neuse River
4692 Estuary: Context-dependent shifts in behavioral avoidance thresholds. *Canadian*
4693 *Journal of Fisheries and Aquatic Sciences* 59:952-963.
- 4694 Erdman, C. and J. Emerson. 2007. An R package for performing a Bayesian analysis of
4695 change point problems. *Journal of Statistical Software* (23):1-13.
- 4696 FDEP. 2009. *Final TMDL Report – Nutrient TMDL for the Caloosahatchee Estuary*
4697 *(WBIDs 3240A, 3240B, and 3240C)*. Florida Department of Environmental Protection,
4698 Tallahassee, FL. September 2009. Available online at
4699 http://www.dep.state.fl.us/water/tmdl/final_tmdl.htm.
- 4700 Fernandez-Carvalho, J., J.L. Imhoff, V.F. Faria, J.K. Carlson and G.H. Burgess. 2014.
4701 Status and the potential for extinction of the largemouth sawfish *Pristis pristis* in the
4702 Atlantic Ocean. *Aquatic Conservation: Marine and Freshwater Ecosystems*
4703 24:478-497.
- 4704 Fisher W.S., J.T. Winstead, L.M. Oliver, H.L. Edminston and G.O. Bailey. 1996.
4705 Physiological variability of eastern oysters from Apalachicola Bay, Florida. *Journal of*
4706 *Shellfish Research* 15:543-555.
- 4707 Flaig, E.G. and J. Capece. 1998. Water use and runoff in the Caloosahatchee Watershed.
4708 pp 73–80 in: Proceedings of the Charlotte Harbor Public Conference and Technical
4709 Symposium, March 15–16, 1997, Punta Gorda, FL. Technical Report No. 98-02,
4710 Charlotte Harbor National Estuary Program, Punta Gorda, FL.
- 4711 Flannery, M.S., E.B. Peebles and R.T. Montgomery. 2002. A percent-of-flow approach for
4712 managing reductions of freshwater inflows from unimpounded rivers to southwest
4713 Florida estuaries. *Estuaries* 25:1318-1332.
- 4714 Frazier, T.K., S.K. Notestein, C.A. Jacoby, C.J. Littles, S.R. Keller and R.A. Swett. 2006.
4715 Effects of storm-induced salinity changes on submersed aquatic vegetation in Kings
4716 Bay, Florida. *Estuaries and Coasts* 29(6A):943-953.
- 4717 French, GT and K.A. Moore. 2003. Interactive effects of light and salinity stress on the
4718 growth, reproduction, and photosynthetic capabilities of *Vallisneria americana* (wild
4719 celery). *Estuaries* 26(5):1255-1268.
- 4720 Funahashi, T., A. Kasai, M. Ueno and Y. Yamashita. 2013. Effects of short time variation
4721 in the river discharge on the salt wedge intrusion in the Yura Estuary, a micro-tidal
4722 estuary, Japan. *Journal of Water Resource and Protection* 5:343-348.
- 4723 FWRI. 2003. Florida Fish and Wildlife Conservation Commission Marine Fisheries
4724 Information System 2002-2003 License/Permit Summary, Florida Fish and Wildlife

- 4725 Research Institute, Florida Fish and Wildlife Conservation Commission,
4726 Tallahassee, FL.
- 4727 Gallegos, C.L. 2001. Calculating optical water quality targets to restore and protect
4728 submersed aquatic vegetation: Overcoming problems in partitioning the diffuse
4729 attenuation coefficient for photosynthetically active radiation. *Estuaries* 24:381-397.
- 4730 Galtsoff, P. 1964. The American oyster, *Crassostrea virginica* Gmelin. *United States Fish*
4731 *and Wildlife Service Fishery Bulletin* 64:1-480.
- 4732 Georgiou, I.Y. 1999. Three-Dimensional Hydrodynamic Modeling of Saltwater Intrusion
4733 and Circulation in Lake Pontchartrain. Dissertation, Department of Civil and
4734 Environmental Engineering, University of New Orleans, New Orleans, LA.
- 4735 Geyer, W.R., R. Chant and R. Houghton. 2008. Tidal and spring-neap variations in
4736 horizontal dispersion in a partially mixed estuary. *Journal of Geophysical Research*
4737 113:1-16.
- 4738 Gillanders, B.M and M.J. Kingsford. 2002. Impact of changes in flow of freshwater on
4739 estuarine and open coastal habitats and the associated organisms. *Oceanography and*
4740 *Marine Biology: An Annual Review* 40:233-309.
- 4741 Gillson, J. 2011. Freshwater flow and fisheries production in estuarine and coastal systems:
4742 Where a drop of rain is not lost. *Reviews in Fisheries Science* 19(3):168-186.
- 4743 Gonzalez-Ortegon, E. and P. Drake. 2012. Effects of freshwater inputs on the lower trophic
4744 levels of a temperate estuary: Physical, physiological, or trophic forcing? *Aquatic*
4745 *Sciences* 74:455-469.
- 4746 Guillian, M. and L. Aguirre-Macedo. 2009. Seasonal variation of physiological parameters
4747 in the eastern oyster *Crassostrea virginica* from a tropical region of the Gulf of Mexico.
4748 *Journal of Shellfish Research* 28(3):439-446.
- 4749 Guillory, V. 2000. Relationship of blue crab abundance to river discharge and salinity.
4750 Pages 213–220 in: *Proceedings Annual Conference Southeastern Association of Fish*
4751 *and Wildlife Agencies*.
- 4752 Gunter, G. and G.E. Hall. 1962. Biological Investigation of the Caloosahatchee Estuary in
4753 Connection with Lake Okeechobee Discharges through the Caloosahatchee River.
4754 Consultant Report to the United States Army Corps of Engineers, Jacksonville, FL.
4755 Serial Number 25.
- 4756 Haller, W.T., D.L. Sutton and W.C. Barlowe. 1974. Effects of salinity on growth of several
4757 aquatic macrophytes. *Ecology* 55:891-894.
- 4758 Halpern, B.S., H.M. Regan, H.P. Possingham and M.A. McCarthy. 2006. Accounting for
4759 uncertainty in marine reserve design. *Ecology Letters* 9:2-11.
- 4760 Hauxwell, J., T.K. Frazer and C.W. Osenberg. 2004. Grazing by manatees excludes both
4761 new and established wild celery transplants: Implications for restoration in Kings Bay,
4762 FL, USA. *Journal of Aquatic Plant Management* 42:49-53.
- 4763 Hauxwell, J, T.K. Frazer and C.W. Osenberg. 2007. An annual cycle of biomass and
4764 productivity of *Vallisneria americana* in a subtropical spring fed estuary. *Aquatic*
4765 *Botany* 87:61-68.

- 4766 Heupel, M.R., B.G. Yeiser, A.B. Collins, L. Ortega and C.A. Simpfendorfer. 2010. Long-
4767 term presence and movement patterns of juvenile bull sharks, *Carcharhinus leuca*, in
4768 an estuarine river system. *Marine and Freshwater Research* 61:1-10.
- 4769 Heupel, M.R., J.K. Carlson and C.A. Simpfendorfer. 2007. Shark nursery areas: Concepts,
4770 definitions, characterization and assumptions. *Marine Ecology Progress Series*
4771 337:287-297.
- 4772 Heupel, M.R. and C.A. Simpfendorfer. 2008. Movement and distribution of young bull
4773 sharks *Carcharhinus leucas* in a variable estuarine environment. *Marine Ecology*
4774 *Progress Series* 1:277-289.
- 4775 Hill, M.O. 1973. Diversity and evenness: A unifying notation and its consequences.
4776 *Ecology* 54:427-432.
- 4777 Hoffacker, A. 1994. 1993 Caloosahatchee River Submerged Aquatic Vegetation
4778 Observations. Letter Report from W. Dexter Bender and Associates, Fort Myers, FL,
4779 to the South Florida Water Management District, West Palm Beach, FL. March 2, 1994.
- 4780 Hopkinson, C.S. and J.J. Vallino. 1995. The relationship among man's activities in
4781 watershed and estuaries: A model of runoff effects on estuarine community
4782 metabolism. *Estuaries* 18:598-621.
- 4783 Hofstetter, R.P. 1977. *Trends in population levels of the American oyster, Crassostrea*
4784 *virginica Gmelin on Public Reefs in Galveston Bay, Texas*. Texas Parks and Wildlife
4785 Department, Austin, TX.
- 4786 Hubbs, C.L. 1943. Terminology of early stages of fishes. *Copeia* 1943(4):260.
- 4787 Hunt, M.J. and P.H. Doering. 2013. Salinity Preferences and Nursery Habitat
4788 Considerations for Blue Crab (*Callinectes sapidus*), Bull Shark (*Carcharhinus leucas*),
4789 and Smalltooth Sawfish (*Pristis pectinata*) in the Caloosahatchee Estuary. Technical
4790 publication WR-2013-001, South Florida Water Management District, West Palm
4791 Beach, FL.
- 4792 Ippen A.T. 1966. Salt Intrusion in Estuaries. In: A.T. Ippen (ed.) *Estuaries and Coastal*
4793 *Hydrodynamics*. McGraw-Hill, New York, NY.
- 4794 Ippen, A.T and Harleman, D.R.F. 1961. *One-Dimensional Analysis of Salinity Intrusion in*
4795 *Estuaries*. Technical Bulletin Number 5, United States Army Corps of Engineers,
4796 Vicksburg, MS.
- 4797 Jarvis, J.C. and K.A. Moore. 2008. Influence of environmental factors on *Vallisneria*
4798 *americana* seed germination. *Aquatic Botany* 88:283-294.
- 4799 Jassby, A.D., W.J. Kimmerer, S.G. Monismith, C. Armor, J.E. Cloern, T.M. Powell,
4800 J.R. Schubel and T.J. Vendlinski. 1995. Isohaline position as a habitat indicator for
4801 estuarine populations. *Ecological Applications* 5:272-289.
- 4802 Jay, D.A., W.R. Grey, R.J. Uncles, J. Vallino, J. Largier and W.R. Boynton. 1997. A review
4803 of recent developments in estuarine scalar flux estimation. *Estuaries* 20(2):262-280.
- 4804 Kalke, R.D. and P.A. Montagna. 1991. The effect of freshwater inflow on macrobenthos
4805 in the Lavaca River Delta and upper Lavaca Bay, Texas. *Contributions in Marine*
4806 *Science* 32:49-72.

- 4807 Kemp, W.M., W.R. Boynton, J.E. Adolf, D.F. Boesch, W.C. Boicourt, G. Brush,
4808 J.C. Cornwell, T.R. Fisher, P.M. Glibert, J.D. Hagy, L.W. Harding, E.D. Houde,
4809 D.G. Kimmel, W.D. Miller, R.I.E. Newell, M.R. Roman, E.M. Smith and
4810 J.C. Stevenson. 2005. Eutrophication of Chesapeake Bay: Historical trends and
4811 ecological interactions. *Marine Ecology Progress Series* 303:1-29.
- 4812 Kemp, W.M., J.M. Testa, D.J. Conley, D. Gilbert and J.D. Hagy. 2009. Temporal responses
4813 of coastal hypoxia to nutrient loading and physical controls. *Biogeosciences*
4814 6:2985-3008.
- 4815 Kennedy, V.S. 1991. American Oyster, *Crassostrea virginica*. Pages 3-1 to 3-20 in: S.L.
4816 Funderburk, S.J. Jordan, J.A. Mihursky and D. Riley (eds.), *Habitat Requirements for*
4817 *Chesapeake Bay Living Resources, Second Edition*. Chesapeake Research Consortium,
4818 Inc., Solomons, MD.
- 4819 Kimes, C.A. and L.C. Crocker. 1999. A historical overview of the Caloosahatchee and its
4820 watershed. *Harbor Happenings, Spring Newsletter of the Charlotte Harbor National*
4821 *Estuary Program* 3(1):8-13.
- 4822 Kimura, R., D.H. Secor, E.D. Houde and P.M. Piccoli. 2000. Up-estuary dispersal of young-
4823 of-the-year bay anchovy *Anchoa mitchilli* in the Chesapeake Bay: Inferences from
4824 microprobe analysis of strontium in otoliths. *Marine Ecology Progress Series*
4825 208:217-227.
- 4826 Konyha, K. and Y. Wan. 2011. *Calibration and Refinement of the Tidal Caloosahatchee*
4827 *Basin Linear Reservoir Model*. Technical report to support the Caloosahatchee Estuary
4828 Water Reservation Project, South Florida Water Management District, West Palm
4829 Beach, FL.
- 4830 Kraemer, G.P., R.H. Chamberlain, P.H. Doering, A.D. Steinman and M.D. Hanisak. 1999.
4831 Physiological responses of transplants of the freshwater angiosperm *Vallisneria*
4832 *americana* along a salinity gradient in the Caloosahatchee Estuary (southwest Florida).
4833 *Estuaries* 22(1):138-148.
- 4834 Kuijper, K and L.C. Van Rijn. 2011. Analytical and numerical analysis of tides and
4835 salinities in estuaries, Part II: Salinity distribution in prismatic and convergent tidal
4836 channels. *Ocean Dynamics* 61:1743-1765.
- 4837 La Peyre, M.K., A.D. Nickens, A.K. Volety, G.S. Tolley and J.F. La Peyre. 2003.
4838 Environmental significance of freshets in reducing *Perkinsus marinus* infection in
4839 eastern oysters *Crassostrea virginica*: Potential management applications. *Marine*
4840 *Ecology Progress Series* 248:165-176.
- 4841 La Peyre, M.K., B. Gossman and J.F. La Peyre. 2009. Defining optimal freshwater flow
4842 for oyster production: Effects of freshet rate and magnitude of change and duration on
4843 eastern oysters and *Perkinsus marinus* infection. *Estuaries and Coasts* 32:522-534.
- 4844 Lamon, E.C., K.H. Reckhow and K.E. Havens. 1996. Using generalized additive models
4845 for prediction of chlorophyll *a* in Lake Okeechobee, Florida. *Lakes & Reservoirs:*
4846 *Research and Management* 2:37-46.
- 4847 Lancelot, C. and K. Muylaert. 2011. Trends in estuarine phytoplankton ecology. Pages 5-
4848 15, Volume 7 in: Wolanski, E. and D.S. McLusky (eds.), *Treatise on Estuarine and*
4849 *Coastal Science*, Academic Press, Waltham, MA.

- 4850 Lane, R.R., J.W. Day, B.D. Marx, E. Reyes, E. Hyfield and J.N. Day. 2007. The effects of
4851 riverine discharge on temperature, salinity, suspended sediment and chlorophyll *a* in a
4852 Mississippi delta estuary measured using a flow-through system. *Estuarine, Coastal,*
4853 *and Shelf Science* 74:145-154.
- 4854 Langevin, C.D. 2003. Simulation of submarine groundwater discharge to a marine estuary:
4855 Biscayne Bay, Florida. *Ground Water* 41(6):758-771.
- 4856 Lauer, N., M. Yeager, A.E. Kahn, D.R. Dobberfuhl and C. Rossa. 2011. The effects of
4857 short term salinity exposure on the sublethal stress response of *Vallisneria americana*
4858 Michx. (Hydrocharitaceae). *Aquatic Botany* 95:207-213.
- 4859 Lehrter, J.C. and J. Cebrian. 2010. Uncertainty propagation in an ecosystem nutrient
4860 budget. *Ecological Applications* 20(2):508-524.
- 4861 Livingston, R.J. 2007. Phytoplankton bloom effects on a gulf estuary: Water quality
4862 changes and biological response. *Ecological Applications* 17(5):S110-S128.
- 4863 Livingston, R.J., X. Niu, F.G. Lewis and G.C. Woodsum. 1997. Freshwater input to a gulf
4864 estuary: Long term control of trophic organization. *Ecological Applications* 7:277-299.
- 4865 Livingston, R.J., F.G. Lewis, G.C. Woodsum, X-F. Niu, B. Galperin, W. Huang, J.D.
4866 Christensen, M.E. Monaco, T.A. Battista, C.J. Klein, R.L. Howell and G.L. Ray. 2000.
4867 Modelling oyster population response to variation in freshwater input. *Estuarine,*
4868 *Coastal, & Shelf Science* 50:655-672.
- 4869 Liu, W-C., M-H. Hsu, A.Y. Kuo and M-S Li. 2001. Influence of bathymetric changes on
4870 hydrodynamics and salt intrusion in estuarine system. *Journal of the American Water*
4871 *Resources Association* 37:1405-1416.
- 4872 Loneragan, N.R. and S.E. Bunn 1999. River flow and estuarine ecosystems: Implications
4873 for coastal fisheries from a review and a case study of the Logan River, southeast
4874 Queensland. *Australian Journal of Ecology* 24:431-440.
- 4875 Longley, W.L., G.L. Powell and A.W. Green. 1994. Freshwater inflows to Texas bays and
4876 estuaries: Ecological relationships and methods for determination of needs. Texas
4877 Water Development Board and Texas Parks and Wildlife Department, Austin, TX.
- 4878 Loosanoff, V.L. 1953. Behavior of oysters in water of low salinities. *Proceedings of the*
4879 *National Shellfish Association* 43:135-151.
- 4880 Loosanoff, V.L. 1965. Gonad development and discharge of spawn in oysters of Long
4881 Island Sound. *Biological Bulletin* (Woods Hole) 129:546-561.
- 4882 Lovett-Doust, J. and G. Laporte. 1991. Population sex ratios, population mixtures and
4883 fecundity in a clonal dioecious macrophyte, *Vallisneria americana*. *Journal of Ecology*
4884 79:477-489.
- 4885 Mackin, J.G. and S.H. Hopkins. 1962. Studies on oyster mortality in relation to natural
4886 environments and to oil fields in Louisiana. *Publications of the Institute of Marine*
4887 *Science, University of Texas* 7:1-131.
- 4888 MacWilliams, M.L., F.G. Salcedo and E.S. Gross. 2009. San Francisco Bay-Delta
4889 UnTRIM Model Calibration Report, Sacramento and Stockton Deep Water Ship

- 4890 Channel 3-D Hydrodynamic and Salinity Modeling Study, Prepared for United States
4891 Army Corps of Engineers, San Francisco, CA.
- 4892 Madden, C.J. and J.W. Day. 1992. An instrument system for high-speed mapping of
4893 chlorophyll *a* and physico-chemical variables in surface waters. *Estuaries* 15:421-427.
- 4894 Mattson, R.A., K.W. Cummins, R.W. Merritt, P.A. Montagna, T. Palmer, J. Mace, J. Slater,
4895 and C. Jacoby. 2012. Benthic Macroinvertebrates. In: E.F. Lowe, L.E. Battoe,
4896 H. Wilkening, M. Cullum and T. Bartol, *The St. Johns River Water Supply Impact*
4897 *Study Final Report*. St. Johns River Water Management District, Palatka, FL.
- 4898
- 4899 Mazzotti, F.J., L.G. Pearlstine, T. Barnes, A. Volety, A. Chartier, A. Weinstein and
4900 D. DeAngleis. 2006. Stressor Response Models for the Blue Crab, *Callinectes sapidus*.
4901 Department of Wildlife Ecology and Conservation, Florida Cooperative Extension
4902 Service, Institute of Food and Agricultural Services, University of Florida,
4903 Gainesville, FL.
- 4904 McFarland, D.G. 2006. *Reproductive Ecology of Vallisneria americana* Michaux. Report
4905 ERDC/TN SAV-06-4, United States Army Engineer Research and Development
4906 Center, Vicksburg, MS.
- 4907 McPherson, B.F. and R.L. Miller. 1987. The vertical attenuation of light in Charlotte
4908 Harbor, a shallow, subtropical estuary, southwestern Florida. *Estuarine, Coastal, and*
4909 *Shelf Science* 25:721-737.
- 4910 McPherson, B.F. and R.L. Miller. 1994. Causes of light attenuation in Tampa Bay and
4911 Charlotte Harbor, southwestern Florida. *Water Resources Bulletin* 30(1):43-53.
- 4912 Meeter, D.A., R.J. Livingston and G.C. Woodsum. 1979. Long-term climatological cycles
4913 and population changes in a river-dominated estuarine system. Pages 315-338 in:
4914 Livingston, R.J. (ed.), *Ecological Processes in Coastal and Marine Systems, Marine*
4915 *Science Volume 10*, Springer, New York, NY.
- 4916 Millero, F. 2010. History of the equation of state of seawater. *Oceanography* 23(3):18-33.
- 4917 Montagna, P.A. and T. Palmer. 2014. *Minimum Flow and Level Analysis of Benthic*
4918 *Macrofauna in the Caloosahatchee Estuary*. Draft report to the South Florida Water
4919 Management District, West Palm Beach, FL.
- 4920 Montagna, P.A., M. Alber, P.H. Doering and M.S. Connor. 2002a. Freshwater inflow:
4921 Science, policy, management. *Estuaries* 25:1243-1245.
- 4922 Montagna, P.A., R.D. Kalke and C. Ritter. 2002b. Effect of restored freshwater inflow on
4923 macrofauna and meiofauna in upper Rincon Bayou, Texas, USA. *Estuaries* 25:1436-
4924 1447.
- 4925 Montagna, P.A., E.D. Estevez, T.A. Palmer and M.S. Flannery. 2008. Meta-analysis of the
4926 relationship between salinity and molluscs in tidal river estuaries of Southwest Florida,
4927 U.S.A. *American Malacological Bulletin* 24:101-115.
- 4928 Montagna, P.A., T.A. Palmer and J.B. Pollack. 2013. Hydrological changes and estuarine
4929 dynamics. *Springer Briefs in Environmental Science*, New York, NY.

- 4930 Moore, KA, E.C. Shields and J.C. Jarvis. 2010. The role of habitat and herbivory on the
4931 restoration of tidal freshwater submerged aquatic vegetation populations. *Restoration*
4932 *Ecology* 18(4):596-604.
- 4933 Moses, C.S., W.T. Anderson, C. Saunders and F. Sklar. 2013. Regional climate gradients
4934 in precipitation and temperature in response to climate teleconnections in the greater
4935 Everglades ecosystem of South Florida. *Journal of Paleolimnology* 49:5-14.
- 4936 Murphy, M.D., A.L. McMillen-Jackson and B. Mahoudi. 2007. *A Stock Assessment of the*
4937 *Blue Crab, Callinectes sapidus, in Florida Waters*. In-House Report 2007-006, Florida
4938 Fish and Wildlife Commission, Florida Wildlife Research Institute, St. Petersburg, FL.
- 4939 Murrell, M., J.D. Hagy, E.M. Lores and R.M. Greene. 2007. Phytoplankton production and
4940 nutrient distributions in a subtropical estuary: Importance of freshwater flow. *Estuaries*
4941 *and Coasts* 30:390-402.
- 4942 Nelson, D.M. (ed.). 1992. *Distribution and Abundance of Fishes and Invertebrates in Gulf*
4943 *of Mexico Estuaries, Volume I: Data Summaries*. Estuarine Living Marine Resources
4944 Report Number 10, National Ocean Service, National Oceanic and Atmospheric
4945 Administration, Rockville, MD.
- 4946 Nixon, S.W. 1981. Freshwater inputs and estuarine productivity. Pages 31–57 in: Cross,
4947 R. and D. Williams (eds.), *Proceedings of the Nation Symposium on Freshwater Inflow*
4948 *to Estuaries, Volume I and II*, FWS/OBS-81/04, United States Fish and Wildlife
4949 Service Washington, DC.
- 4950 Nixon, S.W., S.B. Olsen, E. Buckley and R. Fulweiler. 2004. *Lost to the Tide: The*
4951 *Importance of Freshwater Flow to Estuaries*. Final Report submitted to the Coastal
4952 Resources Center, Narragansett RI., by the Graduate School of Oceanography,
4953 University of Rhode Island, Kingston, RI.
- 4954 Nixon, S.W., C.A. Oviatt, J. Frithsen and B. Sullivan. 1986. Nutrients and the productivity
4955 of estuarine and coastal marine ecosystems. *Journal of the Limnological Society of*
4956 *South Africa* 12(1/2):43-71.
- 4957 NOAA. 2009. *Critical Habitat for the Endangered Distinct Population Segment of*
4958 *Smalltooth Sawfish*. National Oceanic and Atmospheric Administration, Federal
4959 Register, Rules and Regulations 74(169):45353-45378.
- 4960 Norton, S.L., T.R. Wiley, J.K. Carlson, A.L. Frick, G.R. Poulakis and C.A. Simpfendorfer.
4961 2012. Designating critical habitat for juvenile endangered smalltooth sawfish in the
4962 United States. *Marine and Coastal Fisheries: Dynamics, Management, and Ecosystem*
4963 *Science* 4(1):473-480.
- 4964 Nosach, C. 2007. Influence of environmental factors on the germination of South Florida
4965 *Vallisneria Americana*. Senior Thesis, Eckerd College, St. Petersburg, FL.
- 4966 Obeysekera, J., P. Trimble, C. Neidrauer and L. Cadavid. 2007. Consideration of Climate
4967 Variability in Water Resources Planning and Operations – South Florida’s experience.
4968 In: K.C. Kabbes (ed.), *World Environmental and Water Resource Congress 2007:*
4969 *Restoring Our Natural Habitat*, American Society of Civil Engineers, Baltimore, MD.
- 4970 Obeysekera, J., L. Kuebler, S. Ahmed, M.-L. Chang, V. Engel, C. Langevin, E. Swain and
4971 Y. Wan. 2011. Use of hydrologic and hydrodynamic modeling for ecosystem

- 4972 restoration. *Critical Reviews in Environmental Science and Technology* 41(S1):447-
4973 488.
- 4974 Ogden, J.C., S.M. Davis, K.J. Jacobs, T. Barnes and H.E. Fling. 2005. The use of
4975 conceptual ecological models to guide ecosystem restoration in South Florida.
4976 *Wetlands* 25(4):795-809.
- 4977 Ortega, L.A., M.R. Heupel, P. Van Beynen and P.J. Motta. 2009. Movement patterns and
4978 water quality preferences of juvenile bull sharks (*Carcharhinus leucas*) in a Florida
4979 estuary. *Environmental Biology of Fishes* 84:361-373.
- 4980 Paerl, H.W., L.M. Valdes, B.L. Peierls, J.E. Adolf and L.W. Harding. 2006. Anthropogenic
4981 and climatic influences on the eutrophication of large estuarine ecosystems. *Limnology
4982 and Oceanography* 51(1/2):448-462.
- 4983 Palmer, T.A., P.A. Montagna, J.B. Pollack, R.D. Kalke and H.R. DeYoe. 2011. The role
4984 of freshwater inflow in lagoons, rivers, and bays. *Hydrobiologia* 667:49-67.
- 4985 Palmer, T.A., P.A. Montagna, R.H. Chamberlain, P.H. Doering, Y. Wan, K.M. Haunert
4986 and D.J. Crean. 2015. Determining the effects of freshwater inflow on benthic
4987 macrofauna in the Caloosahatchee Estuary, Florida. *Integrated Environmental
4988 Assessment and Management* 9999:1-11.
- 4989 Peebles, E.B., S.E. Burghart and D.J. Hollander. 2007. Causes of inter-estuarine variation
4990 in bay anchovy (*Anchoa mitchilli*) salinity at capture. *Estuaries and Coasts* 30:1060-
4991 1074.
- 4992 Peebles, E.B. and M.F.D. Greenwood. 2009. Spatial abundance quantiles as a tool for
4993 assessing habitat compression in motile estuarine organisms. *Florida Scientist*
4994 72:277-288.
- 4995 Perry, H.M. 1984. *A Profile of the Blue Crab Fishery of the Gulf of Mexico*. Gulf State
4996 Marine Fisheries Commission, Ocean Springs, MS.
- 4997 Perry, H.M. and T.D. McIlwain. 1986. *Species Profiles: Life Histories and Environmental
4998 Requirements of Coastal Fishes and Invertebrates (Gulf of Mexico): Blue Crab*.
4999 Biological Report 82(11.55), United States Fish and Wildlife Service, Washington, DC
5000 and TR EL-82-4, United States Army Corps of Engineers, Washington, DC.
- 5001 Peterson, M.S. 2003. A conceptual view of environment-habitat-production linkages in
5002 tidal river estuaries. *Reviews in Fisheries Science* 11(4):291-313.
- 5003 Petes, L.E., A.J. Brown and C.R. Knight. 2012. Impacts of upstream drought and water
5004 withdrawals on the health and survival of downstream estuarine oyster populations.
5005 *Ecology and Evolution* 2(7):1712-1724.
- 5006 Petrie M.D. and N.A. Brunsell. 2011. The role of precipitation variability on the
5007 ecohydrology of grasslands. *Ecohydrology* DOI: 12.1002/eco.224.
- 5008 Phillips, R. C. and V.G. Springer 1960. *A Report on the Hydrography, Marine Plants and
5009 Fishes of the Caloosahatchee River Area, Lee County, Florida*. Special Report Number
5010 5, Florida State Board of Conservation Marine Lab, Tallahassee, Florida.

- 5011 Pollack, J.B., H-C. Kim, E.K. Morgan and P.A. Montagna. 2011. Role of flood disturbance
5012 in natural oyster (*Crassostrea virginica*) population maintenance in an estuary in South
5013 Texas, USA. *Estuaries and Coasts* 34:187-197.
- 5014 Posey, M.H., T.D. Alphin, H. Harwell and B. Allen 2005. Importance of low salinity areas
5015 for juvenile blue crabs, *Callinectes sapidus* Rathbun, in river-dominated estuaries of
5016 southeastern United States. *Journal of Experimental Marine Biology and Ecology*
5017 319:81-100.
- 5018 Poulakis, G.R., P.W. Stevens, A.A. Timmers, T.R. Wiley and C.A. Simpfendorfer. 2011.
5019 Abiotic affinities and spatiotemporal distribution of the endangered smalltooth sawfish,
5020 *Pristis pectinata*, in a southwestern Florida estuary. *Marine and Freshwater Research*
5021 62:1165-1177.
- 5022 Poulakis, G.R., P.W. Stevens, A.A. Timmers, C.J. Stafford and C.A. Simpfendorfer. 2013.
5023 Movements of juvenile endangered smalltooth sawfish, *Pristis pectinata*, in an
5024 estuarine river system: Use of non-main-stem river habitats and lagged responses to
5025 freshwater inflow related changes. *Environmental Biology of Fishes* 96:763-778.
- 5026 Poulakis, G.R., P.W. Stevens, R.D. Grubbs, D.D. Chapman, J. Gelsleichter, G.H. Burgess,
5027 T.R. Wiley, J.A. Olin, L.S. Hollensead, A.T. Fisk, D.A. Blewett, R.M. Scharer, H.J.
5028 Grier, J.A. DeAngelo, J.M. Darrow, Y. Papstamatiou and M.D. Bakenhaster. 2014.
5029 *Smalltooth Sawfish (Pristis Pectinata) Research and Outreach: An Interdisciplinary*
5030 *Collaborative Program*. Report to Fisheries Species Recovery Grant
5031 NA10NMF4720032, National Oceanic and Atmospheric Administration,
5032 Washington, DC.
- 5033 Powell, E.N., J.M. Klinck, E.E. Hofmann and M.A. McManus. 2003. Influence of water
5034 allocation and freshwater inflow on oyster production: A hydrodynamic-oyster
5035 population model for Galveston Bay, Texas, USA. *Environmental Management*
5036 31:100-121.
- 5037 Powers, S.P., C.H. Peterson, R.R. Christian, E. Sullivan, M.J. Powers, M.J. Bishop and
5038 C. Buzzelli. 2005. Effects of eutrophication on bottom habitat and prey resources of
5039 demersal fishes. *Marine Ecology Progress Series* 302:233-243.
- 5040 Prandle, D. 1985. On salinity regimes and the vertical structure of residual flows in narrow
5041 tidal estuaries. *Estuarine, Coastal Shelf Science* 20:615-635.
- 5042 Prandle, D. 2004. Salinity intrusion in partially mixed estuaries. *Estuarine, Coastal Shelf*
5043 *Science* 54:385-397.
- 5044 Prandle D. 2009. *Estuaries, Dynamics, Mixing, Sedimentation and Morphology*.
5045 Cambridge University Press, Cambridge, United Kingdom.
- 5046 Punt, A.E. 2003. Evaluating the efficacy of managing West Coast groundfish resources
5047 through simulations. *Fisheries Bulletin* 101:860-873.
- 5048 Qian, S.S., Y. Pan and R.S.King. 2004. Soil total phosphorus threshold in the Everglades:
5049 A Bayesian changepoint analysis for multinomial response data. *Ecological Indicators*
5050 4:29-37.

- 5051 Qiu, C. 2002. *Hydrodynamic and Salinity Modeling, Technical Supporting Document for*
5052 *Caloosahatchee River Minimum Flow and Levels Update*. South Florida Water
5053 Management District, West Palm Beach, FL.
- 5054 Qiu, C. 2006. *Addendum to CH3D Calibration Report in Estero Bay and Caloosahatchee*
5055 *Estuary*. South Florida Water Management District, West Palm Beach, FL.
- 5056 Qiu, C. and Y. Wan. 2013. Time series modeling and prediction of salinity in the
5057 Caloosahatchee River Estuary. *Water Resources Research* 49:1-13.
- 5058 Rabalais, N.N., R.J. Diaz, L.A. Levin, R.E. Turner, D. Gilbert and J. Zhang. 2010.
5059 Dynamics and distribution of natural and human-caused hypoxia. *Biogeosciences*
5060 7:585-619.
- 5061 Radabaugh, K.R. and E.B. Peebles. 2012. Detection and classification of phytoplankton
5062 deposits along an estuarine gradient. *Estuaries and Coasts* 35:1361-1375.
- 5063 Reckhow, K.H. 1994. Water quality simulation modeling and uncertainty analysis for risk
5064 assessment and decision making. *Ecological Modelling* 72:1-20.
- 5065 RECOVER. 2012. *2012 System Status Report Interim Update*. Restoration Coordination
5066 and Verification, c/o United States Army Corps of Engineers, Jacksonville, FL, and
5067 South Florida Water Management District, West Palm Beach, FL. Available online at
5068 http://141.232.10.32/pm/ssr_2012/ssr_main_2012.aspx.
- 5069 RECOVER. 2014. *2014 System Status Report*. Restoration Coordination and Verification,
5070 c/o United States Army Corps of Engineers, Jacksonville, FL, and South Florida Water
5071 Management District, West Palm Beach, FL. Available online at
5072 http://141.232.10.32/pm/ssr_2014/ssr_main_2014.aspx.
- 5073 Regan, H.M., M. Colyvan and M.A. Burgman. 2002. A taxonomy and treatment of
5074 uncertainty for ecology and conservation biology. *Ecological Applications*
5075 12(2):618-628.
- 5076 Restrepo, V.R., J.M. Hoenig, J.E. Powers, J.W. Baird and S.C. Turner. 1992. Monte Carlo
5077 simulation applied to *Xiphias gladius* and *Gadus morhua*. *Fishery Bulletin* 90:736-748.
- 5078 Ricker, W.E. 1973. Linear regressions in fishery research. *Journal of the Fisheries*
5079 *Research Board of Canada* 30:409-434.
- 5080 Ricker, W.E. 1975. A note concerning Professor Jolicoeur's comments. *Journal of the*
5081 *Fisheries Research Board of Canada* 32:1494-1498.
- 5082 Robins, J.B., I.A. Halliday, J. Staunton-Smith, D.G. Mayer and M.J. Sellin. 2005.
5083 Freshwater-flow requirements of estuarine fisheries in tropical Australia: A review of
5084 the state of knowledge and application of a suggested approach. *Marine and*
5085 *Freshwater Research* 56:343-360.
- 5086 Rogers, S.G., J.D. Arredondo and S.N. Latham. 1990. *Assessment of the Effects of the*
5087 *Environment on the Georgia Blue Crab Stock*. S-K Project Number NA90AA-H-
5088 SK018, Georgia Department of Natural Resources, Brunswick, GA.
- 5089 Rozas, L.P. and T.J. Minello. 2006. Nekton use of *Vallisneria americana* Michx. (wild
5090 celery) beds and adjacent habitats in coastal Louisiana. *Estuaries and Coasts*
5091 29(2):297-310.

- 5092 Ruggieri, E. 2012. A Bayesian approach to detecting change points in climatic records.
5093 *International Journal of Climatology* DOI: 10.1002/JOC.3447.
- 5094 Sackett, J.W. 1888. *Survey of the Caloosahatchee River, Florida*. Report to the Captain of
5095 the United States Engineering Office, St. Augustine, FL.
- 5096 Sandoz, M.D. and R. Rogers. 1944. The effect of environmental factors on hatching,
5097 molting, and survival of zoea larvae of the blue crab, *Callinectes sapidus*, Rathbun.
5098 *Ecology* 25(2) 216-228.
- 5099 Saundry, P. and C. Cleveland (eds.). 2011. *Wadden Sea, Encyclopedia of Earth*. National
5100 Council for Science and the Environment, Washington, DC.
- 5101 Savenije, H.H.G. 1992. *Rapid Assessment Technique for Salt Intrusion in Alluvial*
5102 *Estuaries*. Ph.D Dissertation, IHE report series, Number 27, Delft, the Netherlands.
- 5103 Savenije, H.H.G. 2005. *Salinity and Tides in Alluvial Estuaries*. Elsevier, Amsterdam
- 5104 Scavia, D., D. Justic and V.J. Bierman. 2004. Reducing hypoxia in the Gulf of Mexico:
5105 Advice from three models. *Estuaries* 27(3):419-425.
- 5106 Schlacher, T.A., A.J. Skillington, R.M. Connolly, W. Robinson and T.F. Gaston. 2008.
5107 Coupling between marine plankton and freshwater flow in the plumes off a small
5108 estuary. *International Review of Hydrobiology*. 93(6):641-658.
- 5109 Schwarz, C.J. 2013. Regression – hockey sticks, broken sticks, piecewise, change points.
5110 Chapter 18 in: C.J. Schwarz, *Sampling, Regression, Experimental Design and Analysis*
5111 *for Environmental Scientist, Biologists and Resource Managers*. Simon Fraser
5112 University, Burnaby, British Columbia. Available online at
5113 [http://people.stat.sfu.ca/~cschwarz/Stat-650/Notes/PDFbigbook-SAS/SAS-](http://people.stat.sfu.ca/~cschwarz/Stat-650/Notes/PDFbigbook-SAS/SAS-part019.pdf)
5114 [part019.pdf](http://people.stat.sfu.ca/~cschwarz/Stat-650/Notes/PDFbigbook-SAS/SAS-part019.pdf)
- 5115 Seaman, W. (ed.). 1988. *Florida Aquatic Habitat and Fishery Resources*. Florida Chapter,
5116 American Fisheries Society, Eustis, FL.
- 5117 SFWMD. 2003. *Caloosahatchee Minimum Flows and Levels Status Update Report*. South
5118 Florida Water Management District, West Palm Beach, FL.
- 5119 SFWMD. 2010. *Final Adaptive Protocols for Lake Okeechobee Operations*. South Florida
5120 Water Management District, West Palm Beach, FL. September 16, 2010.
- 5121 SFWMD. 2012. Appendix 10-2: Caloosahatchee River Watershed Protection Plan 2012
5122 Update. *South Florida Environmental Report – Volume I*, South Florida Water
5123 Management District, West Palm Beach, FL. Available online at
5124 www.sfwmd.gov/SFER.
- 5125 SFWMD. 2014. *Document to Support a Water Reservation Rule for the CERP*
5126 *Caloosahatchee River (C-43) West Basin Storage Reservoir Project*. South Florida
5127 Water Management District, West Palm Beach, FL.
- 5128 SFWMD. 2015. Appendix 10-2: Caloosahatchee River Watershed Protection Plan 2015
5129 Update. *South Florida Environmental Report – Volume I*, West Palm Beach, FL.
5130 Available online at www.sfwmd.gov/SFER.

- 5131 Sheaves, M., R. Baker, I. Nagelkerten and R.M. Connolly. 2015. True value of estuarine
5132 and coastal nurseries for fish: Incorporating complexity and dynamics. *Estuaries and*
5133 *Coasts* 38:401-414.
- 5134 Sheldon, J. and M. Alber. 2006. The calculation of estuarine turnover times using
5135 freshwater fraction and tidal prism models: A critical evaluation. *Estuaries and Coasts*
5136 29(1):133-146.
- 5137 Sheng, Y.P. 1986. A three-dimensional mathematical model of coastal, estuarine and lake
5138 currents using boundary-fitted grid. Technical Report No. 585, Aeronautical Research
5139 Associates of Princeton, N.J.
- 5140 Sheng, Y.P. 1987. On Modeling Three-Dimensional Estuarine and Marine
5141 Hydrodynamics. Pages 35–54 in: J.C.J. Nihoul and B.M. Jamart (eds.), *Three-*
5142 *Dimensional Models of Marine and Estuarine Dynamics*. Elsevier Oceanography
5143 Series, Waltham, MA.
- 5144 Sheng, Y.P. 2002. *Impact of Caloosahatchee Flow on Circulation and Salinity in Charlotte*
5145 *Harbor. Technical Report*. Civil & Coastal Engineering Department, University of
5146 Florida, Gainesville, FL.
- 5147 Sheng, Y.P and C. Villaret, 1989. Modeling the effect of suspended sediment stratification
5148 on bottom exchange processes. *Journal of Geophysical Research*, 94(10):14429-14444.
- 5149 Sheng, Y.P and Y. Zhang. 2006. *Estero Bay and Caloosahatchee Salinity Modeling, Final*
5150 *Report*. Submitted to South Florida Water Management District, West Palm Beach, FL.
- 5151 Shumway, S.E. 1996. Natural Environmental Factors. Pages 467–503 in: V.S. Kennedy,
5152 R.I.E. Newell, and A. Eble (eds.), *The Eastern Oyster (Crassostrea virginica)*..
5153 Maryland Sea Grant College, College Park, MD.
- 5154 Simpfendorfer, C.A., B.G. Yeiser, T.R. Wiley, G.R. Poulakis, P.W. Stevens and
5155 M.R. Heupel. 2011. Environmental influences on the spatial ecology of juvenile
5156 smalltooth sawfish (*Pristis pectinata*): Results from acoustic monitoring. *Plos One*
5157 6(2):1-12.
- 5158 Sklar, F.H. and J.A. Browder. 1998. Coastal environmental impacts brought about by
5159 alterations to freshwater flow in the Gulf of Mexico. *Environmental Management*
5160 22(4):547-562.
- 5161 Spencer, D., C.J. Lemckert, Y. Yu, J. Gustafson, S.Y. Lee and H. Zhang. 2014. Quantifying
5162 dispersion in an estuary. *Journal of Coastal Research* Special Issue 70:29-34.
- 5163 Stanley, J.G. and M.A. Sellers. 1986. American Oyster. In: *Species Profiles: Life Histories*
5164 *and Environmental Requirements of Coastal Fishes and Invertebrates (Gulf of*
5165 *Mexico)*. United States Fish and Wildlife Service, Washington, DC.
- 5166 Stevens, P.W., M.F.D. Greenwood, T.C. MacDonald, C.F. Idelberger and R.H. Michael,
5167 Jr. 2008. Relationships between Freshwater Inflows and Fish Populations in the
5168 Caloosahatchee River Estuary, Florida. File Code: F2706-07-F1, Fish and Wildlife
5169 Research Institute, Florida Fish and Wildlife Conservation Commission,
5170 Tallahassee, FL.

- 5171 Stevens, P.W., M.F.D. Greenwood, C.F. Idleberger and D.A. Blewitt. 2010. Mainstem and
5172 backwater fish assemblages in the tidal Caloosahatchee River: Implications for
5173 freshwater inflow studies. *Estuaries and Coasts* 33:1216-1224.
- 5174 Stevens, P.W., M.F.D. Greenwood and D.A. Blewett. 2013. Fish assemblages in the
5175 oligohaline stretch of a southwest Florida river during periods of extreme freshwater
5176 inflow variation. *Transactions of the American Fisheries Society* 142:1644-1658.
- 5177 Sun, D. 2004. Preliminary Feasibility Study of Saltwater Barrier in the Loxahatchee River
5178 Estuary. Coastal Tech, Vero Beach, FL.
- 5179 Sun, D. 2009. *Development of the CH3D Hydrodynamic Model for the St. Lucie Estuary,*
5180 *Technical Document to Support a Water Reservation Rule for the North Fork of the St.*
5181 *Lucie Estuary.* South Florida Water Management District, West Palm Beach, FL.
- 5182 Sutcliffe, W.H., 1972. Some relations of land drainage, nutrients, particulate material, and
5183 fish catch in two eastern Canadian bays. *Journal of the Fisheries Research Board of*
5184 *Canada* 29:357-362.
- 5185 Sutcliffe, W.H. 1973. Correlations between seasonal river discharge and local landings of
5186 American lobster (*Homarus americanus*) and Atlantic halibut (*Hippoglossus*
5187 *hippoglossus*) in the Gulf of St. Lawrence. *Journal of the Fisheries Research Board of*
5188 *Canada* 30:856-859.
- 5189 Sutherland, K., N.A. Strydom and T.H. Woolridge. 2012. Composition, abundance,
5190 distribution, and seasonality of larval fishes in the Sundays Estuary, South Africa.
5191 *African Zoology* 47(2):229-244.
- 5192 Titus, J.E. and D.T. Hoover. 1991. Toward predicting reproductive success in submersed
5193 freshwater angiosperms. *Aquatic Botany* 41:111-136.
- 5194 Tolley, S.G. A.K. Volety and M. Savarese. 2005. Influence of salinity on the habitat use of
5195 oyster reefs in three Southwest Florida estuaries. *Journal of Shellfish Research*
5196 24:127-137.
- 5197 Tolley, S.G. A.K. Volety, M. Savarese, L.D. Walls, C. Linardich and E.M. Everham III.
5198 2006. Impacts of salinity and freshwater inflow on oyster-reef communities in
5199 Southwest Florida. *Aquatic Living Resources* 19:371-387.
- 5200 Tolley, S.G., D. Fugate, M.L. Parsons, S.E. Burghart and E.B. Peebles. 2010. *The*
5201 *Responses of Turbidity, CDOM, Benthic Microalgae, Phytoplankton, and Zooplankton*
5202 *to Variation in Seasonal Freshwater Inflow to the Caloosahatchee Estuary.* Final
5203 Project Report to the South Florida Water Management District, West Palm Beach, FL,
5204 and the United States Department of Education, Washington, DS.
- 5205 Tolley, S.G., B.M. Brosious, J.T. Evans, J.L. Nelson, L.H. Haynes, L.K. Smith, S.E.
5206 Burghart and E.B. Peebles. 2012. Freshwater inflow effects of larval fish and crab
5207 settlement onto oyster reefs. *Journal of Shellfish Research* 31(3):895-908.
- 5208 Turner, R.E. 2006. Will lowering estuarine salinity increase Gulf of Mexico oyster
5209 landings? *Estuaries & Coasts* 29:345-352.
- 5210 Twilley, R.R. and J.W. Barko. 1990. The growth of submersed macrophytes under
5211 experimental salinity and light conditions. *Estuaries* 12:311-321.

- 5212 Urban, D.L. 2006. A modeling framework for restoration ecology. In D.A. Falk, M.A.
5213 Palmer and R.J. Hobbs (eds.), *Foundations of Restoration Ecology*, Island Press, Boca
5214 Raton, FL.
- 5215 USACE, 1957. General Design Memorandum, Caloosahatchee River and Control
5216 Structures (Canal 43 Lock and Spillway Structures 77, 78, and 79), Part IV: Central
5217 and Southern Florida Project. Serial No. 36. Jacksonville District, United States Army
5218 Corps of Engineers, Jacksonville, FL.
- 5219 USACE 2008. St. John's River Circulation and Salinity for the Jacksonville Harbor
5220 Navigation Study.
- 5221 USACE and SFWMD. 2010. *Central and Southern Florida Project Caloosahatchee River*
5222 *(C-43) West Basin Storage Reservoir Integrated Project Implementation Report and*
5223 *Environmental Impact Statement*. United States Army Corps of Engineers,
5224 Jacksonville, FL, and South Florida Water Management District, West Palm
5225 Beach, FL.
- 5226 Van der Burgh, P. 1972. Ontwikkeling van een methode voor het voorspellen van
5227 zoutverdelingen in estuaria, kanalen en zeeën. Rijkswaterstaat, Deltadienst.
- 5228 Van Engel, W. 1958. The blue crab fishery in Chesapeake Bay. *Com. Fish. Rev.* 20:6-17.
- 5229 Volety, A.K., M. Savarese, S.G. Tolley, W.S. Arnold, P. Sime, P. Goodman,
5230 R.H. Chamberlain and P.H. Doering. 2009. Eastern oysters (*Crassostrea virginica*) as
5231 an indicator for restoration of Everglades ecosystems. *Ecological Indicators*
5232 9:S120-S136.
- 5233 Wan, Y. and K. Konyha. 2015. A simple hydrologic model for rapid prediction of runoff
5234 from ungauged coastal catchments. *Journal of Hydrology* 528:571-583
- 5235 Wan, Y., Z-G. Ji, J. Shen, G.Hu and D. Sun. 2012. Three dimensional water quality
5236 modeling of a shallow sub-tropical estuary. *Marine Environmental Research* 82:76-86.
- 5237 Wan, Y., C. Qiu, P.H. Doering, M. Ashton, D. Sun and T. Coley. 2013. Modelling
5238 residence time with a three-dimensional hydrodynamic model: Linkage with
5239 chlorophyll *a* in a sub-tropical estuary. *Ecological Modelling* 268:93-102.
- 5240 Wang, H., W. Huang, M.A. Harwell, L. Edmiston, E. Johnson, P. Hsieh, K. Milla,
5241 J.D. Christensen, J. Stewart and X. Liu. 2008. Modeling oyster growth rate by coupling
5242 oyster population and hydrodynamic models for Apalachicola Bay. *Ecological*
5243 *Modelling* 211:77-89.
- 5244 Wells, H.W. 1961. The fauna of oyster beds, with special reference to the salinity factor.
5245 *Ecological Monographs* 31:239-266.
- 5246 Wetz, M.S., E.A. Hutchinson, R.S. Lunetta, H.W. Paerl and J.C. Taylor 2011. Severe
5247 droughts reduce estuarine primary productivity with cascading effects on higher trophic
5248 levels. *Limnology and Oceanography* 56:627-638.
- 5249 Whitfield, A.K., M. Elliot, A. Basset, S.J.M. Blaber and R.J. West. 2012. Paradigms in
5250 estuarine ecology – A review of the Remane diagram with a suggested revised model
5251 for estuaries. *Estuarine, Coastal, and Shelf Science* 97:78-90.

- 5252 Wigand, C., R. Wehr, K. Limburg, B. Gorham, S. Longergan and S. Findlay. 2000. Effect
5253 of *Vallisneria americana* (L.) on community structure and ecosystem function in lake
5254 mesocosms. *Hydrobiologia* 418:137-146.
- 5255 Wilbur, D. 1992. Associations between freshwater inflows and oyster productivity in
5256 Apalachicola Bay, Florida. *Estuarine, Coastal, and Shelf Science* 35:179-190.
- 5257 Wilbur, D. 1994. The influence of Apalachicola River flows on blue crab, *Callinectes*
5258 *sapidus*, in north Florida. *Fishery Bulletin* 92:180-188.
- 5259 Wolanski, R., L.A. Boorman, L. Chicharo, E. Langlois-Saliou, R. Lara, A.J. Plater,
5260 R.J. Uncles and M. Zalewski. 2004. Ecohydrology as a new tool for sustainable
5261 management of estuaries and coastal waters. *Wetland Ecology & Management*
5262 12:235-276.
- 5263 Woodward-Clyde. 1999. Distribution of Oysters and Submerged Aquatic Vegetation in the
5264 St. Lucie Estuary. Final Report to the South Florida Water Management District, West
5265 Palm Beach, FL.
- 5266 Zachary, A. and D.S. Haven. 1973. Survival and activity of the oyster drill *Urosalpinx*
5267 *cinerea* under conditions of fluctuating salinity. *Marine Biology* 22:45-52.
- 5268 Zheng, L. and R.H. Weisberg. 2004. Tide, buoyancy, and wind-driven circulation of the
5269 Charlotte Harbor Estuary: A model study. *Journal of Geophysical Research*
5270 109:C0611, doi:10.1029/2003JC001996.
- 5271 Zhu, J., R.H. Weisberg, L. Zheng and S. Han. 2015. Influences of channel deepening and
5272 widening on the tidal and non-tidal circulations of Tampa Bay. *Estuaries and Coasts*
5273 38:132-150.